Wave Impacts on Vertical Breakwaters

final report graduation project

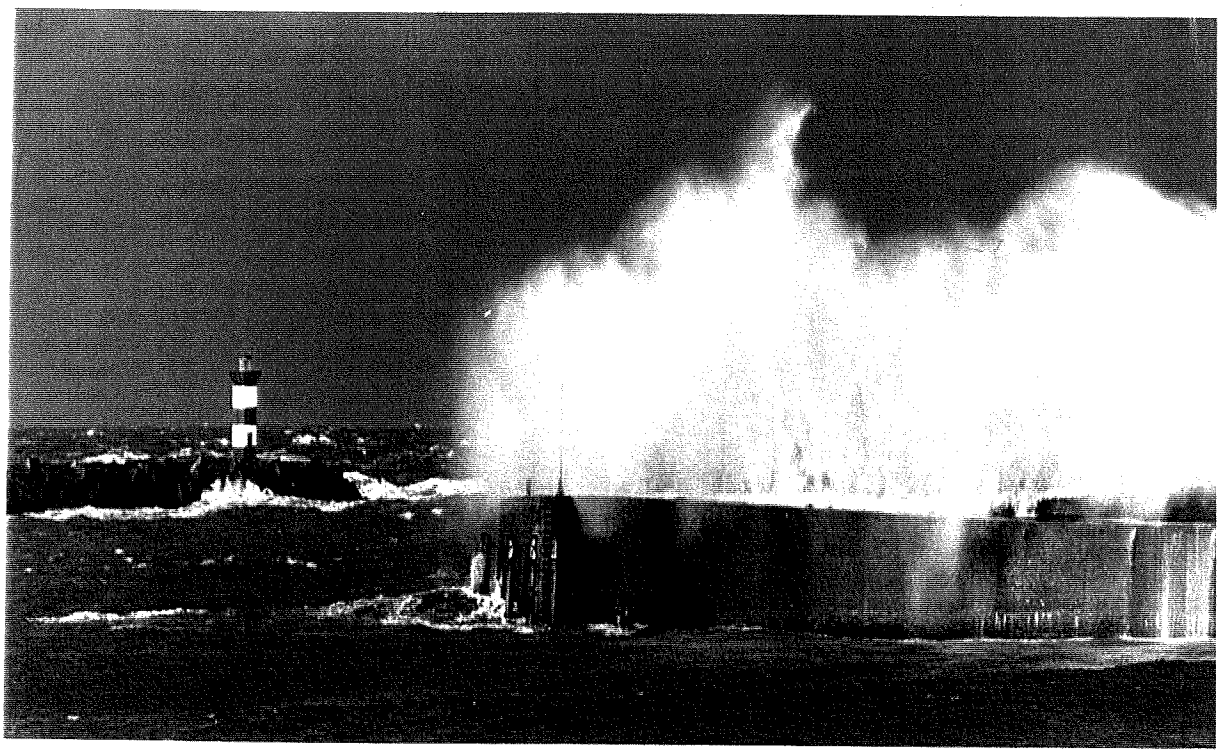

H.A.Th. Vink
May 1997

TU Delft
Delft University of Technology

Faculty of Civil Engineering
Hydraulic and Geotechnical Engineering Division
Hydraulic Engineering Group

Wave Impacts on Vertical Breakwaters

final report graduation project

H.A.Th. Vink
May 1997

under supervision of:

prof. drs. ir. J.K. Vrijling
professor of hydraulic engineering

prof. ir. K. d'Angremond
professor of coastal engineering

prof. dr. ir. F.B.J. Barends
professor of groundwater mechanics

dr. ir. H.A. Dieterman
associate professor of dynamics

No branch of engineering science relies so much upon experience, especially upon the experience gained from disasters, such as that of marine defence works. Nor we lack of disaster examples.

O. Bernardini (1901)

Preface

This is the final report of the graduation project of H.A.Th. Vink. Writing this Master's thesis has been a part of my study Civil Engineering at the Delft University of Technology. Over the past nine months I have been working on a graduation project concerning wave impacts on vertical breakwaters. I have had a *smashing* time.

During my graduation project I have had the opportunity to meet both European and Japanese top-researchers on the subject of (vertical) breakwaters. These meetings have been extremely interesting and instructive. One of these meetings yielded a surprising result as you can see on the last page of this report.

At the beginning of this report, but at the end of my graduation project, I would like to thank everyone who has guided me over the past nine months: (scientific) staff members of Rijkswaterstaat, of the Delft University of Technology and other European (and Japanese) research institutes. I would especially like to thank the chairman of my M.Sc. thesis-committee, prof. drs. ir. J.K. Vrijling, who has supported me enthusiastically and has given me the opportunity to look beyond the Dutch border, as well as the other members: prof. ir. K. d'Angremond, prof. dr. ir. F.B.J. Barends and dr. ir. H.A. Dieterman.

My brother, Ard, ought not to be forgotten.

Dear reader, I hope you will enjoy reading this report.

Delft, May 1997

Heino Vink

Contents

C ANALYSIS OF DIFFERENT TYPES OF WAVE IMPACT LOADS ON A VERTICAL BREAKWATER AND CONCLUSIONS

List of figures

List of tables

List of symbols

Parameter	Dimension	SI-unity	Description
a	L	m	eccentricity of a spring
A_i	L	m	constant used in the modal analysis
	-	rad	
A_i	L	m	factor used to determine eigensolution of a mass-spring
	-	rad	model
b_i	$ML^{-2}T^{-2}$	N/m^3	bed constant
b	L	m	half the width of a breakwater (in x-direction)
$b(t)$	L	m	added function
B_b	L	m	width of rubble berm, at the toe of the wall of a vertical breakwater
B_c	L	m	width of the vertical breakwater (in x-direction)
B_{eff}	L	m	effective width of a vertical breakwater
B_{rel}	L	m	part of the berm width which influences the effective water depth
A_i	L	m	factor used to determine eigensolution of a mass-spring
	-	rad	model
B_i	LT^{-1}	m/s	constant used in the modal analysis
	T^{-1}	rad/s	
c	$MT^{-2}L^{-1}$	N/m^2	cohesion
c	LT^{-1}	m/s	propagation celerity of waves
c_c	LT^{-1}	m/s	velocity of a compression wave (sound) in a structure
$c_{mixture}$	LT^{-1}	m/s	velocity of sound in an air-water mixture
c_w	LT^{-1}	m/s	velocity of sound in water
c_s	-	-	slamming coefficient
c_s	LT^{-1}	m/s	velocity of waves in soil
C_i	L	m	factor used to determine eigensolution of a mass-spring
	-	rad	model
C_d	$MT^{-1}L^{-4}$	Ns/m^5	damping coefficient
C_k	$MT^{-2}L^{-4}$	N/m^5	stiffness coefficient
C_m	ML^{-4}	Ns^2/m^5	inertial coefficient
d	L	m	water depth
d	L	m	water depth at the front wall of a vertical breakwater
$d_{i\ (hor,\ ver)}$	MT^{-1}	Ns/m	friction coefficient
	MLT^{-1}	Ns/rad	
d_b	L	m	the breaking depth measured from still water level (SWL)
d_c	L	m	depth of the vertical breakwater in the foundation
d_m	L	m	effective water depth
d_s	L	m	water surface elevation during breaking directly at a vertical wall
D	L	m	the average space between the front of the water and the vertical breakwater and/or the equivalent diameter of an air pocket at its initial stage
e	-	-	void ratio (volume voids / volume grains)
e	L	m	eccentricity
E	-	-	matrix of eigenvectors
E_{ap}	MLT^{-2}	J/m	transferred energy to an air pocket
E_c	$MT^{-2}L^{-1}$	N/m^2	elasticity modulus of a structure

E_s	$MT^{-2}L^{-1}$	N/m^2	elasticity modulus of the soil
E_w	MLT^{-2}	J/m	available incident wave energy
f or f_i	T^{-1}	s^{-1} (= Hz)	(wave) frequency
F or $F(t)$	MLT^{-2}	N	force
F_b	MT^{-2}	N	force as a result of buoyancy
$F_h(t)$	MT^{-2}	N/m	horizontal force (time function) on a vertical breakwater per linear meter
$F_{h,max}(t)$	MT^{-2}	N/m	maximum horizontal wave force per linear meter
F_{max}	MLT^{-2}	N	maximum force in a spring
$F_{h,q}$	MT^{-2}	N/m	quasi-static horizontal force per linear meter
F_f	MLT^{-2}	N	friction force
$F_{foundation}$	MLT^{-2}	N	horizontal force in the foundation
F_n	MLT^{-2}	N	normal force on the foundation
F_r	MT^{-2}	N/m	response force
F_u	MLT^{-2}	N	uplift force
F_0	MLT^{-1}	Ns	factor to determine magnitude delta-function
$\underline{F}(t)$	MLT^{-2}	N	load, vector notation
	ML^2T^{-2}	Nm	
g	LT^{-2}	m/s^2	gravitational acceleration (9.81 m/s^2)
G_s	$MT^{-2}L^{-1}$	N/m^2	shear modulus of the soil
h	L	m	half the height of a breakwater
h_b	L	m	height of the berm above seabed
h_f	L	m	exposed height on the vertical breakwater
h_m	L	m	waterdepth of the pressure with a peak intensity
h_s	L	m	water depth at the toe of the vertical breakwater / mound
h_r	L	m	depth of the rubble core beneath the vertical breakwater to the seabed
H	L	m	(local) wave height, from trough to crest
H_b	L	m	breaker height at the front wall of the vertical breakwater
$H_{b,max}$	L	m	maximum breaker height at the front wall of the vertical breakwater
H_c	L	m	height of the vertical breakwater (in z-direction)
H_{max}	L	m	maximum wave height in a record
H_s	L	m	significant wave height, average of highest one-third of the wave heights
i_c	-	-	reduction factor Brinch Hansen
i_q	-	-	reduction factor Brinch Hansen
i_γ	-	-	reduction factor Brinch Hansen
I	L^4	m^4	moment of inertia
I_w	MT^{-1}	Ns/m	total force impulse
I_{dyn}	MT^{-1}	Ns/m	dynamic component of the force impulse
$I_{dyn,r}$	MT^{-1}	Ns/m	dynamic component of the force impulse concerning the rise time
I_{stat}	MT^{-1}	Ns/m	static component of the force impulse
I_{max}	MT^{-1}	Ns/m	maximum moment of a wave impact
k	-	-	mass parameter
$k_{i\,(i,A)}$	MT^{-2}	N/m	spring constant
	MLT^{-2}	N/rad	
k	L^{-1}	1/m	wave number ($k = 2\pi/L$)
k	-	-	(slamming) coefficient
k_a	LT^{-1}	m/s	factor of importance concerning wave force oscillations of the double peaked impact force

k_r	-	-	factor to take account for the different geometries of load histories in the case of breaking waves
K	MT^{-2}	N/m	stiffness, matrix notation
	MLT^{-2}	N/rad	
K_a	$MT^{-2}L^{-1}$	N/m^2	compressibility modulus of air
$K_{mixture}$	$MT^{-2}L^{-1}$	N/m^2	compressibility modulus of an air-water mixture
K	-	-	reflection coefficient
K_w	$MT^{-2}L^{-1}$	N/m^2	compressibility modulus of water ($2.2*10^9$ N/m^2)
l	L	m	height of a wave front hitting the vertical wall
l	L	m	half the length of a breakwater (in y-direction)
L	L	m	characteristic length; specific length of a block of water (representing a wave) approaching the wall
L	L	m	wave length, in the direction of propagation
L_b	L	m	wave length of the breaking wave
L_c	L	m	length of the vertical breakwater (in y-direction)
L_p	L	m	deep water wave length related to the peak period (T_p)
L_0	L	m	deep water wave length
m	-	-	cotangent of the bedslope
m	ML^{-1}	kg/m	fluid mass involved in breaking process
m_i	M	kg	mass of a vertical breakwater
m_{cai}	M	kg	mass of a caisson breakwater
$m_{geo\ (hor,\ ver)}$	M	kg	geo-dynamic mass
$m_{hyd\ (hor,\ ver)}$	M	kg	hydro-dynamic mass
m_{rel}	-	-	part of the slope of the berm which influences the effective water depth
$m_{tot\ (hor,\ ver)}$	M	kg	total mass
M	ML^{-1}	kg/m	total mass of a breaking wave
M	M	kg	mass, matrix notation
	ML^2	kgm^2	
M	ML^2T^{-2}	Nm	moment
$M_{foundation}$	ML^2T^{-2}	Nm	moment in the foundation
n_i	-	-	scale factor
N_c	-	-	dimensionless constant Brinch Hansen
N_q	-	-	dimensionless constant Brinch Hansen
N_γ	-	-	dimensionless constant Brinch Hansen
p	$MT^{-2}L^{-1}$	N/m^2 (= Pa)	pressure
$p(t)$	$MT^{-2}L^{-1}$	N/m^2	time dependent pressure
$p(z, t)$	$MT^{-2}L^{-1}$	N/m^2	spatial and time dependent pressure
$p_{average}$	$MT^{-2}L^{-1}$	N/m^2	average pressure
p_{atm}	$MT^{-2}L^{-1}$	N/m^2	atmospheric pressure ($1.01325*10^5$ N/m^2)
$p_{max\ (average)}$	$MT^{-2}L^{-1}$	N/m^2	maximum (average) impact pressure
p_u	$MT^{-2}L^{-1}$	N/m^2	uplift pressure (Goda formula)
p^*	-	-	normalised pressure
p_0	$MT^{-2}L^{-1}$	N/m^2	water pressure before a wave impact
p_0	$MT^{-2}L^{-1}$	N/m^2	equilibrium pressure in an air pocket
p_1 , p_2 , p_3	$MT^{-2}L^{-1}$	N/m^2	pressure (Goda formula)
q	LT^{-1}	m/s	absolute velocity of water particles
q	$MT^{-2}L^{-1}$	N/m^2	pressure (Brinch Hansen)
r	L	m	radius of an air pocket
R	L	m	hydraulic radius
R	L	m	radius
R_c	L	m	crest freeboard, level of crest less static water level
R_i	-	-	factor to determine eigenvector
$R(t)$	L	m	time dependent radius of an air pocket

R_0	L	m	equilibrium radius of a sphere
$s_{(max)}$	-	-	(maximum) wave steepness
s_c	-	-	reduction factor Brinch Hansen
s_q	-	-	reduction factor Brinch Hansen
s_γ	-	-	reduction factor Brinch Hansen
t	T	s	time
t_d	T	s	duration of a horizontal wave impact force
t_r	T	s	rise time, generally for horizontal force F_h
t_t	T	s	total duration of a wave impact event
t^*	-	-	normalised time
T or T_i	T	s	wave period
T or $T(t)$	ML^2T^{-2}	Nm	moment
T_m	T	s	the average period of the waves
T_p	T	s	peak period of the waves
T_s	T	s	the significant period of the waves
$T_{0\,(w)}$	T	s	period of the oscillations of an air pocket near a vertical solid boundary
$u_{(h,\,v)}$	LT^{-1}	m/s	flow velocity (horizontal, vertical
$u_i(t)$	L	m	added function in modal analysis
	-	rad	
$\ddot{u}_i(t)$	LT^{-2}	m/s^2	added function in modal analysis
	T^{-2}	rad/s^2	
$\underline{u}(t)$	L	m	added function in modal analysis, vector notation
	-	rad	
u_0	LT^{-1}	m/s	velocity of an approaching front of water
v	LT^{-1}	m/s	velocity in Froude number
V	L^3	m^3	volume
$V(t)$	L^3	m^3	time dependent volume of an air pocket
$\dot{V}$	L^3T^{-1}	m^3/s	velocity of volume change of an air pocket
$\ddot{V}$	L^3T^{-2}	m^3/s^{-2}	volume acceleration of an air pocket
V_0	L^3	m^3	equilibrium volume of an air pocket
W	MLT^{-2}	N	weight
x	L	m	x-axis, perpendicular to the front face of the vertical breakwater, $x = 0$ at the front face
x_i	L	m	degree of freedom
	-	rad	
$x_i(t)$	L	m	displacement
	-	rad	
x_{bottom}	L	m	horizontal displacement caisson breakwater bottom
$\underline{x}(t)$	L	m	displacement, vector notation
	-	rad	
$\dot{\underline{x}}(t)$	LT^{-1}	m/s	velocity, vector notation
	T^{-1}	rad/s	
$\ddot{\underline{x}}(t)$	LT^{-2}	m/s^2	acceleration, vector notation
	T^{-2}	rad/s^2	
$\hat{\underline{x}}_i$	L	m	eigenvector
	-	rad	
y	L	m	y-axis, longitudinal direction of the vertical breakwater, $y = 0$ in the middle of a section
z	L	m	z-axis, vertical direction, positive upwards, $z = 0$ at the seabed

Parameter	Dimension	SI-unity	Description
α	-	rad or deg	slope angle of the seabed or berm
α	-	rad or deg	angle of contact of an air pocket
α	-	-	air content
α	-	-	parameter Weibull distribution
α^*	-	-	coefficient (extended Goda formula)
α_1, α_2, α_3	-	-	coefficients (Goda formula)
α_I (α_{I0} , α_{I1})	-	-	impulsive coefficient (extended Goda formula)
β	-	rad or deg	direction of the wave propagation relative to the normal to breakwater alignment
β	-	rad or deg	angle of a wave front hitting a vertical wall
β^*	-	rad or deg	equivalent angle of a wave front hitting a vertical wall
β_0	-	rad or deg	adapted angle of a wave front hitting a vertical wall
β	-	-	parameter Weibull distribution
γ	-	-	constant of Poisson
γ	-	-	parameter Weibull distribution
γ_s	$ML^{-2}T^{-2}$	N/m^3	weight of soil
$\gamma_{saturated}$	$ML^{-2}T^{-2}$	N/m^3	weight of saturated soil
γ_w	$ML^{-2}T^{-2}$	N/m^3	weight of water (10.06 kN/m^3)
δ	-	rad or deg	tangential angle to the cord of a curved wave front
$\delta(t)$	T^{-1}	s^{-1}	delta function
δ_1,δ_{11},δ_2,δ_{22}	-	-	coefficients (extended Goda formula)
Δp	$MT^{-2}L^{-1}$	N/m^2	change of pressure
Δt	T	s	time interval
ΔV	L^3	m^3	change of volume
ε	-	-	ratio of the velocity of the a wall to the velocity of the incoming water
η^*	L	m	elevation (Goda formula)
θ	ML^2	kgm^2	mass moment of inertia
θ_{cai}	ML^2	kgm^2	mass moment of inertia of the caisson
θ_{geo}	ML^2	kgm^2	geo-dynamic mass moment of inertia
θ_{hyd}	ML^2	kgm^2	hydro-dynamic mass moment of inertia
θ_{tot}	ML^2	kgm^2	total mass moment of inertia
κ_a	-	-	air thickness coefficient
κ_{a0}	-	-	minimum air thickness coefficient
κ_I	-	-	impact height coefficient
κ_m	-	-	added mass correction factor
μ	-	-	friction coefficient
ν	-	-	Poisson's ratio
ξ	-	-	Irribarren number
ρ	ML^{-3}	kg/m^3	mass density of fresh water (998 kg/m^3)
$\rho_a(t)$	ML^{-3}	kg/m^3	time dependent mass density of air
ρ_c	ML^{-3}	kg/m^3	mass density of concrete
ρ_f	ML^{-3}	kg/m^3	mass density of the fill
ρ_s	ML^{-3}	kg/m^3	mass density of the soil
ρ_c	ML^{-3}	kg/m^3	mass density of a construction
$\rho_{mixture}$	ML^{-3}	kg/m^3	mass density of an air-water mixture

ρ_w	ML^{-3}	kg/m^3	mass density of sea water (1025 kg/m^3)
σ	MLT^{-2}	N/m^2	pressure
$\sigma_{foundation}$	MLT^{-2}	N/m^2	pressure in the foundation
(min, max)			
(hor, ver)			
φ	-	rad or deg	angle of internal friction of the soil
ϕ	L^2T^{-1}	m^2/s	velocity potential
ϕ_i	-	rad or deg	phase
ω or ω_i	T^{-1}	rad/s	radian frequency ($\omega = 2\pi/T$)
ω_d	T^{-1}	rad/s	radian frequency of the damped eigenoscillation
ω_0	T^{-1}	rad/s	radian frequency eigenoscillation

Abstract and outline of this report

The need for coastal structures, such as breakwaters, at great water depths is rapidly increasing as a result of the increasing draught of large vessels and off-shore land reclamations which can, for instance, be used for the benefit of the expansion of harbours and related industrial activities. In water depths greater than approximately 10 m vertical breakwaters may be the best alternative compared to ordinary rubble mound breakwaters, in terms of performance, total costs, environmental aspects, construction time and maintenance.

However, these breakwaters with plane vertical front walls can be exposed to enormous hydraulic loads, such as wave impacts. Wave impacts are dynamical hydraulic loads with, for instance, a very short duration (in the order of magnitude of ms) and a very high peak force which can exceed the quasi-static wave load on a vertical breakwater more than 10 times. As it is described in chapter 1 *"Introduction"*, this report contains the reflection of a research which has been performed on the effect of wave impact loads on the stability of vertical breakwaters. This Master's thesis is divided into three parts:

A Wave impact loads on vertical breakwaters

In chapter 2 *"Hydraulic loads on vertical breakwaters"* different types of quasi-static and wave impact loads are described. Three types of wave impact loads can be distinguished depending on the amount of trapped air between the breaking wave and the plane vertical front wall of a breakwater. In chapter 3 *"Wave impact pressures"*, chapter 4 *"Wave impact forces and momentum"* and chapter 5 *"Special attention to wave impacts with a trapped air pocket"* different formulae are presented which can be used to calculate the characteristics of wave impact loads on vertical breakwaters. In chapter 6 *"Vertical breakwater design formula and wave impacts"* short attention is being paid to the calculation of wave (impact) loads according to the most widely used prediction method for wave (impact) pressures on vertical breakwaters.

B Derivation of models which describe the dynamical behaviour of a vertical breakwater

In chapter 7 *"Derivation of an analytical mass-spring model of a vertical breakwater"*, in chapter 8 *"Derivation of a mass-spring-dashpot TILLY model of the vertical breakwater"* and in chapter 9 *"Analysis of the structure and foundation parameters of the vertical breakwater"* models which can be used to describe the dynamical behaviour and stability of a vertical breakwater which is exposed to wave impacts are treated. A lot of attention is being paid to the influence of the magnitude of the different dynamical properties (mass, stiffness and damping) of such a model.

C Analysis of different types of wave impact loads on a vertical breakwater and conclusions

The *"Analysis of different types of wave impact loads on a vertical breakwater"* is reflected in chapter 10. *"Conclusions and recommendations"* can be found in chapter 11. It can be concluded that the stability of a vertical breakwater against wave impacts entirely depends on the type of wave impact load which is to be expected (i.e. rise time, total duration, magnitude of the peak force, the amount of trapped air) and the dynamical properties of the vertical breakwater and its foundation soil (mass, stiffness and damping). The maximum peak force of a wave impact does not necessarily induce the maximum dynamical response of a vertical breakwater. Wave impacts with relatively low peak forces and long total durations (relative to the eigenperiod(s) of a vertical breakwater, double peaked wave impact forces and wave impacts followed by low frequency force oscillations due to large trapped air pockets seem to be more dangerous for the stability of a vertical breakwater. The amount of momentum is one of the governing properties of a wave impact load concerning the response and stability of a vertical breakwater. The suggestion commonly found in the literature that wave impacts are totally not significant and should not be used for the design of vertical breakwaters could not be confirmed.

A dynamical analysis of the behaviour of a vertical breakwater by means of a mass-(elasto-plastic)-spring-dashpot computer model should become a necessary part of the design process of vertical breakwaters which are exposed to breaking wave loads. The characteristics of the wave impact loads to be expected and the foundation characteristics should be obtained form large scale hydraulic model tests and site investigations.

1 Introduction

1.1 General introduction

Breakwaters and related marine structures can have several functions. They are primarily built to give protection against wave attack on ship moorings, manoeuvring areas, port facilities and adjoining areas of land (breakwaters can serve as a coastal protection). Other functions of breakwaters are that they can serve to reduce the amount of dredging required in a harbour entrance and that they can guide currents in a harbour entrance channel or currents along a coast.

Harbour breakwaters and related marine structures[1] can be divided into two different categories:

- rubble mound structures with permeable and rough side slopes and
- vertical (monolithic, or caisson type) structures which are impermeable and solid with vertical or very steep faces as can be seen in figure 1.1 where three different types of vertical breakwaters are sketched: a vertical caisson breakwater which is placed on a thin (rubble mound) foundation layer, a caisson breakwater which is placed on a thick rubble mound foundation (a vertical composite caisson breakwater) and a caisson breakwater which is placed on a thin (rubble mound) foundation layer and which is armoured by a protection (artificial as well as natural armour units are possible). A caisson is in fact a hollow - in most cases - concrete box which is filled with sand after it has been placed at the right spot.

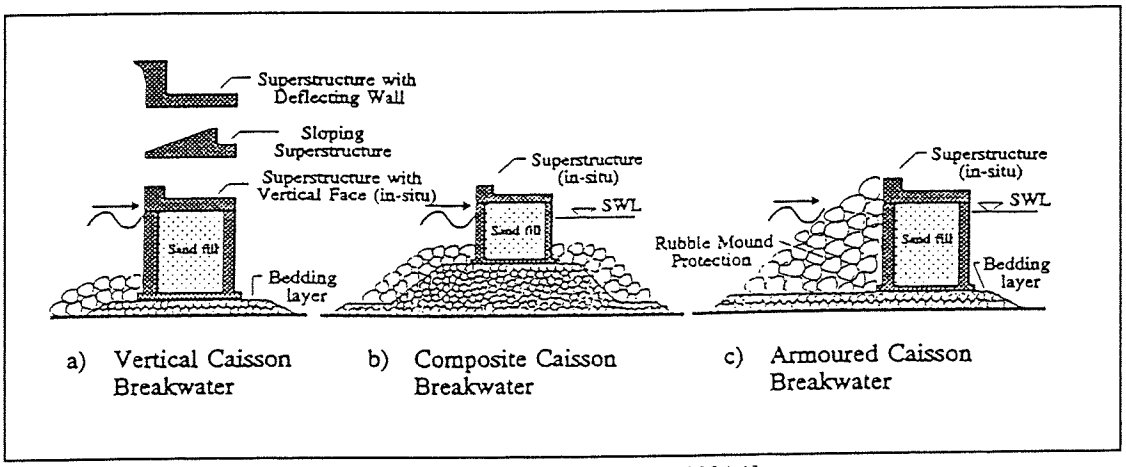

fig. 1.1 Three different types of vertical breakwaters [OUMERACI (1994a)]

A rubble mound breakwater is usually the most economical option if a breakwater has to be constructed in shallow water (i.e. water depths which are approximately smaller than 10 m). Rubble mound breakwaters use more material per cross-section than vertical breakwaters but due to their relative simple construction method they prove to be cheaper than vertical breakwaters. The advantages of rubble mound breakwaters compared with vertical breakwaters are:

- the use of natural material (however, this is increasingly becoming a disadvantage as a result of environmental considerations)
- the fact that they give less wave reflection (this will yield a reduced impact on the adjacent beaches of a breakwater and on the navigation of ships near a breakwater) and
- the fact that they can potentially have a lower crest elevation (this will yield a reduced impact on the offshore view).

[1] This study only deals with vertical breakwaters

However, the recent need of breakwaters at greater depths has made the use of rubble mound breakwaters more prohibitive. Breakwaters at greater depths are for instance needed to suit the increasing draught of large vessels. The recent development of off-shore land reclamations for harbours and their related industries in deep water (i.e. a water depth which is approximately larger than 10 m) does also play an important role in the increasing demand for vertical breakwaters as will be indicated by the following example.

The coastal zone is the most densely populated area in the world. Almost 80% of the world's population lives in the coastal zone. The need for land in the coastal zone is still increasing because of the fact the world's population is still growing. Not only more living space is needed in the coastal zone but also land for the extension of economical activities such as harbours and their related industries. The port of Rotterdam (the Netherlands) has almost reached it economical capacity and has new development plans. One of these plans is the reclamation of new land, the extension of the current Maasvlakte, the so called Maasvlakte 2.

The water depth at the location where this land reclamation is planned to be carried out varies in the range of 15 to 20 m, which is considered to be deep water. As has been mentioned before, vertical coastal structures, such as breakwaters are the most economical at deep water. Vertical coastal structures can be used at Maasvlakte 2 both as breakwaters and as an essential part of the coastal defence of the reclamated area.

Vertical breakwaters increasingly become of economical interest as the water depth increases. At deep water, the reduce of material of a vertical breakwater per cross-section is dominating the rather expensive construction methods. The advantages of vertical breakwaters compared with rubble mound breakwaters are:

- that vertical breakwaters occupy a smaller part of the seabed (this will result in a smaller impact on the flora and fauna in the neighbourhood of a vertical breakwater),
- that less material quantities are needed (less quarry has to be used resulting, for instance, in a smaller water turbidity during the construction of a breakwater),
- that re-use of dredging material for filling the caisson cells is possible (this will yield less land quarrying and less offshore sediment disposal, which are advantages from an environmental point of view),
- the savings in construction time when a breakwater is built at deep water,
- that a safer close navigation is possible (a vertical breakwater is better visible and underwater obstacles are reduced),
- that vertical breakwaters can potentially be removed ("fill out" and float the caissons),
- the reduced environmental impact when a vertical breakwater is constructed (for instance: less trucks are needed, there will be less air pollution and less water turbidity) and
- the less need of maintenance.

The last advantage of a vertical breakwater compared with a rubble mound breakwater is only valid if a vertical breakwater is well designed. A design of a vertical breakwater of poor quality has got a high probability of failure. Vertical breakwaters are extremely sensitive to foundation failure, such as slip, settlements, sliding or failure of the monolithic structure itself. This is a first indication of the fact that the design of a vertical breakwater may be more complicated than the design of an ordinary rubble mound breakwater. There have been numerous vertical breakwater failures in the thirties of this century. Because of this fact, vertical breakwaters have almost been abandoned except in countries like Italy and Japan. However, a number of important (scientific) developments which might promote the revival of vertical breakwaters have taken place in the last decades and nowadays vertical breakwater are becoming more and more of interest due to the increasing draught of vessels and off-shore land reclamations in deep water as has been mentioned before. Oumeraci [OUMERACI (1994)] has reviewed and analysed different vertical breakwater failures. The most important reasons which have led to failures of vertical breakwaters are described in figure 1.2.

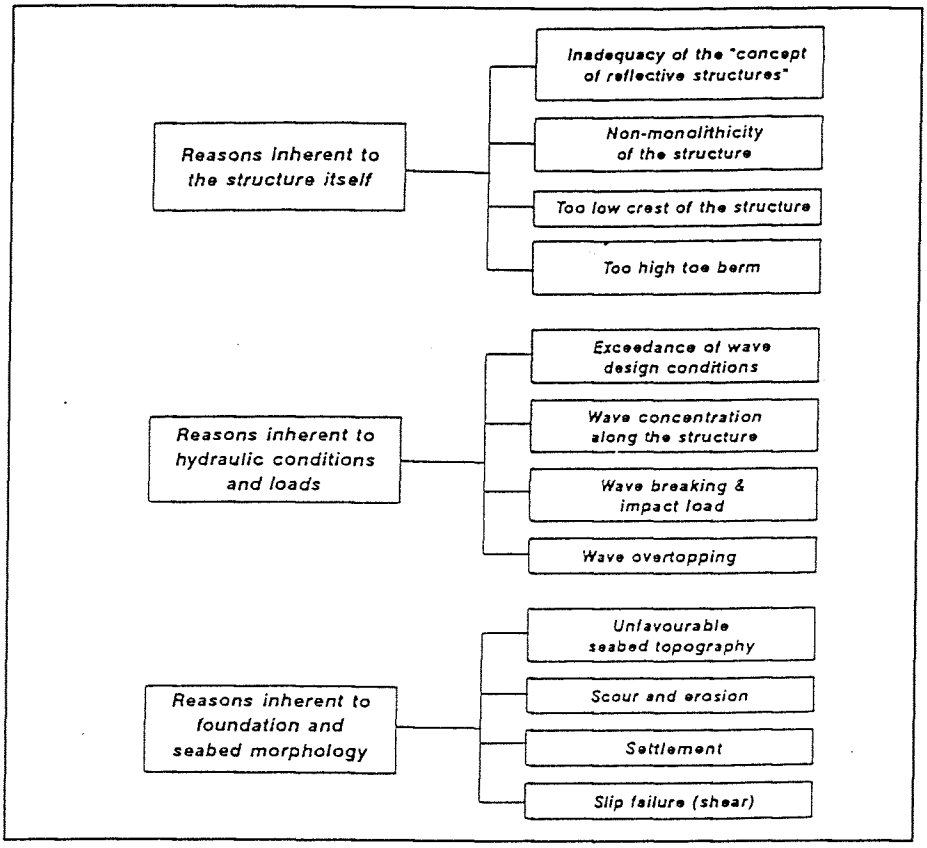

fig. 1.2 Reasons for the failures of vertical structures [OUMERACI (1994)]

The study which is presented in this report deals with wave impacts on vertical breakwaters. Wave impacts are dynamical hydraulic loads with, for instance, a very short duration (in the order of magnitude of ms) and a very high peak force which can exceed the quasi-static wave load on a vertical breakwater more than 10 times. Wave breaking and impact loads on a vertical breakwater can, according to figure 1.2, be a reason of the failure of vertical breakwaters. "Wave breaking and breaking clapotis represent the most frequent damage source of the disasters experienced by vertical breakwaters" writes Oumeraci [OUMERACI (1994)] in his paper which deals with a review and analysis of vertical breakwater failures. Different hydraulic engineers claim that wave impacts are of no significance for the stability of vertical breakwaters, many others claim the opposite. In this graduation project at the faculty of Civil Engineering at the Delft University of Technology, I will try to find an answer to the following general question:

"Are wave impacts important for the stability of vertical breakwaters?"

Several failure modes of vertical breakwaters can be distinguished. These different failure modes are sketched in figure 1.3. The main modes of failure of vertical breakwaters can be divided into two categories: overall failure modes and local failure modes. The failure mechanisms of vertical breakwaters which have been studied in this gradation project are overall failure modes, these are denoted below and considered to be the relevant failure mechanisms of vertical breakwaters which are exposed to wave impacts:

- sliding of a vertical breakwater over its rubble mound foundation,
- overturning of a vertical breakwater and
- exceeding of the bearing capacity of the foundation soil of a vertical breakwater (which will lead to settlements and probably to slip failure of the foundation).

Seaward tilt of a vertical breakwater is neglected in this study. Local failure modes, like the ones which are presented in figure 1.3 as well as for instance rupture of the concrete caisson due to high wave impact pressures are neglected in this study. In this respect it must be stressed that the resultants of these wave impact pressures - which are forces - and the positions of these wave impact forces relative to the centre of gravity of vertical breakwaters are important for overall stability calculations. The actual pressures on the vertical breakwater are in fact important for the calculations of more local failure mechanisms such as rupture of the plane vertical concrete front wall of a breakwater.

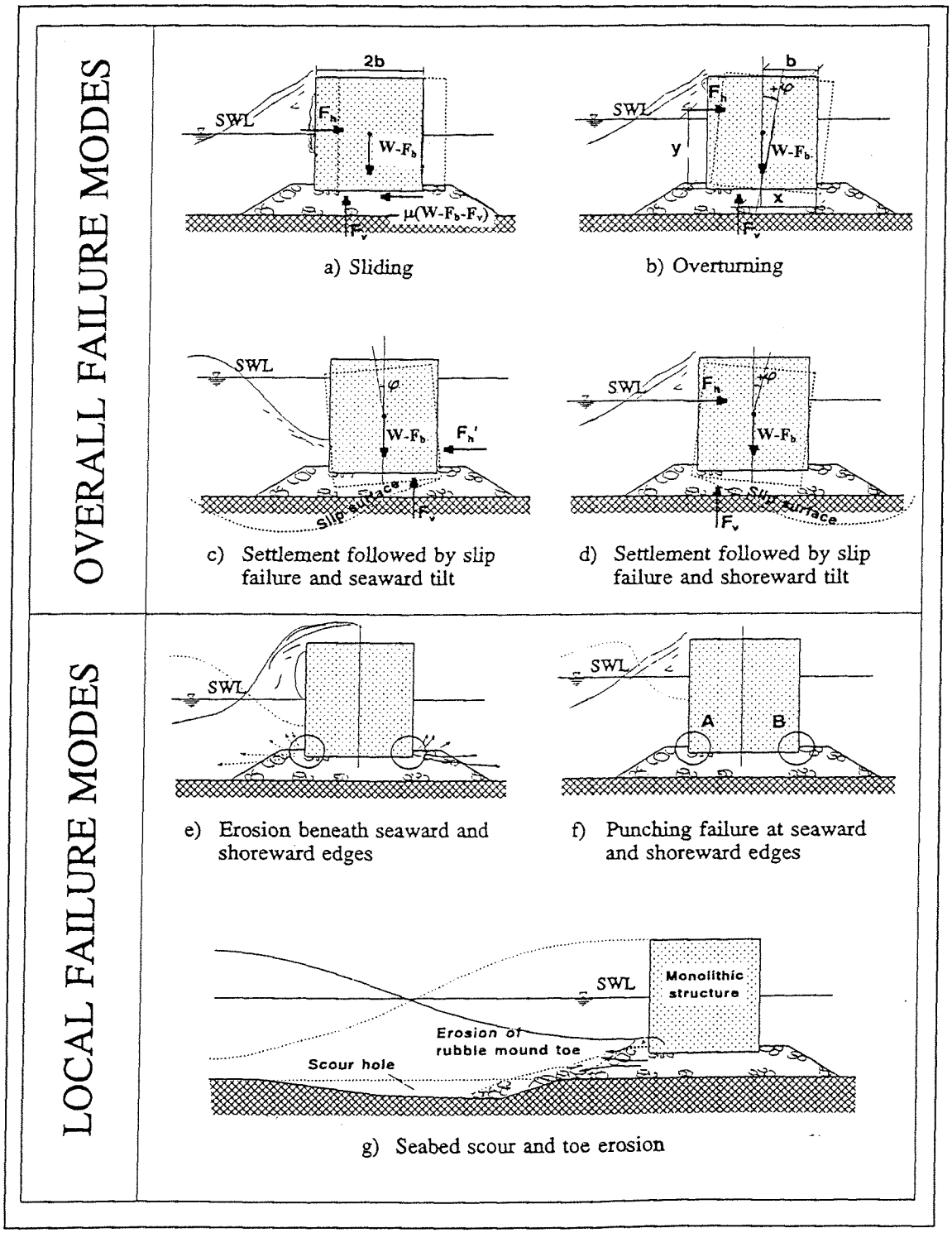

fig. 1.3 Main modes of failure of vertical breakwaters [OUMERACI (1994a)]

1.2 Definition of the problem and the purpose of this graduation project

"It has generally been accepted that dynamic loads can be very important, but it has been argued that many structures are substantially un-affected by such short duration, high intensity loads. Schmidt et al. [SCHMIDT et al. (1992)] remind us that despite more than 80 years of research work on wave impact loads on vertical structures subject to breaking waves, there are two basic attitudes related to the role of wave impact loadings in the design of such structures. The **first** attitude simply assumes that impact pressures (or forces) are not important and thus should not be adopted in the design of vertical structures. The **second** attitude is to skip the problem of evaluating the design impact load by assuming that a structure can be designed in such a way that impact pressures (or forces) will not occur" [ALLSOP et al. (1996)]. However, these two aforementioned attitudes - more or less neglecting the effect of wave impacts on the stability of for instance vertical breakwaters - seem to be very risky, especially because of the fact that vertical breakwaters can be very expensive and important for the safety and serviceability of harbours and coastal zones. Therefore, a different approach of the problem of wave impacts on vertical breakwaters will be treated in this study.

In this study it will be tried to find an answer to the following general question which has been mentioned before in section 1.1:

"Are wave impacts important for the stability of vertical breakwaters?"

To find an answer to this question an extensive study of literature has been carried out and a **third** approach of the problem of the influence of wave impact loads on the stability of vertical breakwaters is pursued. A dynamic analysis of a vertical breakwater, its foundation and the applied wave impact loads has been carried out. For the benefit of this dynamical analysis a mass-(elasto-plastic)spring-dashpot computer model of a vertical breakwater which is exposed to wave impacts has been developed. It ought to be stressed that stability problem of caisson breakwaters which are exposed to wave impacts is a:

- purely dynamical problem (for instance the inertia of a vertical breakwater is important) and
- a multidisciplinary problem requiring and contributions from a number of disciplines (soil mechanics, fluid mechanics (hydrodynamics), structural dynamics, etc.) for its solution.

The purpose of this study is to find an answer to the above mentioned general question. However, it seems advisable to divide this question into the following sub-questions:

- Is there one type of wave impact, or is it possible to distinguish different types?
- If there are different types, which aspects or characteristics of these different types of wave impacts are important for the stability of a vertical breakwater and which are not?
- What is the magnitude of wave impact loads and how is this magnitude related to the duration of the wave impact load?
- What is the influence of the foundation on the dynamical behaviour of a vertical breakwater which is exposed to wave impacts?

In this study a relatively simple mass-(elasto-plastic)-dashpot computer model of a vertical breakwater will be used as a starting step to find an answer to some of these above mentioned questions. However, such a simple model may help to a better understanding of the relative effect of the influencing dynamical properties of the vertical breakwater and its foundation, as well as the effect of the wave impact load and its characteristics.

The answers to the above mentioned questions will be given throughout the whole report. A summary of these answers can be found at the end of the report in chapter 11, where the most important results, conclusions and recommendations of this graduation project are discussed.

1.3 Framework

This Master's thesis has been written as a part of my study Civil Engineering at the Delft University of Technology. My graduation project, which deals with wave impacts on vertical breakwaters, does fit within the framework of a European research programme on vertical breakwaters. This research programme is a part of the project Marine Science and Technology (MAST III), PRObabilistic design of VERtical BreakwaterS (PROVERBS). This research programme is sponsored by the European Union.

This graduation project has among other things been carried out in co-operation with: projectorganisatie Maasvlakte 2 and Rijkswaterstaat. These two organisations are closely involved in the land reclamation of the port of Rotterdam and the design of coastal structures such as vertical breakwaters. At this moment the plans for the land reclamation Maasvlakte 2 are developed and the improvement of the knowledge about the dynamical behaviour and the stability of vertical coastal structures which are exposed to waves and wave impacts seems to be essential for a well-considered design.

A

Wave impact loads on vertical breakwaters

trapped air pocket

2 Hydraulic loads on vertical breakwaters

2.1 Introduction

Coastal structures, such as vertical breakwaters, are exposed to different kinds of loads, e.g. hydraulic loads. The magnitude of these hydraulic loads depends among other things on the (hydraulic) boundary conditions near the coastal structure. The different hydraulic boundary conditions, from which the hydraulic loads can be derived, are related. The principal physical relationships between the relevant hydraulic boundary conditions are shown in the diagram of figure 2.1.

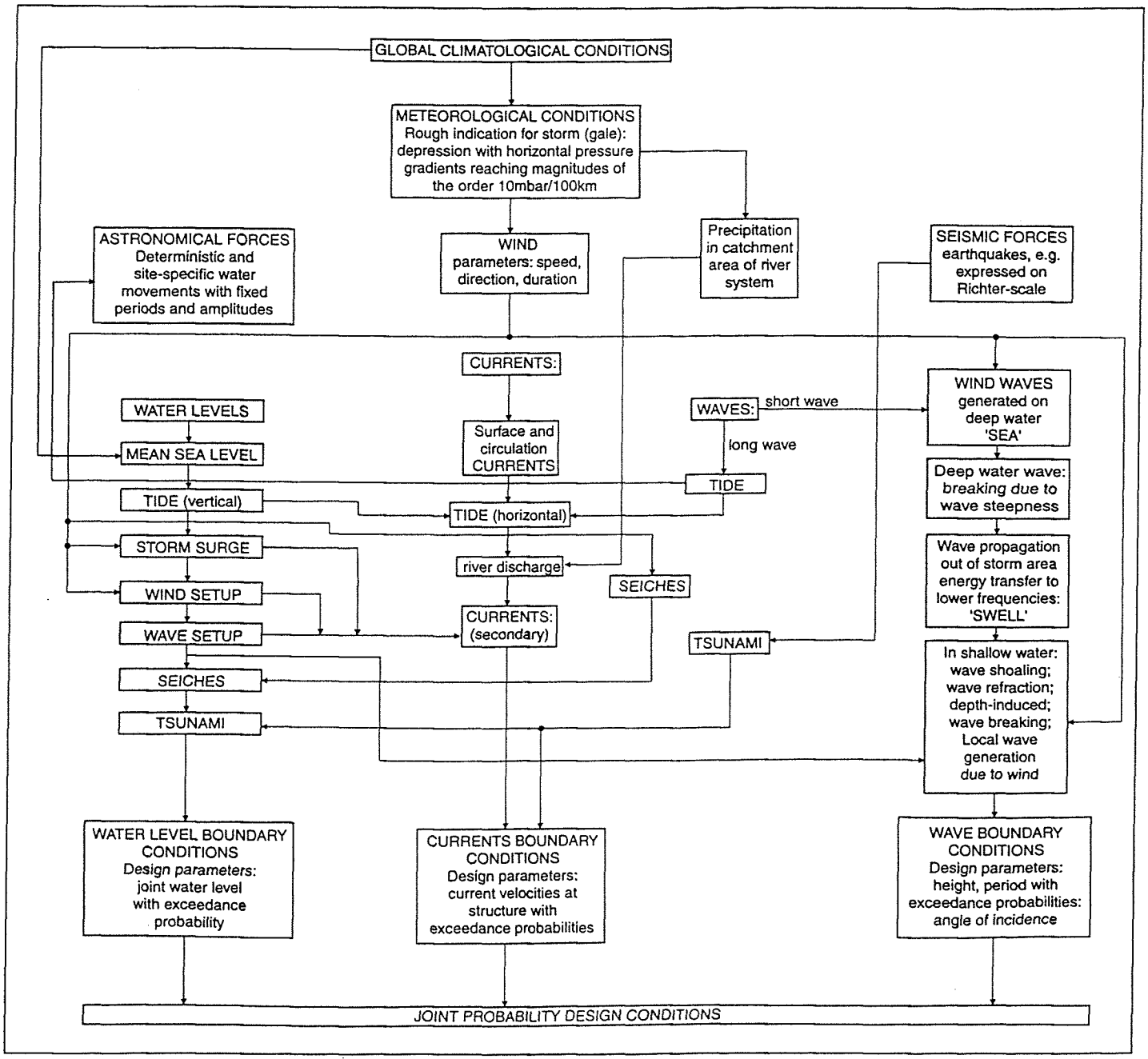

fig. 2.1 Natural hydraulic boundary conditions [CUR/RIJKSWATERSTAAT (1995)]

The magnitude of the hydraulic loads on coastal structures, such as vertical breakwaters, depends on the water level, the currents near the structure and the kind of waves to which the coastal structure is exposed (see figure 2.1). The magnitude of the hydraulic loads on vertical breakwaters, is also influenced by some geometrical factors, such as the geometry of the seabed and the geometry of the coastal structure. Of the three different types of hydraulic loads mentioned above, wave action is in general the most important load on vertical breakwaters. The effect of water level variations and the effect of currents on the stability and dynamical behaviour of a vertical breakwater is neglected in this study.

Waves which travel against a vertical breakwater cause in time varying loads. The magnitude of these loads depends on the wave height, the wave period, the propagation velocity of the wave, the wave angle relative to the alignment of the coastal structure, the bottom geometry and - of course - the size and the shape of the structure surface on which the wave pressures or forces are working. It is often convenient to treat pressures or forces (integrated pressures) which act on vertical breakwaters under wave action in two categories [ALLSOP et al.(1996)]:

- **Quasi-static, or pulsating wave loads**
  Quasi-static or pulsating wave loads change relatively slowly, varying at rates of the same order of magnitude as the wave crest. Traditionally, quasi-static loads are considered for the design of vertical structures, neglecting the effect of shock forces induced by waves breaking directly at the structure. Two principal quasi-static forces may be considered here.
  1. In the first, a wave crest impinges directly against the structure applying a hydro-static pressure difference. The obstruction of the energy of the wave causes the wave surface to rise up the wall, increasing the pressure difference across the wall. The net force is approximately proportional to the wave height, and can be estimated using relatively simple methods.
  2. The second case is the opposite of that above, arising as the wave reflects back from the structure, inducing a net negative force or suction on the wall. Again the magnitudes of the forces are relatively low, and the process is relatively easy to predict.

- **Dynamical, impulsive or impact wave loads**
  Dynamical, or wave impact forces are caused by the special conditions that arise where a wave breaks onto the structure. Impact pressures associated with breaking waves are of substantially greater intensity than pulsating pressures, but are of shorter duration. The magnitude of impulsive or impact wave forces and the duration of these forces depends among other things on the type of wave that breaks onto the structure. The influence of these wave impacts on the dynamical behaviour of vertical breakwaters and its stability (against e.g. sliding, overturning or failure of the foundation) is the subject of this study.

Wave action on vertical breakwaters does not only cause horizontal quasi-static or wave impact forces but also (in time varying) uplift forces which work against the bottom slab of a vertical break-water. A definition sketch of different forces on a vertical breakwater is given in figure 2.2.

This study mainly deals with wave impact forces on vertical breakwaters. Only the in time varying forces are assumed to be of importance when the dynamical behaviour of a vertical breakwater exposed to wave impacts is investigated. In this study, the in time varying force on the vertical breakwater is the horizontal wave impact force. All other forces which have been indicated in figure 2.2 are assumed to be constant and do - in their way - not influence the dynamical behaviour of a vertical breakwater. Thus, the uplift force is assumed to be constant as well in this study, see section 2.5. However, the loads which are assumed to be constant in this study cannot be neglected when the stability of the vertical breakwater against wave impacts forces is investigated. The buoyant force, for example, influences the stability against sliding because of the fact that it reduces the net weight of the vertical breakwater.

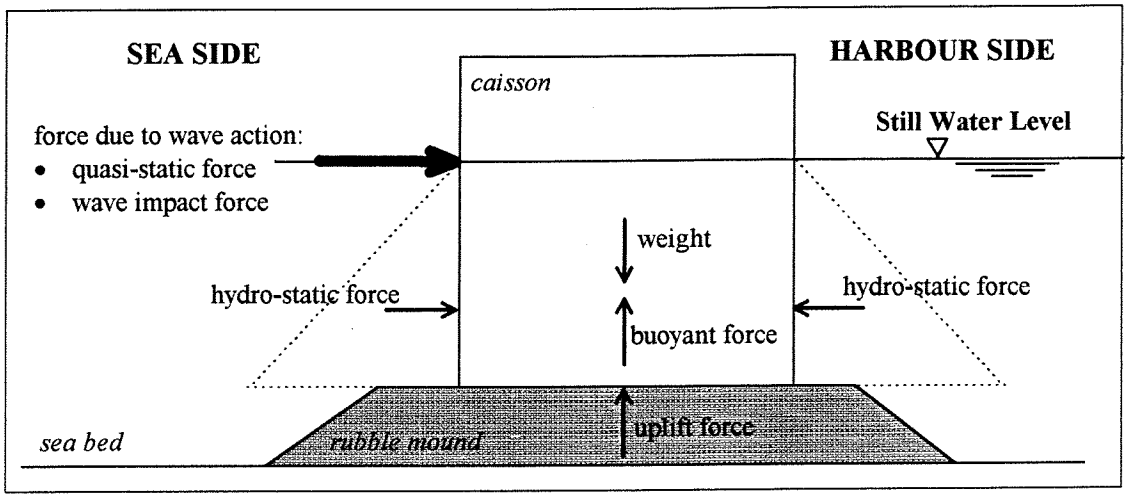

fig. 2.2 Definition sketch of forces on a vertical (composite) breakwater

Quasi-static wave loads are neglected in this study when the dynamical behaviour and the stability of a vertical breakwater against wave impacts is investigated. The breakwater which will be used for the dynamical analysis in chapter 7 to 10 is assumed to be able to withstand the quasi-static wave forces. This assumption is in accordance with the nowadays most widely used prediction method for wave forces on vertical walls. This design formula for vertical breakwaters, the Goda formula [GODA (1985)], is extended by Takahashi et al. [TAKAHASHI et al. (1993)] to include the (extra) load of breaking waves on the vertical front wall of a breakwater, see chapter 6. For breaking wave conditions against vertical breakwaters Takahashi et al. [TAKAHASHI et al. (1993)] propose to enlarge the pressures due to the quasi-static wave loads calculated by the use of the Goda formula by means of a coefficient. Thus, if a vertical breakwater is able to withstand wave impacts forces calculated according to the method of Takahashi et al. [TAKAHASHI et al. (1993)], it will surely be able to withstand quasi-static wave forces calculated according to the Goda formula because of the fact that the quasi-static wave forces will always be less according to the combined method of Goda [GODA (1985)] and Takahashi et al. [TAKAHASHI et al. (1993)].

This chapter gives among other things a general overview of different types of waves which are the cause of these two above mentioned categories of horizontal forces due to wave action on vertical breakwaters: quasi-static wave forces and wave impact forces. In section 2.2, an overview of different types of waves, which cause quasi-static forces on vertical breakwaters, is given. Wave impacts on vertical breakwaters can be caused by some of the waves which are described in section 2.2. In section 2.3, a decision tree is given that describes whether particular structures or sea states will cause a risk of impulsive wave conditions. In section 2.4 a broad - practical - outline of different types of waves impacts is given. Wave impacts will be treated more extensively in chapter 3 ("Wave impact pressures) and chapter 4 ("Wave impact forces and momentum"). Finally, in section 2.5 short attention is being paid to uplift forces and pressures on vertical breakwaters.

2.2 Different types of waves which cause quasi-static loads

As it has been mentioned before, hydraulic loads can be distinguished in two main categories, namely: quasi-static loads and dynamical loads. Quasi-static loads have got the same period as the period of the waves which cause these loads. Dynamic loads, for instance wave impacts, have got a very short duration. As an indication: the duration of the wave impact is 10-200 ms but ups and (especially) downs (1 ms) are possible [DELFT HYDRAULICS (1994)]. After a wave impact pressure has appeared, the quasi-static wave pressure remains.

The movements of waves in water with a free fluid surface are dominated by gravitation. These movements will only originate if energy is supplied. Wind is the most important cause of wave generation, but also waves which are generated by sailing vessels may play an important role in hydraulic engineering.

Compared to the average, wave crests have more potential energy related to gravity and wave troughs have less potential energy. A distorted water surface contains not only potential energy related to gravity, but also potential energy which is related to the so called "surface tension". This component is only important if very small waves with an order of magnitude of the amplitude of a few centimetres are considered (the so called capillary waves). In case of waves with large amplitudes and wave periods, the potential energy related to the surface tension is of minor importance than the potential energy related to gravity. Between the areas of high and low potential energy, a continuous exchange of energy takes place by a transformation of potential energy in kinetic energy [DELFT HYDRAULICS (1994)].

Individual waves are characterised by a period (T), a height (H), a propagation velocity (c) and a propagation direction or, in the case of this study, an angle of wave attack relative to the normal to the breakwater alignment (β). It is important to distinguish between the various types of water waves that may be generated and propagated. One way to classify waves is by wave period T (the time for a wave to travel a distance of one wavelength), or by the reciprocal of T, the wave frequency (f).

Non breaking waves on vertical walls cause quasi-static pressures on these walls. The first order linear wave theory gives a first approximation of the quasi-static wave pressure on the vertical front wall of a breakwater.

The expression for the wave pressure is derived from Bernoulli's equation (equation 2.1; rewritten with $z = 0$ at the seabed and $z = h$ at Still Water Level (SWL), the explanation of the different symbols which are used can be found in the list of symbols),

$$p = -\rho g(z-h) - \rho\frac{\partial\phi}{\partial t} - \frac{1}{2}\rho q^2 \qquad (2.1)$$

in which the first term on the right side is the hydro-static pressure. In a linear approximation the third term on the right side is neglected. The equation which describes the quasi-static wave pressure (e.g. on a vertical breakwater) then becomes:

$$p = -\rho g(z-h) + \frac{1}{2}\rho g H\frac{\cosh(z)}{\cosh(kh)}\sin(\omega t - kx) \qquad (2.2)$$

[BATTJES (1993)].

Different types of waves, which are of importance for vertical breakwaters and cause quasi-static pressures according to equation 2.2, are listed below in order of wave period (varying from short to long waves).

- **wind waves**
  Wind waves are by far the largest contribution of energy from the sea to the coastal zone, so it is obvious that pressures or forces generated by wind waves are usually very essential hydraulic loads on coastal structures such as breakwaters (see figure 2.3). As winds blow over water, waves are generated in a variety of sizes from ripples to large ocean waves as high as 30 meters. Wind waves, which are also known as oscillatory waves, are usually defined by their height, length and period (see figure 2.3). The wave height (H) is the vertical distance from the top of the crest to the bottom of the trough. The wave length (L) is the horizontal distance between successive crests. The wave period (T) is the time between successive crests passing a given point. The propagation velocity of waves is defined as: $c = L/T$. As waves propagate in deep water, only the waveform and a part of the energy of the wave move forward; the water particles move in a nearly circular path [CERC (1984)]. Wave impacts, which are described in section 2.4, are derived from these waves. The period of wind waves at sea is in the range of 5 to 15 seconds.

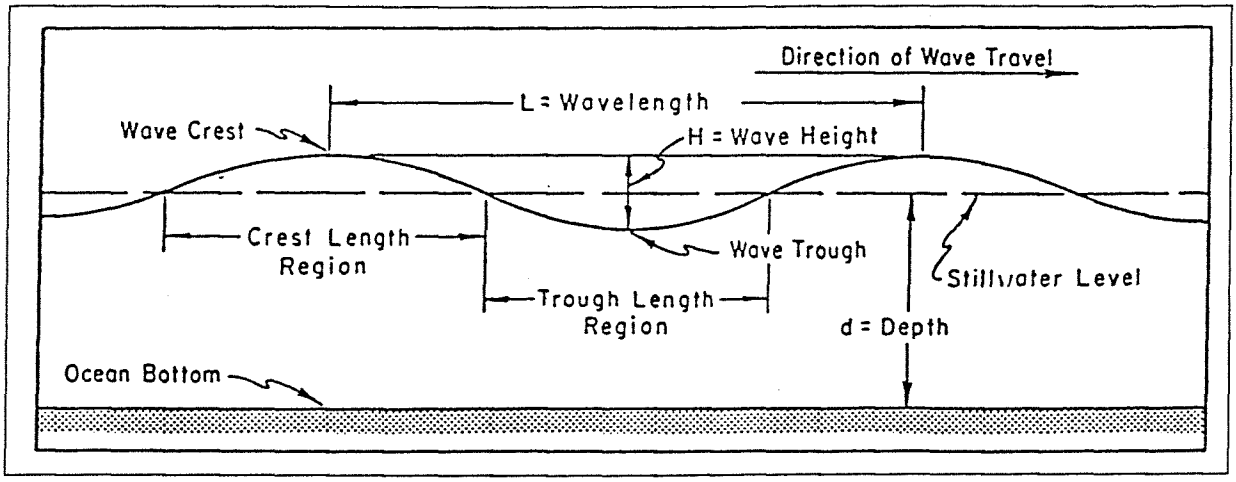

fig. 2.3 Wave characteristics [CERC (1984)]

- **swell**
  Swell are waves which have lengths from 30 to more than 500 times the wave height. They are generated by a distant storm and they may travel through hundreds or even thousands of kilometres of calm wind areas before reaching the shore. Under these conditions, waves decay: short, steep waves are transformed into relatively long, low waves which reach the shore. This wave transformation is caused by frequency dispersion and direction dispersion. Swell waves can have periods of 30 seconds [CERC (1984)].

- **seiches**
  Seiches are oscillations caused by some exciting mechanism and trapped by a susceptible bathymetry, for instance a bay or a harbour basin. Exciting mechanisms can be:

  - local meteorological phenomena like squalls (small depressions) and gusts
  - tsunami (seismically induced gravity waves)
  - storm surges.

  Also long-period wave phenomena like surf beat, induced by variations in shoaling waves (shoaling is a change in wave height when waves propagate in varying water depths), and even current-induced vortices may be such a mechanism. Typical time scales are of the order of minutes (i.e. frequencies are usually less than 0.01 Hz). Observed periods range from 2 to 40 minutes [CUR/RIJKSWATERSTAAT (1995)].

- **tsunamis**
  Tsunamis are seismically induced gravity waves, characterised by wave periods that are in the order of minutes. They occur in seismic active areas. They often originate from earthquakes or other tectonic disturbances below the ocean, where water depths can be more than 1000 m and may travel long distances without reaching any noticeable wave height. However, when approaching a coastline, the height of the wave may increase considerably. This because, due to the large wave length, these waves are subject to strong shoaling and refraction effects (refraction is a process by which the direction of a wave moving in shallow water at an angle to the contours is changed so that the wave crests tend to become more aligned with those contours). Often, wave periods range from 10 to 100 minutes [CERC (1984)].

- **tides**
  Tides are created by the gravitational force of the moon and, to a lesser extent, the sun. These forces of attraction, and the fact that the sun, moon and earth are always in motion relative to each other, cause waters of ocean basins to be set in motion. These tidal motions of water masses are a form of very long period wave motion, resulting in a rise and fall of the water surface at a point. There are normally two tides per day, but some localities have only one per day. Tides constantly change the level at which waves attack coastal structures [CUR/RIJKSWATERSTAAT (1995)]. Along the Dutch coast, the tide has a period of 12 hours and 25 minutes.

- **storm surges**
  Local minima of atmospheric pressures (depressions or "lows") cause a corresponding rise of Mean Water Level (MWL), similarly, high pressures cause low water levels. Due to dynamical effects however, the rise in water level can be amplified significantly. When the depression moves quickly, the elevation of the water level moves correspondingly as a storm surge. A storm surge behaves as a long wave with a wave length approximately equal to the width of the centre of the depression. The height of these long waves may increase considerably due to shoaling [CUR/RIJKSWATERSTAAT (1995)]. The period of these long waves may be in the order of magnitude of a day or more.

Figure 2.4 is an illustration of classification of waves by period or frequency given by Kinsman [KINSMAN (1965)]. The figure shows the relative amount of energy contained in ocean waves having a particular frequency. Of primary concern are the waves referred to in figure 2.4 as gravity waves, which have periods from 1 to 30 seconds. A narrower range of wave periods, form 5 to 15 seconds, is usually more important in coastal engineering problems. Waves in this range are referred to as gravity waves since gravity is the principal restoring force; i.e., the force due to gravity attempts to return the fluid to its equilibrium position. Figure 2.4 also shows that a large amount of the total wave energy is associated with waves classified as gravity waves; hence, gravity waves are extremely important in dealing with the design of coastal and offshore structures [CERC (1984)].

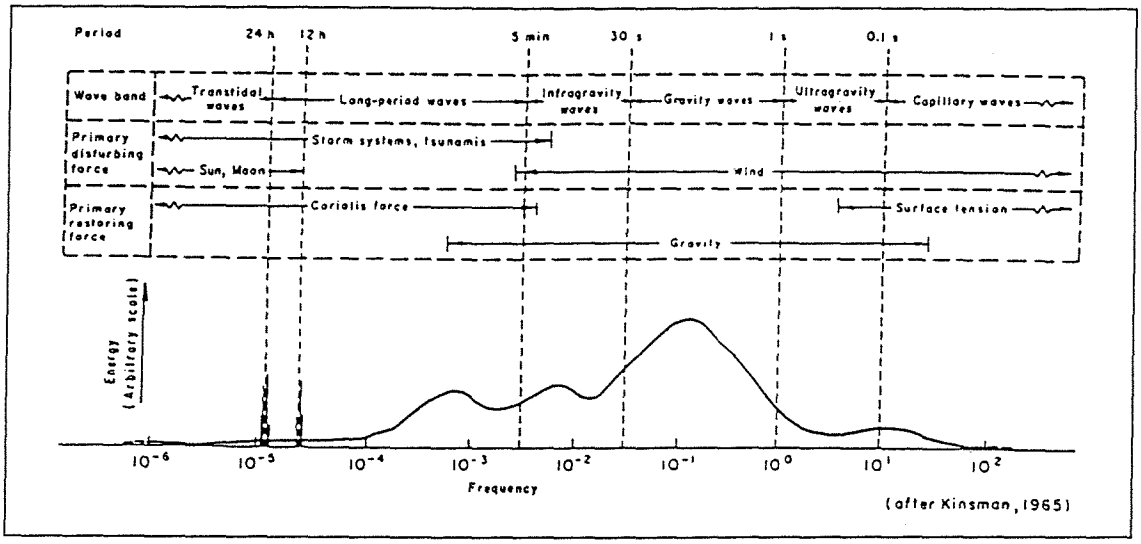

fig. 2.4 Approximate distribution of ocean surface wave energy illustrating the classification of surface waves by wave band, primary disturbing force, and primary restoring force [CERC (1984)]

In section 2.4 different types of wave impacts will be discussed. Only wind waves which break onto a vertical breakwater are discussed in that section. Impact forces or pressures which may occur due to other types of waves, such as tsunamis, will not be treated. Before the different types of wave impacts are treated, the conditions necessary for the occurrence of wave impacts will be treated in section 2.3. In that section a decision tree will be given that describes whether particular structures or sea states will cause a risk of impulsive wave conditions.

2.3 Decision tree for wave impact conditions

Goda [GODA (1985)] describes a number of rules to identify whether particular structures (e.g. vertical breakwaters) or sea states will cause a risk of impulsive (impact) wave conditions. That method is reinterpreted by Allsop et al. [ALLSOP et al. (1996)] and presented here in the flow diagram in figure 2.5.

The different parameters which are shown in figure 2.5 are explained in figure 2.6 and figure 2.7. Figure 2.6 gives the co-ordinate system which is used for vertical breakwater calculations and figure 2.7 gives a definition of the geometric parameters of a vertical breakwater.

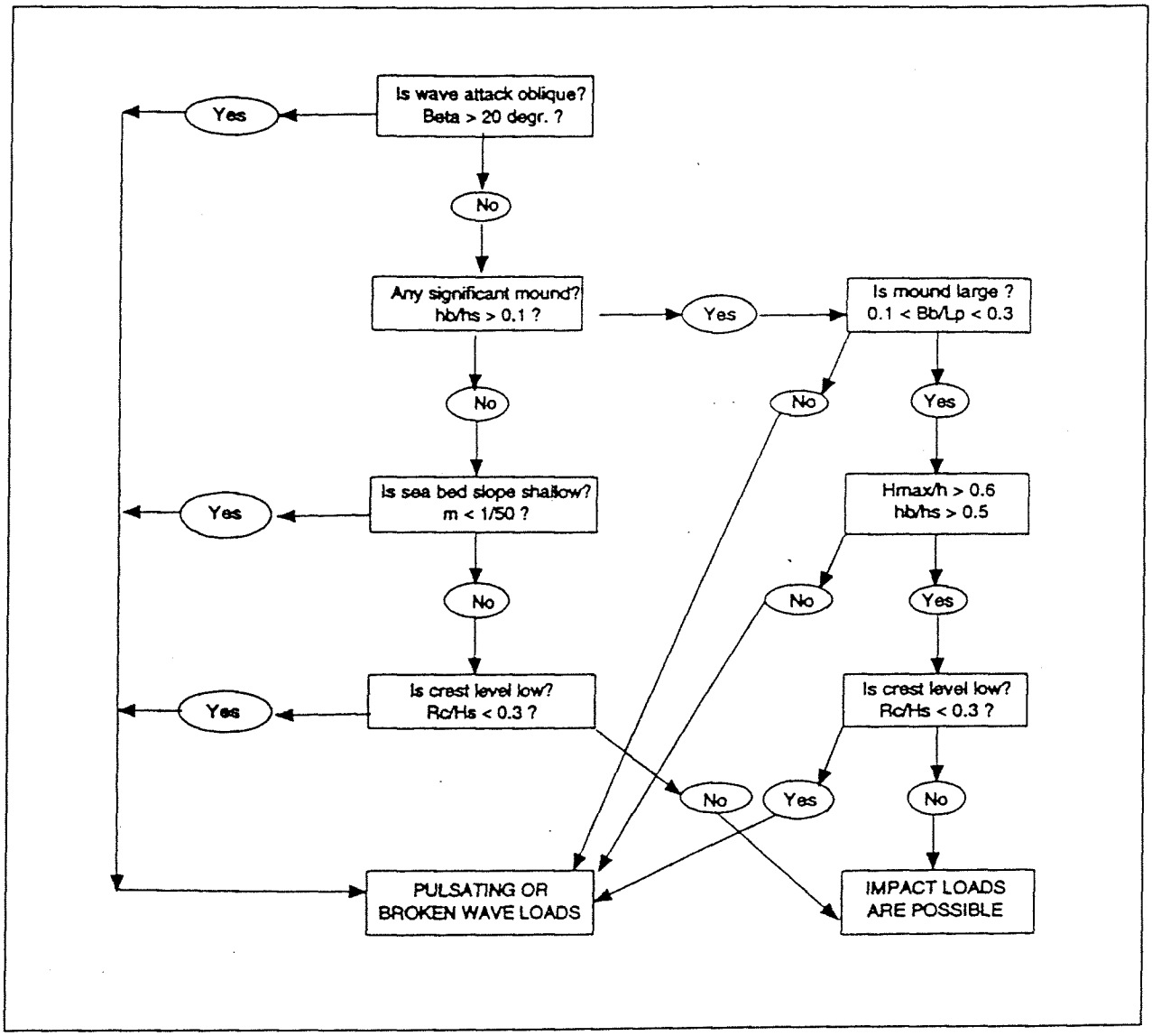

fig. 2.5 Decision tree for impulsive breaking conditions [ALLSOP et al. (1996)]

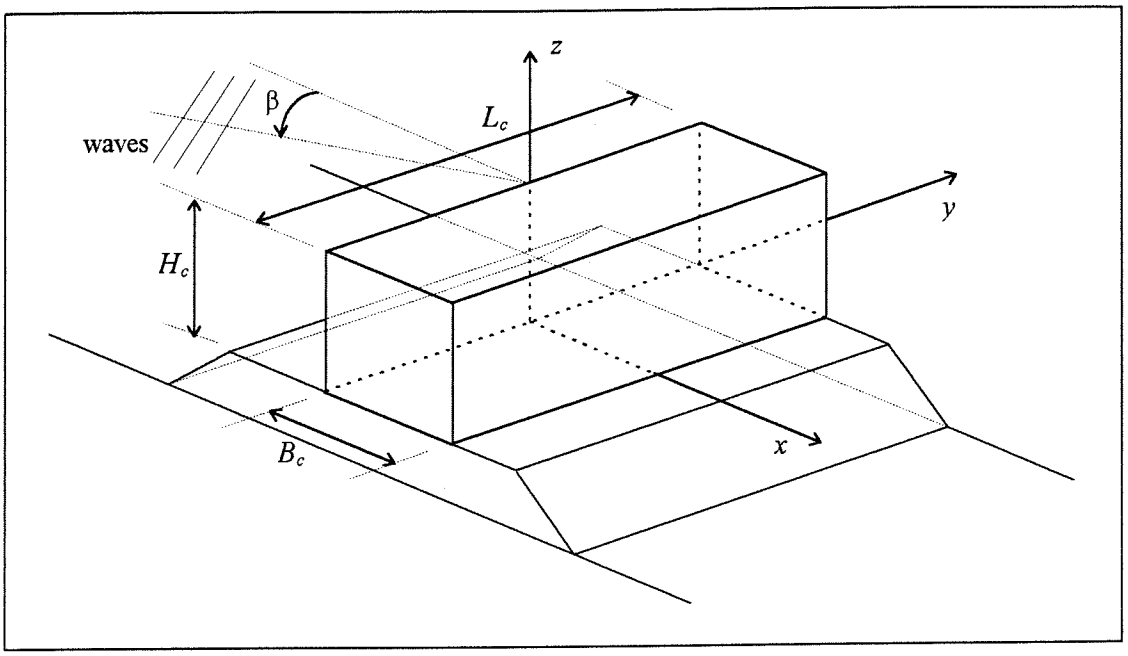

fig. 2.6 Co-ordinate system

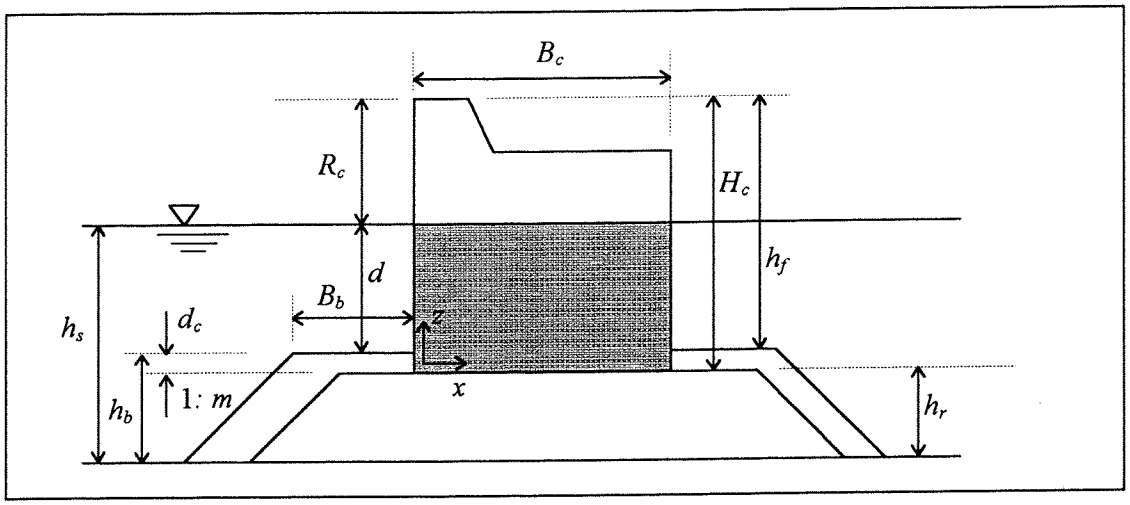

fig. 2.7 Definition of geometric parameters

In the decision tree of figure 2.5 other parameters, such as H_s, H_{max} and L_p, are also used. L_p is the deep water wave length related to the peak period (T_p) and is defined as:

$$L_p = \frac{gT_p^2}{2\pi} \tag{2.3}$$

H_s is defined as the significant wave height which is the average of the highest one-third of the wave heights in a wave record. H_{max} is the maximum wave height in a wave record.

The decision tree of figure 2.5 gives a good idea whether wave impacts will occur or not. Nevertheless, it is important to keep in mind that wave breaking was often observed during the most severe storms which preceded some breakwater disasters, even in water depths where breaking (due to shoaling) was not expected at all [OUMERACI (1994)]. So, one should be very careful in using the decision tree described in figure 2.5 and always keep in mind that breaking wave conditions may occur even when figure 2.5 does not indicate these dangerous conditions.

2.4 Types of wave impacts and related loads

In this section different types of wave impacts and their related loads will be discussed. In literature, all wave generated loads with a short rising time are generally called impact loads or impulsive loads. For each type of wave impact a description of the development in time of the pressure or force on the vertical front wall of the breakwater will be given in this section. The description of wave impacts in this chapter is more practical than the descriptions which will be given in chapter 3 and chapter 4. In those chapters, a more detailed, analytical description of the different types of wave impact pressures, forces and momentum generated by wave impacts will be discussed.

2.4.1 General

The appearance of wave impacts, the magnitude of the impact pressures or forces and the development in time of the pressures or forces on the vertical breakwater are influenced by a lot of factors. These factors are [DELFT HYDRAULICS (1994)]:

geometrical factors:
- the shape of the structure (in connection with trapped air, possibility of water to flow aside and the magnitude of the exposed surface of the structure)
- the angle between the vertical breakwater and the water surface
- the position of the vertical breakwater in relation to the water surface
- the water depth and the slope angle of the seabed near the vertical breakwater (in connection with the propagation of the incoming waves, refraction and breaking)

factors related to the stiffness
- the elasticity of the structure and the compressibility of the water
- the occurrence of trapped air between the water surface and the structure and air bubbles in the water

factors related to the incoming waves
- the wave height and wave period (the higher the wave height and the shorter the wave period, the higher the velocity of the water surface)
- the angle of wave propagation (the smaller the angle between the perpendicular of the breakwater and the wave propagation, the higher the chance of the occurrence of wave impacts; the chance of the occurrence of wave impacts is very little if the angle between the perpendicular of the breakwater and the wave propagation is bigger than 20°)
- dispersion of wave direction
- the shape of the local wave, which is influenced by the reflected wave

factors related to the water
- the salinity of the water (the salinity of the water influences the magnitude and the dispersion of air bubbles in water and influences the propagation of shockpressure waves (see chapter 3 and chapter 4; the mass density of salt water differs from fresh water)
- currents (currents influence a wave field but also the waves near a coastal structure)
- the water level

Wave generated pressures and forces are very complicated functions of the wave conditions and geometry of the structure. When a wave crest approaches a vertical wall the water particles will be forced upwards in a rather sharp curve. The smaller the radius of the particle path, the larger the pressure as it is balanced by centrifugal forces.

Figure 2.8 illustrates three different situations of wave structure interaction [PIANC (1996)]. In figure 2.8 different photographs are added. These photographs give a description of the water surface in different phases before and during the wave hits the vertical wall. These photographs were made during the experiments of Takahashi et al. [TAKAHASHI et al. (1993)]. These photographs are added in figure 2.8 to give a better idea of the shape of the wave profiles, which are also shown by the photographs.

Experiments and prototype measurements indicate that pressures on a breakwater due to the impact of breaking and near-breaking waves may be divided into three overlapping categories. There are sudden violent peaks, somewhat longer duration oscillatory pressures and the longer-lasting moderate pressures that persist until the wave crest is reflected. All three types of pressure can occur in a single wave impact [PEREGRINE (1994)].

The three different types of wave impact forces or pressures which can be found in figure 2.8 are discussed in the next three sub-sections. It should be noted that the three types of wave impacts are divided, depending on the amount of air which is trapped. A strong correlation exists between the shapes of the breaking waves at the vertical wall and the trapped air, which can also be seen in figure 2.8. On the other hand, the latter is known to considerably affect the magnitude as well as the spatial and temporal distribution of the impact pressure [SCHMIDT et al.(1992)]. The highest wave impact force, of very short duration is observed when a vertical wave front strikes the wall while trapping a small amount of air in the form of either bubbles or a thin lens-shaped pocket. The larger the amount of the entrapped air at impact of the plunging breakers, the lower the magnitude and the longer the rise time or compression time of the wave impact force [HATTORI et al. (1994)].

Wave impacts occurring without air entrapment (figure 2.8a) are termed "Wagner type wave impacts" and are discussed in section 2.4.2. Wave impacts occurring with air entrapment (figure 2.8c) are termed "Bagnold type wave impacts" and they are discussed in section 2.4.4. The most severe wave impact forces and pressures take place in the transition region between these types (figure 2.8b), these "transition type wave impacts" will be treated in section 2.4.3. The impact of the transition type arises when a vertical wave face strikes the wall with small trapped air bubbles [HATTORI et al. (1994)].

a) NON-BREAKING WAVE

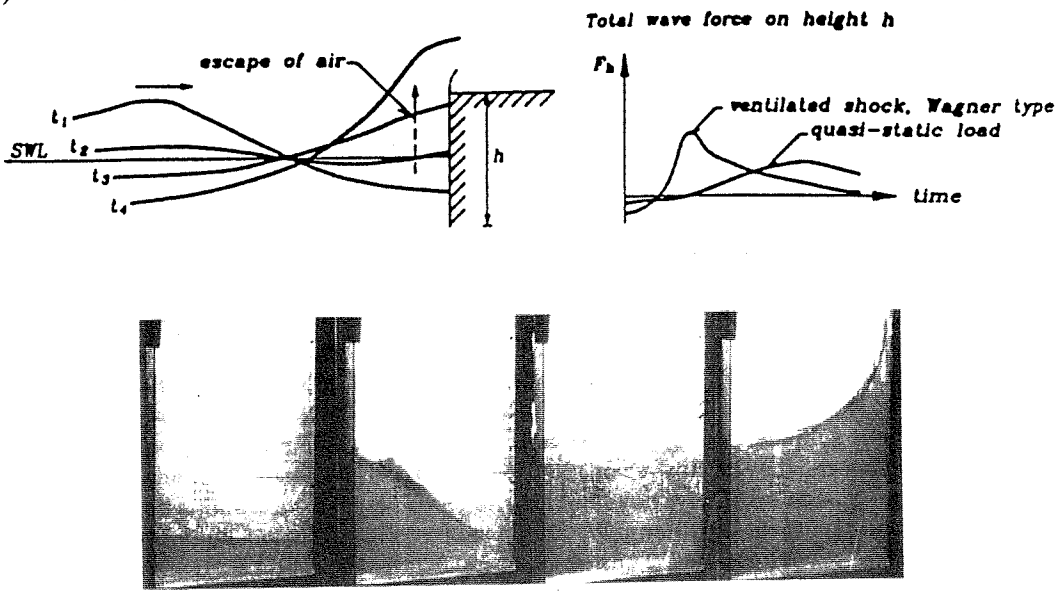

b) BREAKING (PLUNGING) WAVE, ALMOST VERTICAL FRONT, NO TRAPPED AIR POCKET (SINGLE PEAKED)

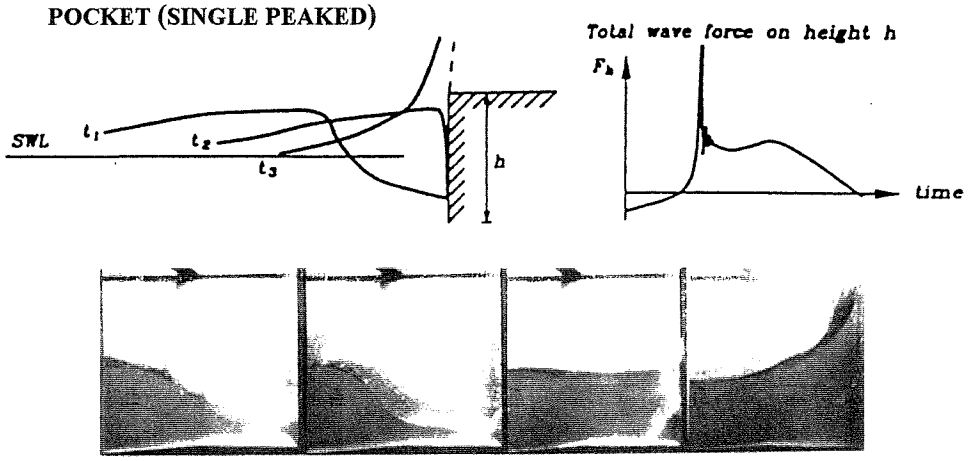

c) BREAKING (PLUNGING) WAVE, LARGE AIR POCKET, DOUBLE PEAKED

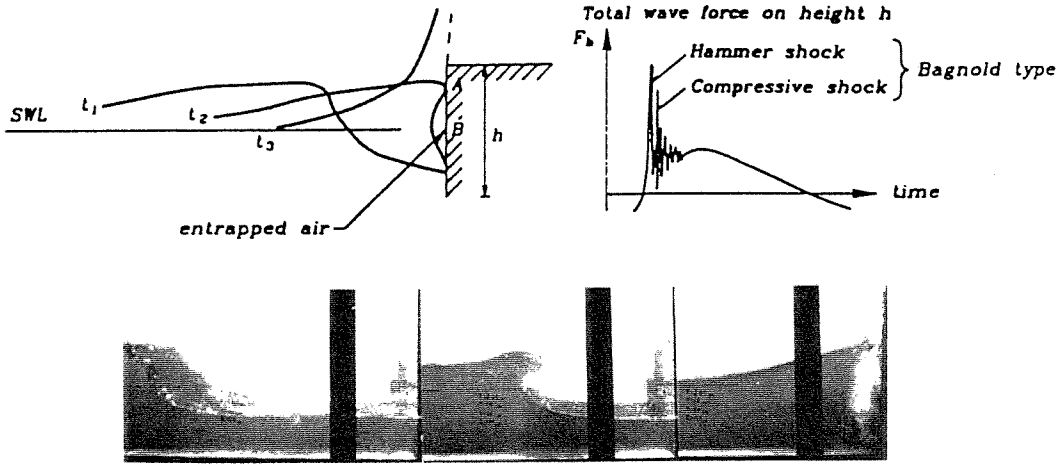

fig. 2.8 Illustration of vertical wall wave forces and wave profiles from non-breaking and breaking waves; [PIANC (1996)] and [TAKAHASHI et al. (1993)]

2.4.2 Wagner type wave impacts

In case of a non-breaking wave no air pocket will be trapped between the wall and the approaching wave front. The pressure at the wall will have a relatively gently variation in time and will be almost in phase with the wave elevation (see figure 2.8a). This kind of wave loads might be called quasi-static loads because the period is much larger than the eigenperiods of oscillation of conventional caisson breakwaters (approximately one order of magnitude larger, see chapter 7). Consequently, the wave load can be treated like a static load in stability calculations, with the exception that special considerations are required if the caisson is placed on fine soils where pore pressures might be built up resulting in significant weakening of the soil [PIANC (1996)].

However, it is not always that loads from what seems to be non-breaking waves can be regarded as quasi-static. A certain asymmetry in terms of steepening of the wave front face can cause a fast rise in the wave pressure, say within some tenths of a second (see figure 2.8a), Lundgren [LUNDGREN (1969)] denotes this a ventilated shock. In the literature it is often referred to as the Wagner type pressure (see also section 3.3) [TAKAHASHI (1995)]. In figure 4.4 on page 4 - 6 the Wagner type wave impact can be found caused by an upward deflected breaker. The time history of a Wagner type pressure is characterised by a sudden rise and exponential decay, see section 3.3.

2.4.3 Transition type wave impacts

The largest impulsive wave loads on vertical breakwaters occur when plunging waves hit the front wall and a small amount of air is trapped (figure 2.8b). This type of wave impacts causes a transition type pressure or force (see also section 3.4). The condition for plunging waves to occur is given by Battjes [BATTJES (1993)] as:

$$0.5 < \xi < 3.3$$

in which:

$$\xi = \frac{\tan\alpha}{\sqrt{H / L_0}} = \text{Irribarren number} \qquad (2.4)$$

H = (local) wave height

$$L_0 = \frac{gT^2}{2\pi} = \text{deep water wave length} \qquad (2.5)$$

g = gravitational acceleration

T = wave period

α = slope angle of the seabed

This fits very well with the results of model tests carried out by Mitsuyasu [MITSUYASU (1962)] from which it can be concluded that the smaller H/L_0 and the larger $\tan\alpha$, the larger the non-dimensional pressure intensity given by $p / (\rho_w g H)$, where p is the average pressure over the wall height ρ_w is the mass density of the water and H is the wave height in front of the wall [PIANC (1996)]. Mitsuyasu [MITSUYASU (1962)] found a maximum non-dimensional pressure [$p / (\rho_w g H)$], for a slope angle of 3.8° (slope 1:15) of approximately 10.5.

In figure 2.9 breaker types according to Battjes [BATTJES (1993)] are portrayed.

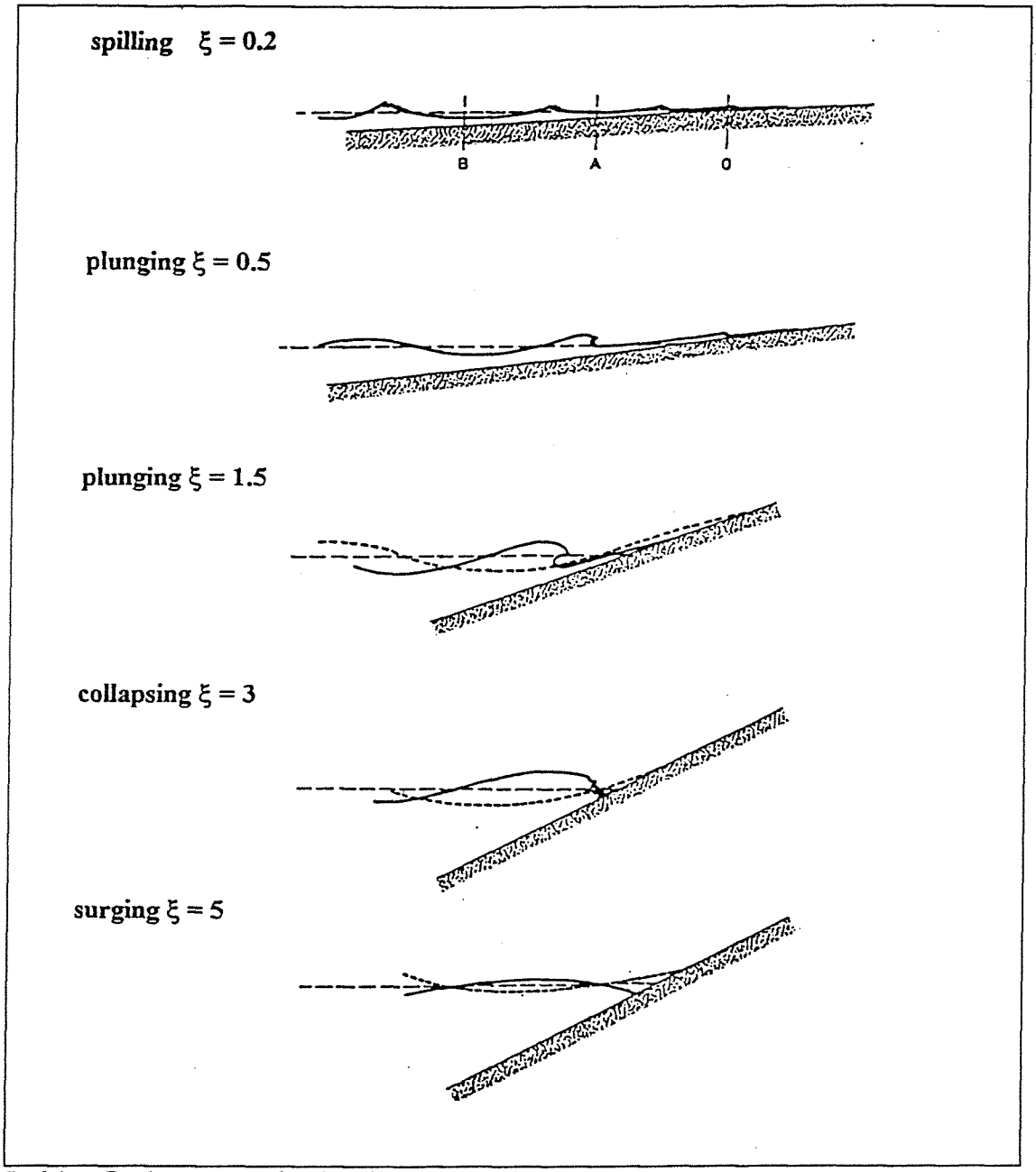

fig. 2.9 Breaker types as a function of ξ [BATTJES (1993)]

Breaking waves of the plunging type develop an almost vertical front before they curl over. If this almost vertical front happens to appear just prior to the contact with the wall then very high but extremely short duration pressures or forces occur.

Figure 2.8b illustrates the case of wave impacts of the transition type where only no or a negligible amount of air is trapped, resulting in a very large single peaked force followed by very small force oscillations. The duration of the peak force is in the order of hundredths of a second. The shorter, the larger is the peak pressure for constant momentum.

The sharp peak of pressure (or force) is due to the impact between the steep overhanging front of the wave and the wall. If the velocity and shape of the oncoming wave are known then the impact can be estimated, by following the type of analysis that has been developed for the impact of moving solid bodies on water (see chapter 3). The most severe type of impact has often been described as the case where the wave face is parallel to the wall at the impact. Cooker et al. [COOKER et al. (1990)] found that in this case a rapid "flip-through" of the surface occurs, rather than a direct impact.

The flip-through occurs because although the front of the wave is approaching the wall at a good velocity, the water in front of the wave at the wall cannot escape and is accelerated upwards. This acceleration increases rapidly, giving the waterline on the wall sufficient velocity that its rise in front of the wave turns the surface around to form an upward jet in the short time in which the oncoming wave might have hit the wall directly [PEREGRINE (1994)]. This effect can be seen in figure 2.8b for the point in time t_3.

The single peaked load history shown in figure 2.8b might by simplified to a "church-roof" shape, see figure 2.10. The response of a structure to such load depends on the eigenfrequencies of the structure and the detailed variation of the load in time (see chapter 7 to 10). Of special importance is the maximum load $F_{h,\max}$, the rise time t_r and the duration t_d of the horizontal force impact. The quasi-static load force $F_{h,q}$. is in most cases, where the wave is depth limited, approximately equal to [GODA (1994)](see figure 2.10) :

$$F_{h,q} = 1.5*\rho_w*g*H_b^2 \tag{2.6}$$

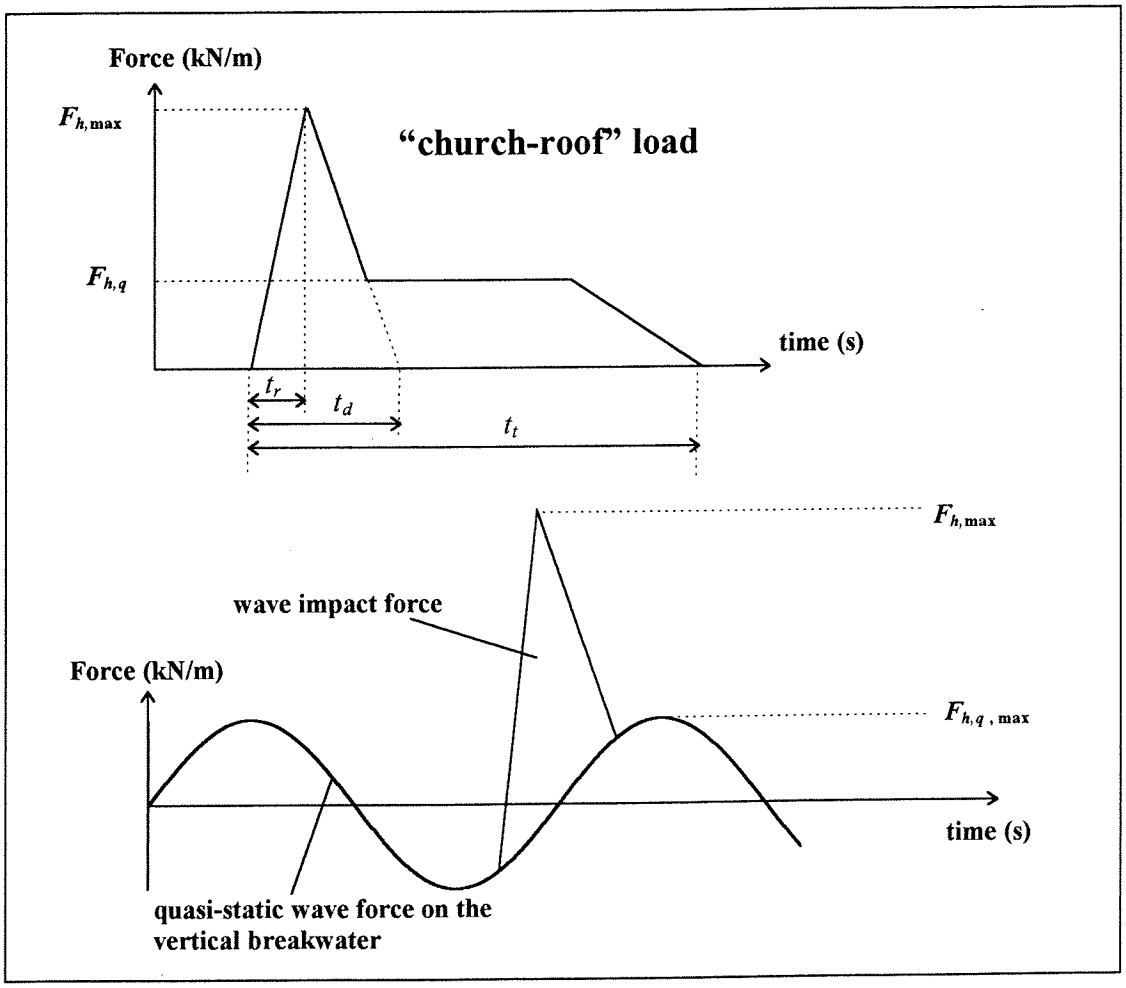

fig. 2.10 Impact load on a vertical breakwater schematised by a church-roof load

Different formulae have been derived to find a the relationship between the peak value $F_{h,\max}$ and the total duration of the peak force t_d . In the case of a single peaked load history the maximum wave impact force may be approximated by the following empirical equation which has been determined on the basis of large-scale model tests performed by Schmidt et al. [SCHMIDT et al. (1992)] (see section 2.4.4):

$$\frac{F_{h,\max}}{\rho_w g H_b^2} = 1.24\left(\frac{t_d}{T_P}\right)^{-0.344} \tag{2.7}$$

in which:

H_b = breaker height at the front wall of the vertical breakwater
T_p = peak period of the waves
ρ_w = mass density of sea water (1025 kg/m^3)

Equation 2.7 has a considerable uncertainty because of the large scatter in the test results (linear correlation coefficient = 0.8). The test result forces can be up to twice the force calculated by equation 2.7 [PIANC (1996)].

In the same tests was found that the point of application of the peak force $F_{h,max}$ is generally located slightly below Still Water Level (SWL) and does not vary significantly during the impact. The ratio of the rise time t_r to the total peak duration t_d was found to vary between $t_r / t_d \approx 0.3$ and $t_r / t_d \approx 0.65$, depending on the amount of trapped air and the magnitude of the force peak. The larger values of t_r / t_d occur for large trapped air volumes and smaller force peaks.

Equation 2.7 is shown in figure 2.11 together with the corresponding data from large scale model tests. The information shown in this figure has some limitations:

- The figure is based on scale tests. The validity for prototype dimensions is a point of discussion, given the uncertainty on scale laws, although the tests have been made at large scale. Scaling problems will shortly be discussed in chapter 4. Waves have been used up to 2 m height and up to a period of 9.4 s. Waves with a period of 9.4 s and a height of 2 m have got a very small wave steepness (H / L_0) of approximately1.5%.
- The tests have been made for a certain group of geometries, the influence of for instance the berm with has not been taken into account.

The horizontal wave impact load can be estimated with the help of equation 2.7. The impact load depends on the value of the relative wave impact duration, t_d / T_p. According to figure 2.11 t_d / T_p may vary roughly between 0.001 and 0.1, with an average of about 0.01. Calculated values of the horizontal wave impact forces for these three values of t_d / T_p are presented in table 2.1 for four different combinations of maximum wave height and peak period.

H_{max}		[m]	5	6.5	8	10
T_p		[s]	8.5	10	11	12
F_h	$t_d/T_p = 0.001$	[kN/m]	3355	5671	8590	13422
	$t_d/T_p = 0.01$	[kN/m]	1520	2568	3890	6079
	$t_d/T_p = 0.1$	[kN/m]	688	1163	1762	2753

table 2.1 Examples of horizontal wave impact loads for a single peak load history

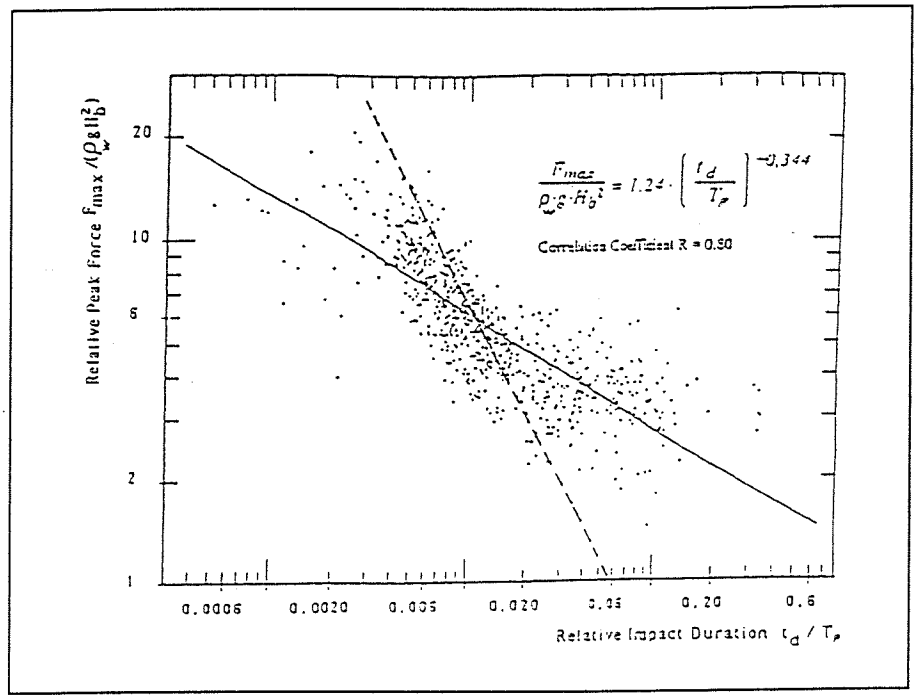

fig. 2.11 Maximum impact force versus impact duration [SCHMIDT et al. (1992)]

In figure 2.11 a dotted line is drawn as well. This line runs through the middle of the cloud and is a line of constant momentum (it is not the best fit). This line is suggested by de Groot (Delft Geotechnics) [GROOT, DE (1996)]. The function of this line is:

$$\frac{F_{h,\max}}{\rho_w g H_b^2} = 0.06\left(\frac{t_d}{T_P}\right)^{-1} \tag{2.8}$$

De Groot suggests this line because the uncertainty of scaling of wave impacts in a model can partly be overcome by expressing the results in terms of momentum (see also chapter 4). However it is still important to know the total duration and/or the rise time of a wave impact. In chapter 10 it will be shown that if a vertical breakwater is exposed to two different wave impacts, which both represent the same amount of momentum, the wave impact with the shortest total duration and rise time causes the largest response of the vertical breakwater. This fact is confirmed by the study of Oumeraci et al. [OUMERACI et al (1994)].

Other horizontal wave impact force prediction formulae, using a consideration of the momentum of breaking waves, can be found in literature as well (equation 2.9) [KLAMMER et al. (1996)]:

$$\frac{F_{h,\max}}{\rho_w * g * H_b^{\,2}} = 2.24 * \left(\frac{t_r}{\sqrt{d_b / g}}\right)^{-1} \tag{2.9}$$

in which t_r is the rise time of the maximum horizontal wave impact force $F_{h,\max}$ and d_b is the water depth of breaking waves. According to Goda [Goda (1985)], [Goda (1994)] the maximum dimensionless wave impact force possible can be approximated by:

$$\frac{F_{h,\max}}{\rho_w * g * H_b^{\,2}} = 15 \tag{2.10}$$

This fact seems to be confirmed by the tests of Schmidt et al. [Schmidt et al. (1992)] see figure 2.11. Note that this maximum wave impact force is 10 times as large as the quasi-static wave force!

Horizontal wave impact force prediction formulae will be extensively treated in chapter 4.

2.4.4 Bagnold type wave impacts

The double peaked force followed by low frequency force oscillations which occurs when a large amount of air is trapped in a pocket (see figure 2.8c) has been described by different researchers. The type of wave impact which causes the wave impact history which is sketched in figure 2.8c is called the Bagnold type wave impact. It is called the Bagnold type wave impact because of the fact that the theoretical approach of the characteristics of these wave impacts has firstly been treated by Bagnold [Bagnold (1939)].

Two different theories of the development in time of the double peaked wave impact force can be found in literature. The two theories differ in the description of the magnitude of the first peak. Lundgren [LUNDGREN (1969)] says that the *first* peak of the total horizontal force (integrated pressures) is the largest one and Schmidt et al. [SCHMIDT et al. (1992)] say that the *second* peak of the total horizontal force is the largest one. The different ideas are reflected below. The results of the study of Schmidt et al. [SCHMIDT et al. (1992)] and the results of their large scale hydraulic model will be treated extensively in this study as well. Not only because of the fact that it gives a good overview of Bagnold type wave impacts but also because of the fact that many other different aspects of wave impact loads are treated as well. The results of the study of Schmidt et al. [SCHMIDT et al. (1992)] are very usefull for a better understanding of different important aspects of wave impact loads.

Lundgren

Figure 2.8c illustrates the case where a large amount of air is trapped in a pocket, resulting in a double peaked force followed by pronounced force oscillations. The first and largest peak is induced by the wave crest hitting the structure in point A (see figure 2.8c), and is denoted a hammer shock (see also section 3.2). The second peak is induced by the subsequent maximum compression of the air pocket B (see figure 2.8c) and is denoted a compression shock [LUNDGREN (1969)]. In literature, this wave impact load is often called the Bagnold type (see also section 3.5). The force oscillations are due to the pulsation of the air pocket. The double peaks are typically spaced in the range of some milliseconds to hundredths of a second. The period of the force oscillations is in the range of 0.2 to 1 s.

Schmidt et al.

Schmidt et al. [SCHMIDT et al. (1992)] have carried out a detailed large-scale model study on impact pressures due to breaking waves of the plunging type on a vertical wall The hydraulic model tests were performed a the large wave flume (length = 320 m, width = 5 m and depth = 7 m) in Hannover (Germany) by using regular and irregular waves up to 2 m height and 9.4 s period. The experimental set-up is given in figure 2.12, showing:

- a sloping seabed 1:20 terminated by a vertical stiff wall of 6 m height instrumented with 28 high resolution pressure transducers (f>35 kHz)
- the locations of eleven wave gauges installed in front of the wall.

Water depths in the flume up to 3.0 m (1.6 m at the wall) were used for the tests. Most of the waves used in the tests arrive at the wall as plunging breakers (see figure 2.9 and figure 2.13), the maximum breaker heights obtained are in the range of $H_b = 1.15 * d_b$, where d_b is the breaking depth measured from Still Water Level (SWL).

Depending on the value of H_b / d and on further parameters seven types of breaking and broken waves - five for the plunging and two for the spilling breaker - in front of the vertical wall have been obtained (see figure 2.13).

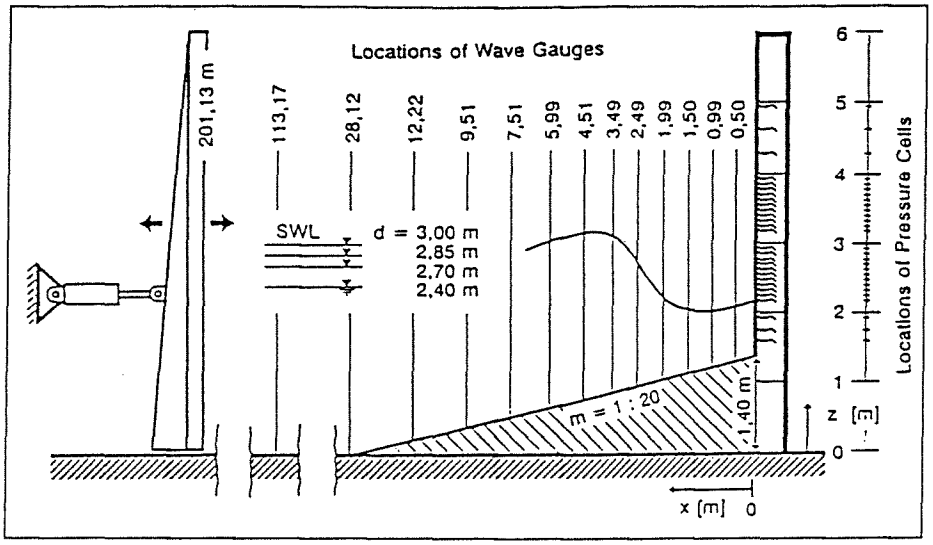

fig. 2.12 Experimental set-up in the large wave flume [SCHMIDT et al. (1992)]

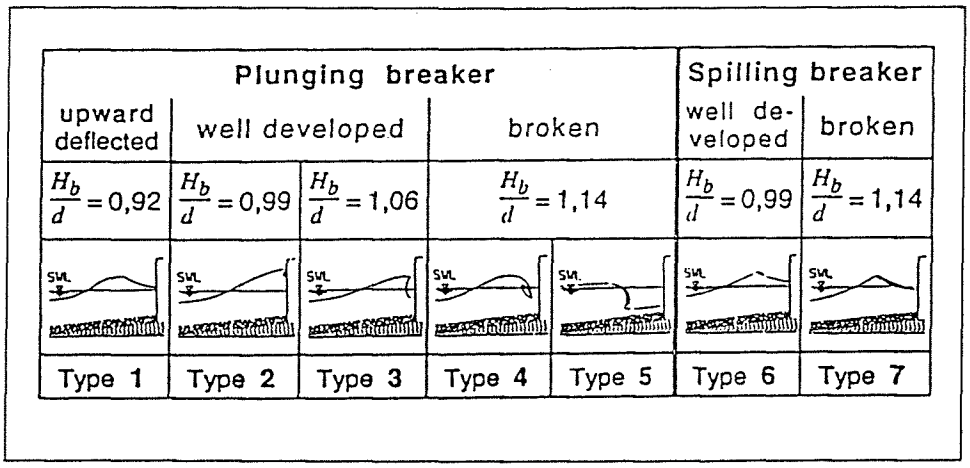

fig. 2.13 Breaker types observed during tests in the large wave flume [SCHMIDT et al. (1992)]

"Unfortunately, the breaker height H_b is extremely difficult to predict with any certainty, so these classifications are of limited practical use" [ALLSOP, et al. (1996)]. The water depth d directly at the vertical wall (see figure 2.7) corresponds to the breaking depth d_b measured from Still Water Level (SWL) by the linear relationship $d = 0.8 * d_b$ (average of 705 breaking waves and correlation coefficient of 0.84).

Some pressure distributions on the vertical wall, which simulates the vertical wall of a vertical breakwater, are given in figure 2.14 (breaker height H_b = 1.57 m and wave period T = 6.75 s).

The horizontal force F_h per linear meter obtained from pressure integration is also given. Figure 2.14 also illustrates that impact pressures are not only limited to small areas but may also occur simultaneously over a large height (in a range up to the wave height) of the front wall of the vertical breakwater.

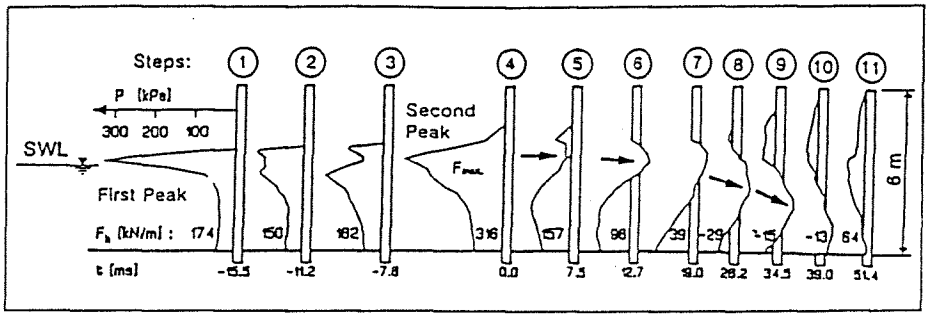

fig. 2.14 Pressure distribution at different time steps (H_b = 1.57 m, T = 6.75 s) [SCHMIDT et al. (1992)]

Particularly in the case of well developed plunging breakers (see figure 2.9 and figure 2.13) with a large trapped air pocket, the spatial integration of the impact pressures generally leads to a total force with a duration which may be much larger than usually assumed. In fact, the duration of total impact forces may reach 5 to 10 times that of the corresponding impact pressures. Since the latter is generally in the range of 0.005 to 0.02 seconds (in the model), the duration of the total impact force may reach values in the range of 0.05 to 0.2 seconds corresponding to values of 0.15 to 0.6 seconds in prototype (see chapter 5 for problems related to scaling); i.e. values which may be in the range of the eigenperiods of oscillation of common prototype vertical breakwaters (see among other things chapter 7).

The origin of negative pressure (see figure 2.14 steps 6 - 10) can also be explained by the fact that the trapped air is compressed so much that in re-expanding it throws the water mass back with such a velocity that the pressure drops below the atmospheric pressure value. Negative pressures are defined here as pressures which have a magnitude below the atmospheric pressure value. The pressure distributions in figure 2.14 clearly characterise the impact of a plunging breaker with a large air pocket trapped between the breaker front and the wall: a Bagnold type wave impact.

Typically, two force peaks (time step 1+4 in figure 2.14) occur which are also seen in the related force history shown in figure 2.15. From this figure can also be seen that the second peak is larger than the first peak for Bagnold type wave impacts according to Schmidt et al. [SCHMIDT et al. (1992)]

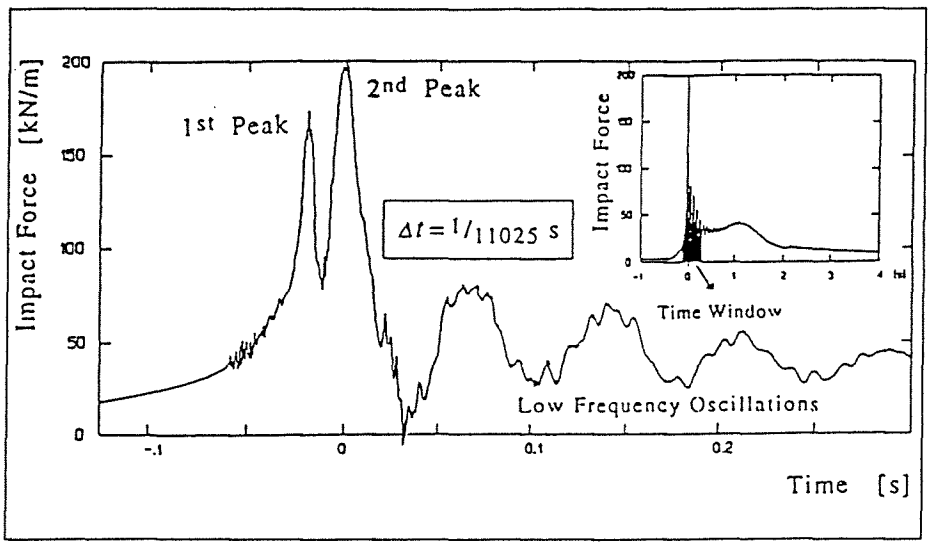

fig. 2.15 Horizontal force history resulting from pressure integration [SCHMIDT et al. (1992)]

A further important characteristic of this Bagnold type wave impact (well developed plunging breaker with trapped large air pocket, see figure 2.13) is the presence of the relative low frequency oscillations after the force peak (see figure 2.15). The latter are caused by the cyclic compressions and expansions of the trapped air pocket under the highly transient pressure fields and are hence related to the size of the trapped air pocket. The most critical situation may occur when the frequency of these oscillations will approach the range of the eigenfrequencies of the motion of a vertical breakwater, leading to resonance or near resonance phenomena. This may be more critical than a high single impact having the same excitation frequency, since it generally needs a number of loading cycles for resonance to build up from rest [OUMERACI et al. (1992)]. Based on a theoretical model as well as on field and laboratory data, the following very simple relationship between the period T_{0w} of the pulsations resulting from the cyclic contractions and expansions of the air pocket trapped between a wall and a plunging breaker with an incident wave height H (in cm) has been developed:

$$T_{0w} = 0.75*10^{-3}*H \tag{2.11}$$

The derivation of this relationship can be found in chapter 5. According to equation 2.11 the force oscillations with $T_{0w} = 0.075$ s in figure 2.15 correspond to an incident wave height in the large scale model of $H = 100$ cm = 1 m. The period of the force oscillations transferred to prototype conditions may also lie in the range of the eigenperiods of prototype vertical (caisson) breakwaters. As has been said before, these force oscillations may lead to near resonance excitation. More detailed information of this phenomenon can be found in chapter 5 and in section 10.6 where the effect of the low frequency force oscillations on the dynamical behaviour and stability on a vertical breakwater is treated.

The typical features of a force history caused by the impact of a breaker plunging on a vertical wall and entrapping a large air pocket are schematically summarised in figure 2.16 which also illustrates the origin of each of these characteristics.

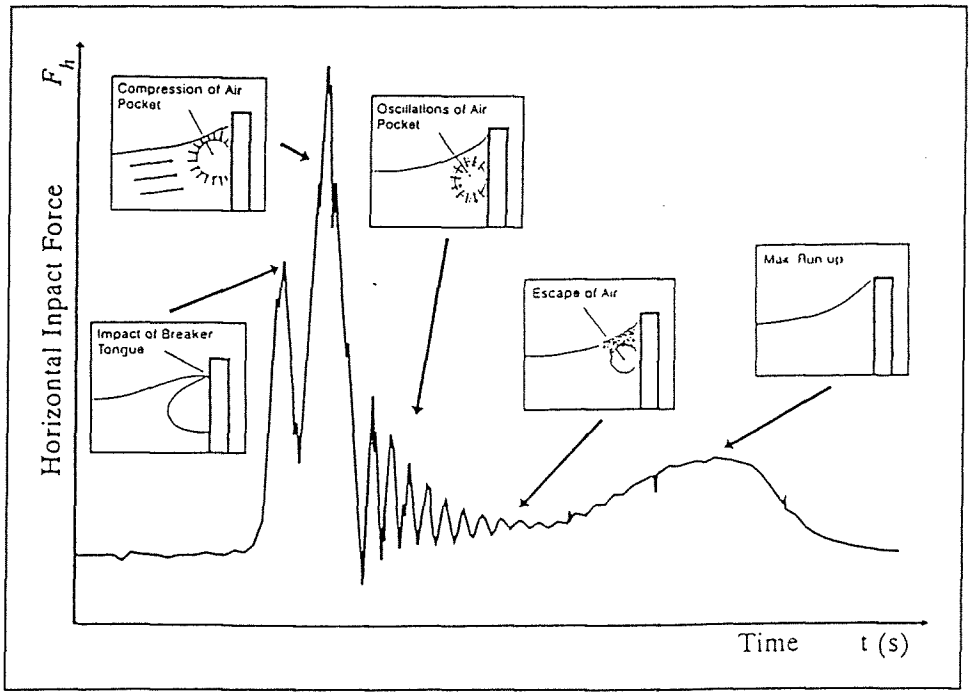

fig. 2.16 Characteristics of impact forces and their origin [SCHMIDT et al. (1992)]

So, although the damped eigenfrequency of typical caisson or vertical breakwaters on sand and gravel is in the order of 0.3 to 0.8 seconds and consequently orders of magnitude larger than the period of impulsive loads from breaking waves of the transition type (see sub-section 2.4.3), there is still a possibility of dynamic amplification of the movements of the caisson, dependent on the rise and decay times of the peak load, the mass of the vertical breakwater, and the elasticity/plasticity of the foundation. The force oscillations caused by a large trapped air pocket, thus the force oscillations after the second peak of the double peaked wave impact force (see figure 2.16), are likely to be dynamically amplified because the frequency of the oscillations is in the same range as the damped eigenfrequency of caisson breakwaters. It can be concluded that these oscillating forces may be very dangerous for (for example) the stability of the vertical breakwater. It may be possible that these oscillating forces have been the cause of previous vertical breakwater failures, see section 10.6.

In literature different equations which describe the period of the force oscillations (T_{0w}) can be found. They all give nearly the same results as will be shown in chapter 5. It can be concluded that the most dangerous load for vertical breakwaters may be the Bagnold type wave impact discussed in this sub-section, although the most severe impact forces take place in the transition region between the Wagner type wave impact and the Bagnold type wave impact, the so called transition type wave impact (discussed in section 2.4.3). Dynamical amplification of the motion of the vertical breakwater may occur when a vertical breakwater is exposed to a Bagnold type wave impact, due to the fact that the force oscillations after the wave impact peak force are in the same order of magnitude as the eigenperiod of the vertical breakwater.

Oumeraci et al. [Oumeraci et al. (1994)] conclude: "Depending upon the purpose of the analysis and upon the shape of the actual load, simplification of the impact load history and its reduction tot very simple shapes (e.g. the "church-roof" (see figure 2.10)) may be either very usefull or quite misleading. For example misleading in the case when low frequency force oscillations may occur when a wave breaks onto a vertical wall. The results achieved so far already indicate, that most of the relevant characteristics of the load history (rise time, single or double force peak, total impact duration period amplitudes and decay rate of the oscillations following the load peak) should be considered in the selection of representative dynamic load histories for the final design of a breakwater."

"Significant dynamic amplification necessitates a thorough dynamic analysis of the response of the structure. Important in such an analysis is the characteristics of the foundation soils under dynamic loads." [PIANC (1996)]

2.5 Uplift forces and uplift pressures on vertical breakwaters

Wave action on vertical breakwaters does not only cause horizontal quasi-static or wave impact forces but also (in time varying) uplift forces which work against the bottom slab of a vertical breakwater, as has been mentioned in the introduction of this chapter. Uplift pressures and / or forces are influenced by the wave action on the vertical breakwater, the permeability of the rubble foundation of the breakwater and the geometry of the structure and the rubble foundation (thickness and height).

The uplift pressure underneath a caisson breakwater consists in fact of a hydro-static pressure and a wave induced pressure. For the calculations of the dynamical behaviour and stability of a vertical breakwater, the horizontal hydro-static pressure is of no significance. However, in contrast to this, the vertical hydro-static pressure is of importance. One should account for his vertical hydro-static force (integrated pressures) or buoyant force in stability calculations. This can be done by reducing the total weight of the caisson, as will be shown in chapter 7.

Relatively little information is available on wave induced up-lift forces acting on the underside of vertical breakwaters of the caisson type. Wave induced uplift forces on caisson breakwaters used for static stability analysis are commonly predicted by empirical and semi-empirical formulae. In this respect the Goda method [GODA (1985)] is mostly used because it applies for breaking and non-breaking wave conditions and also accounts for the height of the foundation. According to Goda [GODA (1985)], see chapter 6, the wave induced uplift pressure, acting on the bottom of the upright section of a vertical breakwater is assumed to have a triangular distribution. The maximum uplift pressure (p_u) occurs at the seaward bottom edge of the caisson and decreases linearly to zero at the shoreward end (see figure 6.1). For wave impact conditions an uplift pressure with the same distribution and magnitude is used, according to Takahashi et al. [TAKAHASHI et al. (1993)] The influence of the characteristics of the rubble foundation (e.g. the permeability) is totally ignored in the Goda method [GODA (1985)].

For a dynamical stability analysis however, temporal and spatial distributions of the uplift loading are actually required. Moreover, the interaction of the dynamical response of the structure and the development of the uplift loading may also be determinant. [MAST II MSC (1995)]. Different breaker types (these types are among other things dependent on the amount of trapped air between the breaking wave and the vertical front wall of a breakwater, see figure 2.13) do cause different pressure distributions underneath the caisson according to Kortenhaus et al. [KORTENHAUS et al. (1994)]. For impulsive loading on the caisson the uplift pressure is not linearly distributed anymore and not equal to zero at the rear edge of the caisson as usually assumed. This is due to the effect of compression waves beneath the structure where the maximum uplift pressure no longer occurs at the seaward edge of the structure. However, in most cases the Goda method [GODA (1985)] seems to give a good first approximation of the magnitude of the resultant of the uplift pressures: the uplift force.

It should be noted that it is extremely difficult to translate the measured uplift pressures of hydraulic scale models to prototype scale. Scale effects may be important in the interpretation of the up-lift data, since the energy dissipation effect of the rubble mound is dependent on the length of the flow path and the flow regime within the material [ALLSOP et al. (1996)].

Although different pressure distributions underneath caisson breakwaters have been found for (different) wave impact conditions, the magnitude of the uplift force according to the Goda method [GODA (1985)] seems to give a usefull approximation for the uplift force used for the benefit of the calculations within the framework of the given analysis of the effect of wave impacts on the dynamical behaviour and stability of vertical breakwaters in this study. This "Goda" uplift force is assumed to be constant in time under different individual wave loading conditions for the benefit of the calculations which will be presented in this report.

3 Wave impact pressures

3.1 Introduction

In the previous chapter different general aspects of hydraulic loads on vertical breakwaters have been treated. Wave impacts passed in review in section 2.4. In this chapter models for wave impact **pressures** will be treated. Wave impact **forces** will be treated in the next chapter. In that chapter different horizontal wave impact force prediction formulae will be discussed.

Wave impact pressures can significantly differ from place to place on the plane vertical front wall of a breakwater as can among other things be seen in figure 2.14 on page 2 - 20, figure 4.4 on page 4 - 6 and figure 6.1 on page 6 - 2. If the spatial distribution of the wave impact pressure on a vertical front wall of a breakwater is known then the total wave impact force on that breakwater can be calculated by means of an integration of the pressure over the total height (and width) of that vertical front wall.

Different wave impact force prediction formulae, which will be treated in the next chapter, can be used for the benefit of the calculation of the dynamical behaviour of a vertical breakwater which is exposed to wave impacts or to calculate its **overall** stability. These calculations will be carried out in chapter 7 to 10. Wave impact pressures have more **local** effects. Large wave impact pressures can be extremely destructive for, for instance, the concrete front wall of a vertical breakwater. However, this study mainly concerns with the overall stability of vertical breakwaters.

Evidence from various sources, including analysis of existing structures, suggests that pressures due to breaking waves on a plane vertical surface will be in the range of 100 to 1000 kN/m^2. In this chapter different theoretical formulae will be presented which make it possible to calculate these (maximum) wave impact pressures. These models are general applicable. The presented analytical formulae in this chapter for the calculation of wave impact pressures are of theoretical use and can be used to get more insight in the phenomena which may occur when waves break onto a plane vertical wall. Design formulae for vertical breakwaters, for instance the Goda formula [GODA (1985)] extended by Takahashi et al. [TAKAHASHI et al. (1993)] give wave (impact) pressures which are of more practical use for the design of vertical breakwater. This design formula will be treated in chapter 6.

The shock wave model, which gives the highest maximum wave impact pressures is treated in section 3.2. In this chapter analytical models for the benefit of the calculations of the pressures of the three different types of wave impacts (treated before in section 2.4) are given as well. Models for the Wagner type pressure (which gives the lowest maximum wave impact pressure), the transition type pressure and the Bagnold type pressure are discussed respectively in section 3.3, section 3.4 and section 3.5. In section 3.6 a summary of the different analytical models is given and for each analytical model the maximum wave impact pressure will be calculated for a prototype situation. Finally, in section 3.7 an example of the highest measured wave impact pressure ever, caused by full-scale waves, will be given: in Dieppe (France) a wave impact pressure of 690 kN/m^2 has been measured.

3.2 Shock wave model

3.2.1 Wave impact on a rigid wall

This model can be used to schematise wave impacts with hammer shock pressures. For example the wave crest of a Bagnold type wave impact which is hitting the structure (see figure 2.8c point *A*). In this model it is assumed that the water approaches perpendicularly to the rigid wall and cannot escape. At the moment of the wave impact, the water is compressed and a shock wave, which moves away from the wall, is created in the water. The celerity of the front of the shock wave is equal to the velocity of sound in water (1480 m/s in pure water [BATTJES (1990)]). Now the following can be deducted:

$$\Delta p = p_{max} - p_0 = \rho c_w u_0 \tag{3.1}$$

in which:

p_{max} = maximum impact pressure
p_0 = water pressure before the impact = p_{atm} at the water surface
p_{atm} = atmospheric pressure
ρ = mass density of fresh water
u_0 = velocity of the approaching front of the water

$$c_w = \sqrt{\frac{K_w}{\rho}} = \text{velocity of sound in water } (\sqrt{\frac{2.2*10^9}{998}} \approx 1480 \text{ m/s}) \tag{3.2}$$

$$K_w = -\Delta p \frac{V}{\Delta V} = \text{compressibility modulus} \tag{3.3}$$

Δp = change of pressure
V = original volume
ΔV = change of volume

With equation 3.2, equation 3.1 can be written as:

$$\Delta p = u_0 \sqrt{K_w \rho} \tag{3.4}$$

It is assumed that the mass density of water ρ is a constant (which is not true in case of a compression wave; however, the variation is relatively small) and that the compressibility modulus is a constant, which means that it is considered as a homogeneous fluid [DELFT HYDRAULICS (1995)].

The shock wave model as described above gives an absolute upper limit for the wave impact pressure. In reality the wave impact pressure will always be lower, because it is very unlikely that the water surface is completely flat and that it hits the wall parallel (the consequence of that is that the water cannot escape quickly enough), and because of the fact that water often contains some air, which reduces the wave impact pressure [DELFT HYDRAULICS (1995)]. The maximum prototype pressure found was about ten percent of that given by equation 3.4 [MASSIE et al. (1986)].

An approximation of the total duration of a wave impact of the hammer shock type can be given [MASSIE et al. (1986)]. The wave which approaches the wall is schematised as a block of water whit a specific length of L. This block of water hits a rigid wall with a velocity u_0. The time during which the shock wave propagates through the block of water with a length L is $\Delta t = L/c_w$. After this time (Δt) the shock wave returns at the same velocity to the starting point. Thus the total time duration of the impact (t_d) is:

$$t_d = 2\Delta t = \frac{2L}{c_w} \tag{3.5}$$

If L is approximated by 5 m and c_w = 1480 m/s than the duration of a wave impact of the hammer shock type can be estimated by 6.8 ms.

3.2.2 Rigid wall and air-water mixture

When water contains some air it can approximately be said that the compressibility of the air-water mixture is determined by the air content and the mass density by the water content. The compressibility modulus of air can be deducted from the equation for the change of the condition of an ideal gas:

$$pV^{\gamma} = constant \tag{3.6}$$

in which:

p	=	pressure
V	=	volume
γ	=	constant of Poisson (isothermal compression (no temperature change during the compression): γ = 1.000; adiabatic compression (no heat exchange with the vicinity during the compression): γ = 1.405)

So, the value of the constant of Poisson is between γ = 1.000 and γ = 1.405. In rather large air pockets the compression is approximately adiabatic.

The differentiation of equation 3.6 has the following result:

$$V^{\gamma}\mathrm{d}p + \gamma\, pV^{(\gamma-1)}\mathrm{d}V = 0 \tag{3.7}$$

or, when the pressure variations are small, compared to the initial pressure (p_0):

$$\frac{\mathrm{d}p}{\mathrm{d}V} = -\frac{p\gamma}{V} \approx -\frac{p_0\gamma}{V} = -\frac{K_w}{V} \tag{3.8}$$

Now, when the air-water mixture is considered homogeneous with α is the air content and (1-α) is the water content, then the following is approximately valid ($0 < \alpha < 1$):

$$K_{mixture} = -\frac{1}{\alpha}\frac{\Delta pV}{\Delta V} = \frac{1}{\alpha}K_w = \frac{1}{\alpha}\gamma p_0 \tag{3.9}$$

$$\rho_{mixture} = (1-\alpha)\rho \tag{3.10}$$

(Because in an air-water mixture only the air-part is compressed, the variation of the volume as a result of a given variation in pressure is a factor α smaller and therefore the compressibility modulus is a factor α^{-1} larger than the compressibility modulus of pure air).

With equations 3.9 and 3.10, equation 3.4 can be written as:

$$\Delta p = u_0 \sqrt{\frac{\gamma p_0 (1-\alpha)\rho}{\alpha}} \tag{3.11}$$

When the water contains little air (for example about 0.1 percent), or when the air is divided up in multiple small bubbles, the compression of the air is nearly isothermal ($\gamma \approx 1.000$), because in that case the warmth can quickly be transferred to the water. To be able to use the above equation, an approximation of the quantity of air in the water is necessary. Nevertheless, in different situations, the quantity of air can vary a lot; this is dependent on the previous history at the impact zone (previous impacts and breaking waves can increase the quantity of air in the water) and on the transport of water (flow or no flow). The maximum quantity of air is perhaps some percents but reliable data do not exist [DELFT HYDRAULICS (1995)].

Führböter [FÜHRBÖTER (1969)], has expressed the influence of air in water on the maximum impact pressure in a factor, by which Δp according to equation 3.1 should be multiplied. This resulted in the following equation:

$$\Delta p = p_{max} - p_0 = \rho c_w u_0 \frac{1}{1 + \alpha\left(\frac{K_w}{K_a} - 1\right)} \tag{3.12}$$

in which:

K_a = compression modulus of air is $\gamma p_0 \approx 1.000*10^5$ N/m^2 in case of isothermal compression and is $\gamma p_0 \approx 1.405*10^5$ N/m^2 in case of adiabatic compression
K_w = compressibility modulus of water is $2.2*10^9$ N/m^2

This equation implies that the maximum pressure, calculated with equation 3.1, is reduced when the compressibility of the air bubbles is included. With equation 3.12 values of impact pressure can be calculated that are closer to reality than the values calculated with equation 3.1. The problem is to make a reliable approximation of the percentage of air in the water. A difficulty is that the air has not always homogeneously been divided and that the percentage of air can strongly vary.

Führböter also found that the effective length L (see equation 3.5) of the approaching water mass is of the same order as the hydraulic radius R of the impact area. This was explained by the fact that the sidewards escape of water develops (via a sideward shock wave) just as fast as the shock wave travels back through the approaching water. The duration the maximum pressure (see also equation 3.12 and equation 3.5) is then:

$$t_d = \frac{R}{c_{mixture}} \tag{3.13}$$

in which:

$c_{mixture}$ = velocity of sound in an air-water mixture; $c_{mixture}$ decreases to a lowest value of about 20 m/s in the case of 50% air in the water; in case of 1% air in the water, $c_{mixture}$ is approximately 100 m/s [KOLKMAN (1992)]

3.2.3 Wave impact on a compressible wall

As a result of a wave impact on a compressible wall, both in the water and in the wall a compression wave is created. The velocity of the approaching water is u_0; the velocity of the wall after the wave impact is considered to be εu_0, the change of the velocity of the water is $(1-\varepsilon)u_0$. The celerity of the compression wave is c_w. The celerity of the compression wave in the wall is c_c. The pressures p_{max} in the contact surface of the water and the wall are equal. Because of an equal initial pressure $p_0 = p_{atm}$, the decline of the pressure over the compression waves is equal too:

$$\Delta p = \rho c_w (1-\varepsilon) u_0 = \rho_c c_c \varepsilon u_0 \tag{3.14}$$

in which:

ρ_c = mass density of the structure

$$c_c = \sqrt{\frac{E_c}{\rho_c}} \quad \text{[DIETERMAN et al. (1993)]} \tag{3.15}$$

E_c = elasticity modulus of a structure

Equation 3.14 can also be written as:

$$\Delta p = \rho c_w u_0 \frac{1}{1+\frac{\rho c_w}{\rho_c c_c}} \tag{3.16}$$

Equation 3.16 shows that including the compressibility of the wall reduces the maximum impact pressure that is calculated with equation 3.1. Compared with the reduction as a result of air in the water, the reduction due to the compressibility of the water can normally be neglected. In reality structures will rather sag than compress; than the above equation is not valid [DELFT HYDRAULICS (1995)]. Flowing aside of water which impinges upon a vertical wall has got a greater influence on the reduction of wave impact pressures than the compressibility of the (concrete) vertical front wall of a breakwater [DELFT HYDRAULICS (1994)].

3.3 Models for Wagner type pressure

Wagner type wave impacts have been mentioned before, among other things in figure 2.8a and in sub-section 2.4.2. Wave impacts which cause Wagner type pressure are also called ventilated shocks. In this section two models are discussed, firstly a simple model, the flow pressure model and secondly a more complex model of Takahashi et al. [TAKAHASHI et al. (1993)].

Flow pressure model

Wave impacts of the Wagner type can be described in a so called flow pressure model which is a very simple model. In this model the maximum wave impact pressure (p_{max}) is by means of a coefficient expressed in the flow pressure ($\frac{1}{2}*\rho*u_0^2$):

$$p_{max} - p_0 = k\left(\frac{1}{2}\rho u_0^2\right) \tag{3.17}$$

in which:

k = coefficient which determines the impact pressure

For a given geometry and given hydraulic boundary values the coefficient k should experimentally be determined. In some cases a theoretical approximation is possible, for example in case of a circular cylinder. In marine engineering k is defined as the slamming coefficient c_s. For a circular cylinder, different researchers have determined the magnitude of c_s. The magnitude varies between approximately 2 and 6, dependent on the theories and geometries of the cylinder which are used.

The magnitude of the impact pressure found here with the flow pressure model is probably the lowest impact pressure which can be found when analytical models are used. This pressure is considerably lower then observed impact pressures, even though the velocity of the approaching flow is the comparable to the celerity of a wave in shallow water [MASSIE et al. (1986)].

In the flow pressure model it is assumed that no water is trapped between the front of the water and the structure; so the angle between the front of the water and the perpendicular of the (vertical) wall of the breakwater is small and there are no standing edges which could hinder the escape of the air. It is also assumed that the water can escape fast enough to the sides, as a result, the compression of the water can be neglected.

The wave impact pressure is determined by the inertia phenomena connected with the 'blocking' of the water. According to Newton's second law the following equation is valid:

$$p = \frac{d(mu)}{dt} = \rho L \frac{du}{dt} \tag{3.18}$$

It is assumed that the mass density of the water ρ is constant. The longitudinal measure L is a measure for the quantity of water which has to be blocked ($m = \rho L$). L can be determined by a added water mass consideration. The added water mass is a mass which has to be taken into account when the dynamical behaviour of hydraulic structures is investigated. Hydraulic structures which move in water excite water movements. These water movements influence on their turn the movement of the hydraulic structure. This influence can by modelled by taking into by adding a virtual mass (an added mass) to the structure (see also chapter 7 of this report).

Now it is assumed that the velocity of the approaching wave front u_0 is reduced to 0, therefore $du = -u_0$. When the front of the water hits the structure under a certain angle, the time for slowing down, dt, can be set proportional to D/u_0, in which D is the average space between the front of the water and the vertical breakwater. Thus the wave impact pressure can be calculated with the following equation:

$$p_{max} - p_0 = \frac{\rho L u_0^2}{D} = k\left(\frac{1}{2}\rho u_0^2\right) \tag{3.19}$$

The larger the angle between the front of the water and the structure, the smaller the coefficient k and the smaller the maximum pressure. With equation 3.19 a good first approximation of the pressure can be given, if it is assumed that there is no air trapped. If air is trapped, the air compression model derived by Bagnold [BAGNOLD (1939)], discussed in section 3.5, should be used. A limitation of the flow pressure model is that for some geometry's there is no slamming coefficient k known.

Slamming coefficients are often determined by letting fall an object on the water. When the object hits the water a certain quantity of water mass (the added water mass) is given an acceleration and pressure waves occur in the water. This is the same quantity of water mass that is slowed down when the water hits a rigid object. Both experiments produce the same slamming coefficient, if the added water mass is not related to the acceleration. The added water mass is not related to the acceleration when the acceleration is short-lived.

The added water mass does not change when both the water surface and the object are moving. But the time for slowing down the water mass (dt) is then related to the difference of the velocity of the water surface and the velocity of the object. The velocity if the water surface that is to be reduced is an absolute quantity though. Equation 3.28 cannot be used when both the water surface and the object are moving. The velocity (u_0) could be replaced by a relative velocity; nevertheless then it is dubious to use a slamming coefficient which is determined with a unmoving water surface [DELFT HYDRAULICS (1995)].

Model of Takahashi et al.

Takahashi et al. [TAKAHASHI et al. (1993)] have developed a theoretical model to describe the generation mechanism of impact pressures. Different models have been developed for each type of pressure. The type of impact pressure changes with the amount of trapped air. The model for the Wagner type pressure is discussed in this section. In section 3.4 the model for the transition type pressure is discussed and in section 3.5 discusses the model for the Bagnold type pressure.

Nota bene: The other models which are described in this chapter also take the atmospheric pressure (p_0 or p_{atm}) into account when the maximum wave impact pressure is calculated. Takahashi et al. omit do this. So the atmospheric pressure has to be added afterwards if the results of the theory of Takahashi et al. [TAKAHASHI et al. (1993)] are compared to the results of the other theories which are described in this chapter (see section 3.6).

The three models are defined for three different regions of the attack angle (β) of the wave front surface against the wall. A special feature of the model is that the wave front surface has a curvature defined by the tangential angle (δ) to the cord of the curved wave front as shown in figure 3.1.

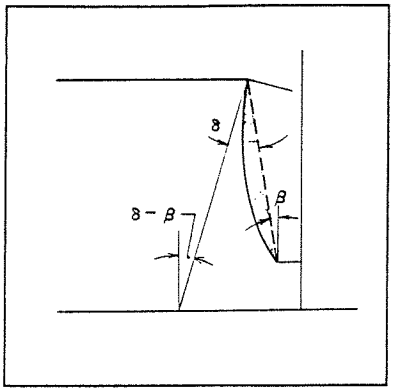

fig. 3.1 Diagram showing the curved wave front for the impact pressure generation model [TAKAHASHI et al. (1993)]

Therefore a small amount of air is trapped even when the attack angle (β) is zero and Bagnold type pressure acts when $0 \geq \beta$. Wagner type pressure acts when the attack angle is $\beta \geq \delta$ and is also assumed to act in the transition region of $\delta > \beta > 0$ (see figure 3.2) even though the pressure is changed due to the trapped air. Takahashi et al. [TAKAHASHI et al. (1993)] found that at $\beta \approx 20°$ the transition is between the Wagner type pressure and the transition type pressure. When $\beta \approx 20°$ the maximum pressure of the Wagner type occurs (see figure 3.3). As mentioned before, the three regions (see figure 3.2) are discussed respectively in this section, section 3.4 and section 3.5.

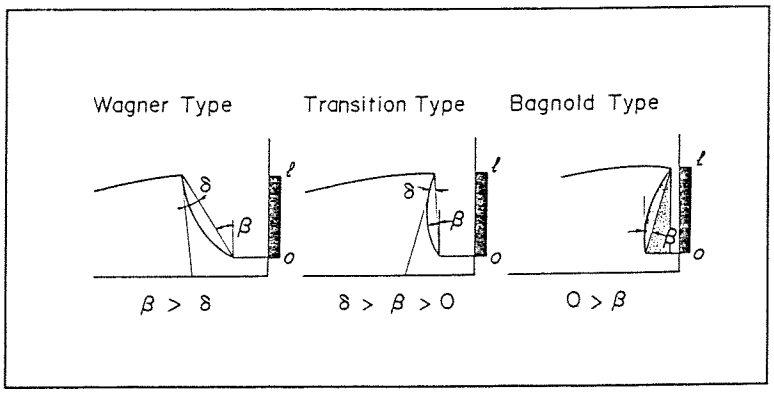

fig. 3.2 Wave action models for the three applied regions [TAKAHASHI et al. (1993)]

Figure 3.3 gives an idea of the magnitude of the three types of impact pressures compared to each other, calculated with the three models of Takahashi et al. [TAKAHASHI et al. (1993)]

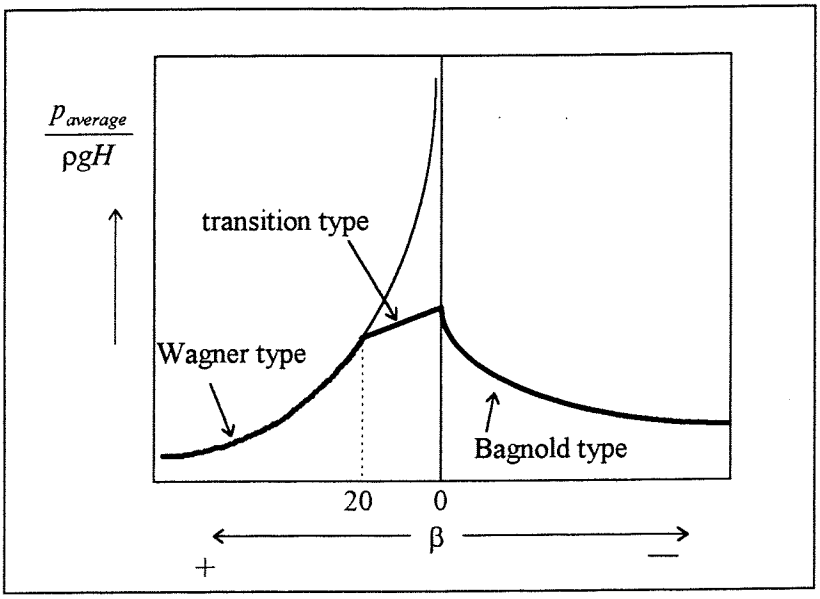

fig. 3.3 Impact pressure versus the angle β [TAKAHASHI et al. (1993)]

Figure 3.3 shows again that the most severe impact pressures take place in the transition region between the Wagner type pressure and the Bagnold type pressure.

When $\beta \geq \delta$, the Wagner type pressure acts (see figure 3.4) and the wave front hits the vertical wall with the height ($l = \kappa_l H$), speed (u_0) and angle (β). The impact pressure acts along l of the wall. Using the Wagner theory, [TAKAHASHI et al. (1983)] the pressure $p(z,t)$ is (for the definition $z = 0$, the lowest point of the impact pressure, and $z = l$, the highest point of the impact pressure, see figure 3.4):

$$p(z,t) = \frac{1}{2}\rho u_0^2 \kappa_m^2 \left\{ \frac{\pi \cot\beta}{\sqrt{1-\left(\frac{x}{b(t)}\right)^2}} - \frac{\left(\frac{x}{b(t)}\right)^2}{1-\left(\frac{x}{b(t)}\right)^2} \right\} \tag{3.20}$$

$$b(t) = \frac{\pi}{2u_0 t \cot\beta} \tag{3.21}$$

In which:

κ_m = added mass correction factor
κ_l = impact height coefficient

Equation 3.20 is similar to equation 3.17, the only differences are that the (slamming) coefficient k is replaced by a different coefficient and the atmospheric pressure is not added.

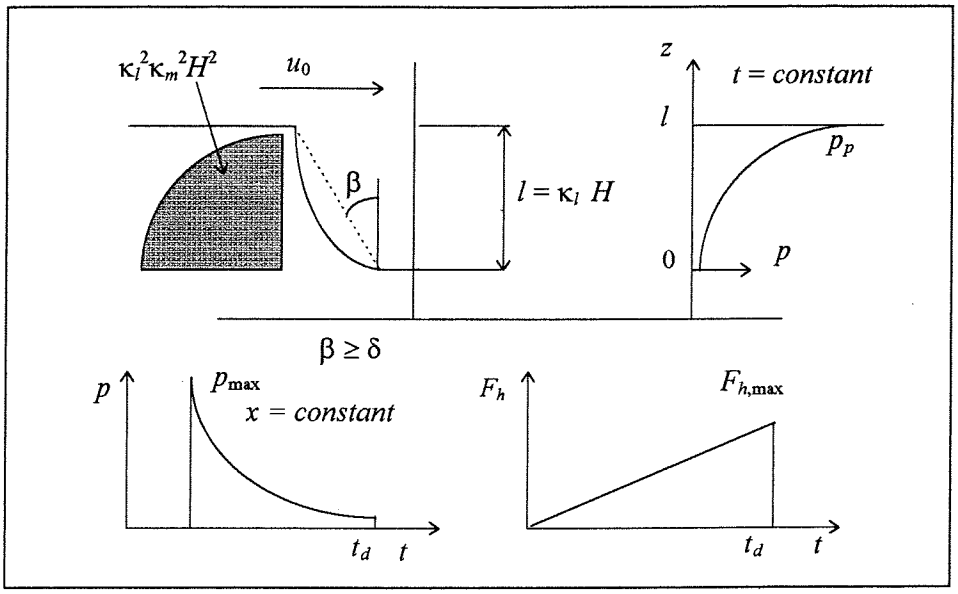

fig. 3.4 Collision of a wave front on a vertical wall ($\beta \geq \delta$) [TAKAHASHI et al. (1993)]

The peak pressure p_{max} of $p(x)$ is:

$$p_{max} = \frac{1}{2}\rho u_0^2 \kappa_m^2 \left(\frac{\pi^2}{4} \cot^2 \beta + 1 \right) \tag{3.22}$$

The total impact force $F_h(t)$ on the wall increases linearly with the time t, reaches its peak $F_{h,max}$ and instantaneously goes to zero. The peak value $F_{h,max}$ and the average peak pressure $p_{max,average}$ along l ($= \kappa_l H$) are related as:

$$p_{max,average} = \frac{F_{h,max}}{\kappa_l H} = \frac{\rho \pi^2 u_0^2 \kappa_m^2}{4} \cot\beta \tag{3.23}$$

The duration time t_d of F_h is:

$$t_d = \frac{\kappa_l H}{\frac{\pi}{2} u_o \cot\beta} \tag{3.24}$$

It should be noted that the impact pressure only acts where the water surface hits the vertical wall ($z = 0$ to l), with $p_{max,average}$ being the average peak pressure within this particular region. Although the peak pressure at each point is quite high, the average peak pressure is lower since the high pressure moves from $z = 0$ to l as defined by equation 3.20. This is the typical feature of the Wagner type pressure [TAKAHASHI et al. (1993)].

3.4 Model for transition type pressure

The model Takahashi et al. [TAKAHASHI et al. (1993)] have made for the transition type pressure (see also sub-section 2.4.3 and figure 2.8b) uses the model for the Wagner type pressure described in the previous section. When $0 < \beta < \delta$, it is assumed that the impact pressure can be modelled as Wagner type pressure and also that the peak pressure is decreased and the duration time increased by the existence of air (see figure 3.2). This effect is expressed by the equivalent angel β^* which is used in this region instead of β, i.e.:

$$\beta^* = \beta_0 + \frac{\delta - \beta_0}{\delta}\beta \tag{3.25}$$

$$\beta_0 = \tan\left\{\frac{2}{\pi\kappa_m^2}\left[\frac{p_{max}}{\frac{1}{2}\rho u_0^2}\right]_{\beta=0}\right\} \tag{3.26}$$

In figure 3.3 can be seen that the adapted angle described in equation 3.25 and 3.26 reduces the average impact pressure calculated with the equation of the Wagner type pressure (equation 3.23). If the adapted angle, described in equation 3.25 and 3.26, was not used, the impact pressures would grow infinite (see figure 3.3). The Wagner type pressure becomes infinite if $\beta \rightarrow 0$ (see equation 3.23).

3.5 Models for Bagnold type pressure

When there is some air trapped between the water surface and the structure and this air is compressed, the air compression model can be used. This model can be used to describe the Bagnold type wave impacts (see also sub-section 2.4.4 and figure 2.8c). With this model not only the maximum impact pressure can be calculated but it also gives information about the duration of the impact and the frequency of the oscillating air pocket which is trapped between the breaking wave and the plane vertical wall of a breakwater. More information about the phenomenon of oscillating air pockets which can cause low frequency force oscillations on the vertical front wall of a vertical breakwater can among other things be found in sub-section 2.4.4 and chapter 5.

Breaking waves of the plunging type can cause large amounts of trapped air (see among other things figure 2.8c). Air entrapment can also occur where vertical and horizontal slabs come together. The air will not equally be compressed on a large surface; there normally is an angle between the approaching water surface and the surface of the structure and therefore the trapped air will be pushed to the corners. Where the water surface hits the structure first, the air compression model is not valid. The quantity of air that is considered in the air compression model is one order of magnitude larger than the quantity of air in the shock wave model. In the shock wave model, the compression of the air is isotherm ($\gamma = 1.000$; no temperature change during the compression). In the air compression model the compression will be adiabatic ($\gamma = 1.405$; no heat exchange with the vicinity during the compression) because the volume of the trapped air is relatively large.

In this section the models of Bagnold [BAGNOLD (1939)] and Takahashi et al. [TAKAHASHI et al. (1993)] are treated.

Model of Bagnold

Bagnold [BAGNOLD (1939)], was the first to formulate an equation for the compression of air that is trapped along with a wave impact. He considered piston model as reproduced in figure 3.5; the spring element is the trapped air, the water mass is the piston.

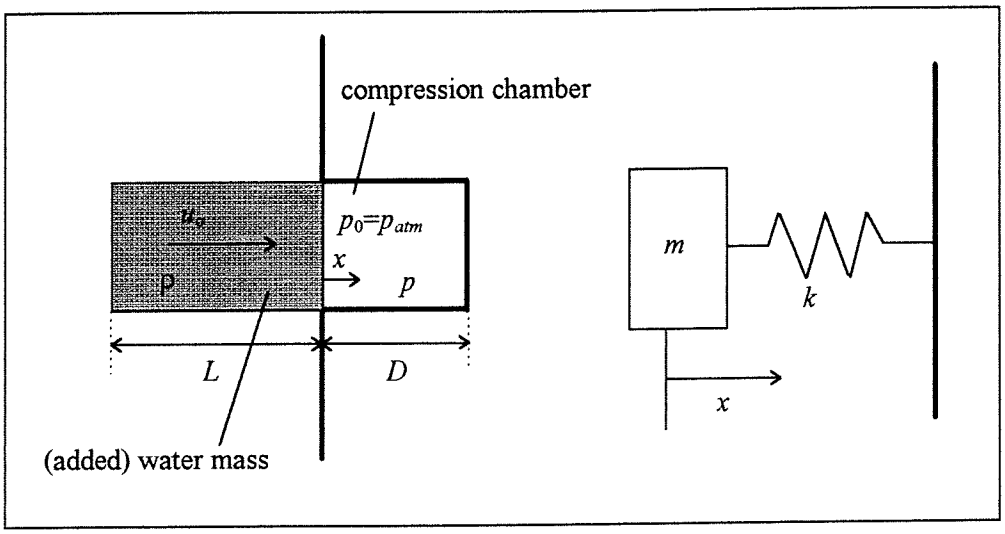

fig. 3.5 Bagnold's piston model [DELFT HYDRAULICS (1995)]

The water mass m can be determined by an added water mass consideration and is equal to ρL per unit piston surface.

The stiffness of the air is assumed constant (linear approximation). This is only allowed when the air is compressed not too much. The initial pressure p_0 in the compression chamber is equal to the atmospheric pressure p_{atm}. According to Poisson:

$$p(D-x)^{\gamma} = constant \tag{3.27}$$

The differentiation of equation 3.27 has the following result (see equation 3.7):

$$dp(D-x)^{\gamma} - \gamma p(D-x)^{\gamma-1} dx = 0 \tag{3.28}$$

When the compression of the air is small than $x \approx D$ and $p \approx p_0 = p_{atm}$ is valid. The stiffness k of the air per unit piston surface is:

$$k = \frac{dp}{dx} = \frac{\gamma p_0}{D} \tag{3.29}$$

The differential equation for the mass-spring system can be written as:

$$\rho L \frac{d^2x}{dt^2} + \frac{\gamma p_0}{D} x = 0 \tag{3.30}$$

in which:

$$x = (p-p_0)/k \tag{3.31}$$

The solution of the differential equation described in equation 3.30 and 3.31 is:

$$p - p_0 = u_0\sqrt{\frac{\gamma p_0 \rho L}{D}}\sin\left(\sqrt{\frac{\gamma p_0}{D\rho L}}\right)t \tag{3.32}$$

This is an oscillation that is not damped. The maximum pressure is:

$$p_{max} = p_0 + u_0\sqrt{\frac{\gamma p_0 \rho L}{D}} \tag{3.33}$$

The period of the oscillation is:

$$T = 2\pi\sqrt{\frac{D\rho L}{\gamma p_0}} \tag{3.34}$$

Ramkema has measured frequencies of prototype wave impact low frequency force oscillations. The frequencies measured and those calculated with Bagnold's theory show (see equation 3.34) good similarity [DELFT HYDRAULICS (1979)]. The pressure calculated with this Bagnold air compression model proves to give the same (calculated) pressure as with the linear shock wave model when $(1-\alpha)/\alpha = L/D$ (compare equation 3.11 to equation 3.33), so when the relations between the volume of water and the volume of air are equal. In reality the content of air of an air-water mixture is not higher than about 1 %. The quantity of air, trapped along with a wave impact, can substantially be bigger. Therefore the linear air compression model will lead to a lower pressure than the linear shock wave model [DELFT HYDRAULICS (1995)], [RAMKEMA (1978)].

Model of Takahashi et al.

The model of Takahashi et al. [TAKAHASHI et al. (1993)] includes also Bagnold type pressure (see figure 3.2). When $\beta = 0$, air is trapped due to the curvature of the wave front (see figure 3.2) having a volume which increases as the absolute value of β increases ($0 \geq \beta$, see also figure 3.3). The air compression pressure can be obtained by the thickness of the air layer D, the with L of the water mass compressing the air and the speed u_0 of the compressing water.

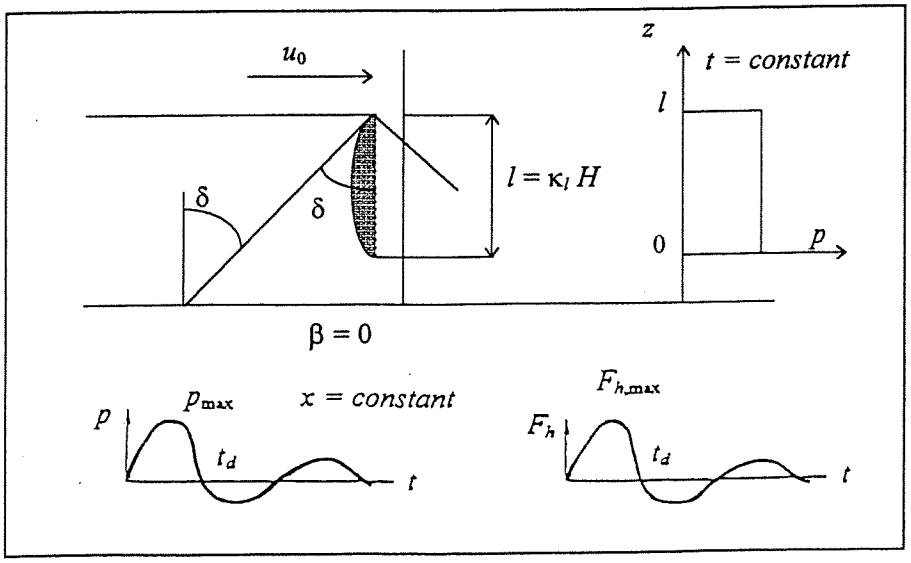

fig. 3.6 Collision with trapped air ($\beta = 0$) [TAKAHASHI et al. (1993)]

The average thickness of the air layer D is defined by:

$$D = \kappa_a l \tag{3.35}$$

$$\kappa_a = \kappa_{a0} + 0.5\tan|\beta| \tag{3.36}$$

$$\kappa_{a0} = \frac{1}{4}\left(\frac{\delta}{\sin^2\delta} - \cot\delta\right) \tag{3.37}$$

In which:

κ_{a0}= the minimum air thickness coefficient at $\beta = 0$
κ_a = air thickness coefficient for $\beta < 0$

The effective width L of the water mass compressing the air is:

$$L = \frac{\pi}{4}\kappa_m^2 \kappa_l H \tag{3.38}$$

The pressure due to the compression of the air layer is obtained by solving a set of differential equations, representing D, L and u_0. The impact pressure is assumed to act on the wall where the water surface entraps the air (z = 0 to l). The impact pressure is a sinusoidal oscillation with relatively high damping. The impact pressure is assumed to simultaneously act only within z = 0 to l with the same intensity, even though the air compression pressure propagates in the water. The peak pressure p_{max} can be estimated with figure 3.7 using the Bagnold number which is defined as:

$$\frac{\rho\pi\kappa_m^2 u_0^2}{4p_0\kappa_a} = \frac{\rho L u_0^2}{p_0 D} \tag{3.39}$$

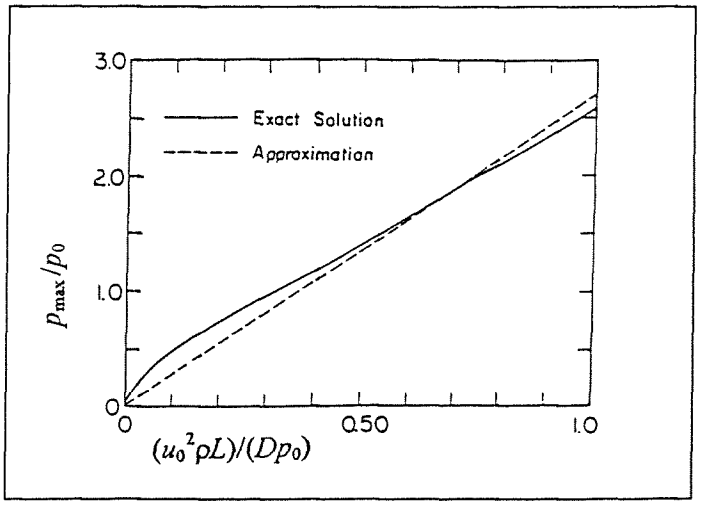

fig. 3.7 Pressure due to air compression versus Bagnold number [TAKAHASHI et al. (1993)]

The approximate linear solution of the theoretical equations is shown in figure 3.7, where p_{max} / p_0 is proportional to 2.7 times the Bagnold number. The air compression pressure can be approximated by a damping oscillation, with p_{max} being:

$$p_{max} = p_{max,average} = 1.6\left(\frac{\rho L u_0^2}{D p_0}\right) p_0 \tag{3.40}$$

Equation 3.40 is considered to provide a good approximation of the exact solution, especially for impact pressures on a prototype vertical breakwater. Note that the exact solution does take air leakage during air compression into account. In the approximate linear solution presented here this air leakage is neglected.

The oscillation period is approximated by:

$$T = 2\pi\sqrt{\frac{\pi\rho\kappa_m^2\kappa_l^2\kappa_a H^2}{4\gamma p_0}} \tag{3.41}$$

where $\gamma = 1.405$ for adiabatic compression. This approximation is in fact the same as equation 3.34 which was found before for the linear air compression model.

3.6 Summary of the analytical models

In this section a summary of the different analytical models is given and for each analytical model the maximum wave impact pressure will be calculated for a prototype situation.

The period of the oscillation of the air pocket of the Bagnold type pressure will also be given for this prototype situation

The following situation is considered:

p_0 = $1.01325*10^5$ N/m^2 ($= p_{atm}$)
c_w = 1480 m/s
u_0 = 10 m/s
γ = 1.000 (isotherm compression) → α = 0.1%
γ = 1.405 (adiabatic compression) → α = 5.0%
K_a = $1.000*10^5$ N/m^2 (isotherm compression); $1.405*10^5$ N/m^2 (adiabatic compression)
K_w = $2.2*10^9$ N/m^2
ρ = 998 kg/m^3 (fresh water is used in these computations)
ρ_c = 2100 kg/m^3
E_c = $2.85*10^{10}$ N/m^2
c_c = 3680 m/s
k = 6
κ_{a0} = 0.06 → $\beta = 0°$ → κ_a = 0.06 → D = 0.15 m
→ $\beta = \pm 20°$ → κ_a = 0.24 → D = 0.6 m
κ_l = 0.5
κ_m = 0.9
H = 5 m
l = 2.5 m
L = 1.6 m

SHOCK WAVE MODEL:

- **Wave impact on a rigid wall:**

$$\Delta p = p_{max} - p_0 = \rho c_w u_0 \qquad (3.1)$$

$$p_{max} = 1.01325*10^5 + 998*1480*10 = 14872 \text{ kN/m}^2$$

- **Rigid wall and air -water mixture:**

$$\Delta p = u_0 \sqrt{\frac{\gamma p_0 (1-\alpha)\rho}{\alpha}} \qquad (3.11)$$

$$p_{max} = 1.01325*10^5 + 10* \sqrt{\frac{1.000*1.01325*10^5*(1-0.001)*998}{0.001}} = 3280 \text{ kN/m}^2$$

(the water contains a small amount of air: 0.1%)

A small amount of air does significantly reduce the wave impact pressure as it can be seen when the results of equation 3.1 and 3.11 are compared to each other.

Führböter:

$$\Delta p = p_{max} - p_0 = \rho c_w u_0 \frac{1}{1+\alpha\left(\frac{K_w}{K_a}-1\right)} \qquad (3.12)$$

$$p_{max} = 1.01325*10^5 + 998*1480*10* \frac{1}{1+0.001\left(\frac{2.2*10^9}{1.000*10^5}-1\right)} = 744 \text{ kN/m}^2$$

(the water contains a small amount of air: 0.1%)

- **Wave impact on a compressible wall:**

$$\Delta p = \rho c_w u_0 \frac{1}{1+\frac{\rho c_w}{\rho_c c_c}} \qquad (3.16)$$

$$p_{max} = 1.01325*10^5 + 998*1480*10* \frac{1}{1+\frac{998*1480}{2100*3680}} = 12502 \text{ kN/m}^2$$

The reduction of the wave impact pressure as a result of a compressible wall is much smaller than due to a small amount of trapped air (0.1%) as it can be seen when the results of equation 3.11 and 3.12 are compared to the results of equation 3.16.

MODELS FOR WAGNER TYPE PRESSURE:

Flow pressure model:

$$p_{max} - p_0 = \frac{\rho L u_0^2}{D} = k\left(\frac{1}{2}\rho u_0^2\right) \qquad (3.17)$$

$$p_{max} = 1.01325*10^5+6*(\frac{1}{2}*998*10^2) = 401 \text{ kN/m}^2$$

Takahashi et al.:

$$p_{max} = \frac{1}{2}\rho u_0^2 \kappa_m^2\left(\frac{\pi^2}{4}\cot^2\beta + 1\right) \qquad (3.22)$$

(including the atmospheric pressure, the maximum Wagner type pressure occurs for $\beta = 20°$ as can be seen in figure 3.3)

$$p_{max} = 1.01325*10^5+\frac{1}{2}*998*10^2*0.9^2\left(\frac{\pi^2}{4}\cot^2 20 + 1\right) = 895 \text{ kN/m}^2$$

MODEL FOR TRANSITION TYPE PRESSURE:

The maximum pressure occurs when $\beta = 0$ and is equal to the maximum pressure for the Bagnold type pressure according to Takahashi et al. (see figure 3.3).

MODELS FOR BAGNOLD TYPE PRESSURE

Model of Bagnold:

$$p_{max} = p_0 + u_0\sqrt{\frac{\gamma p_0 \rho L}{D}} \qquad (3.33)$$

$$p_{max} = 1.01325*10^5+10\sqrt{\frac{1.405*1.01325*10^5*998*1.6}{0.6}} = 296 \text{ kN/m}^2$$

The period of the oscillation is:

$$T = 2\pi\sqrt{\frac{D\rho L}{\gamma p_0}} \qquad (3.34)$$

$$T = 2\pi\sqrt{\frac{0.6*998*1.6}{1.405*1.01325*10^5}} = 0.52 \text{ s.}$$

The magnitude of the period and the maximum pressure is calculated for the case that a relatively large air pocket is trapped (D = 0.6 m and γ = 1.405), which is typical for the Bagnold type pressure. As has been indicated before in chapter 2, a period is found which magnitude is in the range of the eigenperiods of a vertical breakwater of the caisson type (e.g. 0.2 - 0.8 s). Dynamic amplification of the displacement of a vertical breakwater may occur when it is exposed to an impact load with a low frequency force oscillation - due to a large trapped air pocket - which is in the range of the natural periods of the breakwater (see sub-section 2.4.4, chapter 5 and section 10.6).

Takahashi et al.:
The model of Takahashi et el. [TAKAHASHI et al. (1993)] gives almost the same value of the maximum pressure as mentioned above, when $D = 0.6$ m and $\gamma = 1.405$.

The maximum pressure of a Bagnold type wave impact in the model of Takahashi et al. [TAKAHASHI et al. (1993)] occurs when $\beta = 0$ (see figure 3.3) and this is the upper limit for this model.

The maximum pressure can be determined, using figure 3.7:

$$\frac{\rho\pi\kappa_m^2 u_0^2}{4p_0\kappa_a} = \frac{\rho L u_0^2}{p_0 D} = \frac{998*1.6*10^2}{1.01325*10^5*0.6} = 2.63 \qquad (3.39)$$

p_{max}/p_0 can not be determined in figure 3.7, but its value will be approximately (including the atmospheric pressure):

$p_{max} = 1.01325*10^5 + 1.6*2.63*1.01325*10^5 = 528$ kN/m^2 (see equation 3.40)

The approximation of the period of the force oscillations using the Takahashi et al. model is, when $\beta = -20°$:

$$T = 2\pi\sqrt{\frac{\pi\rho\kappa_m^2\kappa_l^2\kappa_a H^2}{4\gamma p_0}} \qquad (3.41)$$

$$T = 2\pi\sqrt{\frac{\pi*998*0.9^2*0.5^2*0.24*5^2}{4*1.405*1.01325*10^5}} = 0.51 \text{ s}$$

which is in fact almost the same as found before for the air compression model of Bagnold (equation 3.34)

Conclusion:
The maximum wave impact pressures - of the models described in this chapter - differ substantially. Dependent on the prototype situation, one of the models can be chosen to make a first approximation of the maximum wave impact pressure which may occur.

Equations 3.34 and 3.41 show that the period of the oscillation of the Bagnold type pressure may be in the range of the natural period of a vertical breakwater of the caisson type. This can be dangerous (see section 10.6).

3.7 Wave impact pressures caused by full-scale sea waves

In this section different wave impact pressure records can be found in figure 3.8 to 3.10. These are records of pressure impulses caused by full-scale sea waves in Dieppe (France). In figure 3.8 to 3.10 the unity *tonnes per square metre* is used, 1 *tonne per square metre* is approximately equal to 10 kN/m^2. The wave impact pressure records can be found in [ROUVILLE et al. (1938)] and [BAGNOLD (1939)].

- In figure 3.8 the largest measured full-scale wave impact pressure ever is sketched. In Dieppe (France) a wave impact pressure of 690 kN/m^2 has been measured on the 23rd of February 1937. The height of the breaking waves was found to be H_b = 2.5 m. Compare this impact pressure of 690 kN/m^2 to the results found by the general analytical models described in the previous section. In figure 3.19 it can be seen that t_r = 20 ms and t_d = 50 ms.

- In figure 3.9 a wave impact pressure history is sketched which is caused by breaking waves with a height of H_b = 4.0 m. The low frequency pressure oscillations can easily be seen in figure 3.9. The period of these oscillations is approximately 0.3 sec. This datum fits perfectly well in the equation given in the previous chapter which describes the relationship between the wave height and the period of the low frequency force or pressure oscillations (H in cm, the derivation of this equation will be given in chapter 5):

$$T_{0w} = 0.75*10^{-3}*H \qquad (2.11)$$

- In figure 3.10 a wave impact pressure history is sketched which is caused by breaking waves with a height of H_b = 2.9 m. The period of the first cycle of the oscillations is approximately 0.15 s.

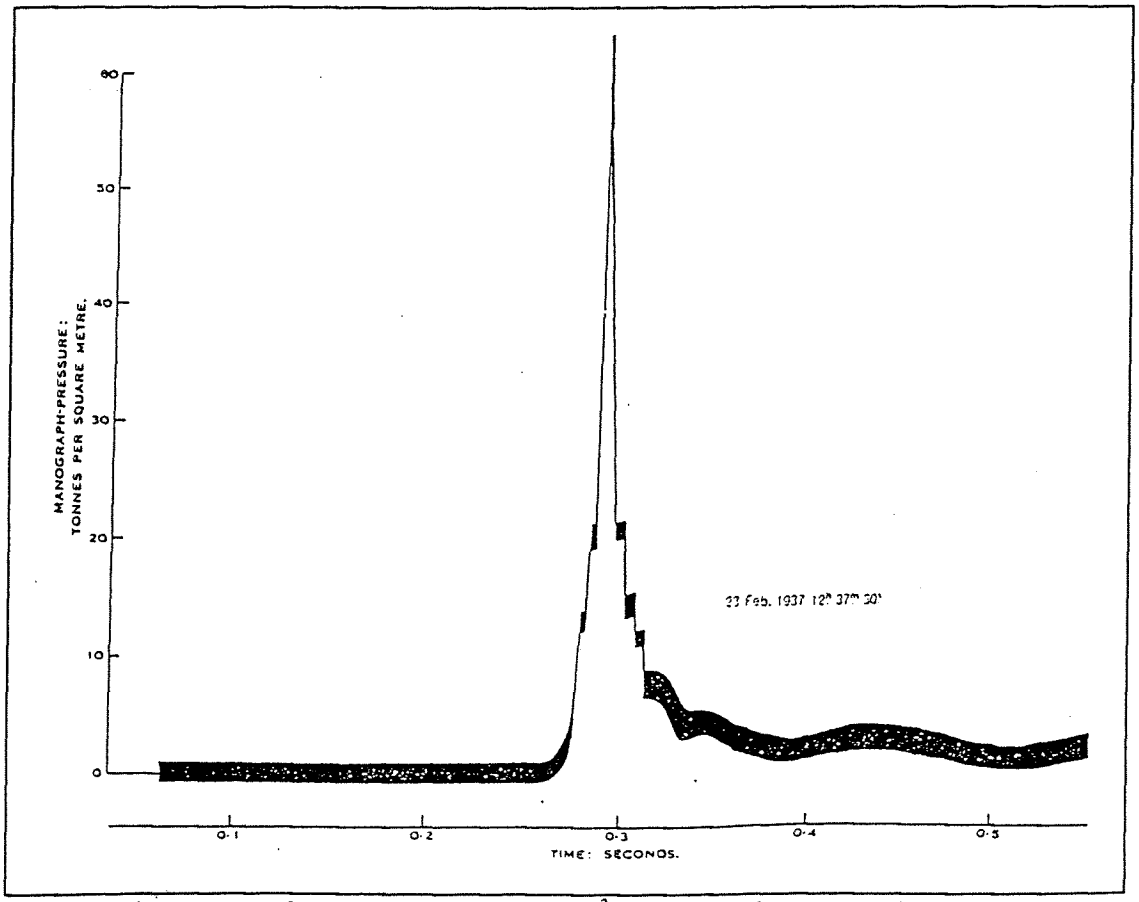

fig. 3.8 Highest measured wave pressure ever: 690 kN/m^2 , H_b = 2.5 m [BAGNOLD (1939)]

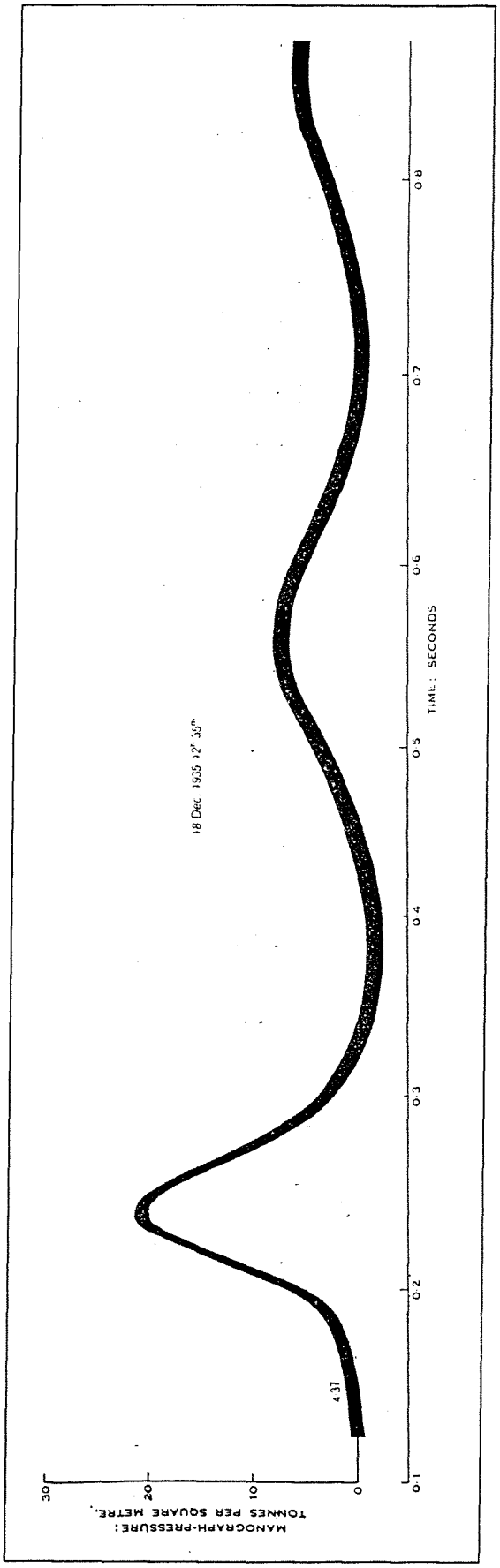

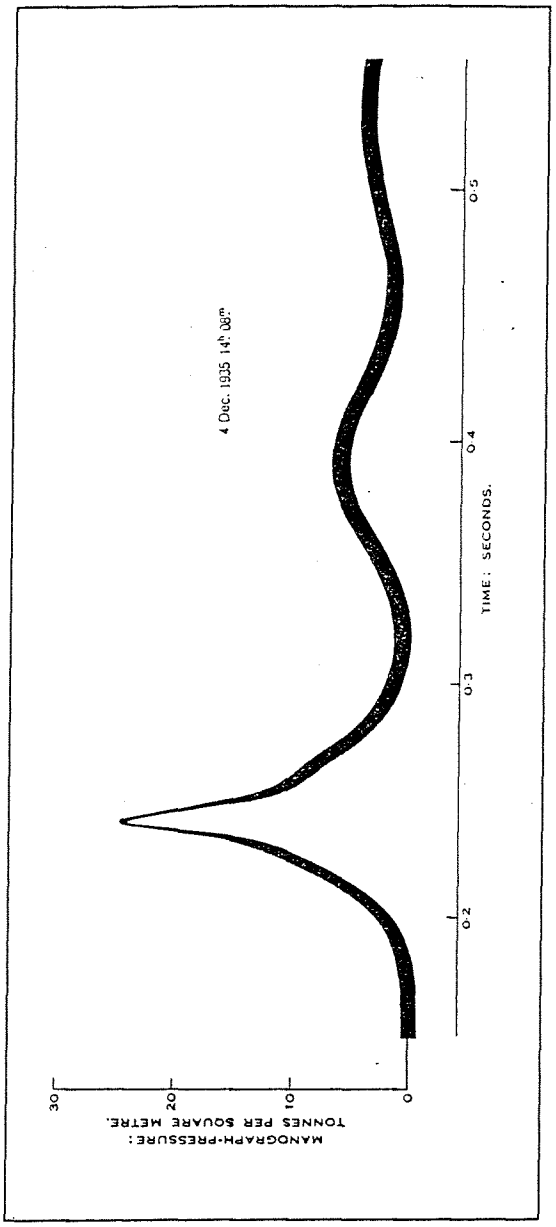

fig. 3.10 Wave impact pressure history with low frequency force oscillations, T_{0w} = 0.15 s, H_b = 2.9 m [BAGNOLD (1939)]

fig. 3.9 Wave impact pressure history with low frequency force oscillations, T_{0w} = 0.3 s, H_b = 4.0 m [BAGNOLD (1939)]

4 Wave impact forces and momentum

4.1 Introduction

In this chapter the derivation of a prediction formulae for maximum horizontal wave impact forces will be treated. In this chapter only a triangular wave impact force history is assumed (as it has been described in chapter 2 before). So, there is taken no account of the effect of pulsating air pockets etc.. One of the derivations has been published by Klammer et al. [KLAMMER et al. (1996)] and will be reflected here again in section 4.2, together with an analysis of the important parameters of this formula. In section 4.3 some other horizontal wave impact force prediction formulae are given as well. An analysis of the total amount of momentum of a wave impact is given in section 4.4 and finally in section 4.5 brief attention is being paid to scaling of wave impacts from model tests to full scale situations.

Nota bene:

All prediction formula which are given in this chapter will be derived for one linear meter. So the SI- unity of $F_{h,\max}$, the maximum horizontal wave impact force, is a force per linear meter [N/m].

4.2 Derivation of a prediction formula for horizontal wave impact forces

Klammer et al. [KLAMMER et al. (1996)] have derived a formula for the maximum wave impact force using the momentum theory and the solitary wave theory. Missing parameters in the formula were obtained from PIV (particle image velocity) tests conducted at the University of Edinburgh [OUMERACI et al. (1995)]. The obtained formula has been compared to hydraulic model tests performed in the large wave flume of Hannover (GWK).

A breaking wave impinging on a vertical wall generally induces impulsive pressures on the wall which are difficult to predict in terms of their magnitude as well as in terms of their spatial and temporal distribution (see figure 4.1)

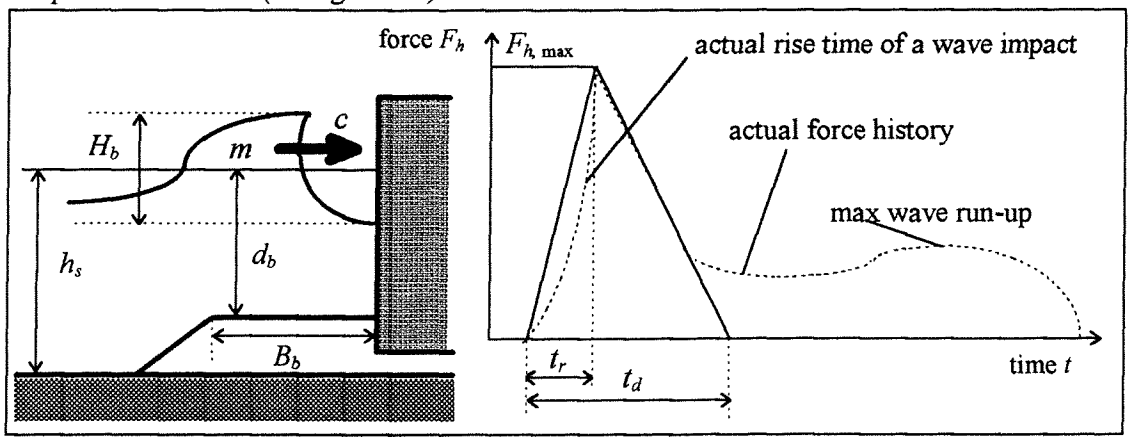

fig. 4.1 Impact loading of a vertical structure - definition sketch

The forward momentum of a fluid mass m hitting the a wall with a horizontal velocity c will induce a force impulse (see figure 4.1):

$$\int_0^{t_r} F_h(t) * \mathrm{d}t = m * c \qquad (4.1)$$

where t_r is the rise time of the peak force $F_{h,\max}$ and $F_h(t)$ is the horizontal force time function.

Assuming a linear temporal increase of the force $F_h(t)$, equation 4.1 yields:

$$^1/_2 * F_{h,\max} * t_r = m * c \tag{4.2}$$

thus leading to the peak force:

$$F_{h,\max} = 2 * \frac{m * c}{t_r} \tag{4.3}$$

The most difficulties encountered in applying equation 4.3 for the prediction of impact forces originate from the lack of information on the magnitude of the fluid mass m which is involved in the impact process and which accounts only for a small portion of the total mass M of the breaking wave impinging on the wall (k is a dimensionless mass parameter):

$$m = k * M \tag{4.4}$$

Assuming that the actual wave at breaking may be approximated by a solitary wave, its total mass M is given by the following relationship (see figure 4.2):

$$M = \rho_w * \sqrt{\frac{16}{3} * H_b * d_b^{\,3}} \tag{4.5}$$

The maximum horizontal velocity is approximated by (see figure 4.2):

$$c = \sqrt{g * (d_b + H_b)} \tag{4.6}$$

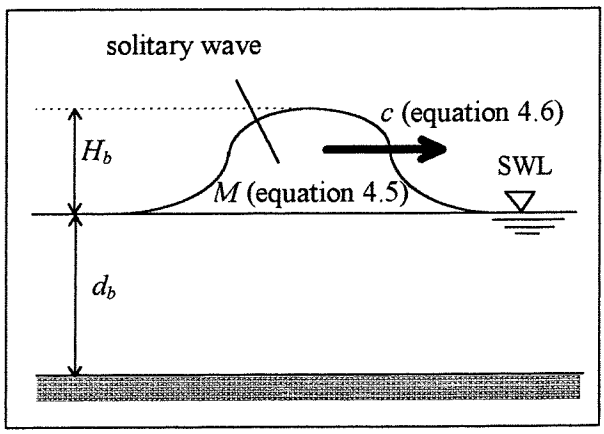

fig. 4.2 Definition sketch solitary wave

If the breaking criterion of equation 4.7 is used:

$$\frac{H_b}{d_b} = 0.78 \tag{4.7}$$

equations 4.5 and 4.6 can be written as:

$$c = \sqrt{g * d_b * (1 + 0.78)} = 1.33 * \sqrt{g * d_b} \tag{4.8}$$

$$M = \rho_w * \sqrt{\frac{16}{3} * H_b * \left(\frac{H_b}{0.78}\right)^3} = 3.35 * \rho_w * H_b^2 \tag{4.9}$$

The forward momentum of the fluid mass m involved in the impact process is obtained from equation 4.4, 4.8 and 4.9:

$$m * c = (k * M) * c = 4.47 * k * \rho_w * H_b^2 * \sqrt{g * d_b} \tag{4.10}$$

Considering equation 4.3, the dimensionless peak force is obtained as a function of the dimensionless rise time:

$$\frac{F_{h,\max}}{\rho_w * g * H_b^2} = k * 8.94 * \left(\frac{\sqrt{d_b / g}}{t_r} \right) = k * 8.94 * \left(\frac{t_r}{\sqrt{d_b / g}} \right)^{-1} \tag{4.11}$$

So far, this method is purely based on theoretical considerations. But the formula contains a non dimensional mass parameter k which represents the portion of the total mass of the breaking wave involved in the impact process. This parameter has to be determined experimentally for each breaker type because of the fact that for different breaker types different portions of the total fluid mass M are involved in the wave impact process.

According to Bagnold [BAGNOLD (1939)] the magnitude of k can be approximated by 0.2 ("... it is possible that the maximum value to be allowed for k may have to be slightly greater..."). Besides the mass parameter k, important parameters in equation 4.11 are the breaker height H_b, which is related to the breaker depth d_b - which is another important parameter - and the rise time t_r of the wave impact which is dependent on the breaker type. It must be noted that the breaker type determines the mass parameter and the rise time. The determination of the breaker height and the mass parameter will be treated below.

Estimation of the wave height H_b

An estimation of the incident wave height in the presence of a vertical structure can be made by using the formula which is given by Oumeraci et al. for irregular waves [OUMERACI et al. (1994a)]. In the formula, which is described in equation 4.12, the total reflection of the structure and its influence on wave breaking is considered by the reflection coefficient K_r.

$$H_b = L_b * \left[0.1025 + 0.0217 * \left(\frac{1 - K_r}{1 + K_r} \right) \right] * \tanh\left(\frac{2 * \pi * d_b}{L_b} \right) \tag{4.12}$$

In equation 4.12, d_b is the water depth at the breaking point of the wave and L_b is the wave length of the breaking wave. Equation 4.12 is sketched in figure 4.3 for different reflection coefficients K_r. Besides the breaking criterion for irregular waves which is described by equation 4.12 also the breaking criterion for regular waves are sketched in figure 4.3 [OUMERACI et al. (1994a)].

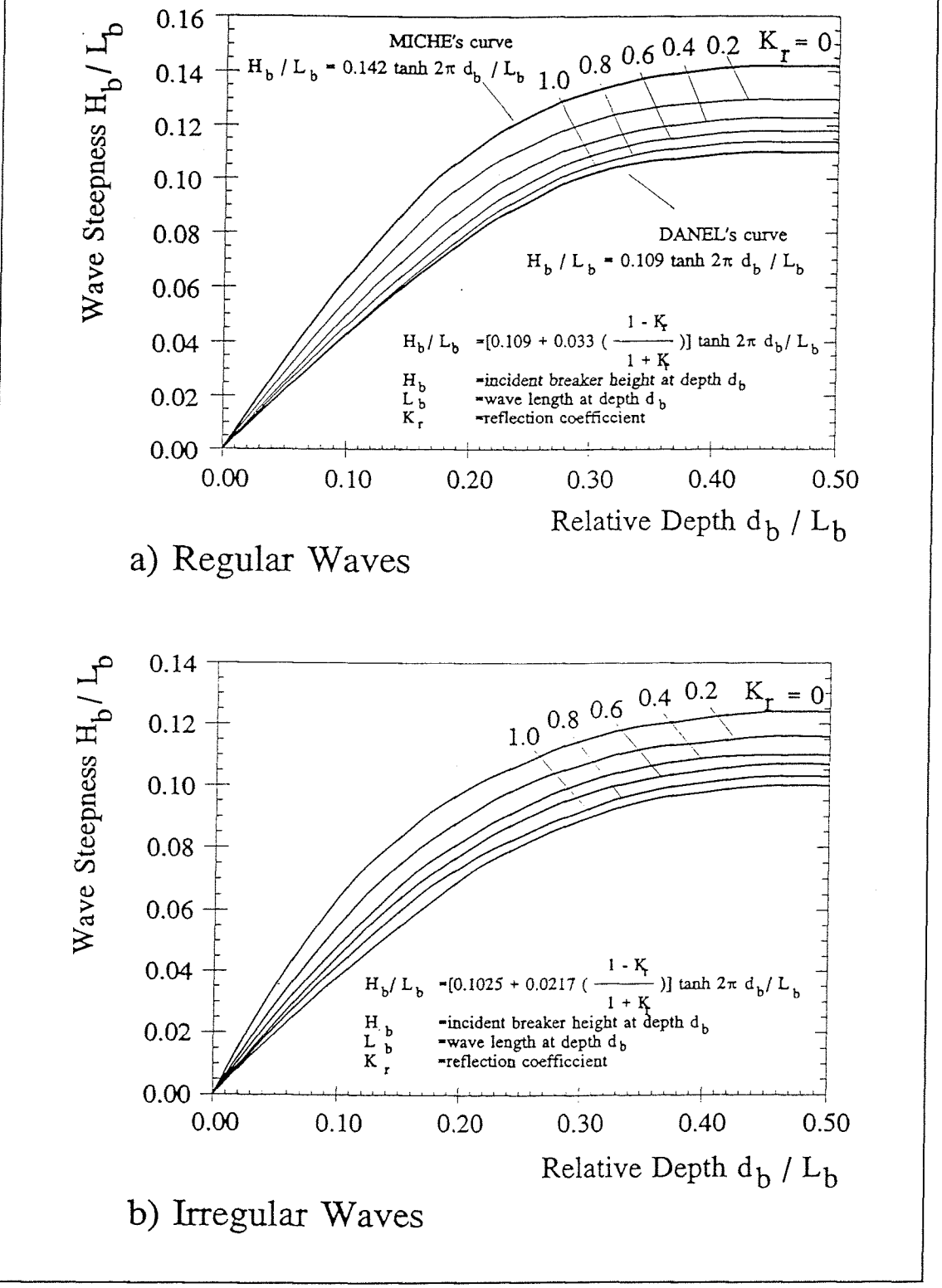

fig. 4.3 Breaking criteria in the presence of vertical structures for regular (a) and irregular (b) waves [OUMERACI et al. (1994a)]

The water depth in front of the structure can be regarded as the governing parameter for the magnitude of the resulting wave height H_b . It can be assumed that a relatively short berm in front of the structure (0. 15 $\geq$ (B_b /L_b) will only have a small influence on wave breaking. Therefore, it would not be correct to use the water depth d in front of the structure as an input ($d = d_b$) for equation 4.12. On the other hand using the water depth h_s (see figure 4.1) at the toe of the berm would certainly overestimate the breaker height as the influence of the berm on the breaking would be neglected. It is assumed that the berm width B_b , the wave length L_b and the lope of the berm 1 : m (in which m = cot α and α is the slope angle of the berm) will influenced the breaking of waves. Therefore an affective water depth d_m can be derived which takes into account the aforementioned parameters (see figure 1):

$$d_m = d + B_{rel} * m_{rel} * (h_s - d) \qquad (4.13)$$

In equation 4.13 B_{rel} is the part of the berm width which influences the effective water depth:

$$B_{rel} = 1 \qquad \text{for } B_b / L_b > 1 \qquad (4.14)$$

$$B_{rel} = 1 - 0.5 * B_b / L_b \qquad \text{for } B_b / L_b \leq 1$$

The parameter m_{rel} in equation 4.13 is a part of the slope of the berm which influences the effective water depth and is assumed to be:

$$m_{rel} = 1 \qquad \text{for } m < 1 \qquad (4.15)$$

$$m_{rel} = m - 0.5 \qquad \text{for } m \geq 1$$

For solitary waves the effective water depth d_m is very close to the depth h_s ($d_m = h_s$), so that B_{rel} = 1 and m_{rel} = 1. This is confirmed by comparing the calculated wave height using equation 4.12 and this assumption with measurements in the Large Wave Flume of Hannover (GWK). A relatively good agreement between measured and calculated values is also obtained for regular and random wave tests [KLAMMER et al. (1996)].

Experimental determination of the mass parameter *k*

Model tests in the wave flume at the University of Edinburgh were conducted to experimentally define the water mass m involved in the impact process under different loading conditions [OUMERACI et al. (1995)]. For three breaker types the mass parameter k could be determined using the particle image velocity (PIV) tests (see table 4.1 and figure 4.4 (note that the resultant wave impact force is slightly below Still Water Level (SWL) for the three different cases)):

BREAKER TYPE	MASS PARAMETER *k*
well developed plunging breaker with a large trapped air pocket	0.11
plunging breaker with a small trapped air pocket	0.16
upward deflected breaker	0.28

table 4.1 Mass parameter for different breaker types

It can be seen from table 4.1 that the value of the experimentally determined mass parameter k (0.11-0.28) has got the same order of magnitude as the average value k = 0.2 proposed by Bagnold [BAGNOLD (1939)].

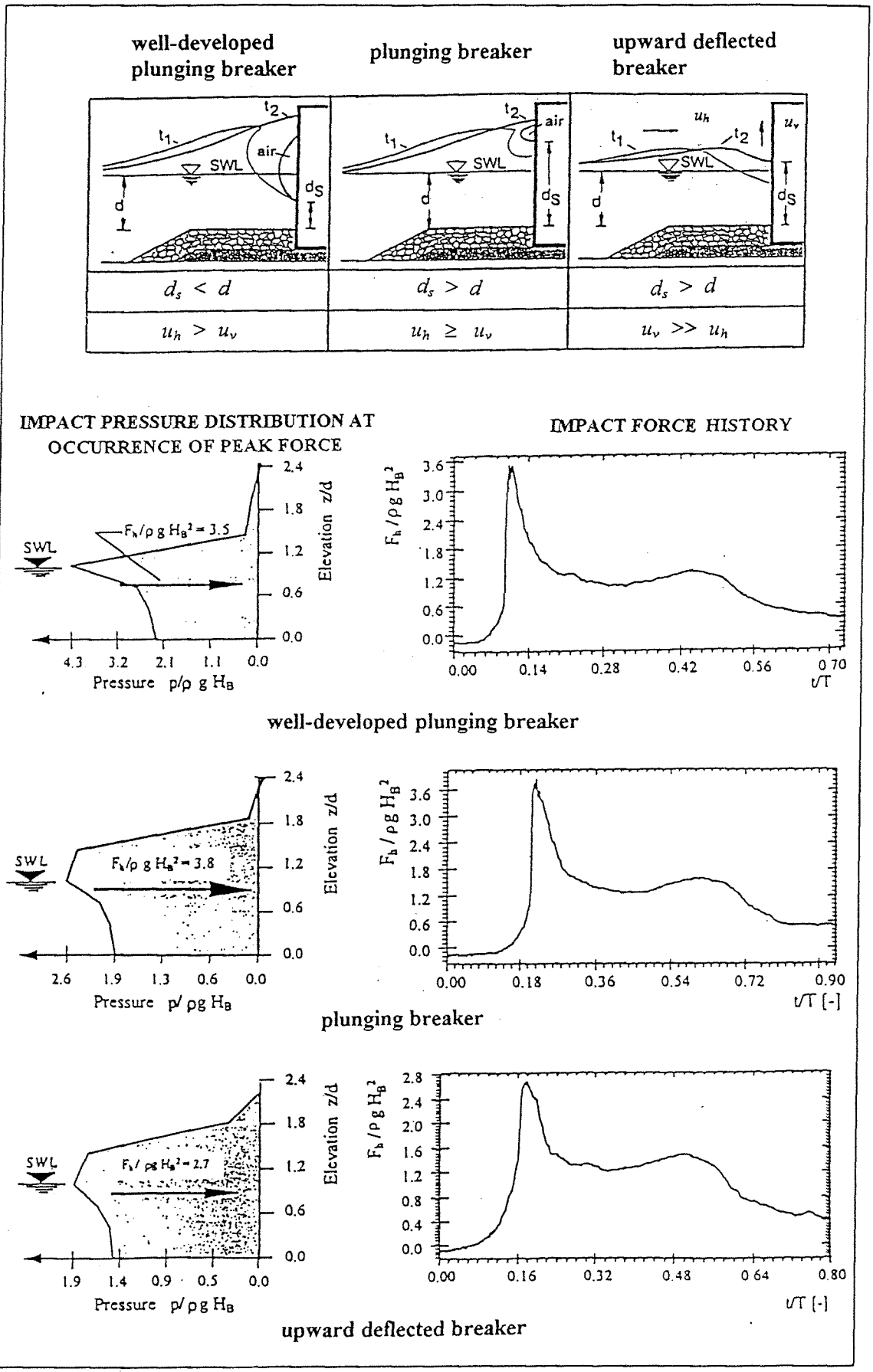

fig. 4.4 Different breaker types [OUMERACI et al. (1995)]

Prediction formula for impact loading of vertical structures

If k is chosen as 0.2 and substituted in equation 4.11, the following wave impact prediction formula can be derived (equation 4.16) presented in terms of a dimensionless peak force:

$$\frac{F_{h,\max}}{\rho_w * g * H_b^{\,2}} = 1.79 * \left(\frac{t_r}{\sqrt{d_b / g}} \right)^{-1} \tag{4.16}$$

Equation 4.16 is based on the assumption of a linear rise of the horizontal force to the maximum load as can be seen in figure 1 and this is reflected in equation 4.2. Actually the shape of this force increase is strongly dependent on the breaker types. Therefore a reduction factor k_r is introduced by Klammer et al. [KLAMMER et al. (1996)]. This reduction factor accounts for the different geometries of load histories in the case of breaking waves. The factor k_r is the value which has to be multiplied with the rise time t_r in order to obtain a triangle with the same area (force impulse). For the horizontal force this can be calculated as follows (see figure 4.5):

$$k_r = \frac{2 * I_{dyn,r}}{F_{h,\max} * t_r} \qquad \text{with } k_r < 1 \tag{4.17}$$

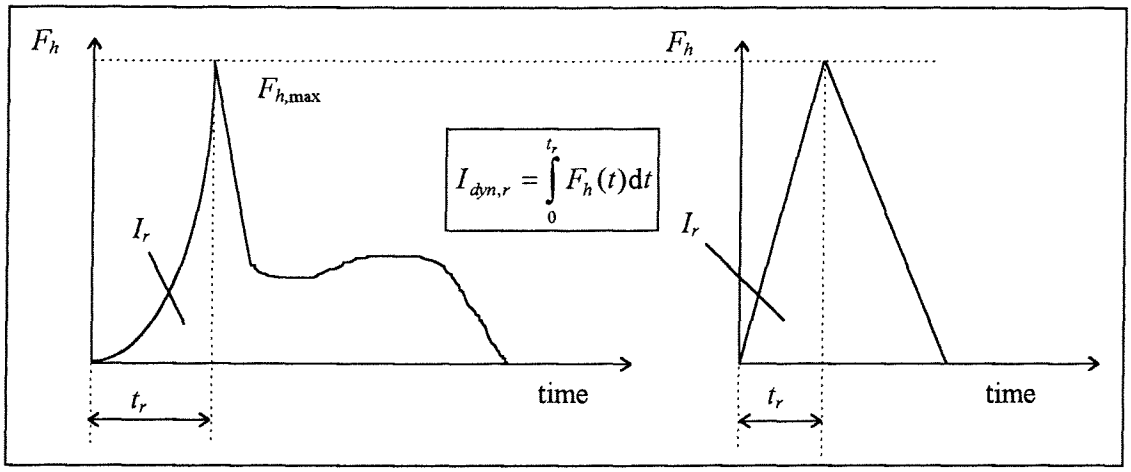

fig. 4.5 Substitution of the real force history by an equivalent triangular force

Using equation 4.17 is substituted in equation 4.11 the following result can be obtained, again presented in terms of a dimensionless peak or maximum force:

$$\frac{F_{h,\max}}{\rho_w * g * H_b^{\,2}} = \frac{k}{k_r} * 8.94 * \left(\frac{t_r}{\sqrt{d_b / g}} \right)^{-1} \tag{4.18}$$

The magnitude of the reduction factor k_r has been obtained from PIV measurements as well (see table 4.2.

BREAKER TYPE	REDUCTION FACTOR k_r
well developed plunging breaker with a large trapped air pocket	0.8
plunging breaker with a small trapped air pocket	0.8
upward deflected breaker	1.0

table 4.2 Reduction factor k_r for different breaker types

If k is chosen as 0.2 and k_r as 0.8 the following horizontal wave impact force prediction formula can be derived for the dimensionless maximum wave impact force:

$$\frac{F_{h,\max}}{\rho_w * g * H_b^{\,2}} = 2.24 * \left(\frac{t_r}{\sqrt{d_b / g}} \right)^{-1} \tag{4.19}$$

This prediction formula can be compared with measurements obtained from tests performed in the large wave flume of Hannover (GWK) [KORTENHAUS et al. (1994)] see figure 4.6. The wave types which were generated throughout the tests are among other things: solitary waves and random waves. Data of the tests is given in table 4.3:

	wave height (m)	wave period (s)	water depth (m)
SOLITARY WAVES	0.40 - 0.60	-	3.10 - 3.50
	0.65 - 1.10	-	3.50 - 3.90
RANDOM WAVES	0.30 - 1.10	3.50 - 3.60	3.70 - 4.30

table 4.3 Data of large scale model test

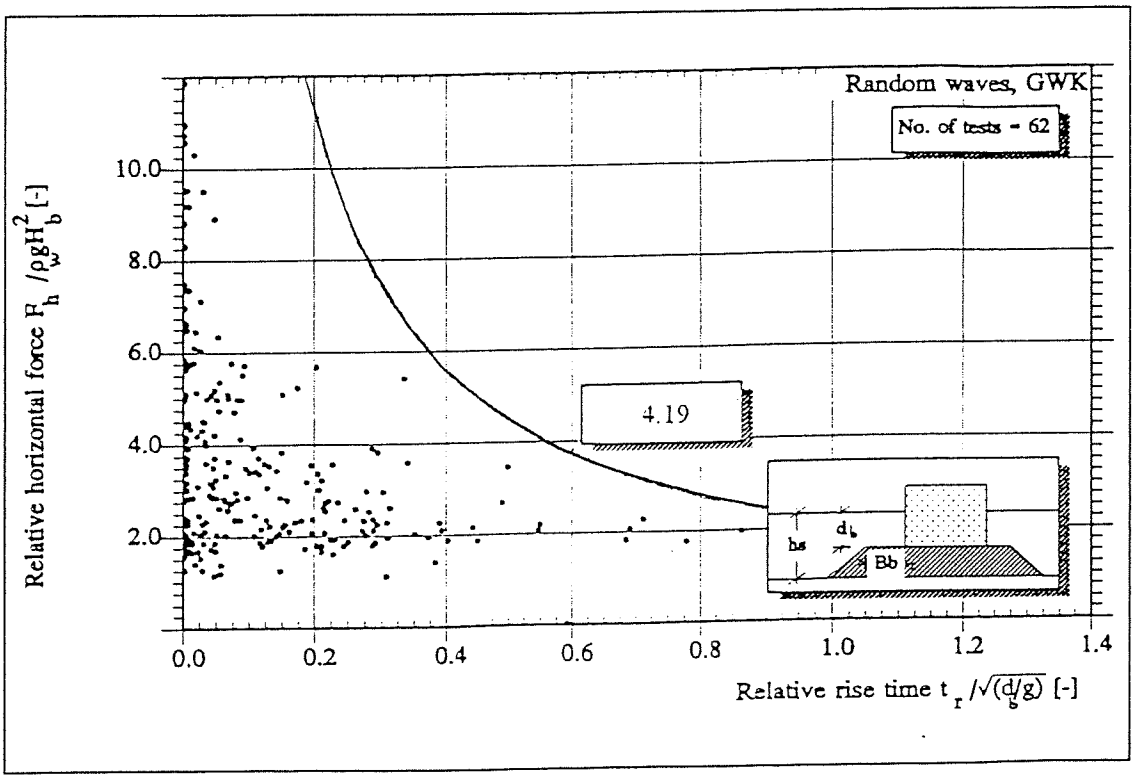

fig. 4.6 Comparison of the prediction formula to large-scale measurements (random waves) [KLAMMER et al. (1996)]

It can be seen from figure 4.6 that the prediction formula in equation 4.19 approximately represents the upper envelope to the random wave test results. This was to be expected because of the fact that a conservative approach, the solitary wave theory, was used. Therefore, for solitary waves the prediction formula better fits the data obtained from the model tests. (see figure 4.7).

From figure 4.6 and 4.7 it is obvious that the shorter the rise time of the wave impact, the higher the impact force. In fact the horizontal wave impact force can be infinite if the rise time of the wave impact approaches zero. According to Goda [GODA (1985)], [GODA (1994)], who is referring to different measurements in the past, the maximum dimensionless wave impact force on a vertical wall can be set about 15 (see equation 4.20). Goda's findings are treated more extensively in the next chapter where some other wave impact force prediction formulae will be treated as well.

$$\frac{F_{h,\max}}{\rho_w * g * H_b^{\,2}} = 15 \tag{4.20}$$

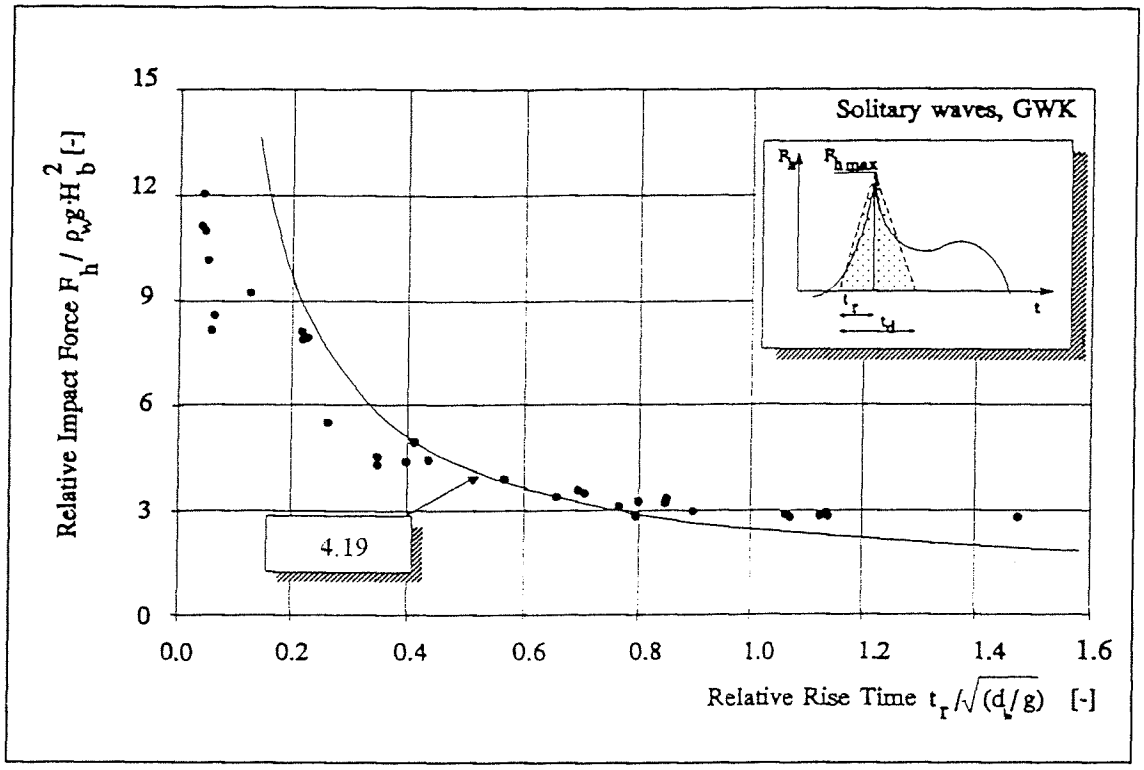

fig. 4.7 Comparison of prediction formula to large-scale measurements (solitary waves) [KLAMMER et al. (1996)]

4.3 Other prediction formulae for horizontal wave impact forces

In chapter 2 the horizontal wave impact force prediction formula derived by Schmidt et al. [SCHMIDT et al. (1992)] has already been given. This formula has been derived based on large scale model tests by using waves up to 2 m height and with wave periods of 9.4 s. (the experimental set-up of the tests has already been described in chapter 2). The relation between the peak value $F_{h,max}$ per linear meter and the total peak duration t_d may be approximated by:

$$\frac{F_{h,max}}{\rho_w g H_b^2} = 1.24 * \left(\frac{t_d}{T_P}\right)^{-0.344} \tag{4.21}$$

Equation 4.21 is sketched again in figure 4.8, together with two other wave impact prediction formulae which will be treated later on. This wave impact force prediction formula does not represent wave impacts with a constant amount of momentum. Wave impacts with a long total duration t_d represent a greater amount of momentum than wave impacts with very short total duration. The wave impact prediction formula which has been given in the previous section, see equation 4.19, has been derived for a wave impacts with a constant amount of momentum: $F_{h,max}$ linearly decreases with a linearly increasing rise time of the wave impact.

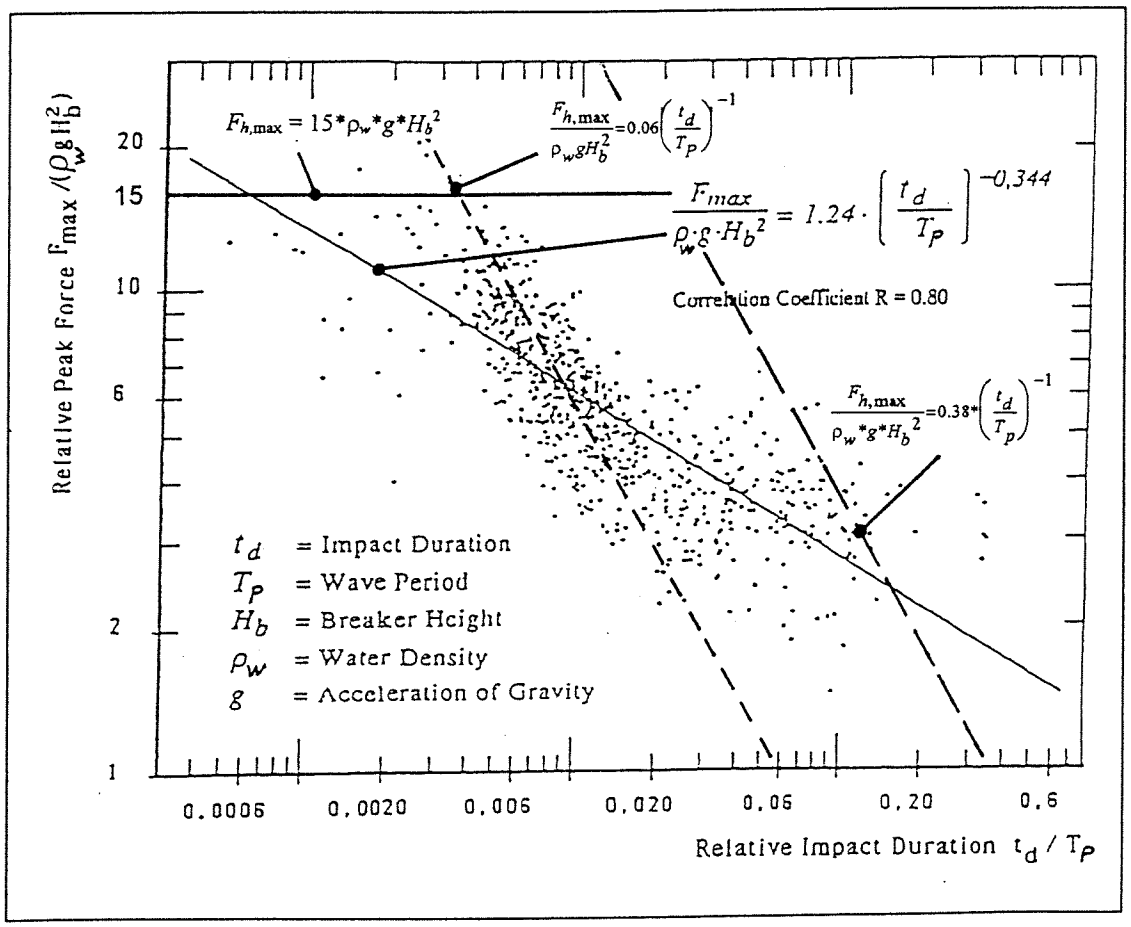

fig. 4.8 Maximum impact force versus impact duration [SCHMIDT et al. (1992)]

The theoretical basis of equation 4.21 is weak. It is an empirical formula based on a fit of plotted points. The formula has a considerable uncertainty because of the large scatter in the test results (linear correlation coefficient = 0.80). The test forces can be up to twice the force calculated by equation 4.22. No restrictions are given for the ratio t_d / T_P .

In figure 4.8 the wave impact force formula which is given by equation 4.22 is also given. This equation describes wave impact forces per linear meter with a constant amount of momentum and runs through the middle of the cloud of points.

$$\frac{F_{h,\max}}{\rho_w g H_b^2} = 0.06\left(\frac{t_d}{T_P}\right)^{-1} \tag{4.22}$$

In the tests of Schmidt et al. [SCHMIDT et al. (1992)] it was found that:

$$0.3 \le \frac{t_r}{t_d} < 0.65 \tag{4.23}$$

The ratio of the rise time to the total peak duration is depending on the amount of trapped air and the magnitude of the force peak. The larger values of t_r / t_d occur for large trapped air volumes and smaller force peaks. According to Walkden et al. [WALKDEN et al. (1995)] the reduction in the impact force and the associated increase in the impact duration are due to the combined influence of the increase in compressibility of the air/water mixture and the observed change in the wave profile at the impact.

In the derivation of the horizontal wave impact force prediction formula which has been described in the previous chapter, the effect of the wave period of the waves which might break on the vertical wall has not been taken into account because of the fact that the solitary wave theory has been used. The derivation of a horizontal wave impact force prediction formula which accounts for the wave period of the waves will be treated below.

The mass of an incoming sinusoidal wave can be approximated by (see figure 4.9):

$$M = \rho_w * \frac{H_b * L_b}{2 * \pi} \tag{4.24}$$

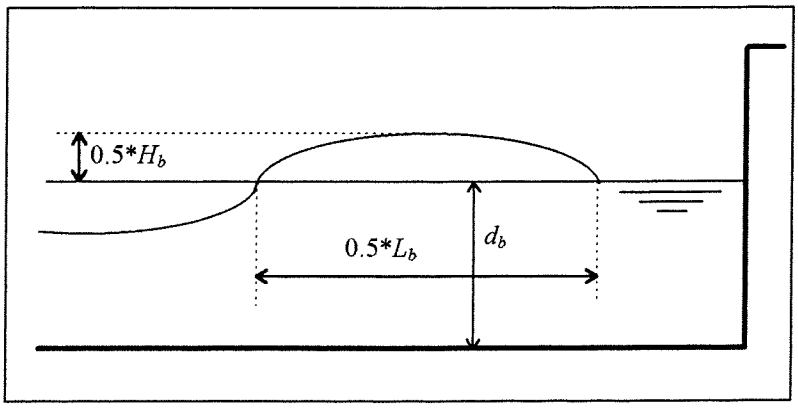

fig. 4.9 Incoming sinusoidal wave

If the following breaker criterion is used:

$$\frac{H_b}{d_b} = 0.78 \tag{4.7}$$

The maximum velocity of the incoming wave can be approximated by:

$$c = \sqrt{g(d_b + 0.5 * H_b)} = 1.18 * \sqrt{g * d_b} \tag{4.25}$$

The wave length and the wave peak period which contains the most are related by the following relation (the peak period of the waves is that period of the waves in the wave field at which the most energy is accumulated in the energy density spectrum):

$$L_b = c * T_p \tag{4.26}$$

So the total amount of momentum of the incoming wave is:

$$M*c = \rho_w * \frac{H_b * L_b}{2 * \pi} * c = \rho_w * \frac{H_b * c * T_p}{2 * \pi} * c = 0.22 * \rho_w H_b g d_b T_p \tag{4.27}$$

In equation 4.3 the following relation has been given for the relation between the maximum horizontal peak force, the rise time and the forward momentum of a wave:

$$F_{h,\max} = 2* \frac{M * c}{t_r} \tag{4.28}$$

The following horizontal wave impact force prediction formula can be obtained using equation 4.26, 4.27 and 4.7 if is assumed that the total mass of the incoming wave causes the wave impact (the dimensionless peak force is a function of the rise time and the peak period of the waves):

$$\frac{F_{h,\max}}{\rho_w * g * H_b^{\,2}} = 0.57 * \left(\frac{t_r}{T_p}\right)^{-1} \tag{4.29}$$

The maximum wave impact force per linear meter obtained by equation 4.29 can be reduced if it is assumed that only a part of the total mass of the incoming wave causes the wave impact instead of the total mass, as has been assumed here. According to Bagnold [BAGNOLD (1939)] the total mass of the incoming wave can be multiplied by a factor 0.2 to obtain the actual mass involved in the wave impact process (adaptation of the formula by the use of the factor k_r see section 4.2 will not be carried out here). Now equation 4.30 can be determined:

$$\frac{F_{h,\max}}{\rho_w * g * H_b^{\,2}} = 0.11 * \left(\frac{t_r}{T_p}\right)^{-1} \tag{4.30}$$

As has been stated before , Schmidt et al. [SCHMIDT et al. (1992)] have found the following ratio

$$0.3 \le \frac{t_r}{t_d} < 0.65 \tag{4.23}$$

According to this ratio, the maximum forces can be expected if $t_r = 0.3*t_d$. This leads to the following equation for the dimensionless maximum wave impact force:

$$\frac{F_{h,\max}}{\rho_w * g * H_b^{\,2}} = 0.38 * \left(\frac{t_d}{T_p}\right)^{-1} \tag{4.31}$$

This equation is sketched in figure 4.8 as well. It can be seen that this formula is more conservative than the two other formulae which are sketched in figure 4.8. Nearly all points are plotted under the line which represents equation 4.31.

Goda [GODA (1994)] uses the same method to derive a wave force prediction formula as in this section and in section 4.2. The time integral or the amount of momentum of a breaking wave force exerted upon a vertical wall must be equal to the forward momentum of the breaking wave impinging upon the wall. He suggests that the upper limit of the momentum of a breaking wave can be approximated with that of a semi-circular cylinder having a diameter of H_b which advances with the speed of the wave celerity c. Goda [GODA (1994)] has found the following relation for the dimensionless peak force:

$$\frac{F_{h,m\max}}{\rho_w * g * H_b^{\,2}} = \frac{\pi * c}{4 * g * t_r} \tag{4.32}$$

If the breaking criterion of equation 4.7 is used than the speed of the wave celerity can be approximated by:

$$c = \sqrt{g(d_b + 0.5 * H_b)} = 1.18 * \sqrt{g * d_b} \tag{4.25}$$

than the findings of Goda can be presented in the following formula (equation 4.33)

$$\frac{F_{h,\max}}{\rho_w * g * H_b^{\,2}} = 0.93 * \left(\frac{t_r}{\sqrt{d_b / g}} \right)^{-1} \tag{4.33}$$

Although the breaking wave pressure measured by a pressure gauge with a small sensor area often exceeds 100 times the hydrostatic head of the wave height, the total thrust upon the whole area of the vertical wall does not rise to such a high level. By referring to the measurements by Mitsuyasu (1962, 1966a,b) and Horikawa and Noguchi (1970), the upper limit of the dimensionless wave impact force can be set to about 15 [GODA (1994)], see equation 4.20:

$$\frac{F_{h,\max}}{\rho_w * g * H_b^{\,2}} = 15 \tag{4.20}$$

Equation 4.20 is sketched in figure 4.8 as well.

After the wave impact the standing wave force on the vertical wall remains which can be estimated by:

$$\frac{F_{h,\max}}{\rho_w * g * H_b^{\,2}} = 1.5 \tag{4.34}$$

Nota bene:

The fact that wave impact forces hardly exceed a value of $F_{h,\max} = 15*\rho_w*g*H_b^2$ N/m has been investigated by the author of this report for many wave impact situations generated by random waves of small scale and large scale hydraulic model tests which could be found in the literature. Only a very few wave impacts for random wave conditions were found to exceed a value of $F_{h,\max} = 15*\rho_w*g*H_b^2$. This can among other things be seen in figure 4.10 and 4.8 where only a few points ($\approx$5) are plotted above the line which indicates the maximum horizontal wave impact force. So for the benefit of the analysis which is presented in this report, this value of $15*\rho_w*g*H_b^2$, will be seen as the upper limit for wave impact forces per linear meter on vertical breakwaters.

One should bear in mind that if a vertical breakwater is designed, a probabilistic design approach can be very useful. In this way one is able to take into account that specific extreme wave impact, which might exceed the value of say $F_{h,max} = 15*\rho_w*g*H_b^2$ N/m and might lead to failure of a vertical breakwater, in a - from a designers point of view - more "realistic" way. It is essential to know the return period of these extreme wave impacts (actually this is essential for all kinds of wave impacts). For instance: it seems unwise to design a vertical breakwater with a proposed life time of 50 years for a wave impact force of say $F_{h,max} = 25*\rho_w*g*H_b^2$ N/m which will lead to vertical breakwater failure, but has a return period of say 1000 years.

For the benefit of a probabilistic design the statistical distribution of the (dimensionless) horizontal forces has to be derived. Such a distribution function has been developed by Klammer et al. [KLAMMER et al. (1996)] by modifying the standard Weibull distribution function. This gives the following conditional formula (only valid for wave impacts):

$$F(x) = 1 - e^{[-\gamma(\ln x - \beta)]^{\alpha}} \qquad x > 0 \tag{4.35}$$

In equation 4.35 α, β, and γ are the parameters of the modified Weibull functions whereas $F(x)$ is the distribution function. Figure 4.10 shows the non exceedance probabilities of the dimensionless ("relative") horizontal forces taken from large scale measurements with random waves [KORTENHAUS et al. (1994)].

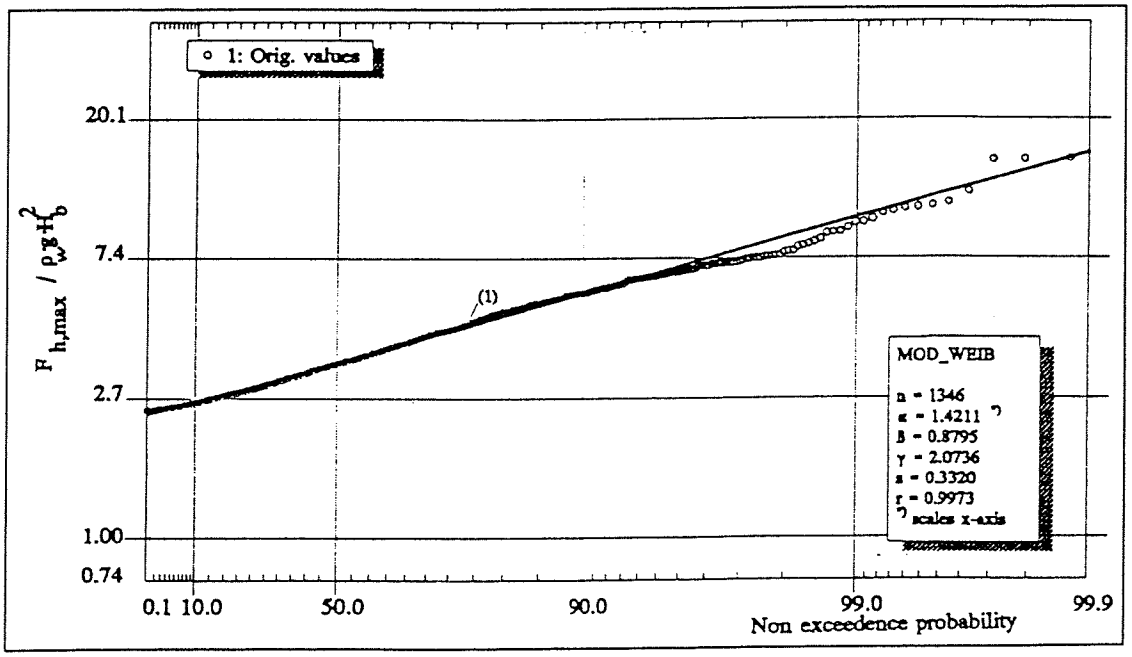

fig. 4.10 Statistical distribution function of dimensionless horizontal forces [KLAMMER et al. (1996)]

The following value of wave impact forces on vertical breakwaters may be used for a *preliminary design* according to Oumeraci [KORTENHAUS (1996)]:

$$F_{h,max} = 8.0*\rho_w\, gH_b^2 \tag{4.36}$$

This formula has been derived from experiments on a large-scale breakwater model for the design of a high water protection wall in Hamburg, Germany.

From statistical analysis it has been found that the non exceedance probability of the relative horizontal force $F_{h,max} / \rho_w *g*H_b^2$ in equation 4.36 is about 10 to 15%. The point of application of the force is close to the height of the Still Water Level (SWL).

The two wave impact force formula, which have been derived in this chapter, can be compared with the formula of Schmidt et al. [SCHMIDT et al. (1992)] and the formula which has been derived by Goda [GODA (1994)], see table 4.4. In section 4.2 the following formula was found [KLAMMER et al. (1996)] (for reasons of comparison, the formula without the correction factor k_r is used here (see section 4.2)):

$$\frac{F_{h,\max}}{\rho_w * g * H_b^2} = 1.79 * \left(\frac{t_r}{\sqrt{d_b / g}} \right)^{-1} \tag{4.16}$$

In this section equation 4.31 was found:

$$\frac{F_{h,\max}}{\rho_w * g * H_b^2} = 0.38 * \left(\frac{t_d}{T_p} \right)^{-1} \tag{4.31}$$

The formula of Schmidt et al. [SCHMIDT et al. (1992)] is

$$\frac{F_{h,\max}}{\rho_w * g * H_b^2} = 1.24 * \left(\frac{t_d}{T_p} \right)^{-0.344} \tag{4.21}$$

The formula of Goda [GODA (1994)] is

$$\frac{F_{h,\max}}{\rho_w * g * H_b^2} = 0.93 * \left(\frac{t_r}{\sqrt{d_b / g}} \right)^{-1} \tag{4.33}$$

For reasons of comparison it is assumed that in equation 4.19 and equation 4.33: $t_r = 0.3 * t_d$.; t_d is chosen as 0.1 s. Wave data can among other things be found in table 4.3.

$t_d = 0.1$ s	equation 4.16 ($t_r = 0.3 * t_d$) $\frac{F_{h,\max}}{\rho_w g H_b^2}$	equation 4.31 $\frac{F_{h,\max}}{\rho_w g H_b^2}$	equation 4.33 ($t_r = 0.3 * t_d$) $\frac{F_{h,\max}}{\rho_w g H_b^2}$	equation 4.21 $\frac{F_{h,\max}}{\rho_w g H_b^2}$
$H_b = 0.3$ m $T \approx T_p = 3.55$ s $d_b = 3.7$ m (see table 4.3)	36.64	13.49	19.04	4.23
$H_b = 1.1$ m $T \approx T_p = 3.55$ s $d_b = 4.3$ m (see table 4.3)	39.50	13.49	20.87	4.23
$H_b = 10$ m $T \approx T_p = 12$ s $d_b = 15$ m (see chapter 7)	73.78	45.6	45.08	4.23

table 4.4 Comparison wave impact force prediction formula

Some of the dimensionless forces which can be found in table 4.4 are much higher than the maximum value of 15 given by Goda in equation 4.20. This is because of the fact that the input parameters of the horizontal wave impact force prediction formulae described in equation 4.16, 4.31, 4.33 and 4.21 are not restricted to any range of values. So, in fact, much higher values are possible according to these formulae, but in the remainder of this report 15 will be regarded as the maximum dimensionless wave impact force ($F_{h,\max} / \rho_w * g * H_b^2$), because of the fact that this has proven to be a good approximation according to a lot of hydraulic model tests.

For the data which is presented in table 4.4 it can be seen that the formula of Klammer et al. [KLAMMER et al. (1996)] gives the highest horizontal wave impact forces.

If equation 4.16 and 4.31 are compared and it is assumed that $t_r = 0.3*t_d$ than it can be concluded that equation 4.31 only gives higher values than equation 4.16 if the following condition is fulfilled:

$$15.70\sqrt{\frac{d_b}{g}} < T_p \tag{4.37}$$

For full scale situations under breaking conditions for short waves at vertical wall breakwaters this is condition is nearly never fulfilled. So it can be concluded that the formula of Klammer et al. [KLAMMER et al. (1996)] gives higher horizontal wave impact forces than equation 4.31 which has been derived in this chapter.

It should be noted that the rise time of a wave impact is dependent on the angle of the wave front as can be seen from figure 4.11

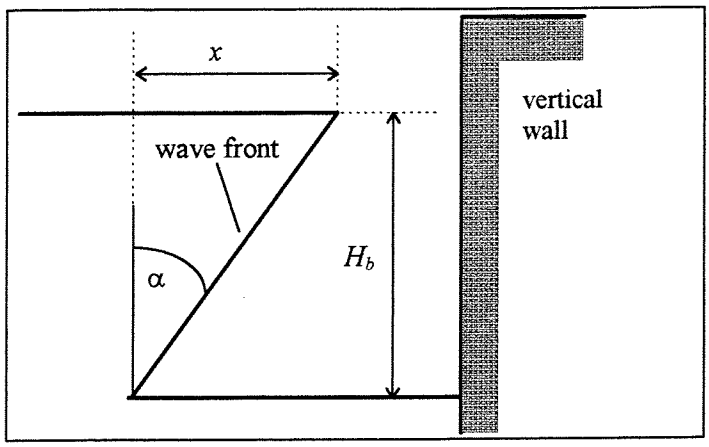

fig. 4.11 Angle of the wave front

The rise time of the wave impact and the angle of wave front are related by the relation which is reflected in equation 4.29:

$$t_r = \frac{x}{c} = \frac{H_b * \tan\alpha}{\sqrt{g(d + 0.5 * H_b)}} \quad \propto \quad \sqrt{\frac{d_b}{g}} \tan\alpha \quad \propto \quad \sqrt{\frac{d_b}{g}} \tag{4.38}$$

This relation has been used in the horizontal wave impact force prediction formula of Klammer et al. [KLAMMER et al. (1996)] presented in the previous section and the formula of Goda [GODA (1994)] which has been given in this section. In the way the rise time is schematised here Froude scaling seems applicable. When Froude scaling is used time should be scaled from model scale to full scale by the square root of the length (or a characteristic size), see equation 4.45.

4.4 Momentum of a wave impact

In chapter 10 it will be shown that especially the total amount of momentum of a breaking wave impinging on a vertical breakwater is very important for the overall stability of the vertical breakwater against sliding, overturning or other modes of failure. As it will be shown in chapter 8, a very high horizontal wave impact peak force will not threaten the overall stability of the structure as long as the duration of the wave impact is sufficiently short enough. In that case the total amount of momentum of the breaking wave will be only very small. For smaller horizontal wave impact peak forces - but longer durations - situations may arise which cause vertical breakwater failure because of the fact that the total amount of momentum of these breaking waves (which will be transferred to the vertical breakwater) is too large: the breakwater cannot withstand such amounts of momentum.

In the previous sections the amount of momentum of a breaking wave has been used to determine horizontal wave impact force prediction formulae. It has been shown that some of these horizontal wave impact force prediction formulae represent an upper envelope to random wave test results of wave impact forces.

Schmidt et al. [SCHMIDT et al. (1992)] have investigated the wave momentum and the force impulse of wave impacts caused by plunging breakers. Some results of their study has already been presented in the previous section, among other things in figure 4.8 and in chapter 2. Schmidt et al. [SCHMIDT et al. (1992)] have determined "dynamic" and "quasi-static" components I_{dyn} and I_{stat} of the force impulse of wave impacts separately. These are defined in figure 4.12 where the point (M) of maximum wave run-up is also shown.

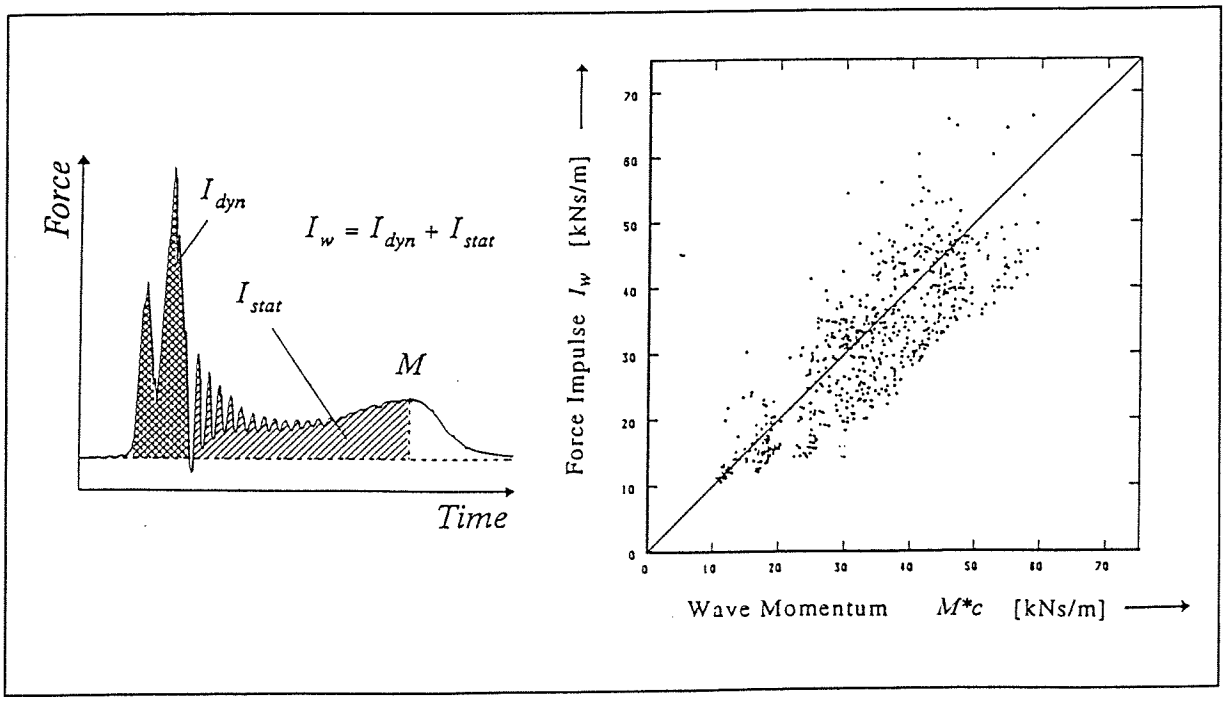

fig. 4.12 Force impulse definition sketch and force impulse versus wave momentum [SCHMIDT et al. (1992)]

From the part of figure 4.12 where the definition sketch is given, it can be seen that the dynamic component of the force impulse I_{dyn} is the part which "belongs to" the actual peak force. This dynamic force impulse I_{dyn} has been used in the previous sections to determine the horizontal wave impact force prediction formulae.

According to Schmidt et al. [SCHMIDT et al. (1992)] the force impulse $I_w = I_{dyn} + I_{stat}$ should be equal to the momentum of the wave with a mass M impinging on a wall with a horizontal velocity c by assuming conservation of momentum and the solitary wave theory:

$$M = \rho_w * \sqrt{\frac{16}{3} * H_b * d_b^3} \tag{4.5}$$

$$c = \sqrt{g * (d_b + H_b)} \tag{4.6}$$

in which d_b is the breaking depth measured from Still Water Level (SWL) and H_b the breaker height. After analysing the results of the large scale tests the solitary wave theory proved to give the best approximation of the velocity of the breaking wave and the mass of the breaking wave.

The momentum of the wave was calculated using equations 4.5 and 4.6 and compared to the force impulse I_w in figure 4.12. It can be seen that despite the large scatter, the solitary wave theory still represents a good mean for the approximate evaluation of the loads of vertical structures by breaking waves. In average, the wave momentum was slightly larger (7%) than the force impulse I_w (correlation coefficient 0.83).[SCHMIDT et al. (1992)]

In the previous sections some horizontal wave impact force prediction formula have been derived using the momentum of an incoming (solitary) wave as well. The (dimensionless) forces which can be predicted by among other things equation 4.16, 4.31 and 4.33 were found to be (very) conservative compared to (dimensionless) wave impact forces measured in hydraulic scale model tests. Here, a good agreement is found between the measured force impulse and the predicted wave momentum while in the previous sections large differences were to be found. This is because of the fact that the "quasi-static" component I_{stat} has been neglected in the previous sections. The total wave momentum, approximated by $M*c$ (see equation 4.5 and 4.6) is set to be equal to I_{dyn} leading to very high wave impact forces, while it should in fact be set equal to the total force impulse $I_w = I_{stat} + I_{dyn}$ according to the results which are shown in figure 4.12. The latter approach leads to a mean for the approximate evaluation of the loading of vertical structures induced by breaking waves, while the approach presented in section 4.2 and 4.3 leads to horizontal wave impact force prediction formulae which represent an upper envelope to random wave test results of wave impact forces.

In figure 4.13 equation 4.19 is sketched together with the upper bound given by Goda [GODA (1994)] presented in equation 4.20.

$$\frac{F_{h,\max}}{\rho_w * g * H_b^2} = 2.24 * \left(\frac{t_r}{\sqrt{d_b / g}}\right)^{-1} \tag{4.19}$$

$$\frac{F_{h,\max}}{\rho_w * g * H_b^2} = 15 \tag{4.20}$$

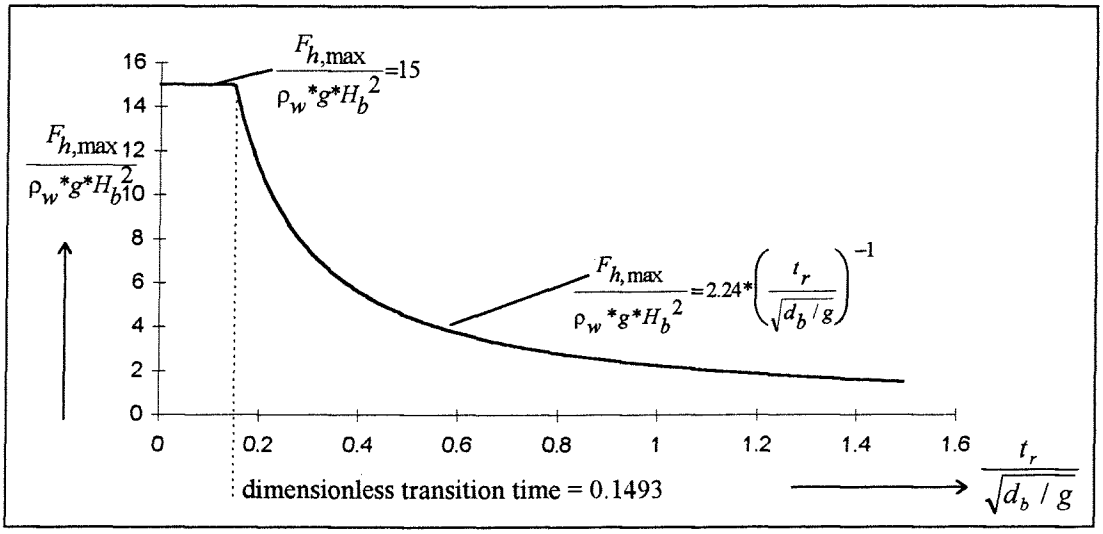

fig. 4.13 Prediction formula 4.19 with the maximum dimensionless wave impact force of 15

Figure 4.13 can be used to determine the maximum momentum of wave impacts. The transition rise time of the two formulae (equation 19 and equation 20) presented in figure 4.13 is given in equation 4.39:

$$t_r = \frac{2.24}{15} * \sqrt{\frac{d_b}{g}} = 0.1493 * \sqrt{\frac{d_b}{g}} \qquad (4.39)$$

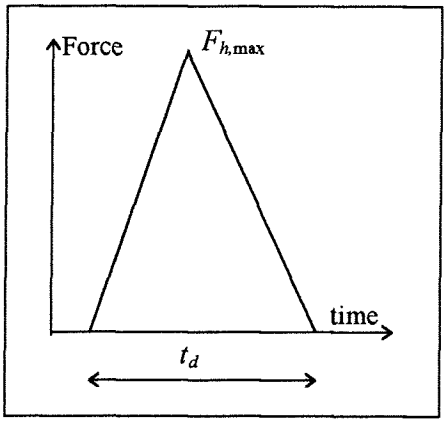

fig. 4.14 Definition sketch maximum momentum

The maximum momentum of a wave impact can be determined as (see figure 4.14)

$$I_{max} = 0.5 * t_d * F_{h,max} \qquad (4.40)$$

The following formulae of the maximum momentum of a wave impact can be used:

$$\text{If } t_r < \frac{2.24}{15} * \sqrt{\frac{d_b}{g}} \qquad I_{max} = 0.5 * \rho_w * g * H_b^2 * 15 * t_d \qquad (4.41)$$

$$\text{If } t_r > \frac{2.24}{15} * \sqrt{\frac{d_b}{g}} \qquad I_{max} = 0.5 * \rho_w * g * H_b^2 * 2.24 * \sqrt{\frac{d_b}{g}} * \frac{t_d}{t_r} \qquad (4.42)$$

In figure 4.15 the maximum momentum of a wave impact is sketched for the following situations (see also equation 4.23):

- H_b = 10 m, d_b = 15 m and $t_r = 0.30 * t_d$
- H_b = 10 m, d_b = 15 m and $t_r = 0.65 * t_d$

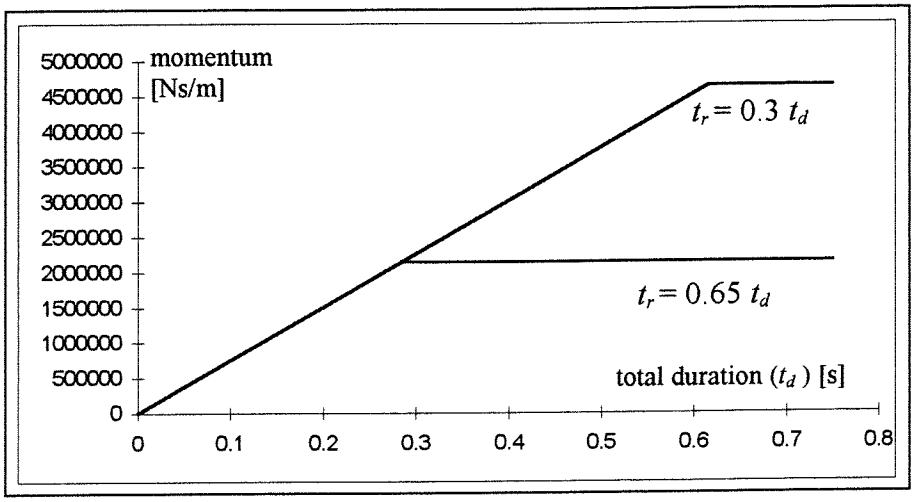

fig. 4.15 Maximum momentum for H_b = 10 m, d_b = 15 m and $t_r = 0.65 * t_d$ and $t_r = 0.30 * t_d$

The linear branch of the graph presented in figure 4.15 indicates equation 4.41. The constant branches of the graph indicate equation 4.42 for different rise times. It is obvious that these branches are constant because equation 4.42 has been derived using the horizontal wave impact formula of the previous sections which has been derived using the consideration of a constant amount of momentum. From figure 4.15 it can be seen that the amount of momentum of wave impacts with the same total duration, but with a shorter rise times ($t_r = 0.3\ t_d$) can be much higher than wave impacts with longer rise times ($t_r = 0.65\ t_d$). This is logical because the two investigated wave impacts have got the same total duration and wave impacts with the shortest rise times give the highest wave impact forces, according to the formulae which have been derived in the previous chapter.

Figure 4.15 will be used in chapter 10 to indicate the danger of the maximum wave impacts forces for different (total) durations of these wave impacts.

The same procedure as has been used here to derive the momentum of wave impacts using the formula of Klammer et al. [KLAMMER et al. (1996)] can be used to derive the momentum of wave impacts using the formula which takes the peak period T_p of the waves into account:

$$\frac{F_{h,\max}}{\rho_w * g * H_b^{\,2}} = 0.38 * \left(\frac{t_d}{T_p}\right)^{-1} \tag{4.31}$$

Now, the following formulae of the maximum momentum of a wave impact can be derived, using equation 4.31 and the maximum dimensionless horizontal wave impact force of 15 (see equation 4.20 and also figure 4.14):

$$\text{If } t_d < \frac{0.38}{15} * T_p \qquad I_{\max} = 0.5 * \rho_w * g * H_b^{\,2} * 15 * t_d \tag{4.43}$$

$$\text{If } t_d > \frac{0.38}{15} * T_p \qquad I_{\max} = 0.5 * \rho_w * g * H_b^{\,2} * 0.38 * T_p \tag{4.44}$$

Using T_p = 12 s and H_b = 10 m , the maximum momentum becomes (equation 4.44): I_{max} = 2292597 Ns/m; using equation 4.42 with $t_r = 0.65\ t_d$ gives I_{max} = 2142440 Ns/m (see figure 4.15. It can be concluded that these two formulae give almost the same results.

4.5 Brief attention to scaling of wave impacts

In this section attention is paid to scaling of wave impacts from small and large scale hydraulic model tests to prototype situations.

As gravity forces are predominant in the case of surface water waves which are to be modelled, the Froude number should be identical in the hydraulic scale model and in nature (prototype scale). The Froude number is given by:

$$\frac{u}{\sqrt{gL}} \tag{4.43}$$

in which:

u = velocity
g = acceleration of gravity
L = characteristic dimension of the caisson

From this the scale factor follows for:

- velocity $n_u = \sqrt{n_L}$ (4.44)
- time $n_t = \sqrt{n_L}$ (4.45)
- mass $n_m = n_L^3$ (4.46)
- pressure $n_p = n_L$ (4.47)

in which:

$$n_i = \frac{\text{value in nature}}{\text{value in model}} \qquad (i \text{ indicates the parameter which is considered}) \tag{4.48}$$

Impact forces caused by breaking waves can not always be modelled according to the Froude number. Compression of the trapped air by the breaking wave and subsequent oscillation of air bubbles give model scales which deviate from the above mentioned scale law [DELFT HYDRAULICS (1993)]. Impact loads are potentially influenced by scale and other model effects, so impact loads converted directly by Froude scaling will over-estimate prototype loads. Froude scaling does not take account of air entrainment which causes compressibility of the air / water mixture. Only in the case of pulsating wave forces (quasi-static wave forces) where the relationships between wave momentum, pressure impulse, and horizontal force are relatively simple, the assumption of Froude scaling is realistic.

It has long been argued and is well accepted that wave impacts in small scale hydraulic model tests will be grater in magnitude , but shorter in duration than their equivalents at full scale in (invariably aerated) sea water. The reduction in the impact force and the associated increase in impact duration are due to the combined influence of the increase in compressibility of the air/water mixture and the observed change in the wave profile. It is very probable therefore that the higher impact forces measured in model tests can be scaled to lower values, but that the impulse durations must be scaled to longer values. On the other hand, a comparison between large scale model tests and different small scale hydraulic model tests suggests that Froude scaling should be used to obtain an upper limit to the impact force to be expected. It may be noted in passing that the largest forces occur when there is least air entrained or trapped, and these impacts may therefore actually be less influenced by scale effects on air compression [ALLSOP et al. (1996)].

Many of the uncertainties concerning scaling of wave impacts have been studied by various researchers. Among other things the effect of using salt and fresh water has been tested. It has been shown by Walkden et al. [WALKDEN et al. (1995a)] that lower impact forces can be expected from a sea water wave impact than from a similar fresh water wave impact, due to the differences in bubble characteristics and higher aeration levels in sea water. It can be seen from hydraulic model tests that bubbles in sea water are approximately one order of magnitude (a factor 10) smaller than fresh water bubbles for the same entrainment rate. It has previously been argued that the addition of only small fractions of air may dramatically change force or pressure transmission characteristics of the water, thus substantially modifying pressures or forces that might be experienced by the structure. Numerical modelling studies by Peregrine et al. [PEREGRINE et al. (1995)] suggest that scale errors due to air effects might be limited to about 50%. In his study it has been theoretically shown that even a small volume fraction of air (as bubbles) in water can significantly lower the sound speed (4% air causes a speed reduction by 96%), and thus the impact force.

The results of small scale hydraulic model tests - done at HR Wallingford and described in [ALLSOP et al. (1996)] - suggest that even small changes of the level of the rubble mound compared to the Still Water Level (SWL) will change wave impact forces by factors 5 of even more. This suggests that the influence of small changes to the geometry may be of greater effect than the uncertainties introduced by scale effects.

It will be shown in chapter 5 - where special attention will be paid to wave impacts with a trapped air pocket - that the pulsation period of a trapped air pocket which is generally visible in the force history of plunging breakers must be transferred to prototype by using the Mach-Cauchy scaling law instead of the Froude scaling law [OUMERACI et al. (1991)].

5 Special attention to wave impacts with a trapped air pocket

5.1 Introduction

A general overview of hydraulic loads on vertical breakwaters has been given in chapter 2. Wave impacts on vertical breakwaters, the subject of this graduation project and a special type of hydraulic loads, have been treated concisely in that chapter: an overview of different types of wave impacts has been given. Three types of wave impacts have been defined: wave impacts of the Wagner type without trapped air, wave impacts of the Bagnold type with large trapped air pockets (a trapped air pocket between the breaking wave and the plane vertical front wall of a breakwater caused by breakers of the plunging type) and wave impacts of a transition type. These three types of wave impacts have been described more extensively in chapter 3 by some general analytical formulae which can be used to calculate wave impact pressures. In chapter 4 different formulae have been treated which can be used to predict the maximum horizontal wave impact forces on vertical breakwaters.

In this chapter (see figure 5.1) wave impacts with a large amount of trapped air (a large trapped air pocket) between the plane vertical front wall of a breakwater and the breaking wave (a wave impact of the Bagnold type) will be treated elaborately because they can be considered as a dangerous type of wave impacts. This has been mentioned before in chapter 2 and chapter 3 and will also be shown in this chapter and further on in this report (see chapter 10).

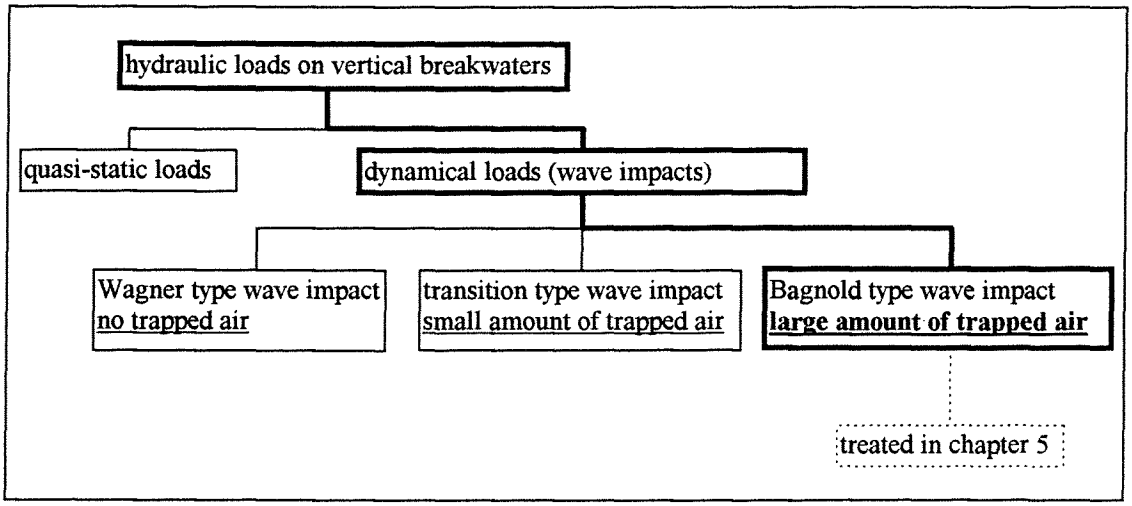

fig. 5.1 Position of the Bagnold type wave impact

Wave impacts of the Wagner type are not treated in this study because they show more or less quasi-static behaviour.

Wave impacts of the transition type have got very high peak forces and very short durations. By means of an analytical study in chapter 7 and a study by means of a computer model (a mass-(elasto-plastic)spring-dashpot TILLY model) in chapter 8 to 10 the danger of this type of wave impacts will be indicated.

Wave impacts of the Bagnold type can be more dangerous than wave impacts of the transition type although their peak forces are lower. The force history of a wave impact of the Bagnold type has been shown in figure 2.16 previously but is shown here as well in figure 5.2.

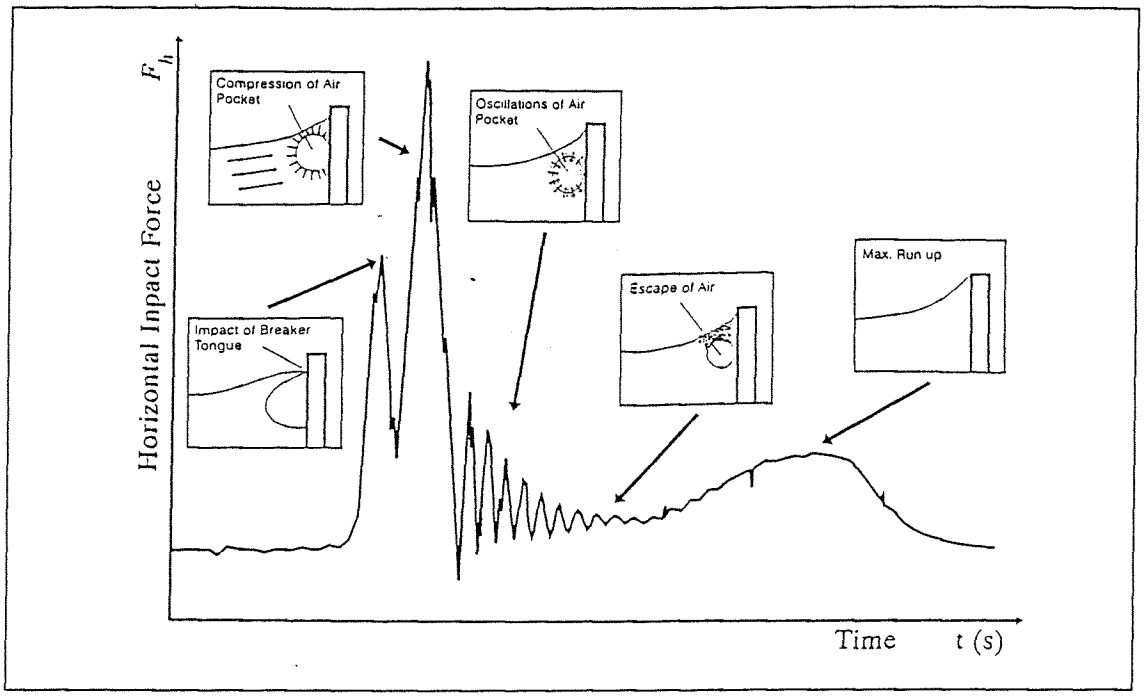

fig. 5.2 Characteristics of a Bagnold type wave impact (a large trapped air pocket) [SCHMIDT et al. (1992)]

The Bagnold type wave impact can be more dangerous because of the large air pocket which is trapped between the breaking wave and the plane vertical front wall of a vertical breakwater, although the two peak forces (see figure 5.2) of the Bagnold type wave impact are lower than the peak force of the transition type wave impact. "Generally, it is believed that the main effect of air entrapment is to damp the shock pressure, and thus favourably acts on the stability of the breakwater. If this is true for the damping of the pressure, it is not likely the case for the dynamic response of the structure" [OUMERACI et al. (1991)]. This large air pocket is the cause of force oscillations and the cause of two peaks instead of one peak. These two aspects can both be very important:

- The direct collision of a wave crest onto a plane vertical wall causes the first peak and the compression of an enclosed air pocket causes the second peak (see also figure 10.22 on page 10 - 22). If the second peak occurs within such a time that it hits the structure while the structure is moving in the same direction as the direction of the wave impact (i.e. while the vertical breakwater is moving shoreward) it will have to overcome no or at least only a part of the inertia of the structure. The cumulative response is expected to be much higher than it would be if only a single impact occurred or if the second peak was applied at a time when the structure was moving opposite to the direction of the wave impact. The effect of double peaked wave impacts will be shown elaborately in chapter 10, section 10.5.
- A large trapped air pocket between a plunging breaker and the plane vertical front wall of a breakwater will start to oscillate as will be shown in this chapter. The air cushion which is subject to a highly transient pressure field expands and contracts cyclically. It acts therefore as an oscillator which starts to cyclically excite the structure just as the peak of the impact load passes. These excitations can be clearly identified as oscillations following the first peak in the impact force. In fact the second peak in the force history is the first peak of the low frequency force oscillations. The most critical situation may occur when the period of these force oscillations approaches the range of natural periods of the structure, thus leading to resonant excitations, this can cause breakwater failure as will be shown in chapter 10. The existence and the origin of these low frequency force oscillations will be treated extensively in this chapter.

In this chapter an extensive analysis of this wave impact with a large trapped air pocket caused by a plunging breaker is treated. Special attention will be paid to the origin and the existence of the low frequency force oscillations. It will be shown that these low frequency force oscillations really exist in nature and that they are not a disturbance of the force signal on the front wall of a vertical breakwater by the eigenmotion of the vertical breakwater itself (see section 5.2). These force oscillations can be described by analytical formulae. The derivation of a formula which gives a relationship between the incident wave height and the period of the force oscillations of a Bagnold type wave impact can be found in section 5.3. This formula confirms measured values of these force oscillations in hydraulic scale models and full-scale situations. In section 5.4 some attention will be paid to the scaling of the period of the force oscillations of Bagnold type wave impacts from hydraulic model scale to full-scale situations.

5.2 Hydraulic scale model tests and wave impacts with a trapped air pocket

5.2.1 Introduction

In this section the existence of low frequency force oscillations due to a trapped air pocket is proved using several results of two hydraulic scale model tests. As it has been mentioned before, these low frequency force oscillations can be very dangerous for the stability of a vertical breakwater. In chapter 10 it will be proved that these low frequency force oscillations can result in vertical breakwater failure. The various results of two different hydraulic scale model tests are described here because it is very dangerous to use only one result of a single hydraulic scale model test as an evidence for the existence of these low frequency force oscillations due to large trapped air pockets. In sub-section 2.4.4 in figure 2.15 these low frequency force oscillations have already been shown. But as has been said before, it is dangerous to use only the results of these single tests to draw conclusions. *Poor measurements may result in wrong conclusions.*

For instance: it can be possible that the wave impact force signal which is measured on a model of a vertical breakwater by measuring instruments (which are among other things placed on the front wall of the vertical breakwater) is disturbed by the eigenoscillation of the breakwater itself. A wave impact on a vertical breakwater will cause an oscillation of this structure. The structure will still oscillate in its eigenfrequency after the wave impact, which has only got a very short duration, is disappeared. If the structure is not fixed rigidly one will also measure this eigenoscillation of the vertical breakwater besides the wave impact itself, because the measuring instruments are moving in the water together with the structure itself because of the fact that they are placed on the front wall of the vertical breakwater. The measuring instruments will translate the eigenoscillation of the vertical breakwater into a force. The force signal will then show a very high peak and after the peak low frequency force oscillations. This may lead to the wrong conclusion that a wave impact will not only cause a high peak force but also low frequency force oscillations which have got the same frequency as the eigenfrequency of the vertical breakwater.

So one must be sure that the model structure on which one is measuring is fixed rigidly: the measuring structure must have a very high eigenfrequency compared to the frequency of the oscillating air pockets to make sure that the low frequency force oscillations which are measured are the consequence of the wave impact load itself (a wave impact with a large trapped air pocket which is oscillating) and not the consequence of the eigenoscillation of the structure. In section 5.2.2 special attention is being paid to these hydraulic scale model tests. The low frequency force oscillations due to trapped air pockets which are measured are compared with the eigenfequency of the structure which is exposed to plunging breakers which are able to cause these wave impacts.

5.2.2 Hydraulic scale model tests

Hydraulic scale model tests of Hattori et al. [HATTORI et al. (1994)]

"The physics and characteristics of the impact pressure significantly depend on the colliding conditions of breaking waves. These were studied for the following colliding conditions: flip-through (an upward deflected breaker), collision of the vertical wave front and plunging wave collision [HATTORI et al. (1994)]." These colliding conditions have already been discussed in figure 2.8 on page 2 - 12 and figure 4.4 on page 4 - 6. Hattori et al. have found as well that when plunging and curling of the breaking wave develop well, a thick air pocket is trapped and damped force oscillations, due to the air pocket pulsation, appear immediately after the peak of the impact force. Hattori et al. have carried out experiments for all kinds of wave impacts. Here only the results are shown concerning wave impacts with a large trapped air pocket.

The experimental set-up of the scale model tests of Hattori et al. is shown in figure 5.3.

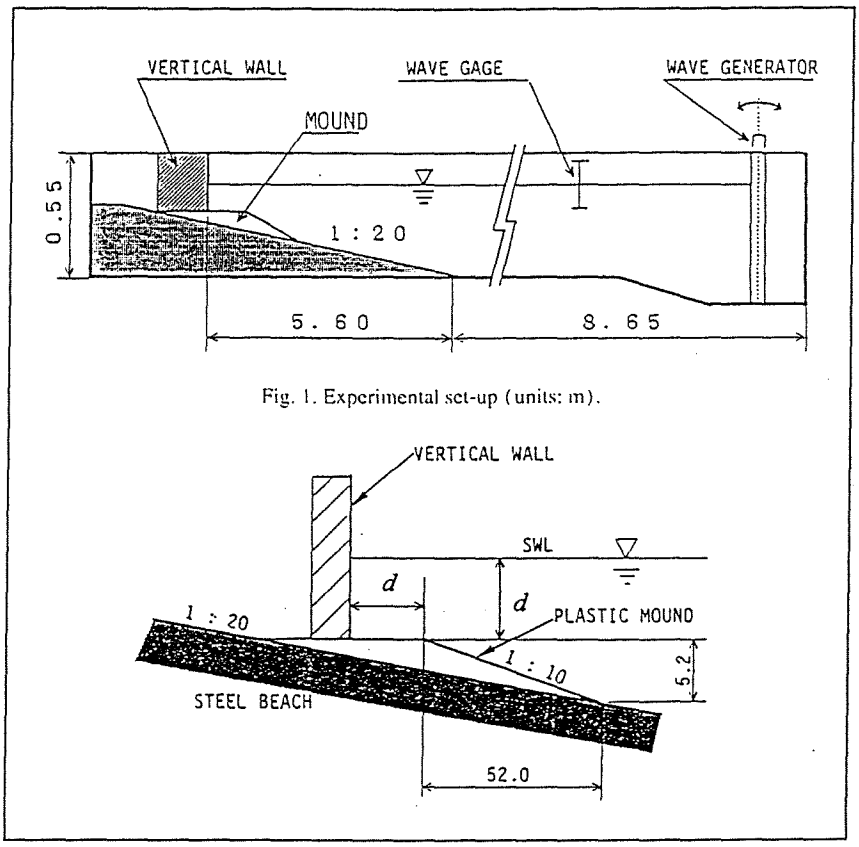

fig. 5.3 Experimental set-up [HATTORI et al. (1994)]

The experiments were carried out in a glass walled wave flume, 0.30 m wide, 0.55 m high and 20 m long in which a steel beach of 1/20 slope was installed. Thus, these tests can be considered as two dimensional tests. Regular waves were produced by a reflection-absorbing wave generator. A vertical plane wall of a 35 mm thick plastic plate (0.30 m wide and 0.50 m high) was firmly shored up with steel frames. The wall complex, having an eigenfrequency of 1.2 kHz in water, was mounted rigidly on a plastic mound with a foreshore slope of 1:10, modelling the rubble mound of composite type breakwaters (see figure 5.3). The impact pressures were measured by semi-conductor type transducers 10 mm in diameter. Their natural frequency in water and frequency range of flat high cutoff are 9,6 kHz and DC to 4.8 kHz, respectively.

As it is shown in figure 5.4, four pressure transducers were located vertically along the centreline of the wall at an interval of 2.0 cm. The maximum pressures occur most likely in the vicinity of the still water level as has been shown by Takahashi et al. [TAKAHASHI et al. (1993)]. Two additional transducers were set at 1.0 cm below and above the still water level and 5.0 cm apart from the centreline. Pressure records will be presented in a normalised form:

$$p^* = \frac{p}{\rho g H_b} \tag{5.1}$$

$$t^* = \frac{t c_w}{H_b} \tag{5.2}$$

H_b = breaker height at the front wall of the vertical breakwater
c_w = velocity of sound in water (1480 m/s)

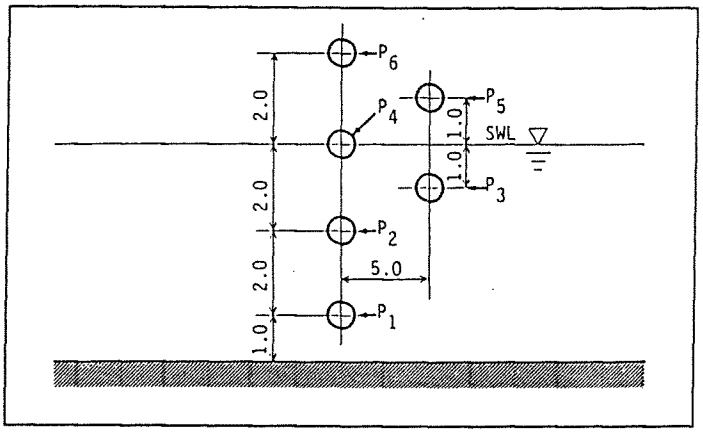

fig. 5.4 Arrangement of pressure transducers (units: cm) [HATTORI et al. (1994)]

Hattori et al. have specified wave impacts in different categories. The characteristics of the impact pressures caused by a plunging breaker which causes a large pocket of trapped air (relative to the waterdepth; i.e. the scale of the hydraulic model tests) are shown in figure 5.5. High speed motion pictures of this type of wave impact are shown in figure 5.6. The letters in figure 5.5 correspond to the letters which belong to the high speed motion pictures in figure 5.6.

At the instant of the impact, a large amount of air is entrapped between the wave and the wall. The governing tip of the plunging breaker is in free fall (figures 5.6 a - d) and collides with the wall in the vicinity of transducer P4 (figure 5.6 e). A large 1.1 cm thick air pocket (relative to the waterdepth and wave height, of course) is clearly trapped and it breaks up into air bubbles (figures 5.6 f - g). The air pocket disintegrates into a group of bubbles, which are compressed and stretched as a whole with the wave run-up (figures 5.6 h - l). The pressure records between the limits of the locations of the thick air pocket (P1 to P4 in figure 5.5) display regular pressure oscillations with decreasing amplitude, having a frequency of 210 Hz.

The eigenfrequency of the wall complex is 1.2 kHz in water, this is almost five times higher than the measured frequency of the force oscillations due to the oscillating air pocket. The conclusion can be drawn that in this test with a fully developed plunging breaker, the pressure signal has not been disturbed by the eigenmotion of the vertical breakwater.

The frequency of the pressure oscillations is low compared to the frequency of the pressure oscillations which has been found in the same hydraulic scale model tests for other kinds of wave impacts. For an impact with a small amount of trapped air (D = 0.4 cm, see figure 5.5) a frequency of 625 Hz was found. For a vertical wave front in fact a wave impact of the transition type, with almost no entrapped air (D = 0.0 cm) a frequency of 1100 Hz was found for the force oscillations, see figure 5.7.

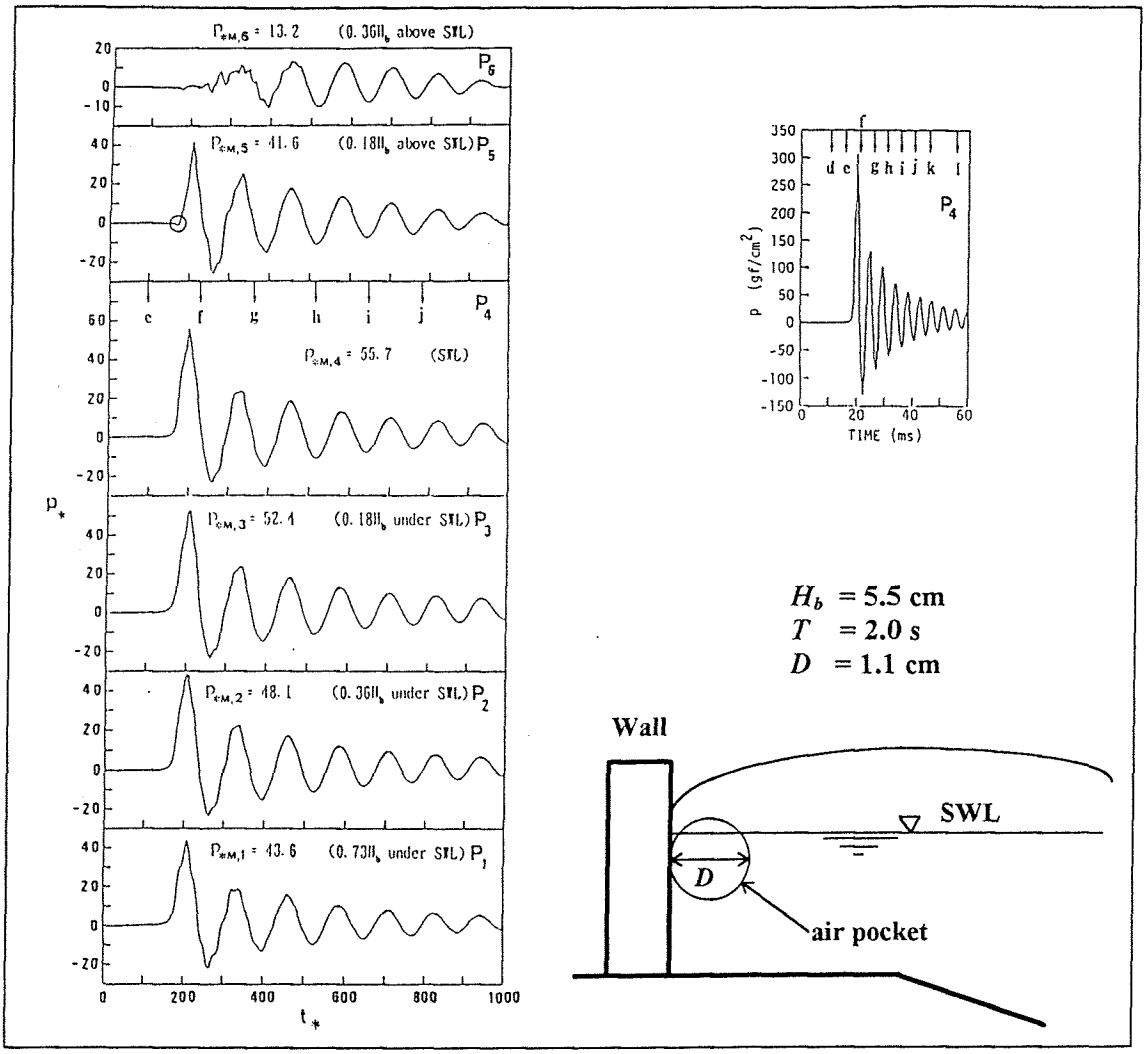

fig. 5.5 Dimensionless wave pressure records from collision of a fully developed plunging breaker [HATTORI et al. (1994)]

In the study of Hattori et al. it has been found that with the development of plunging and curling incident waves, a large amount of air in the form of an air pocket is trapped and damped pressure oscillations start immediately after the impact. The larger the amount of entrapped air, the lower the peak pressure maxima and the longer the rising time of the impact. Subtle variations in the primary wave cause variations in the shape of the air pocket, resulting in high variability in the pressure characteristics.

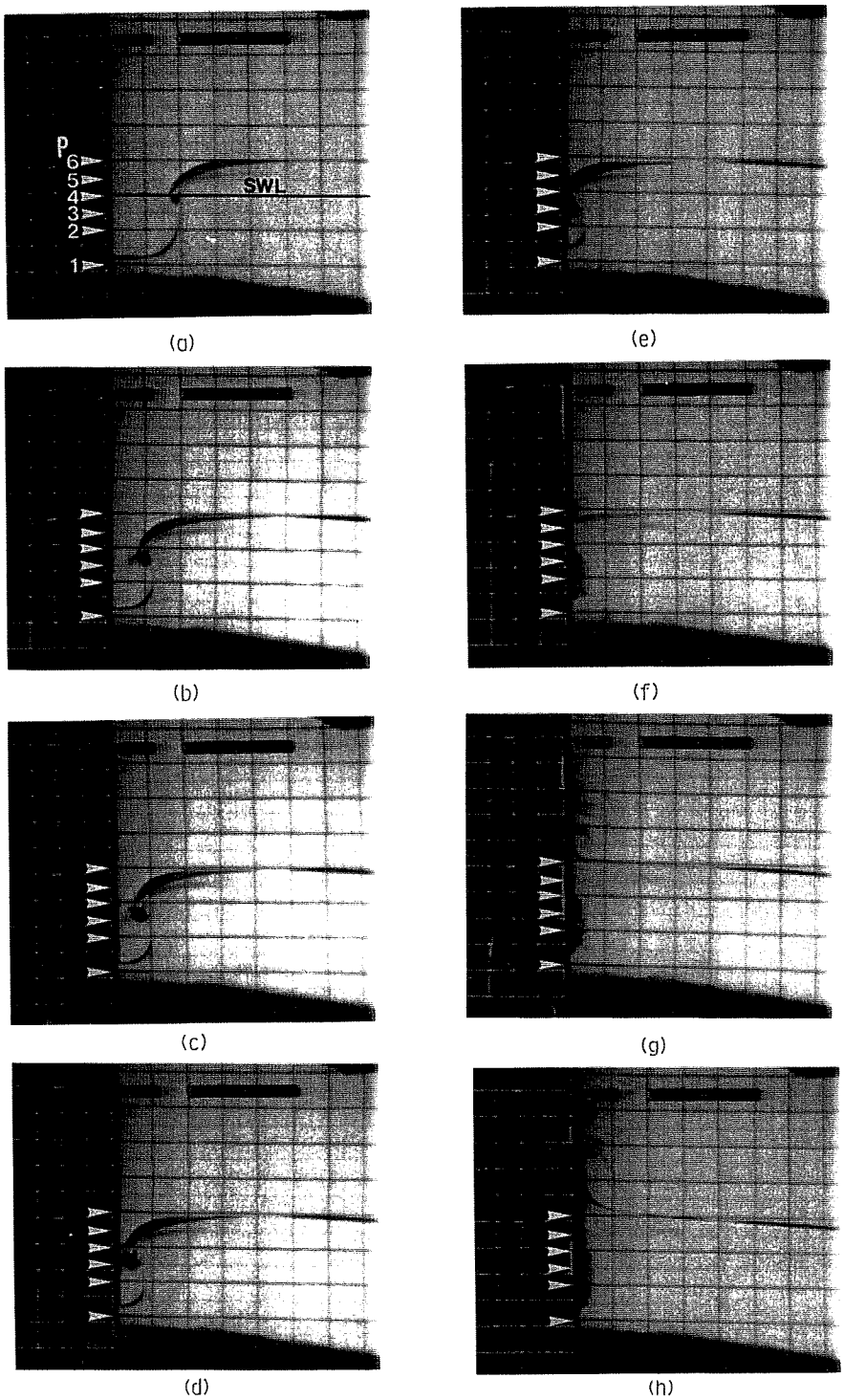

fig. 5.6 High speed motion pictures of the collision of a fully developed plunging breaker [HATTORI et al. (1994)]

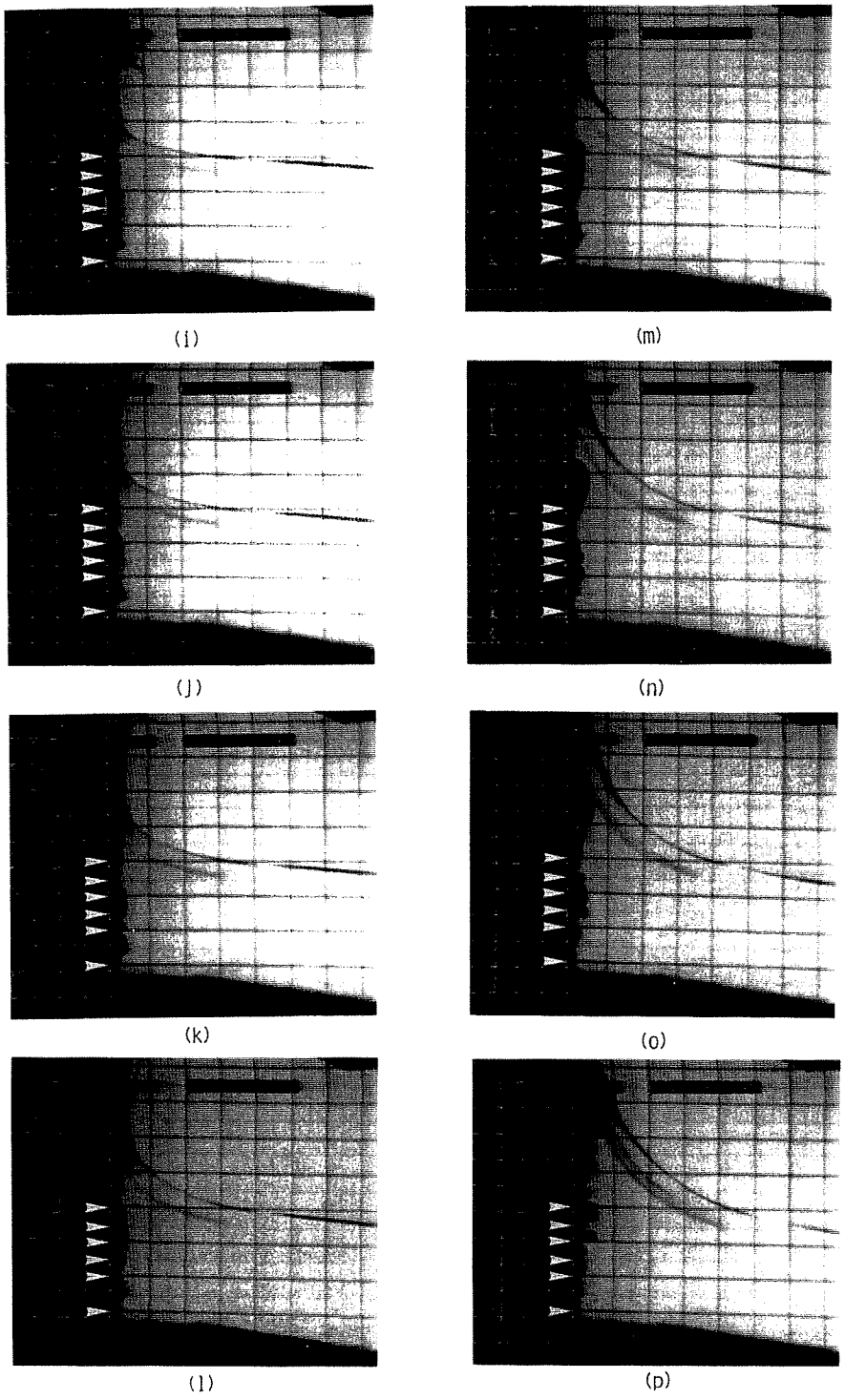

fig. 5.6 High speed motion pictures of the collision of a fully developed plunging breaker [HATTORI et al. (1994)]

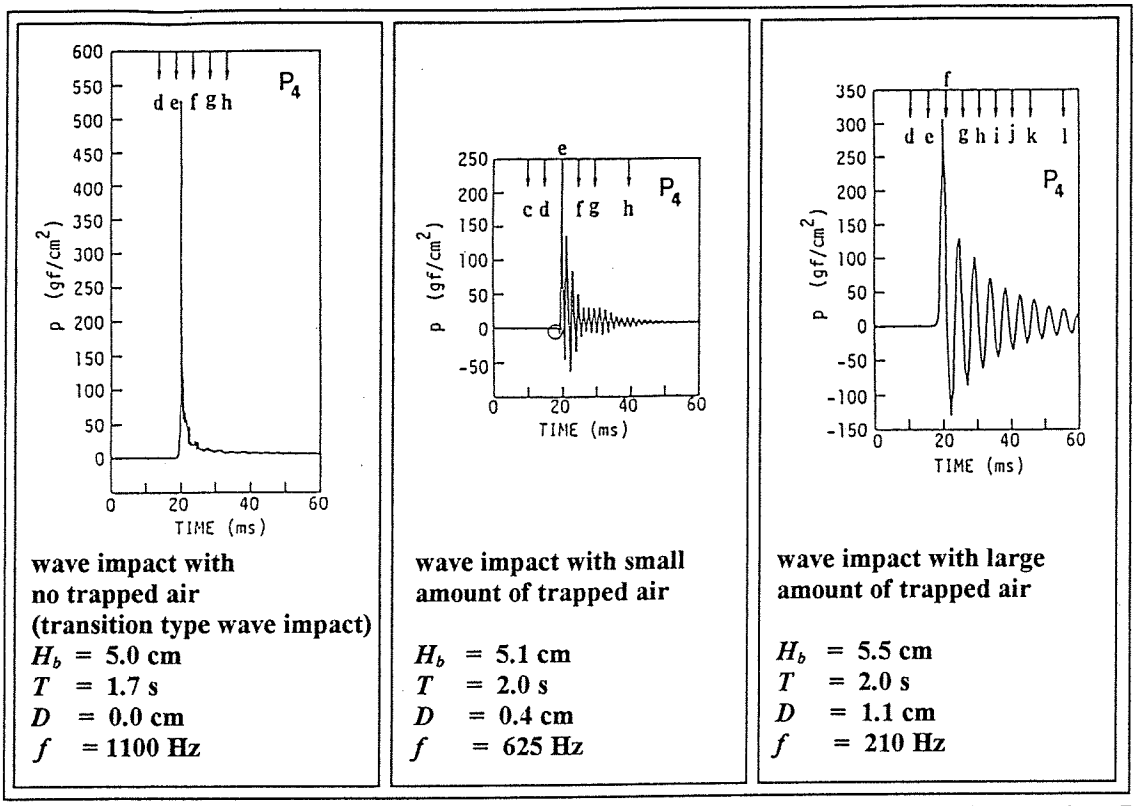

fig. 5.7 Comparison of pressures and frequencies for different types of wave impacts measured by transducer P4 [HATTORI et al. (1994)]

Hydraulic scale model tests of Delft Hydraulics [DELFT HYDRAULICS (1993)]

In the report of Delft Hydraulics [DELFT HYDRAULICS (1993)] the results of model investigations which have been performed to measure the distribution of wave impacts at the front face of a caisson breakwater are described. This breakwater which consists of concrete caissons is the extended breakwater of the existing rubble mound breakwater of the harbour of Civitavecchia (Italy).

The tests were performed in a flume in De Voorst Laboratory (the Netherlands). The length of this flume is about 50 m, the width is 1 m and the height is 1.2 m. The front side of the tested caisson was constructed of a 10 mm thick steel plate. The rear side was strengthened by steel diaphragms to ensure a rigid model construction. The caisson was founded on a rigid steel base, the berm in front of the caisson was constructed of concrete (see figure 5.8). The following scale has been used: 1 m in the hydraulic scale model is the full-scale situation 38 m. Waves have been used in the hydraulic scale model with a height in the order of magnitude of H = 0.20 m

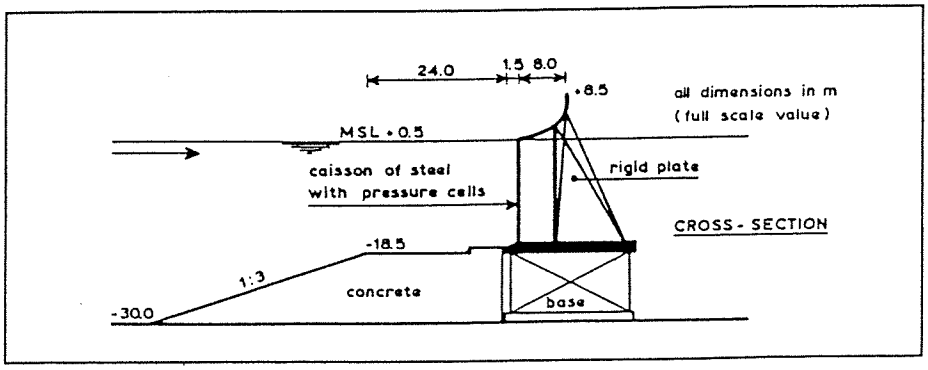

fig. 5.8 Test set - up for wave impact study [DELFT HYDRAULICS (1993)]

"The caisson was constructed of steel to obtain a model with a great stiffness. Natural frequencies were measured with water in the flume. Frequencies of 1250, 2000 and 5000 Hz were measured. Although the lowest frequency of 1250 Hz is in the range of impact frequencies, the stiffness of the caisson is much larger than the stiffness of air and water mixture and therefore pressure variations by the natural frequency will be negligible [DELFT HYDRAULICS (1993)].

In figure 5.9 different wave impacts which have been measured are sketched.

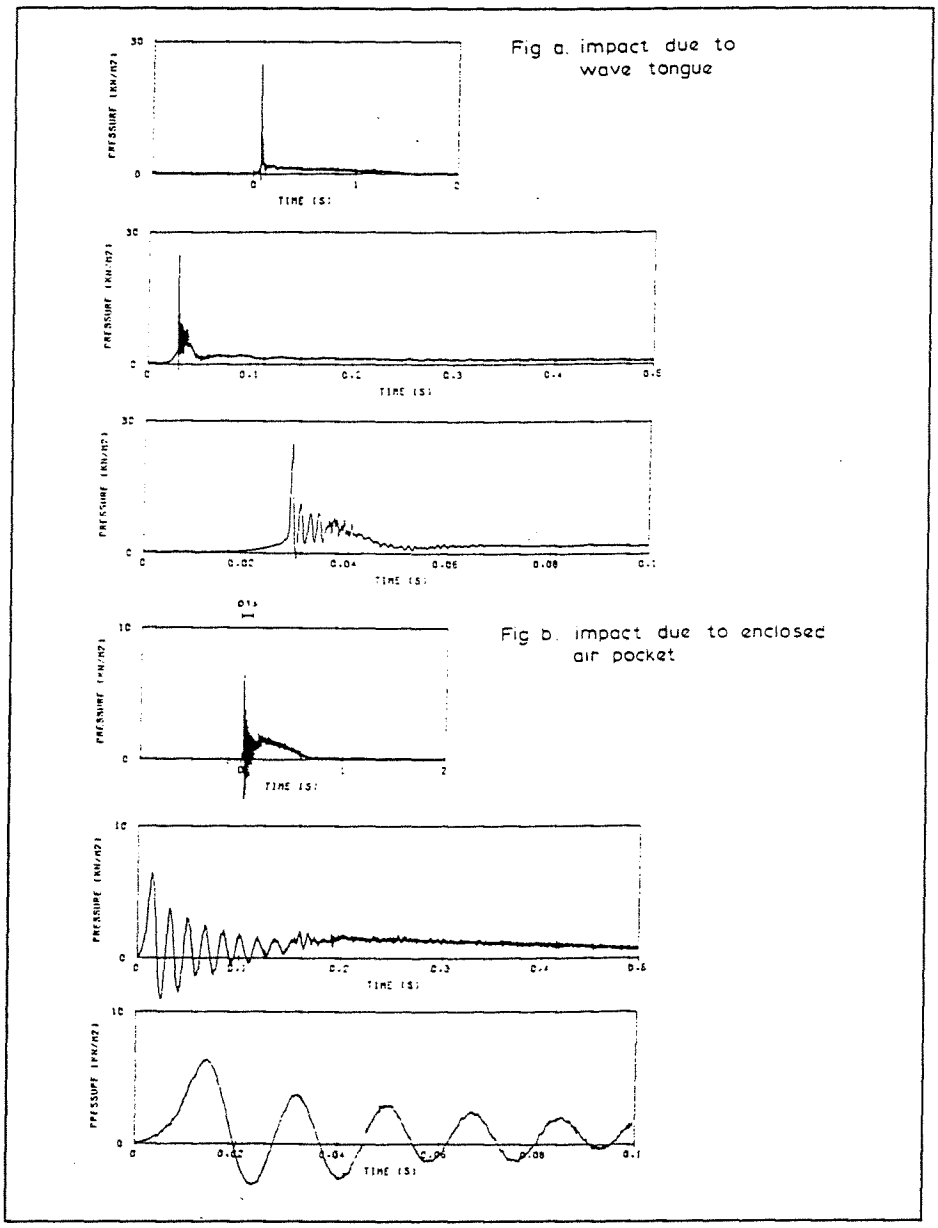

fig. 5.9 Wave impacts at different time scale [DELFT HYDRAULICS (1993)]

The location of the different impact types is sketched in figure 5.10

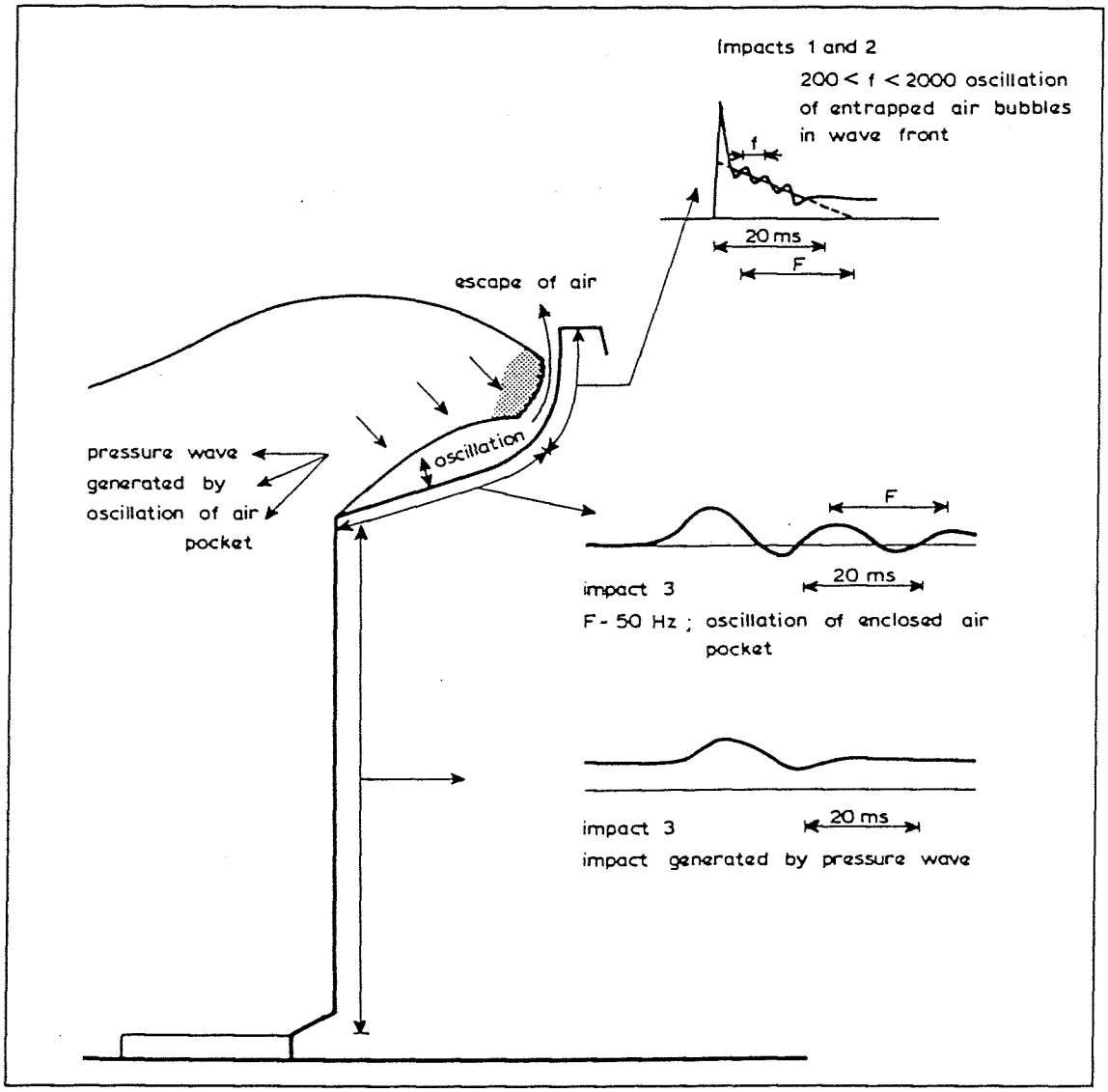

fig. 5.10 Location of impact types [DELFT HYDRAULICS (1993)]

The following results have been found in the hydraulic scale model tests of Delft Hydraulics [DELFT HYDRAULICS (1993)] concerning the oscillation of air pockets:

- the range of frequencies of air pocket oscillation: $33 < f < 80$ Hz
- the range of air bubble oscillations: $200 < f < 2000$ Hz

Again it can be seen that the frequencies of the air pocket oscillation due to a wave impact which encloses this large air pocket are different from the eigenfrequencies of the structure on which the wave impacts have been measured. Thus, the conclusion can be drawn that for this test of the collision of a fully developed plunging breaker the pressure signal has not been disturbed by the eigenmotion of the vertical breakwater.

Conclusion:
It can be concluded that the air pocket oscillation is a phenomenon purely caused by a wave impact load itself; the wave impact pressure signal has not been disturbed by the eigenmotion of the vertical breakwater.

5.3 Formulae for the pulsation of an air pocket

In the previous chapter it has been shown that the low frequency force oscillations, caused by a large air pocket which is enclosed between a breaking wave and a vertical front wall of a breakwater, is a phenomenon purely caused by the wave impact load itself. The low frequency force oscillations are not caused by the eigenmotion of a vertical breakwater, on which is measured in a model, which disturbs the force signal. The low frequency force oscillations can, by accident, have a frequency which is in the range of the eigenfrequencies of a vertical breakwater .

Bagnold [BAGNOLD (1939)] and many others, such as Ramkema [RAMKEMA (1978)], have used air trapped by a piston as a model (see chapter 3) to determine the force oscillations which occur after the second force peak caused by a plunging wave with a large air pocket. Bagnold [BAGNOLD (1939)] has found the following relationship for the period of an oscillating air pocket which can be caused by a breaking wave of the plunging type:

$$T = 2\pi\sqrt{\frac{D\rho L}{\gamma p_0}} \tag{3.34}$$

Takahashi et al. [TAKAHASHI et al. (1993)] have found approximately the same result:

$$T = 2\pi\sqrt{\frac{\pi\rho\kappa_m^2\kappa_l^2\kappa_a H^2}{4\gamma p_0}} \tag{3.41}$$

Both results show that the period of the oscillations of an enclosed air pocket is proportional to the wave height or a "length": $\sqrt{DL}$. A definition of the different symbols can be found in the list of symbols.

The derivation of a relationship between the wave height and the period of the force oscillations will be given here. This derivation has been presented earlier by Oumeraci et al. [OUMERACI et al. (1991)]. This derivation can be denoted as the Lumped-Mass approach.

Lumped-Mass approach [OUMERACI et al. (1991)]
"Force and pressure histories and the simultaneously recorded video pictures show that a correlation is apparent between the size of the pulsating air pocket, the incident wave height and the period of pulsations. In spite of the stochastic nature of the phenomena involved a semi-empirical relationship between the resonant period of pulsations and the incident wave height may be derived, based on the test results and the basic knowledge in gas bubbles dynamics, as well as in the thermodynamics and acoustics. (...) only very approximate solutions can be obtained, since linear pulsations are assumed for the development of the equation of motion. Even with these shortcomings, the proposed relationship will allow us to evaluate the importance of the phenomena involved(...). For reasons of simplification the air pocket will first be assumed as a sphere pulsating in infinite incompressible water. [OUMERACI et al. (1991)].

The spherical air pocket (figure 5.11) is assumed as a linear oscillating system, a mass-spring-dashpot model.

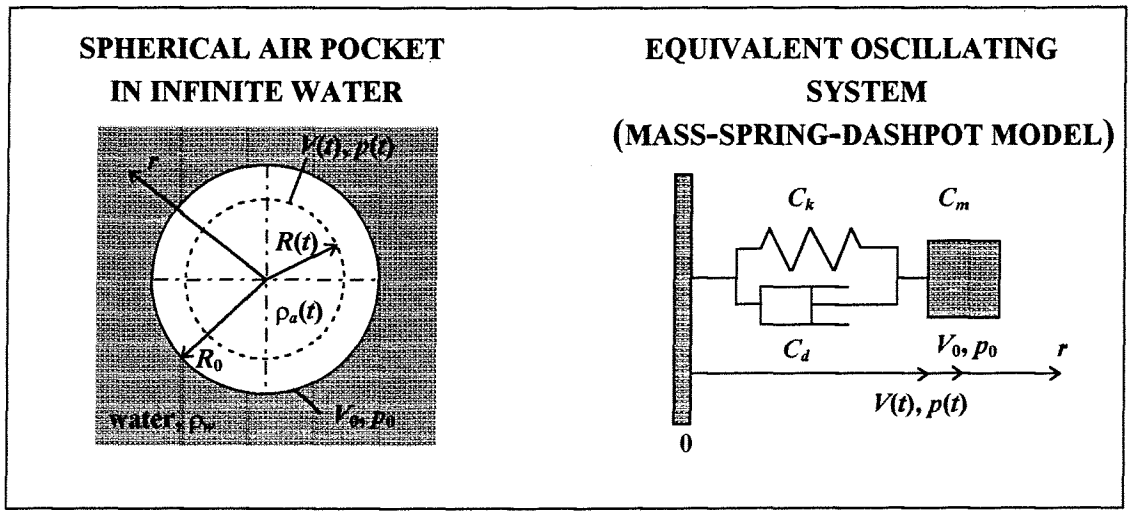

fig. 5.11 Pulsating air pocket and equivalent oscillating system [OUMERACI et al. (1991)]

The linear second-order equation of free motion is formulated in terms of the air volume $V(t)$ oscillating around an equilibrium volume of V_0 :

$$C_m \frac{d^2V}{dt^2} + C_d \frac{dV}{dt} + C_k V = 0 \qquad [\text{Pa}=\text{N/m}^2] \qquad (5.3)$$

in which :

C_m	=	inertial coefficient	[Ns^2/m^5]
C_d	=	damping coefficient	[Ns/m^5]
C_k	=	stiffness coefficient	[N/m^5]

Neglecting the dissipating effect during the first oscillation cycle the resonant period T_0 can be obtained:

$$T_0 = 2\pi\sqrt{\frac{C_m}{C_k}} \qquad (5.4)$$

Nota bene:

The period of the oscillating trapped air pocket will increase due to the effect of damping as can be seen in equation 5.5:

$$T = 2\pi \frac{1}{\sqrt{\frac{C_k}{C_m} - \frac{C_d^2}{4C_m^2}}} \qquad (5.5)$$

The generalised mass or inertial coefficient C_m represents in this case the pressure dp required to give the water a volume acceleration:

$$\ddot{V} = \frac{d^2V}{dt^2} \tag{5.6}$$

$$C_m = \frac{dp}{\ddot{V}} \tag{5.7}$$

Substituting the following relationships [LAMB (1932)] in equation 5.7:

$$p = \rho_w \phi \tag{5.8}$$

$$\phi = \frac{\dot{V}}{4\pi R_0} \tag{5.9}$$

gives:

$$C_m = \frac{\rho_w}{4\pi R_0} \tag{5.10}$$

in which:

ϕ = velocity potential of a water particle at distance R_0
ρ_w = mass density of water
$\dot{V}$ = dV/dt = velocity of volume change of the air pocket

The stiffness coefficient C_k can be defined as the change of pressure dp inside the air pocket associated with its volume change dV:

$$C_k = \frac{dp}{dV} \tag{5.11}$$

In thermodynamics generally is made use of the Poisson equation in the following form:

$$p = p_0\left(\frac{V_0}{V}\right)^{\gamma} \tag{5.12}$$

Differentiation of this equation leads to the following result (assumed is that the pressure variations are small, compared to the initial pressure, see chapter 3, equation 3.7):

$$\frac{dp}{dV} = \gamma\left(\frac{p_0}{V_0}\right) \tag{5.13}$$

in which:

V, p = instantaneous volume and air pressure, respectively
V_0, p_0 = equilibrium values of V and p, respectively
γ = constant of Poisson (isothermal compression (no temperature change during the compression): γ = 1.000; adiabatic compression (no heat exchange with the vicinity during the compression): γ = 1.405)

The trapped air pocket at its equilibrium state can be assumed to have a volume V_0 which is equal to a volume of a sphere with a radius R_0:

$$V_0 = {}^4/_3 * \pi * R_0^3 \tag{5.14}$$

This assumption will not significantly affect the final result, since the natural frequency of oscillations is only slightly dependent on the shape of the trapped air [PEREGRINE (1994)].

Combining equations 5.11, 5.13 and 5.14 gives:

$$C_k = \frac{3\gamma p_0}{4\pi R_0^3} \tag{5.15}$$

So, finally the period of the oscillations of the air pocket can be found (substituting the equations 5.10 and 5.15 in equation 5.4):

$$T_0 = 2\pi\sqrt{\frac{C_m}{C_k}} = 2\pi\sqrt{\frac{\frac{\rho_w}{4\pi R_0}}{\frac{3p_0\gamma}{4\pi R_0^3}}} = 2\pi R_0\sqrt{\frac{\rho_w}{3p_0\gamma}} \tag{5.16}$$

This equation shows good agreement with the equation of Bagnold (equation 3.34) and Takahashi (equation 3.41) which have been given in chapter 3.

Oumeraci et al. [OUMERACI et al. (1991)] show by an energy approach of the problem of the oscillating trapped air that the pulsation process of the air pocket is adiabatic, this means that $\gamma = 1.4$. This result is not surprising due to the relatively large volume of the trapped air. In previous studies is also experimentally shown that the process is clearly adiabatic when the initial volume (V_0) is greater than 4 cm^3.

Using equation 5.16, equation 5.17 can be derived when $\gamma = 1.4$, $p_0 = p_{atm} = 1.01325 * 10^5$ N/m^2 and $\rho_w = 1025$ kg/m^3:

$$T_0 = 0.3084 * R_0 \tag{5.17}$$

Equation 5.17 ($T_0 = 0.3084*R_0$) is obtained by assuming the air pocket oscillating in infinite water. However, due to the presence of the solid boundary (front wall of the vertical breakwater) the resonant period is expected to increase. Based on the geometric considerations in figure 5.12 and following Blue (1966), Oumeraci et al. [OUMERACI et al. (1991)] have obtained a relationship between the increase of the period of the oscillations of the trapped air pocket and the relative distance form the wall expressed by the angle α which is described in equation 5.18:

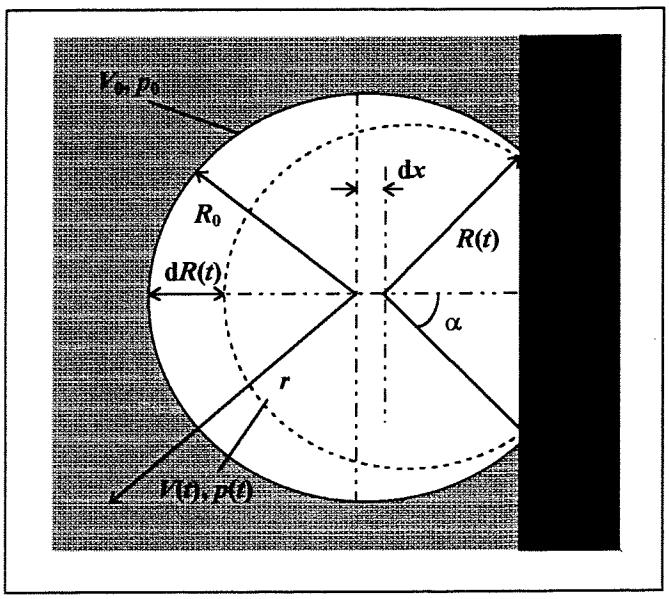

fig. 5.12 Pulsating air pocket in the presence of a solid boundary [OUMERACI et al. (1991)]

$$T_{0w} = T_0\sqrt{1+\cos(\alpha)} \tag{5.18}$$

in which:

T_{0w} = period of the oscillations of an air pocket near a vertical solid boundary
T_0 = period of the oscillations of an air pocket in infinite water

According to equation 5.18 and assuming that the spherical air pocket is at its equilibrium stage when the angle of contact is $\alpha = 60°$ equation 5.17 becomes:

$$T_{0w} = T_0\sqrt{1+\cos(\alpha)} = 0.3084*R_0*\sqrt{1+\cos(60)} = 0.378*R_0 \tag{5.19}$$

According to a number of observations of trapped air pockets by plunging breakers during model tests (video) and prototype (photographs) the following approximate relationship between the equivalent radius R_0 and the incident wave height H may be assumed:

$$R_0 = 0.2*H \tag{5.20}$$

Finally, the relationship between the period of pulsations T_{0w} (in seconds) and the incident wave height H (in cm) is obtained:

$$T_{0w} = 0.75*10^{-3} * H \tag{5.21}$$

Prototype measurements of force oscillations and experimental results from small and large-scale tests are plotted in figure 5.13, showing a relatively good agreement with equation 5.21 [OUMERACI et al. (1991)].

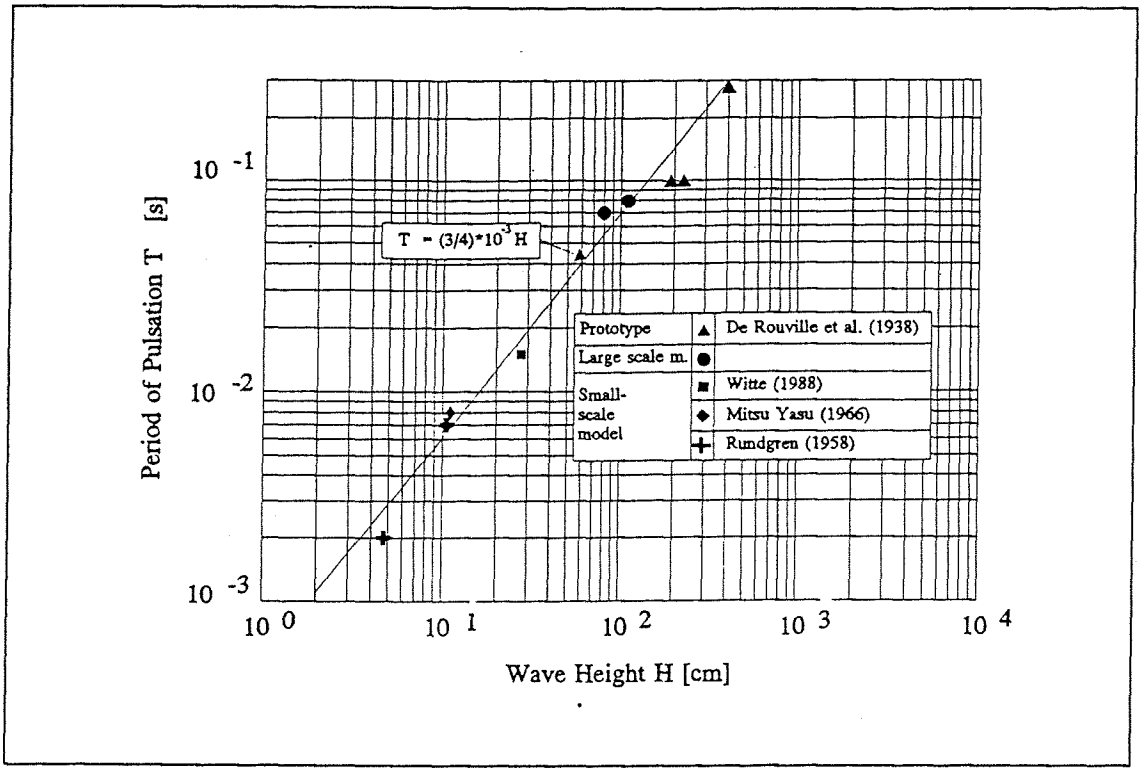

fig. 5.13 Pulsation period of air pocket versus incident wave height [OUMERACI et al. (1991)]

The meaning of the result shown in figure 5.13 may be formulated as follows:

- If a plunging breaker is impinging on a vertical caisson front in such a way that a large air pocket is trapped, the latter will perform volume oscillations with a period which is directly proportional to the incident wave height.
- Prototype scale values for wave heights are 1 - 10 m. This leads to periods of the force oscillations in the range of 0.075 - 0.75. Muraki [MURAKI (1966)] found that the damped natural frequency of typical caisson or vertical breakwaters on sand and gravel is in the range of 0.3 to 0.6 seconds (see also chapter 7).[1] The period of the low frequency force oscillations is in the range of the eigenperiods of the structure. Dynamic amplification of the displacement of a vertical breakwater may occur due to these resonant or quasi-resonant force oscillations. In chapter 10 it will be shown that if a plunging breaker hits the vertical breakwater and a large air pocket is entrapped, the breakwater can fail. This situation is not likely to occur very often, a very special situation (dependent on the geometry of the structure and the foreshore and the characteristics of the waves) is necessary to cause this kind of load, but it can occur! One should regard this load as an important load which may lead to breakwater failure.

[1] Lamberti et al. [LAMBERTI et al. (1996)] have reanalysed the prototype measurements of Muraki et al. [MURAKI et al. (1966)] with modern methods and found a different conclusion than the author himself. For one of the tested caissons Muraki et al. found a period of oscillation of 0.2 s while Lamberti et al. found larger periods. Two dominant periods have been found, one which is slightly smaller (0.7 s) and one which is slightly larger than (1.3 s) than 1 s.

Oumeraci et al. [OUMERACI et al. (1991)] do also give an evaluation of the amount of energy which is transferred from an approaching wave to an enclosed air pocket. The available incident wave energy E_w will be transferred through a half-cylindrical water-air boundary to the air pocket (see figure 5.14). This transferred energy E_{ap} will be presented within the air cushion as internal energy during the first compression; i.e. when the air volume reaches its minimum value.

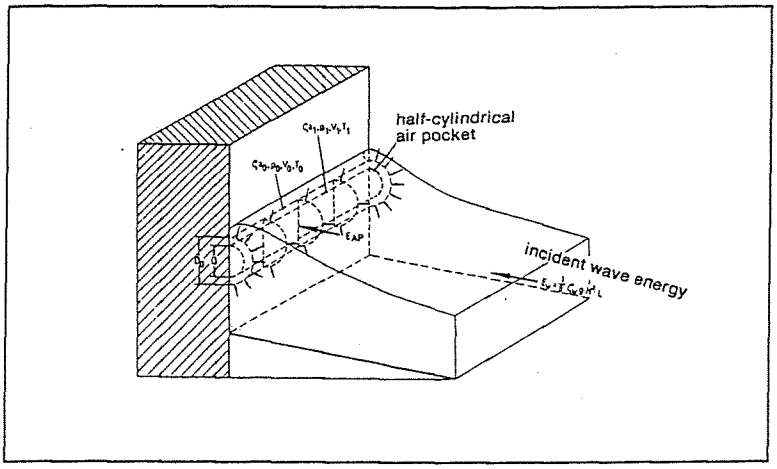

fig. 5.14 Entrapped air pocket as a wave energy reservoir [OUMERACI et al. (1991)]

The ratio of the transferred energy E_{ap} to the available incident wave energy E_w (E_{ap}/E_w) is plotted in figure 5.15 versus the dimensionless maximum pressure p_{max}/p_0 inside the air pocket for different wave lengths L = 10 m (small hydraulic scale model), L = 20 - 40 m (large hydraulic scale model) and L = 100 - 200 m (full-scale) (p_0 is the initial pressure or the equilibrium pressure in the air pocket).

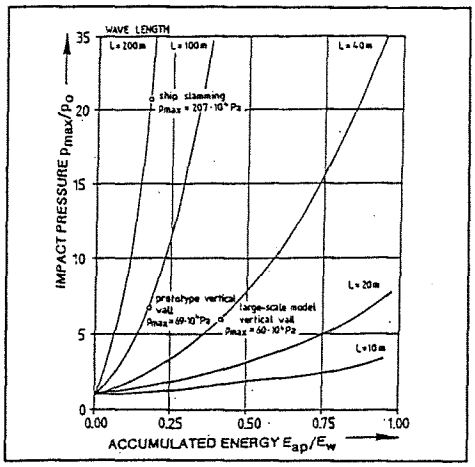

fig. 5.15 Wave energy accumulated by the entrapped air pocket [OUMERACI et al. (1991)]

From figure 5.15 it can be seen that:

- the accumulated wave energy rate increases with the maximum pressure inside the air pocket
- the smaller the model scale, i.e. the smaller the air pocket, the larger the portion of the available wave energy that is accumulated by the air pocket
- for full-scale situations the wave energy accumulated by the entrapped air pocket is approximately 20 to 25%.

5.4 Brief attention to scaling of wave impacts with a trapped air pocket

As has been shown before in section 4.5 the scale factor for the time according to Froude's law is (see equation 4.45)

$$n_t = \sqrt{n_L} \tag{4.45}$$

However, the period of the pulsation of an air pocket which is enclosed when a plunging breaker hits a plane vertical front wall of a breakwater in a hydraulic scale model must be transferred to full-scale situations by multiplying the hydraulic scale model value by the length scale n_L instead of $\sqrt{n_L}$, i.e. according to Mach-Cauchy's scaling law instead of Froude's law. "This result can also be found by applying a dimensional analysis to the wall motion and the pressure field of the air pocket" [OUMERACI et al. (1991)].

It is obvious to see from the presented formulae in the previous section that the period of the oscillations of an air pocket is proportional to a "length scale" e.g. the wave height H or $\sqrt{DL}$. The three equations which have been treated in this chapter and which can be used to calculate the period of an oscillating air pocket which is enclosed by a breaking wave of the plunging type are reflected here again:

[BAGNOLD (1939)]:

$$T = 2\pi\sqrt{\frac{D\rho L}{\gamma p_0}} \tag{3.34}$$

[TAKAHASHI et al. (1993)]:

$$T = 2\pi\sqrt{\frac{\pi\rho\kappa_m^2\kappa_l^2\kappa_a H^2}{4\gamma p_0}} \tag{3.41}$$

[OUMERACI et al. (1991)]:

$$T_{0w} = 0.75*10^{-3} * H \tag{5.21}$$

The formula presented in equation 5.21 will be used to calculate the period of the low frequency force oscillation (caused by a large trapped air pocket) in this study.

6 Vertical breakwater design formula and wave impacts

6.1 Introduction

In this chapter the most widely used prediction method for wave forces on vertical breakwaters will be treated. This method is known as Goda's method [GODA (1985)]. This method was primarily developed to calculate the horizontal forces for concrete caissons on rubble mound foundations, and was calibrated against laboratory tests and back-analysis of historic failures. It assumes that wave pressures on the wall can be represented by a trapezoidal distribution, see figure 6.1, with the highest value at Still Water Level (SWL), regardless of whether waves are breaking or non-breaking [ALLSOP et al. (1996)]. In section 6.2 this method will be treated more extensively.

Goda's method does not consider frequent wave breaking close to and at a vertical breakwater. Therefore, Takahashi et al. [TAKAHASHI et al. (1993)], [TAKAHASHI et al. (1994)] have developed a modification to the Goda method, often termed the "Takahashi extension". This extension will be treated in section 6.3.

The pressures which can be calculated by means of the presented design method in this chapter can be used to calculate wave (impact) forces on a vertical breakwater. These forces can be used in a **(quasi-)static** stability analysis. In this study, however, a **dynamical** (stability) analysis will be used to calculate the effect of wave impact forces on the stability of a vertical breakwater. This analysis will be carried out in chapter 7 to 10 by means of the calculation of the dynamical behaviour of a vertical breakwater which is exposed to wave impacts. For a dynamical (stability) analysis the development in time of wave impact forces has to be known. The forces or pressures which can be calculated by means of the presented method(s) in this chapter do not give the development in time of the wave (impact) forces and are therefore of limited use for this study.

6.2 The Goda formula

Wave pressure formulae have been developed by Goda [GODA (1985)] for the case of a conventional vertical front where wave breaking on the wall is not enhanced by a steep seabed or structural configurations. The method was primarily developed to calculate the horizontal force for concrete caissons on rubble mound foundations. The formulae are based on model test in head-on waves but were modified to cover oblique waves as well. The formulae include the effect of breaking waves to the extent of normal accidental (non-provoked) wave breaking. The formulae are currently used in the Japanese as well as in the European standards. The Goda formula is the most widely used prediction method for wave forces on vertical walls.

The Goda method is based on non linear wave theory and assumes that wave pressures on the wall can be represented by a trapezoidal distribution, with the highest value at Still Water Level (SWL), regardless of whether waves are breaking or non-breaking (see figure 6.1). It is assumed, for the sake of simplicity, that wave overtopping does not have an influence on this distribution.

Goda's method represents wave pressure characteristics by considering two components, the breaking wave (impacts) and the deflected wave (slowly varying or pulsating pressures), represented in the method by coefficients α_1, α_2, and α_3 [ALLSOP et al. (1996)]. According to Goda these coefficients have got the following meaning:

- Coefficient α_1 accounts for the influence of the wave period: the influence of the relative depth to the wave length on the slowly varying component.
- Coefficient α_2 accounts for the tendency of the pressure to increase with the height of the rubble-mound foundation. It accounts for the effect of impulsive wave breaking due to the relative level of the mound.
- Coefficient α_3 is the result of an interpolation between α_1 and α_2 and accounts for the relative crest level of the caisson and the relative water depth over the toe mound.

The results of the Goda formula are presented by means of pressures on the vertical front wall of a vertical breakwater and pressures and underneath a vertical breakwater (uplift pressures). These results can be used to calculate the forces on the caisson breakwater which can, in their way, be used to calculate the stability of a vertical breakwater for instance against sliding and / or overturning.

In the Goda formula: "the highest wave in the design sea state is to be employed. The adoption of this H_{max} in the pressure formulae was first proposed by Ito. It is based on the principle that a breakwater should be designed to be safe against the single wave with the largest pressure among storm waves" [GODA (1985)].

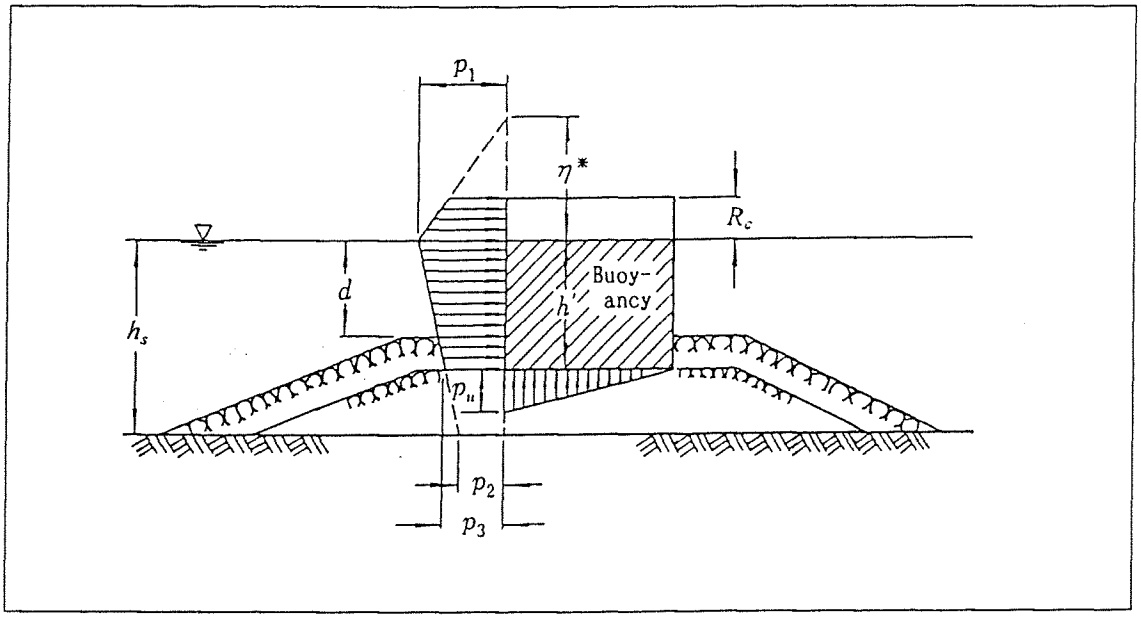

fig. 6.1 Wave pressure distribution by Goda's formulae [GODA (1985)]

In figure 6.1 four parameters regarding the geometry (lay-out) of a breakwater are denoted. R_c is the crest freeboard, the level of the crest less the static water level, h_s is the water depth in front of the vertical breakwater, d is the water depth over the berm at the vertical front wall of the breakwater and h' is the distance from the design water level to the bottom of the upright section (the upright section is the actual *vertical breakwater*; in fact, figure 6.1 denotes a *vertical composite breakwater*, consisting of an upright section and a rubble mound berm, see figure 7.4).

The wave pressures (and forces) on the upright section can be calculated using the following equations:

$$\eta^* = 0.75 * (1 + \cos\beta) * \lambda_1 * H_{max} \tag{6.1}$$

$$p_1 = 0.5 * (1 + \cos\beta)(\lambda_1\alpha_1 + \lambda_2\alpha_2 \cos^2\beta) * \rho_w * g * H_{max} \tag{6.2}$$

$$p_2 = \frac{p_1}{\cosh\left(\frac{2\pi}{L} * h\right)} \tag{6.3}$$

$$p_3 = \alpha_3 * p_1 \tag{6.4}$$

$$p_u = 0.5*(1+\cos\beta)\lambda_3 *\alpha_1*\alpha_3*\rho_w*g*H_{max} \tag{6.5}$$

in which:

β = angle of incidence of waves (angle between the wave crests and the normal of the front of the structure)

H_{max} = the design wave height defined as the highest wave in the design sea state at a location just in front of the breakwater. If seaward of a surf zone a value of 1.8 H_s might be used corresponding to the 0.1% exceedence value for Rayleigh distributed wave heights. This corresponds to $H_{1/250}$ (mean of the heights of the waves included in 1/250 of the total number of waves, counted in descending order of height form the highest wave). If within a surfzone H_{max} is taken as the highest of the random breaking waves at a distance $5*H_s$ seaward of the structure [BURCHARTH et al. (1994)] [PIANC (1996)]. "The Goda formula might, according to van der Meer et al. (1992), be regarded as a good central approximation for the maximum wave force in a sea state with a duration of approximately 2500 waves" [BURCHARTH et al. (1994)].

L = wave length corresponding to that of the significant wave $T_s \cong 1.1*T_m$, where T_m is the average period

$$\alpha_1 = 0.6 + 0.5 * \left[\frac{(4\pi * h_s)/L}{\sinh[(4\pi * h_s)/L]}\right]^2 \tag{6.6}$$

$$\alpha_2 = \text{the smallest of } \frac{h_b - d}{3 * h_b}\left(\frac{H_{max}}{d}\right)^2 \text{ or } \frac{2*d}{H_{max}} \tag{6.7}$$

$$\alpha_3 = 1 - \frac{h'}{h_s} * \left[1 - \frac{1}{\cosh[(2\pi * h_s)/L]}\right] \tag{6.8}$$

h_b = water depth at the location at a distance of $5*H_s$ seaward of the breakwater front wall

$\lambda_1, \lambda_2, \lambda_3$ = modification factors dependent on the structural type; 1 for the condition of both standing and non-provoked breaking waves on a vertical wall

Although the wave induced uplift pressure, p_u (equation 6.5), at the front edge of the base plate is equal to p_3 it is suggested by Goda to use the somewhat reduced value given by equation 6.5. This is because analyses of the behaviour of Japanese breakwaters revealed that the use of $p_u = p_3$ together with an assumed triangular distribution of the uplift pressure gave too conservative results [PIANC (1996)].

"The caissons on rubble mound foundations considered by Goda (1974) had natural periods around 0.1 to 0.3 s. When subjected to loads of durations shorter than the most dominant eigenperiod of the oscillation of a vertical breakwater, the effective load will itself be smaller than the applied load. Thus for the very short peak pressures caused by breaking waves, the Goda formula does not give the actual peak pressure, but pressures which give the equivalent static load for the dynamic system of caisson, mound and foundation. This method was not intended to predict pressures of short duration, or of limited restricted spatial extent. Goda (1974) noted that impulsive pressures caused by waves which break in front of or onto the wall may rise to

$$10*\rho_w *g*H_b \tag{6.9}$$

but judged that vertical breakwaters would not be designed to be exposed to direct impulsive pressures" [ALLSOP et al (1996)].

Goda considers wave impacts not to be that important for the stability of vertical (composite) breakwaters. "It is found in laboratory experiments that the front face of an impinging breaking wave is always curved and a small amount of air is entrapped at the instant of collision. As suggested by Bagnold [BAGNOLD (1939)] and by Takahashi and Tanimoto (1983), the entrapped air acts to dampen the impulsive pressure and prevents it from becoming abnormally high. Furthermore, the rubble mound foundation and the ground around a prototype breakwater will be elastically deformed under the application of an impulsive breaking wave pressure, and this softens the wave impact on the upright section" [GODA (1985)]. In Goda's opinion impact forces are not important for the design of vertical breakwaters. "It would be rather foolish to design a vertical breakwater to be directly exposed to impulsive breaking wave pressures. A rubble mound breakwater would be the natural choice in such a situation. If space is limited, or if little wave transmission is to be allowed, a vertical breakwater protected by a mound of concrete blocks of the energy-dissipating type might be an alternative design. From the engineering point of view, it is not the magnitude of the greatest pressure but, rather the occurrence of the impulsive breaking wave pressure that is the most important" [GODA (1985)].

"Various researchers have found uncertainties with the Goda's method, and some have identified differences with measurements of forces / pressures. (...) Despite these limitations, the methods developed by Goda (1975), Goda [GODA (1985)] and others constitute the best methods available, and include many points of good advice" [ALLSOP et al. (1996)].

6.3 Extended Goda formula by Takahashi et al.

Goda's formula does not consider frequent wave breaking close to and at a vertical breakwater. Therefore, Takahashi et al. [TAKAHASHI et al. (1993)], [TAKAHASHI et al. (1994)] have developed a modification to the Goda method, often termed the "Takahashi extension". This modification has been developed to estimate equivalent wave forces under breaking wave impacts and was obtained by re-analysing the results of comprehensive model tests of caissons sliding under wave impacts, together with analysis of the breakwater movements at Sakata Port, Japan 1973-1974. The modification is applied to the Goda method by changing the formulation for the α_2 coefficient of the Goda formula. Takahashi introduces a new coefficient α^* which is the maximum of α_2 or a new impulsive coefficient α_I, itself given by two coefficients representing the effect of the wave height on the mound, and the shape of the mound (see figure 6.2). This modification only operates where the water depth over the toe mound is relatively small, and the mound is therefore likely to generate wave breaking onto the wall. Takahashi's method does not change the uplift pressures calculated by Goda's method.

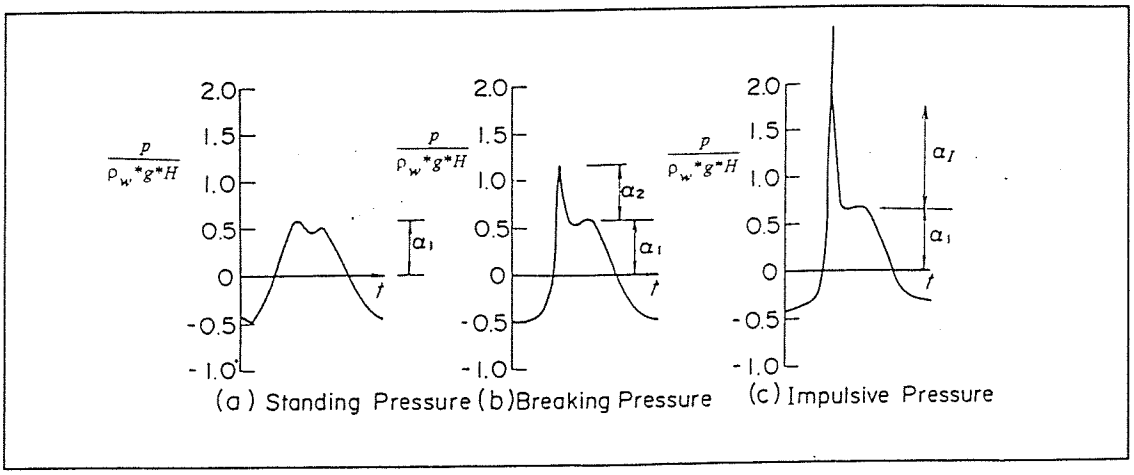

fig. 6.2 Transition of wave pressure [TAKAHASHI (1995)]

According to Takahashi et al. [TAKAHASHI et al. (1993)] the pressure p_1 at the water surface in the Goda pressure formula can be expressed as (see also equation 6.2):

$$p_1 = 0.5 * (1 + \cos\beta)(\lambda_1\alpha_1 + \lambda_2\alpha^* \cos^2\beta) * \rho_w * g * H_{max} \tag{6.10}$$

where α^* represents the coefficients of impulsive pressure and α_1 is the pressure coefficient for the slowly varying pressure. The coefficient α^* is expressed by:

$$\alpha^* = \text{the largest of } \alpha_2 \text{ and } \alpha_I \tag{6.11}$$

In figure 6.3 a calculation diagram for the impulsive pressure coefficient α_I is presented. This diagram has been obtained from sliding tests [TAKAHASHI et al. (1993)].

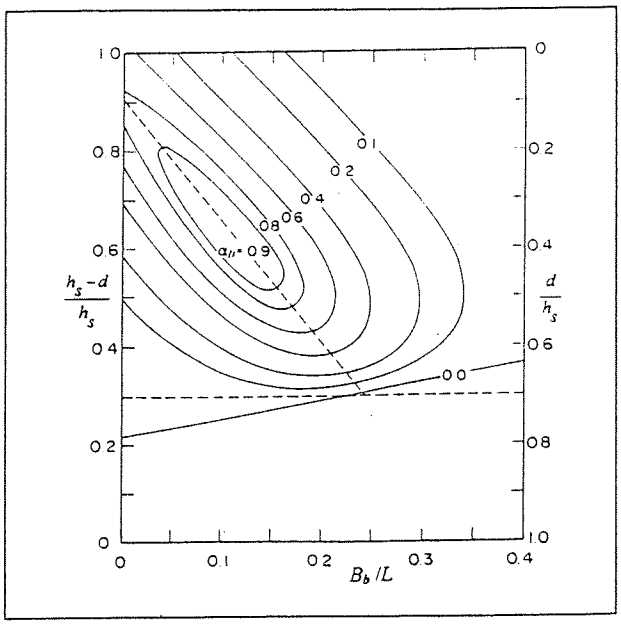

fig. 6.3 Calculation diagram of the impulsive pressure coefficient [TAKAHASHI et al. (1993)]

The coefficient α_I is expressed by the product of α_{I0} and α_{I1}:

$$\alpha_I = \alpha_{I0} * \alpha_{I1} \tag{6.12}$$

where α_{I0} represents the effect of wave height on the mound, i.e.,

$$\alpha_{I0} = H_{max}/1.8*d \quad : \quad H_{max}/1.8*d \leq 2 \tag{6.13}$$

$$\alpha_{I0} = 2.0 \quad : \quad H_{max}/1.8*d > 2$$

and α_{I1} represents the shape of the rubble mound:

$$\alpha_{I1} = \frac{\cos\delta_2}{\cosh\delta_1} \quad : \quad \delta_2 \leq 0 \tag{6.14}$$

$$\alpha_{I1} = \frac{1}{\cosh\delta_1 * \sqrt{\cosh\delta_2}} \quad : \quad \delta_2 > 0$$

$$\delta_1 = 20*\delta_{11} \quad : \quad \delta_{11} \leq 0 \tag{6.15}$$

$$\delta_1 = 15*\delta_{11} \quad : \quad \delta_{11} > 0$$

$$\delta_{11} = 0.93\left(\frac{B_b}{L} - 0.12\right) + 0.36\left(\frac{h_s - d}{h_s} - 0.6\right) \tag{6.16}$$

$$\delta_2 = 4.9*\delta_{22} \quad : \quad \delta_{22} \leq 0 \tag{6.17}$$

$$\delta_2 = 3*\delta_{22} \quad : \quad \delta_{22} > 0$$

$$\delta_{22} = -0.36\left(\frac{B_b}{L} - 0.12\right) + 0.93\left(\frac{h_s - d}{h_s} - 0.6\right) \tag{6.18}$$

L is defined as for the Goda formula and B_b is the width of the rubble berm at the toe of the wall of a vertical breakwater.

The value of α_I reaches a maximum of 2 when $B_b/L = 0.12$, $d/h_s = 0.4$ and $H_{max} / 1.8d \geq 2$. When the term $d/h_s > 0.7$, then impulsive pressures rarely occur and α_I is close to zero (as can be seen in figure 6.3) and smaller than α_2. It should be noted that impulsive pressures are significantly reduced when the angle of incidence β increases.

In using Goda's or Takahashi's methods, it is assumed that wave pressures are distributed approximately trapezoidally over the height of the caisson, with the maximum at the water level. Impact conditions considered by Takahashi et al. [TAKAHASHI et al. (1993)] are assumed not to alter the shape of the pressure distribution, so gradients are relatively mild.

For vertical (composite) breakwaters with high rubble mounds $0.6 \leq h_b / h_s < 0.9$ (see figure 2.7) Allsop et al. [ALLSOP et al. (1996)] suggest that: "An extremely crude, and safe approach for wave forces in this region is to use the Takahashi prediction, described in this section, multiplied by 2. This gives a generally safe result for the combinations of conditions tested here (see [ALLSOP et al. (1996)], but has little other merit except its relative simplicity."

B

Derivation of models which describe the dynamical behaviour of a vertical breakwater

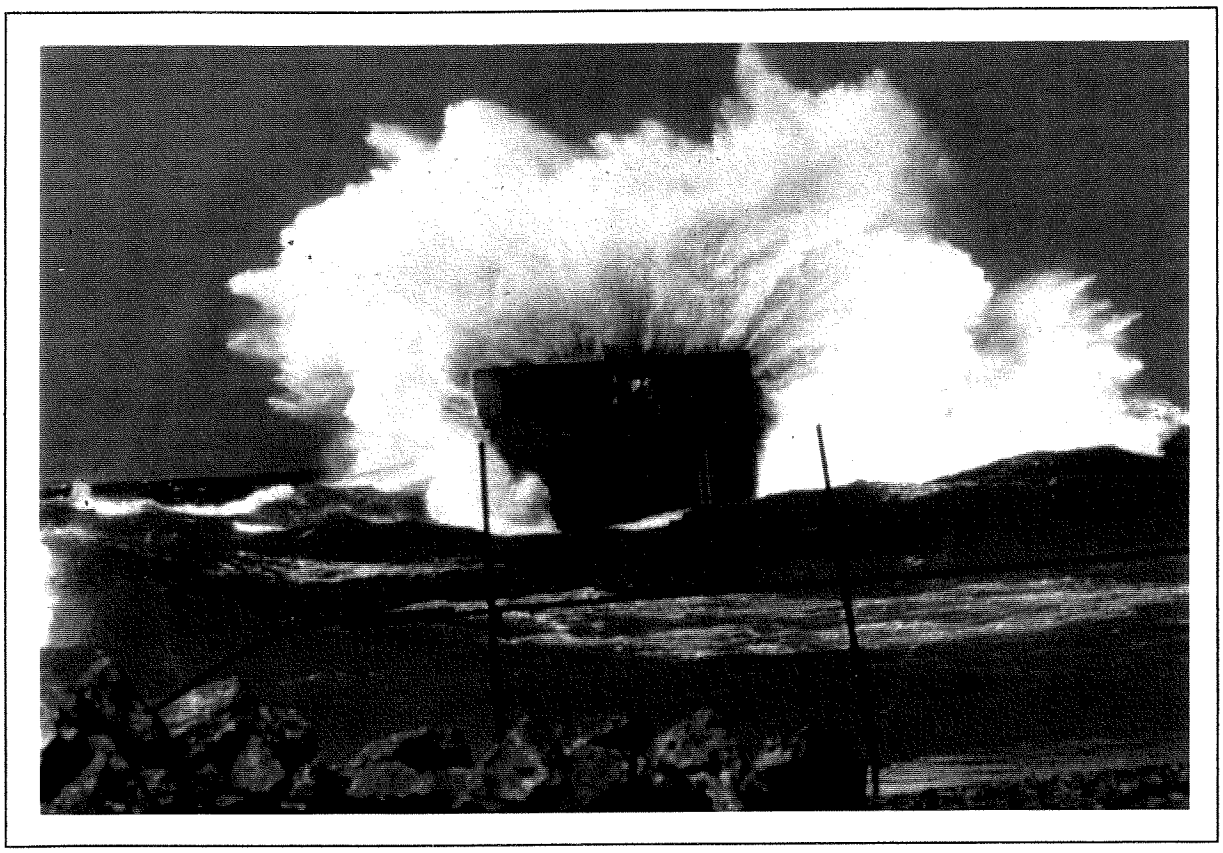

Civitavecchia (Italy), inspection tower of a cooling-water intake

7 Derivation of an analytical mass-spring model of a vertical breakwater

7.1 Introduction

In this chapter the derivation of a simple mass-spring model of a vertical breakwater will be treated. This model will be used to calculate the dynamical behaviour of a vertical breakwater which is exposed to a transition type wave impact. This calculation is also treated in this chapter. The transition type wave impact has been treated before in section 2.4.3. A transition type wave impact on a vertical breakwater is caused by a breaking wave with an almost vertical front, so there is almost no trapped air. Because of this almost vertical front the rise time and total duration of a transition type wave impact is very short and the peak force is very high.

The dynamical behaviour of a vertical breakwater can be calculated by the use of a mass-spring model. If the dynamical behaviour of a vertical breakwater is known, the displacement of different points on the vertical breakwater is known and the forces in the foundation of the vertical breakwater are known as well. The masses which are used in this mass-spring model describe the mass and the mass moment of inertia of the vertical breakwater. The springs which are used in this mass-spring model describe the behaviour of the foundation of the vertical breakwater and they are linear-elastic. The mass-spring model which will be treated in this chapter has three degrees of freedom and damping and elasto-plastic behaviour of the foundation are neglected. Because of the fact that linear-elastic springs are used and that there is taken no account of damping a rather simple analytical solution of this problem is possible.

In the next chapter the derivation of a more sophisticated model will be treated. In that chapter a description is given of the derivation of a mass-spring-dashpot computer model with elasto-plastic springs and damping which describes the behaviour of the foundation of a vertical breakwater more accurately. Results of this more sophisticated model will be calculated by the use of TILLY, which is a computer programme. It is very usefull to find an analytical solution of the dynamical behaviour of a vertical breakwater which is exposed to a wave impact of the transition type in advance because it can give some insight in the problems involved when a mass-spring-dashpot model is derived by using a computer programme. The analytical solution can also serve as a check of the solution of the dynamical behaviour of the vertical breakwater which is generated by the computer model.

In section 7.2 the derivation of a mass-spring model which describes the dynamical behaviour of a vertical breakwater will be treated. The derivation of this model will be carried out for a general case. The result of this derivation is written in parameters which can be chosen in conformance with the situation one would like to calculate. In this chapter (and in the remainder of this report) all calculations will be carried out for a situation along the Dutch coast, so the parameters are also chosen in conformance with the situation at this location. In this chapter and in the next chapter the chosen parameters will not be varied. The effect of the variation of different parameters of the models - which are described in chapter 7 and 8 - will be treated in chapter 9. In that chapter the masses and mass moment of inertia are varied (e.g. by changing the design of the vertical breakwater: if the width and the length of a vertical breakwater of the caisson type are constant, a vertical breakwater on a low rubble mound will weight more than a vertical breakwater on a high rubble mound in the same waterdepth) and the stiffness, strength and damping of the foundation are varied in order to give an idea of the importance of the magnitude of the different parameters. The wave impact load and water depth will not be varied in chapter 9. Calculations with different loads will be carried out in chapter 10. In chapter 10 an analysis of different types of wave impact loads on a vertical breakwater will be treated. In that chapter the structure and foundation parameters will not be varied, but the load on the vertical will.

To determine the magnitude of the parameters which are necessary for the calculations with the model - which will be derived for a general case in section 7.2 - a lay-out of a vertical breakwater is chosen which applies to the situation at the planned land reclamation of the port of Rotterdam: "Maasvlakte 2". The water depth, the wave impact load, the structure size and masses and the characteristics of the foundation are chosen in conformance with the situation at that location.

The masses, size and shape of the vertical breakwater, and the characteristics of the foundation of the vertical breakwater at the chosen location are given in section 7.3. In section 7.4 the eigenvalues of the chosen vertical breakwater are calculated. In section 7.5 the dynamical behaviour of the vertical breakwater, exposed to a wave impact of the transition type (here only the triangular part of the "church-roof" load) is calculated. The stability of the vertical breakwater which is exposed to a transition type wave impact will be discussed in section 7.6. Comments on the calculations carried out in this chapter can be found in section 7.7.

7.2 Derivation of an analytical mass-spring model

In figure 7.1 an overview of the different parameters which are used for the determination of the mass-spring model is given (F_1 (=$F_1(t)$) and F_2 (=$F_2(t)$) are external forces, T (= $T(t)$) is an external moment). This model has three degrees of freedom: vertical, horizontal and rotational displacements are possible.

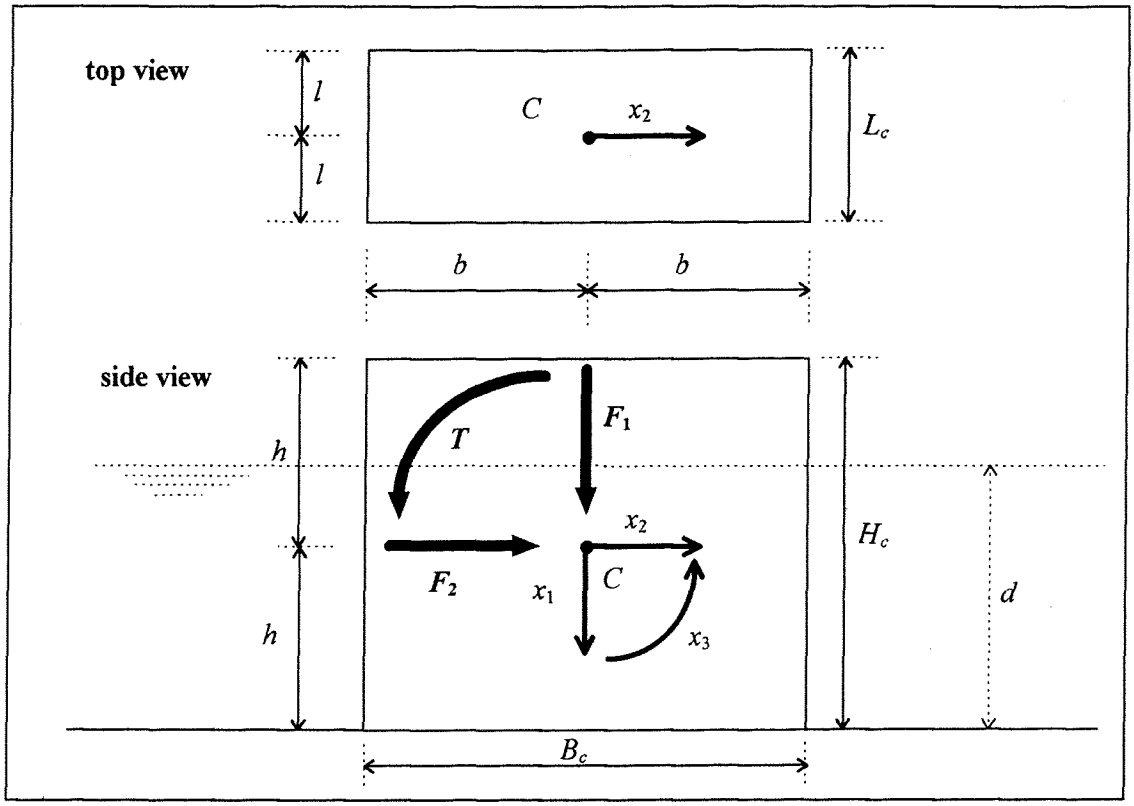

fig. 7.1 Definition sketch parameters

The dynamical behaviour of the system sketched in figure 7.1 can be described by the following differential equation (a description of the different parameters can be found in the list of symbols and figure 2.5 and 2.6):

$$M\ \underline{\ddot{x}}(t) + K\ \underline{x}(t) = \underline{F}(t) \qquad (7.1)$$

in which:

M = mass matrix
K = stiffness matrix
$\underline{F}(t)$ = load vector
$\underline{x}(t)$ = displacement vector ($\underline{x}^T(t) = [\ x_1(t)\ x_2(t)\ x_3(t)\ ]$; $x_1(t)$, $x_2(t)$ [m], $x_3(t)$ [rad])
$\underline{\ddot{x}}(t)$ = acceleration vector ($\underline{\ddot{x}}^T(t) = [\ddot{x}_1(t)\ \ddot{x}_2(t)\ \ddot{x}_3(t)]$;
$\ddot{x}_1(t)$, $\ddot{x}_2(t)$ [m/s^2], $\ddot{x}_3(t)$ [rad/s^2])

Equation 7.1 represents three differential equations, one for each degree of freedom:

- vertical: translation x_1
- horizontal: translation x_2
- rotational: rotation x_3.

These three differential equations can be derived using the so called displacement method. The reaction force of the foundation must be derived when each degree of freedom is given a unit displacement (see figure 7.2); b_1 and b_2 are the so called "bed constants" which represent respectively the stiffness of the foundation in vertical and horizontal direction (b_1 , b_2 [N/m^3] see section 7.3.2).

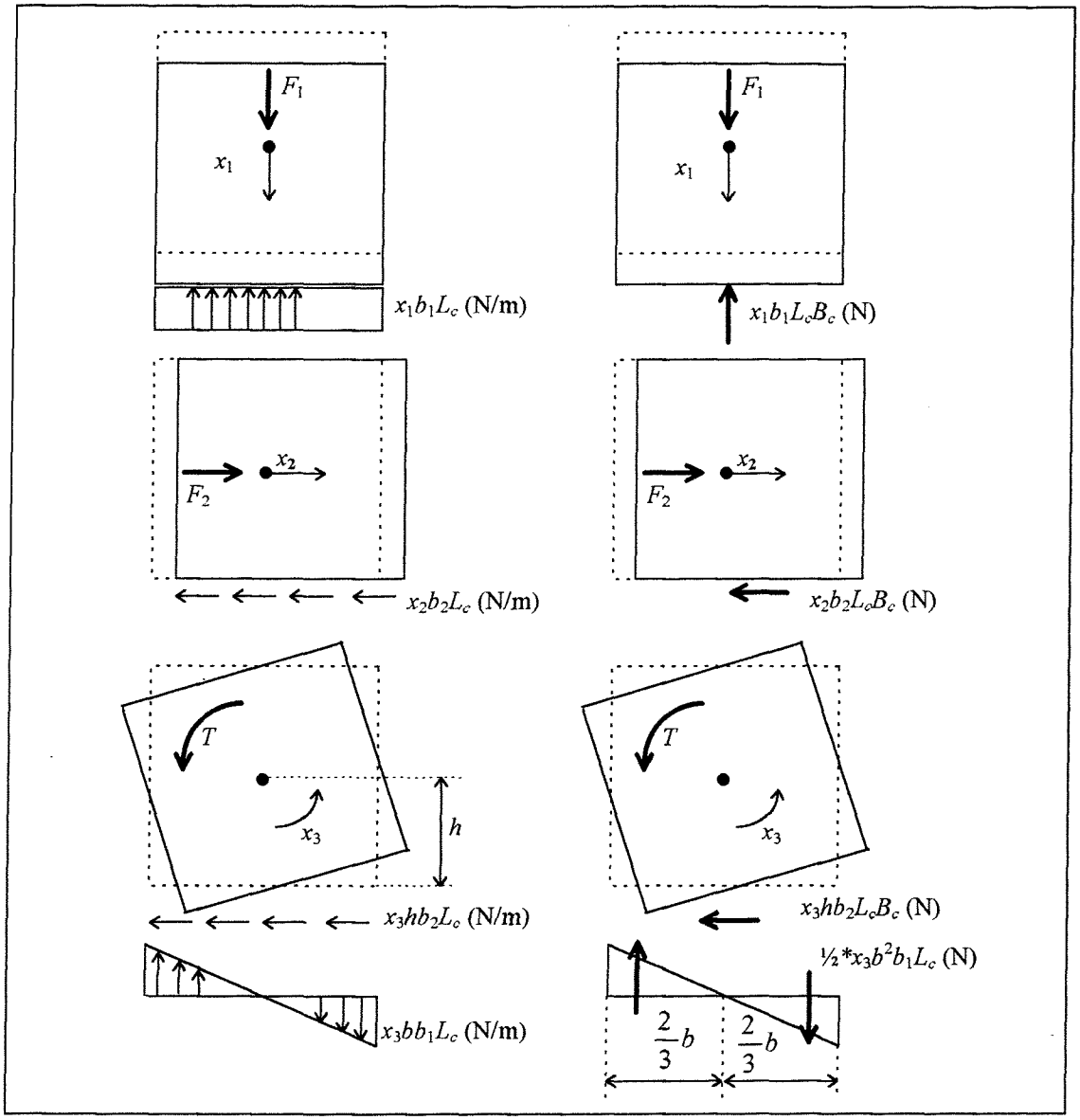

fig. 7.2 Unit displacements and forces

The three equations for the three degrees of freedom can now be derived:

$$m_1 \ddot{x}_1 = -b_1 L_c B_c * x_1 + 0 * x_2 - 0 * x_3 + F_1 \tag{7.2}$$

$$m_2 \ddot{x}_2 = 0 * x_1 - b_2 L_c B_c * x_2 - h b_2 L_c B_c * x_3 + F_2 \tag{7.3}$$

$$\theta \ddot{x}_3 = 0 * x_1 - h b_2 L_c B_c * x_2 - h^2 b_2 L_c B_c * x_3 - \frac{2}{3} b^3 b_1 L_c * x_3 + T \tag{7.4}$$

In which b = ½*B_c and h = ½*H_c .

This can be written in a matrix notation:

$$\begin{bmatrix} m_1 & 0 & 0 \\ 0 & m_2 & 0 \\ 0 & 0 & \theta \end{bmatrix} \begin{bmatrix} \ddot{x}_1 \\ \ddot{x}_2 \\ \ddot{x}_3 \end{bmatrix} + \begin{bmatrix} b_1 L_c B_c & 0 & 0 \\ 0 & b_2 L_c B_c & h b_2 L_c B_c \\ 0 & h b_2 L_c B_c & h^2 b_2 L_c B_c + (^2/_3) b^3 b_1 L_c \end{bmatrix} \begin{bmatrix} x_1 \\ x_2 \\ x_3 \end{bmatrix} = \begin{bmatrix} F_1 \\ F_2 \\ T \end{bmatrix} \tag{7.5}$$

Check of the elements of the stiffness matrix: $k_{12} = k_{21}$
$k_{13} = k_{31}$
$k_{23} = k_{32}$ → OK!

In the matrix notation (equation 7.5), the different stiffnesses of the springs (as sketched in figure 7.3) can be found. The stiffnesses of the two translational springs (k_1 and k_2) and the rotational spring (k_3) can be found in equation 7.6, 7.7 and 7.8.

$$k_1 = b_1 L_c B_c \tag{7.6}$$
$$k_2 = b_2 L_c B_c \tag{7.7}$$
$$k_3 = b_1 {}^*{}^1/_{12} {}^* L_c {}^* B_c{}^3 = b_1 {}^* I \tag{7.8}$$

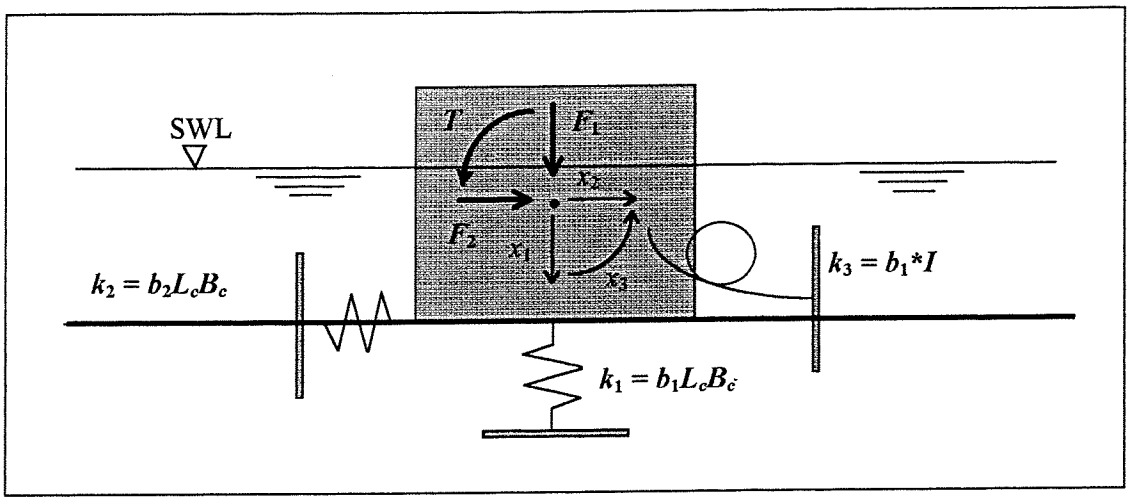

fig. 7.3 Mass-spring model

The position of the translational springs in figure 7.3 (k_1 and k_2) is important and is as sketched in figure 7.3. The position of the rotational spring is not relevant. The position of the springs is of course also assimilated in equation 7.9.

Substitution of the equations 7.6, 7.7 and 7.8 in equation 7.5 gives:

$$\begin{bmatrix} m_1 & 0 & 0 \\ 0 & m_2 & 0 \\ 0 & 0 & \theta \end{bmatrix} \begin{bmatrix} \ddot{x}_1 \\ \ddot{x}_2 \\ \ddot{x}_3 \end{bmatrix} + \begin{bmatrix} k_1 & 0 & 0 \\ 0 & k_2 & h k_2 \\ 0 & h k_2 & h^2 k_2 + k_3 \end{bmatrix} \begin{bmatrix} x_1 \\ x_2 \\ x_3 \end{bmatrix} = \begin{bmatrix} F_1 \\ F_2 \\ T \end{bmatrix} \tag{7.9}$$

7.3 Structure and foundation parameters of the chosen vertical breakwater

In the previous section a general analytical model which describes the dynamical behaviour of a vertical breakwater has been derived. The magnitude of the different parameters of the model will be described in this section. The magnitude of these parameters is chosen in conformance with a prototype situation, in this case: along the Dutch coast at the site of the planned land reclamation of the harbour of Rotterdam: "Maasvlakte 2".

Vertical or caisson breakwaters are usually placed on a rubble mound. This rubble mound usually consists of coarse stones (e.g. 10 - 1000 kg). To protect the rubble mound in front of the vertical breakwater, it is usually covered with armour blocks (e.g. heavy stones or concrete blocks). Dependent on the height of the rubble mound, these breakwaters are called high mound or low mound vertical composite breakwaters (see figure 7.4). These breakwaters are called vertical *composite* breakwaters because they consist of several layers in a vertical direction.

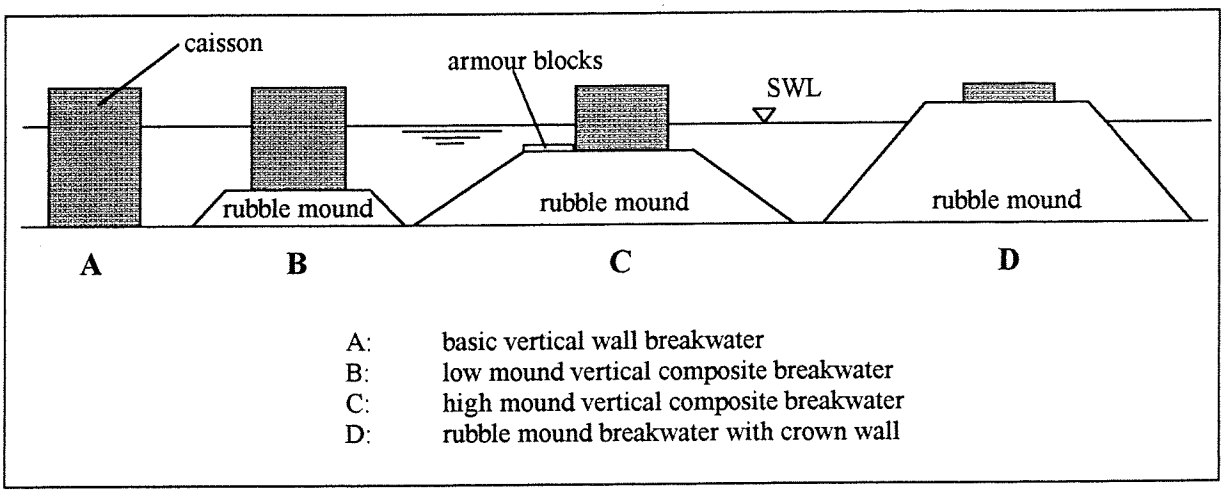

fig. 7.4 Vertical type breakwaters

The rubble mound (foundation) under the vertical breakwater has several functions:

- The rubble mound can level out an uneven seabed, so the caissons can be placed on an even foundation.
- During placing of the vertical (caisson) breakwater, high flow velocities can occur between the caissons and the seabed which, for example, consists of sand along the Dutch coast (caisson breakwaters are usually constructed elsewhere at a construction site and floated in after they are completed). The rubble mound stabilises the foundation (the seabed) in order to prevent enormous scour during placing of the caissons.
- The rubble mound serves as a filter in order to prevent local liquefaction of the foundation of the vertical breakwater. As a result of the movements of a caisson breakwater which are caused by wave action, the groundwater pressure under the caisson breakwater will fluctuate considerably. At some points high pressure differences can occur which can cause local liquefaction. To prevent this local liquefaction a geometrical closed filter is necessary [SCHIERECK (1995)]. A geometrical closed filter is designed in such a way that the grains in and under the filter layer cannot move. This often leads to a conservative design, since the filter can stand any load: there is no critical gradient at which the grains will start to move.
- The rubble mound prevents erosion of the sandy seabed at the toe of a vertical breakwater.

The calculations which are carried out in this study - and described in this report - are carried out as if the rubble mound is absent. This is assumption does not influence the calculations in the way as they are carried out here, but one should always bare in mind that in a real situation a rubble mound berm is usually necessary.

The vertical breakwater of which the dynamical behaviour will be calculated in this chapter, is a vertical breakwater of the caisson type and is directly placed on the seabed which consists of sand. Both the rubble mound and the armour layer are absent. In fact this is an basic vertical wall breakwater (see figure 7.4). The caisson breakwater is constructed at the construction site and floated in after it is completed. After the caisson is placed at the right spot, it is filled, for instance with sand. The width of the caisson is 20 m and the height is 23 m. The length of one individual caisson is chosen as 30 m (a total breakwater consists of several individual caissons which are placed next to each other). The water depth at both sides of the caisson is 15 m. The breakwater is assumed to be rigid, it will not distort. The lay-out of the vertical breakwater of the caisson type is described in figure 7.5.

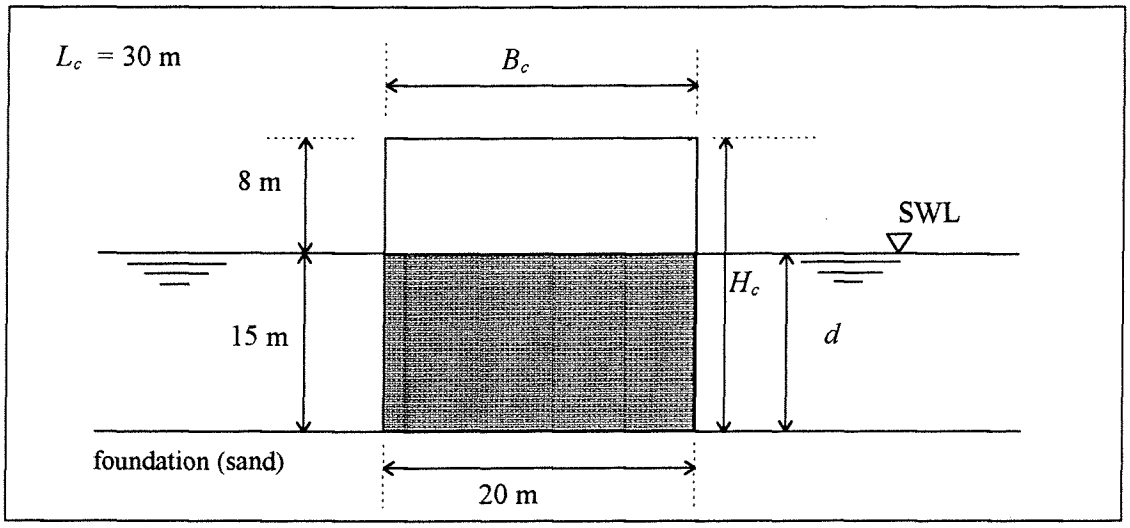

fig. 7.5 Lay-out of the vertical breakwater of the caisson type

Nota bene:

The design of the chosen breakwater is a realistic one. A high rubble mound that is lower than Still Water Level (SWL) occasionally generates impulsive wave forces due to wave breaking [TAKAHASHI (1995)]. A low mound - in this case no mound is assumed - is favourable for the stability of the vertical breakwater because:

- less breaking waves will act directly against the vertical breakwater and
- a larger caisson is needed. A caisson on a high mound will weight less than a caisson which is placed on a thin rubble mound, because the dimensions of the breakwater on a high rubble mound can be smaller (the height is smaller and the width is the same) A heavy caisson is more stable against sliding and overturning than a light caisson as will be shown later on in this report in section 9.5.

The calculations which will be carried out in this study will be carried out for a design which will give the fewest breaking wave conditions under the given circumstances at the location of the vertical breakwater (at a waterdepth of 15 m). If one is interested in the effect of wave impact forces on a vertical breakwater one should choose a realistic design to calculate the effect of wave impacts and not a design of a vertical breakwater where wave impacts are generated by the chosen design itself (e.g. by a high rubble mound). That would be a very *unwise* design!

The most interesting thing is to know if wave impacts are important - and, if so, which wave impacts are important - for a chosen design which would give the fewest wave impact forces on a vertical breakwater under the given circumstances. A comparison between a vertical breakwater at a waterdepth of 15 m on a low mound and a vertical breakwater at a waterdepth of 15 m on a high mound (the *stupid* design) will be made in section 9.5.

A vertical breakwater without damping can be schematised by a mass-spring model with three degrees of freedom: vertical (translation x_1), horizontal (translation x_2) and rotational (rotation x_3) displacements are possible (see section 7.2 and figure 7.6). The origin of these displacements is chosen in the centre of gravity (C) of the caisson. When the dynamical behaviour of a caisson breakwater is investigated, the following parameters must be known:

- the masses (m_1 and m_2) and the mass moment of inertia (θ) of the caisson breakwater
- the stiffnesses (k_1 , k_2 and k_3) of the foundation which can be represented by springs.

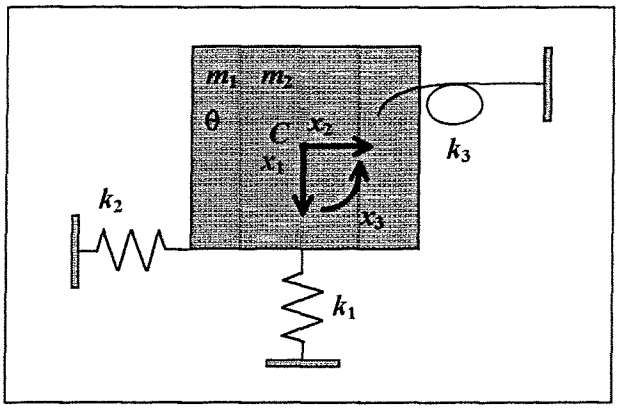

fig. 7.6 Mass-spring model with three degrees of freedom

The magnitude of the masses and the mass moment of inertia is treated in sub-section 7.3.1 and the (linear-elastic) characteristics of the foundation are treated in sub-section 7.3.2.

7.3.1 Masses and mass moment of inertia of the vertical breakwater

The masses and the mass moment of inertia of the caisson breakwater are determined for the vertical breakwater with a height of 23 m, a width of 20 m and a length of 30 m.

Masses

The mass which should be taken into account (m_{tot}) is the mass of the caisson breakwater itself (m_{cai}), the added hydraulic mass (m_{hyd}) and the added mass of soil (m_{geo}):

$$m_{tot} = m_{cai} + m_{hyd} + m_{geo} \tag{7.10}$$

The mass of the caisson breakwater (m_{cai}) can be calculated if the amount and the mass density of concrete and the amount and the mass density of the fill are know. Usually, a caisson breakwater consists of approximately 10% concrete, the mass density of reinforced concrete (ρ_c) is 2400 kg/m^3. The fill (sand) has a mass density (ρ_f) of 1900 kg/m^3 (almost saturated sand). Thus, the total mass of the vertical breakwater is:

$$\begin{aligned} m_{cai} &= L_c*B_c*H_c*(0.1*\rho_c+0.9*\rho_f) = \\ &= 30*20*23*(0.1*2400+0.9*1900) = 26910.0*10^3 \text{ kg} \end{aligned} \tag{7.11}$$

When the caisson which is exposed to a wave impact load oscillates, a certain body of water is forced to move with the structure. This added mass of water is called hydro-dynamic mass in the following. By using a theoretical calculation based on an incompressible and irrotational two dimensional potential flow it can be shown [OUMERACI et al. (1994)] that for horizontal oscillations:

$$m_{hyd,\,hor} = L_c * 0.543 * \rho_w * d^2 \qquad (7.12)$$

in which:

$m_{hyd,\,hor}$ = the hydro-dynamic mass for horizontal oscillations
d = water depth next to a vertical breakwater

Nota bene:

Equation 7.12 refers to the water on the seaward side of the structure only.

Pendulum tests on a caisson have been conducted for different water depths d [OUMERACI et al. (1992a)]. The results of these tests show that equation 7.12 will lead to underestimated values of the added mass. For calculating the hydro-dynamic mass of the system, equation 7.13 will be used [MAST II, ANNEX 1 (1995)]:

$$m_{hyd,\,hor} = L_c * 1.40 * \rho_w * d^2 \qquad (7.13)$$
$$= 30 * 1.40 * 1025 * 15^2 = 9686.3 * 10^3 \text{ kg}$$

Equation 7.12 and 7.13 are plotted in figure 7.7 (L_c is chosen as 1 m).

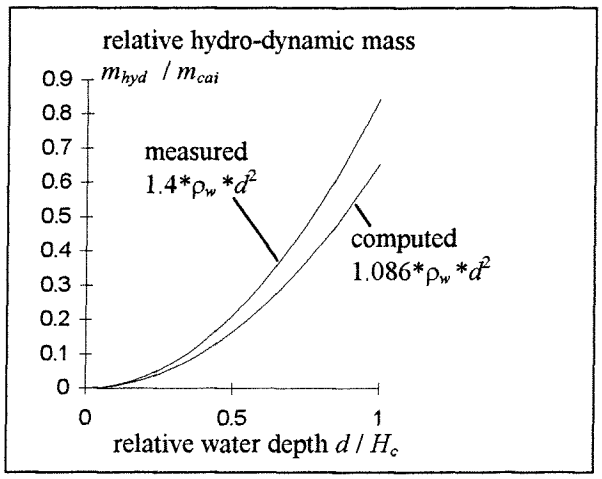

fig. 7.7 Hydro-dynamic mass resulting from horizontal caisson oscillations

The hydro-dynamic mass for vertical motions is assumed to be zero.

$$m_{hyd,\,ver} = 0 \text{ kg} \qquad (7.14)$$

Nota bene:

The theoretical basis of the added hydraulic mass or hydro-dynamic mass is weak. It seems logical that the hydro-dynamic mass is dependent on the frequency of oscillation of the structure, but all formulae given here are independent of the frequency of oscillation. The value for the hydro-dynamic mass which is used by different researchers within the MAST project is used here as well, so a hydro-dynamic mass which is independent of the frequency of oscillation of the vertical breakwater. According to MARIN (faculty of Marine Technology, Delft University of Technology) the hydro-dynamic mass can be estimated by the displaced mass of water by the vertical breakwater, which is $30*15*20*1025 = 9225.0*10^3$ kg. This is slightly lower than the value of $9686.3*10^3$ kg which is used in this study.

When the caisson exhibits oscillating motions, a certain mass of the soil beneath the structure is forced to move with the latter, this added mass of soil is called in the following geo-dynamic mass. For the determination of the geo-dynamic mass, the approximation which can be found in [MAST II, ANNEX 1 (1995)] (see equation 7.15) is used. In fact this is the geo-dynamic mass for horizontal oscillations. The geo-dynamic mass is assumed to be the same for horizontal and vertical oscillations. This assumption will not influence the results of the calculations very much because of the fact that a wave impact of the transition type will cause horizontal and rotational oscillations and almost no vertical oscillations.

$$m_{geo} = m_{geo,hor} = m_{geo,ver} = \frac{0.76 * \rho_s * \left(\frac{B_c L_c}{\pi}\right)^{\frac{3}{2}}}{2 - \nu} \qquad (7.15)$$

$$= \frac{0.76 * 2000 * \left(\frac{20 * 30}{\pi}\right)^{\frac{3}{2}}}{2 - 0.3} = 2359.9 * 10^3 \quad \text{kg}$$

in which:

ρ_s = mass density of the foundation soil (2000 kg/m^3)

ν = Poisson's ratio. (The Poisson ratio is normally within the range of 0.2-0.4 for sandy soils. Here 0.3 is chosen, assuming drained conditions)

Nota bene:

Just as for the hydro-dynamic mass, the theoretical basis of the geo-dynamic mass is weak. Again a formula is used which is independent of the frequency of oscillation of the vertical breakwater. Expression 7.15 is also independent of the height and weight of the vertical breakwater. This formula is also being used within the MAST project and will be used here as well.

The total mass for vertical oscillations is:

$$m_1 = m_{tot,\,ver} = m_{cai} + m_{hyd,\,ver} + m_{geo,\,ver} \qquad (7.16)$$
$$= 26910.0*10^3+0+2359.9*10^3 = 29269.9*10^3 \text{ kg}$$

The total mass for horizontal oscillations is:

$$m_2 = m_{tot,\,hor} = m_{cai} + m_{hyd,\,hor} + m_{geo,\,hor} \qquad (7.17)$$
$$= 26910.0*10^3+9686.3*10^3+2359.9*10^3 = 38956.2*10^3 \text{ kg}$$

Mass moment of inertia

For the determination of the mass moment of inertia, the same procedure can be followed as for the determination of the mass of the vertical breakwater:

$$\theta_{tot} = \theta_{cai} + \theta_{hyd} + \theta_{geo} \tag{7.18}$$

θ_{cai} , θ_{hyd} , θ_{geo} must be determined individually.

A good approximation of the magnitude of θ_{tot} can be found when θ_{hyd} and θ_{geo} are neglected and $m_{tot,\,hor}$ is used instead of m_{cai} in equation 7.19.

$$\theta_{cai} = \frac{1}{12} * m_{cai} * (B_c^2 + H_c^2) \tag{7.19}$$

This equation represents the mass moment of inertia of the caisson around the centre of gravity (C, see figure 7.1) for a rectangular caisson with equally distributed density.

$$\theta = \theta_{tot} = \frac{1}{12} * m_{tot,hor} * (B_c^2 + H_c^2) \tag{7.20}$$

$$= \frac{1}{12} * 38956.2 * 10^3 * (20^2 + 23^2) = 3.016 * 10^9 \quad \text{kgm}^2$$

Nota bene:

It is assumed that the mass of the vertical breakwater is equally distributed over its length, height and width. The centre of gravity is assumed to be placed in the centre of the cross section as is shown in figure 7.1.

7.3.2 Soil characteristics

The soil characteristics (e.g. the stiffness of the foundation soil) must be known to determine the stiffness of the springs of the mass-spring model. The determination of the stiffness of the springs will be carried out in the next section. Here, only the so called "bed constants" will be given. These constants are different for different foundation soils. The following values are to be found in the literature for a static situation (these values are approximations!):

- clay or peat: $1*10^6$ N/m^3
- sand: $1*10^7$ N/m^3
- gravel: $1*10^8$ N/m^3

Here a value of $2.5*10^7$ N/m^3 will be chosen. This value will be chosen the same for the horizontal and vertical direction. A rather high value is chosen. It is assumed that the vertical breakwater will be placed on compact sand. Another reason for choosing a rather high value is the fact that the vertical breakwater is exposed to a highly dynamical load. The stiffness of the soil, when exposed to a dynamical load, may expected to be higher than the static value. The stiffnesses of the springs of the mass-spring model can now be determined:

$$k_1 = b_1 L_c B_c = 2.5*10^7 * 30 * 20 = 1.5*10^{10} \text{ N/m} \tag{7.6}$$

$$k_2 = b_2 L_c B_c = 2.5*10^7 * 30 * 20 = 1.5*10^{10} \text{ N/m} \tag{7.7}$$

$$k_3 = b_1 * {}^1/_{12} * L_c * B_c^{\,3} = b_1 * I = 2.5*10^7 * {}^1/_{12} * 30 * 20^3 = 5.0*10^{11} \text{ Nm/rad} \tag{7.8}$$

Nota bene:

Within the MAST-project the spring constants are often calculated using the method of Richart et al. [RICHART et al. (1970)]. Using the method which is used here, with the bed constants with a magnitude of $2.5*10^7$ N/m^3 gives results which are comparable with the results using the method of Richart et al..

The formulae given by Richart et al. are dependent on the size of the structure (especially the ratio B_c / L_c). The following approximations can be given for the stiffnesses of the different springs:

$$k_1 = 1.1 * E_s * \sqrt{B_c * L_c} * \frac{1}{1-\nu^2} \quad \text{N/m} \tag{7.21}$$

$$k_2 = 0.82 * k_1 \quad \text{N/m} \tag{7.22}$$

$$k_3 = 2.73 * B_c^{\,2} * {}^1/_{12} * k_1 \quad \text{N/m} \tag{7.23}$$

The properties of the soil are usually expressed in terms of a shear modulus G_s and the Poisson ratio ν instead of an elasticity modulus E_s. The elasticity modulus can be derived from the shear modulus and the Poisson ratio with the following relation:

$$E_s = 2*(1+\nu)*G_s \tag{7.24}$$

Pedersen [PEDERSEN (1994)] uses equation 7.25 for the determination of the shear modulus G_s, which has been derived for sandy normally consolidated soils which consist of angular-grained material [RICHART et al. (1970)]:

$$G_s = 0.4 * 1230 * \frac{(2.973-e)^2}{1+e} \sqrt{\frac{F_n}{B_c * L_c}} \tag{7.25}$$

where e is the void ratio. Expression 7.25 is developed as a best fit to a number of tests and is seen not to be dimensionally correct. G_s and $\frac{F_n}{B_c * L_c}$ must be evaluated in [lbf/in^2] (1 lbf/m^2 = $1.4503*10^{-4}$ N/m^2).

If e is chosen as 0.6, ν = 0.3 and $F_n = 152.4*10^6$ N (see equation 7.88) than E_s can be calculated using equation 7.24 and 7.25. This calculation results in: $E_s = 188*10^6$ N/m^2.

7.4 Determination of the eigenvalues of the vertical breakwater

All structure and foundation parameters which are needed for the determination of the mass-spring model of the vertical breakwater of the caisson type at the chosen location are known. The mass-spring model of the chosen breakwater for this specific location can now be derived.

If there is no load on the vertical breakwater ($F_1 = 0$, $F_2 = 0$ and $T = 0$) equation 7.9, which described the dynamical behaviour of the breakwater, will be homogeneous:

$$\begin{bmatrix} m_1 & 0 & 0 \\ 0 & m_2 & 0 \\ 0 & 0 & \theta \end{bmatrix} \begin{bmatrix} \ddot{x}_1 \\ \ddot{x}_2 \\ \ddot{x}_3 \end{bmatrix} + \begin{bmatrix} k_1 & 0 & 0 \\ 0 & k_2 & hk_2 \\ 0 & hk_2 & h^2k_2 + k_3 \end{bmatrix} \begin{bmatrix} x_1 \\ x_2 \\ x_3 \end{bmatrix} = \begin{bmatrix} 0 \\ 0 \\ 0 \end{bmatrix} \tag{7.26}$$

In this section the solution of this homogeneous equation will be given. This solution is called the eigensolution of the mass-spring system.

This solution represents the free oscillations of the breakwater, which will occur when no energy is added to the mass-spring system which represents the vertical breakwater.

The solution of the homogeneous equation 7.26 is:

$$\underline{x}(t) = \underline{\hat{x}}_i \sin(\omega_i t + \phi_i) \quad (i = 1, 2, 3) \tag{7.27}$$

in which

$\underline{\hat{x}}_i$ = eigenvector

The mass-spring system (see equation 7.26) can be divided in two sub-systems:

$$m_1 \ddot{x}_1(t) + k_1 x_1(t) = 0 \tag{7.28}$$

and

$$\begin{bmatrix} m_2 & 0 \\ 0 & \theta \end{bmatrix} \begin{bmatrix} \ddot{x}_2(t) \\ \ddot{x}_3(t) \end{bmatrix} + \begin{bmatrix} k_2 & hk_2 \\ hk_2 & h^2k_2 + k_3 \end{bmatrix} \begin{bmatrix} x_2(t) \\ x_3(t) \end{bmatrix} = \begin{bmatrix} 0 \\ 0 \end{bmatrix} \tag{7.29}$$

The solution of this system is as follows:

$$\underline{x}(t) = \begin{bmatrix} x_1(t) \\ x_2(t) \\ x_3(t) \end{bmatrix} = A_1 \begin{bmatrix} 1 \\ 0 \\ 0 \end{bmatrix} \sin(\omega_1 t + \phi_1) + A_2 \begin{bmatrix} 0 \\ 1 \\ R_2 \end{bmatrix} \sin(\omega_2 t + \phi_2) + A_3 \begin{bmatrix} 0 \\ 1 \\ R_3 \end{bmatrix} \sin(\omega_3 t + \phi_3) \tag{7.30}$$

In this section R_2, R_3, ω_1, ω_2 and ω_3 will be determined. A_1, A_2, A_3, ϕ_1, ϕ_2 and ϕ_3 will be determined in the next section.

In section 7.3 the structure and foundation parameters have already been given, they will all be repeated here.

m_1	=	$29269.9*10^3$ kg			
m_2	=	$38956.2*10^3$ kg			
θ	=	$3.016*10^9$ kgm^2			
B_c	=	20 m	b	=	10.0 m
H_c	=	23 m	h	=	11.5 m
L_c	=	30 m	l	=	15.0 m
k_1	=	$1.5*10^{10}$ N/m			
k_2	=	$1.5*10^{10}$ N/m			
k_3	=	$5.0*10^{11}$ Nm/rad			

The first system, only the vertical oscillation, degree of freedom $x_1(t)$

$$29269.9 * 10^3 \ddot{x}_1(t) + 1.5 * 10^{10} x_1(t) = 0 \tag{7.31}$$

$$\omega_1 = \sqrt{\frac{k_1}{m_1}} = \sqrt{\frac{1.5 * 10^{10}}{29269.9 * 10^3}} = 22.638 \text{ rad/s} \tag{7.32}$$

$$f_1 = \frac{\omega_1}{2\pi} = \frac{22.638}{2\pi} = 3.603 \text{ Hz} \tag{7.33}$$

$$T_1 = \frac{1}{f_1} = \frac{1}{3.603} = 0.278 \text{ s} \tag{7.34}$$

$$\text{eigenvector } \underline{\hat{x}}_1 = \begin{bmatrix} 1 \\ 0 \\ 0 \end{bmatrix} \tag{7.35}$$

The second system, the horizontal oscillation and the rotational oscillation, degrees of freedom $x_2(t)$ and $x_3(t)$

$$\begin{bmatrix} 38956.2 * 10^3 & 0 \\ 0 & 3.016 * 10^9 \end{bmatrix} \begin{bmatrix} \ddot{x}_2(t) \\ \ddot{x}_3(t) \end{bmatrix} + \begin{bmatrix} 1.5 * 10^{10} & 1.725 * 10^{11} \\ 1.725 * 10^{11} & 2.48375 * 10^{12} \end{bmatrix} \begin{bmatrix} x_2(t) \\ x_3(t) \end{bmatrix} = \begin{bmatrix} 0 \\ 0 \end{bmatrix} \tag{7.36}$$

Solution of this eigenvalue problem:

$$\left(\omega^2\right)_{2,3} = \frac{\omega_{22}^2 + \omega_{33}^2}{2} \pm \sqrt{\left(\frac{\omega_{33}^2 - \omega_{22}^2}{2}\right)^2 + \left(\omega_{23}\right)^4} \tag{7.37}$$

in which:

$$\omega_{22}^2 = \frac{k_{22}}{m_2} = \frac{1.5 * 10^{10}}{38956.2 * 10^3} = 385.048 \tag{7.38}$$

$$\omega_{33}^2 = \frac{k_{33}}{\theta} = \frac{2.48375 * 10^{12}}{3.016 * 10^9} = 823.525 \tag{7.39}$$

$$\omega_{23}^4 = \frac{k_{23}k_{32}}{m_2\theta} = \frac{1.725 * 10^{11} * 1.725 * 10^{11}}{38956.2 * 10^3 * 3.016 * 10^9} = 253262.140 \tag{7.40}$$

$$\left(\omega^2\right)_{2,3} = \frac{385.048 + 823.525}{2} \pm \sqrt{\left(\frac{385.048 - 823.525}{2}\right)^2 + 253262.140} \tag{7.41}$$

$$\omega_2^2 = 604.287 - 548.933 = 55.354 \qquad \omega_2 = 7.440 \text{ rad/s} \tag{7.42}$$

$$f_2 = \frac{\omega_2}{2\pi} = \frac{7.440}{2\pi} = 1.184 \text{ Hz} \tag{7.43}$$

$$T_2 = \frac{1}{f_2} = \frac{1}{1.184} = 0.845 \text{ s} \tag{7.44}$$

$$\text{eigenvector } \underline{\hat{x}}_2 = \begin{bmatrix} 0 \\ 1 \\ R_2 \end{bmatrix} = \begin{bmatrix} 0 \\ 1 \\ -0.07445 \end{bmatrix} \tag{7.45}$$

in which

$$R_2 = \frac{-\omega_2^2 m_2 + k_{22}}{-k_{23}} = \frac{-55.354 * 38956.2 * 10^3 + 1.5 * 10^{10}}{-1.725 * 10^{11}} = -0.07445 \tag{7.46}$$

$$\omega_3^2 = 604.287 + 548.933 = 1153.220 \qquad \omega_3 = 33.959 \text{ rad/s} \tag{7.47}$$

$$f_3 = \frac{\omega_3}{2\pi} = \frac{33.959}{2\pi} = 5.405 \text{ Hz} \tag{7.48}$$

$$T_3 = \frac{1}{f_3} = \frac{1}{5.405} = 0.185 \text{ s} \tag{7.49}$$

$$\text{eigenvector } \underline{\hat{x}}_3 = \begin{bmatrix} 0 \\ 1 \\ R_3 \end{bmatrix} = \begin{bmatrix} 0 \\ 1 \\ 0.17348 \end{bmatrix} \tag{7.50}$$

in which

$$R_3 = \frac{-\omega_3^2 m_2 + k_{22}}{-k_{23}} = \frac{-1153.220 * 38956.2 * 10^3 + 1.5 * 10^{10}}{-1.725 * 10^{11}} = 0.17348 \tag{7.51}$$

Check: $R_2 * R_3 = -\frac{m_2}{\theta}$ → OK!

Summary of eigenvalues and solution of equation 7.30

$\omega_1 = 22.638$ rad/s $\quad f_1 = 3.603$ Hz $\quad T_1 = 0.278$ s $\quad \underline{\hat{x}}_1 = \begin{bmatrix} 1 \\ 0 \\ 0 \end{bmatrix}$

$\omega_2 = 7.440$ rad/s $\quad f_2 = 1.184$ Hz $\quad T_2 = 0.845$ s $\quad \underline{\hat{x}}_2 = \begin{bmatrix} 0 \\ 1 \\ -0.07445 \end{bmatrix}$

$\omega_3 = 33.959$ rad/s $\quad f_3 = 5.405$ Hz $\quad T_3 = 0.185$ s $\quad \underline{\hat{x}}_3 = \begin{bmatrix} 0 \\ 1 \\ 0.17348 \end{bmatrix}$

$$\underline{x}(t) = \begin{bmatrix} x_1(t) \\ x_2(t) \\ x_3(t) \end{bmatrix} = A_1 \begin{bmatrix} 1 \\ 0 \\ 0 \end{bmatrix} \sin(22.638t + \phi_1) + A_2 \begin{bmatrix} 0 \\ 1 \\ -0.07445 \end{bmatrix} \sin(7.440t + \phi_2) + A_3 \begin{bmatrix} 0 \\ 1 \\ 0.17348 \end{bmatrix} \sin(33.959t + \phi_3)$$

Nota bene:

The results found here show good agreement with the results found in the literature. Lamberti et al. [LAMBERTI et al. (1996)] have calculated eigenperiods for caisson breakwaters in Italy (Genoa, Naples and Brindisi). In their study it has been shown that for these caissons the eigenperiods for horizontal movements are in the range of 0.65 - 0.85 s and the eigenperiods for rotational movements are in the range of 0.20 - 0.30 s.

7.5 The vertical breakwater exposed to a "transition type" wave impact

In this section the horizontal and rotational movements of the breakwater which is exposed to a transition type wave impact will be calculated. Thus, according to equation 7.30, only A_2, A_3, ϕ_2 and ϕ_3 have to be determined. The vertical motion will be zero because there is no vertical load.

The breakwater will be exposed to a transition type wave impact load. Chosen is for the "church-roof" load which is among other things described in chapter 2. The equation which has been derived by Schmidt [SCHMIDT et al. (1992)] is used here (see equation 7.52). No other loads on the breakwater due to wave action are taken into account for the benefit of the dynamical analysis presented in this report. The uplift force and the quasi-static wave forces are assumed to be constant. This assumption will be made throughout the whole report and will not influence the calculation of the dynamical behaviour of the vertical breakwater because of the fact that these forces are constant.

$$\frac{F_{h,\max}}{\rho_w g H_b^2} = 1.24 \left(\frac{t_d}{T_P} \right)^{-0.344} \tag{7.52}$$

The vertical breakwater will be exposed to a wave impact with a magnitude of 13422 kN/m (see table 2.1; $H_b = 10$ m, $T_p = 12$ s, $(t_d / T_p) = 0.001$, so $t_d = 12$ ms). Only the triangular part of the "church-roof" load will be taken into account (see figure 7.8). According to Oumeraci [OUMERACI et al. (1994)] substitution of an actual impact load by a triangular pulse may lead to useful results if only the maximum response is needed. The maximum response of the vertical breakwater is what will be calculated here. This maximum response will be used for the stability analysis in the next section, so the substitution of the actual load by a force pulse seems permissible in this case.

The wave impact will act over the total length of the vertical breakwater which is a very pessimistic assumption. The total horizontal force of the wave impact with a peak force of 13422 kN/m is 13422*30=402660 kN.

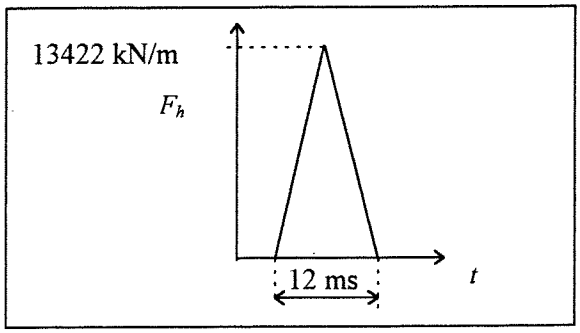

fig. 7.8 Triangular load on the vertical breakwater

According to Takahashi et al. [TAKAHASHI et al. (1993)] the peak pressure of the wave impact of the transition type acts at Still Water Level (SWL). It is supposed that the total wave impact force (resultant of the wave impact pressures) acts at SWL. As stated before, it is assumed that this wave impact is the only load on the structure. The total uplift force under the caisson due to wave action is assumed to be constant. Together with the buoyancy, which is also assumed to be constant, the uplift force will not influence the horizontal and rotational motions of the vertical breakwater.

The wave impact is schematised by a pulse load. A pulse load can be schematised using a delta-function [DIETERMAN (1994)]

$$F(t) = F_0\delta(t) \tag{7.53}$$

in which:

$$\int_{0^-}^{0^+} \delta(t)\mathrm{d}t = 1 \tag{7.54}$$

$$F_0 = 0.5*12*10^{-3}*30*13422*10^3 = 2415960 \text{ Ns} \tag{7.55}$$

The time between t = 0- and t = 0+ is very short. Because this pulse will act excentric on the front wall relative to the centre of gravity, it will also cause a pulse moment. The centre of gravity is 11.5 m above the seabed. The wave impact force (the resultant of the wave impact pressures) acts at SWL, thus 15 m above the seabed. Thus, the wave impact force acts 3.5 m excentric relative to the centre of gravity. The magnitude of the force and the moment on the vertical breakwater ($F_2(t)$ and $T(t)$) are:

$$F_2(t) = 2415960*\delta(t) \text{ N} \tag{7.56}$$

$$T(t) = -3.5*F_2 = -8455860*\delta(t) \text{ Nm} \tag{7.57}$$

$F_2(t)$ and $T(t)$ can be substituted in equation 7.36:

$$\begin{bmatrix} 38956.2*10^3 & 0 \\ 0 & 3.016*10^9 \end{bmatrix}\begin{bmatrix} \ddot{x}_2(t) \\ \ddot{x}_3(t) \end{bmatrix}+\begin{bmatrix} 1.5*10^{10} & 1.725*10^{11} \\ 1.725*10^{11} & 2.48375*10^{12} \end{bmatrix}\begin{bmatrix} x_2(t) \\ x_3(t) \end{bmatrix}=\begin{bmatrix} 2415960*\delta(t) \\ -8455860*\delta(t) \end{bmatrix} \tag{7.58}$$

If the solution of equation 7.58 has to be determined, this equation has to be integrated from $t = 0-$ to $t = 0+$ to get rid of the delta-function in the load vector. This is done for degree of freedom $x_2(t)$.

$$\int_{0^-}^{0+} 38956.2*10^3\ddot{x}_2(t)dt+\int_{0^-}^{0^+} 1.725*10^{11}x_2(t)dt+\int_{0^-}^{0^+} 1.725*10^{11}x_3(t)dt=\int_{0^-}^{0^+} 2415960*\delta(t)dt \tag{7.59}$$

The second and the third term of equation 7.59 are zero because $x_2(t)$ and $x_3(t)$ are zero: in a very short period the breakwater will not move.

$$38956.2*10^3*\dot{x}_2(0^+)-38956.2*10^3*\dot{x}_2(0^-)=2415960 \tag{7.60}$$

with:

$$\dot{x}_2(0^-)=0 \tag{7.61}$$

follows:

$$\dot{x}_2(0^+)=\frac{2415960}{38956.2*10^3}=0.0620173\ \text{m/s} \tag{7.62}$$

The same can be done for degree of freedom x_3:

$$\dot{x}_3(0^+)=\frac{-8455860}{3.016*10^9}=-0.0028036\ \text{rad/s} \tag{7.63}$$

At $t = 0+$ there is no wave impact any more. Thus, the elements of the load vector in equation 7.58 become zero. Again, it is a homogeneous system for $t > 0+$

$$\begin{bmatrix} 38956.2*10^3 & 0 \\ 0 & 3.016*10^9 \end{bmatrix}\begin{bmatrix} \ddot{x}_2(t) \\ \ddot{x}_3(t) \end{bmatrix}+\begin{bmatrix} 1.5*10^{10} & 1.725*10^{11} \\ 1.725*10^{11} & 2.48375*10^{12} \end{bmatrix}\begin{bmatrix} x_2(t) \\ x_3(t) \end{bmatrix}=\begin{bmatrix} 0 \\ 0 \end{bmatrix} \tag{7.64}$$

With the initial values:

$$\underline{x}(0^+)=\begin{bmatrix} x_2(t) \\ x_3(t) \end{bmatrix}=\begin{bmatrix} 0 \\ 0 \end{bmatrix} \tag{7.65}$$

$$\underline{\dot{x}}(0^+)=\begin{bmatrix} \dot{x}_2(t) \\ \dot{x}_3(t) \end{bmatrix}=\begin{bmatrix} 0.0620173 \\ -0.0028036 \end{bmatrix} \tag{7.66}$$

The solution of equation 7.64 and 7.65 and 7.66 can be found using the modal analysis [SPIJKERS et al.(1993)]:

$$\underline{x}(t) = \sum_{i=2}^{3} \underline{\hat{x}}_i u_i(t) = \left[\underline{\hat{x}}_2 \; \underline{\hat{x}}_3 \right] \begin{bmatrix} u_2(t) \\ u_3(t) \end{bmatrix} = E\underline{u}(t) \tag{7.67}$$

Substitution of:

$$M\underline{\ddot{x}}(t) + K\underline{x}(t) = \underline{0} \tag{7.68}$$

gives:

$$\ddot{u}_i(t) + \omega_i^2 u_i(t) = 0 \quad (i=2,3) \tag{7.69}$$

Equation 7.69 has as solution:

$$u_i(t) = C_i \sin(\omega_i t + \phi_i) \qquad (i=2,3) \tag{7.70}$$

in which:

$$C_i = \sqrt{A_i^2 + \left(\frac{B_i}{\omega_i}\right)^2} \tag{7.71}$$

$$\tan\phi_i = \frac{A_i \omega_i}{B_i} \tag{7.72}$$

in which:

$$A_i = \frac{\underline{\hat{x}}_i^T M \underline{x}(0)}{\underline{\hat{x}}_i^T M \underline{\hat{x}}_i} \tag{7.73}$$

$$B_i = \frac{\underline{\hat{x}}_i^T M \underline{\dot{x}}(0)}{\underline{\hat{x}}_i^T M \underline{\hat{x}}_i} \tag{7.74}$$

For the problem which is described in the equations 7.64, 7.65 and 7.66, A_2, A_3, ϕ_2 and ϕ_3 can now be determined:

$A_2 = 0$ (7.75) $A_3 = 0$ (7.76)

$B_2 = 0.0547027$ (7.77) $B_3 = 0.0073161$ (7.78)

$C_2 = \sqrt{\left(\frac{0.0547027}{7.440}\right)^2} = 7.3525*10^{-3}$ (7.79) $C_3 = \sqrt{\left(\frac{0.0073161}{33.959}\right)^2} = 2.1544*10^{-4}$ (7.80)

$\phi_2 = 0$ (7.81) $\phi_3 = 0$ (7.82)

Now, $x_2(t)$ and $x_3(t)$ can be determined using again equation 7.67 and 7.70:

$$\underline{x}(t) = \sum_{i=2}^{3} \underline{\hat{x}}_i u_i(t) = \left[\underline{\hat{x}}_2 \; \underline{\hat{x}}_3 \right] \begin{bmatrix} u_2(t) \\ u_3(t) \end{bmatrix} = E\underline{u}(t) \tag{7.67}$$

$$u_i(t) = C_i \sin(\omega_i t + \phi_i) \qquad (i=2,3) \tag{7.70}$$

$$\underline{x}(t) = \begin{bmatrix} x_2(t) \\ x_3(t) \end{bmatrix} = \begin{bmatrix} 7.3525 * 10^{-3} \\ -5.4739 * 10^{-4} \end{bmatrix} \sin(7.440t) + \begin{bmatrix} 2.1544 * 10^{-4} \\ 3.7375 * 10^{-5} \end{bmatrix} \sin(33.959t) \tag{7.83}$$

Equation 7.83 describes the horizontal and rotational oscillations of the centre of gravity of the caisson breakwater.

7.6 Stability of the vertical breakwater

In this section the stability of the vertical breakwater which is exposed to the wave impact (which is described in figure 7.8) will be discussed. The stability of a vertical breakwater against wave action can be examined for a lot of modes of failure. The most important failure modes are: sliding, overturning and collapse of the foundation. In this section these failure modes will be checked: sliding in sub-section 7.6.1, overturning in sub-section 7.6.2 and possible collapse or yielding in the foundation will be discussed in sub-section 7.6.3. In this chapter, the foundation is schematised by linear-elastic springs which can in fact not collapse. Collapse of the foundation will be treated in the next chapters, when the springs are not linear-elastic anymore, but elasto-plastic. The plastic part of the springs "represents" the collapse of the foundation.

Before the stability of the vertical breakwater against sliding and overturning is treated, the force in the foundation must be known. Therefore, the displacement of the bottom of the caisson must be calculated in advance. The force in the foundation can be calculated easily when the displacement of the bottom of the caisson is know.

The horizontal displacement of the centre of gravity of the caisson is $x_2(t)$ and the rotation of the centre of gravity of the caisson breakwater is $x_3(t)$. The horizontal displacement of the bottom of the caisson is a function of $x_2(t)$ and $x_3(t)$, see equation 7.84 and equation 7.85. Equation 7.85 is sketched in figure 7.9 together with the equations which are described in the matrix notation of equation 7.83.

$$x_{\text{bottom}}(t) = x_2(t) + 11.5 * x_3(t) \tag{7.84}$$

$$x_{\text{bottom}}(t) = 1.0575*10^{-3} * \sin(7.440\,t) + 6.4525*10^{-4} * \sin(33.959\,t) \tag{7.85}$$

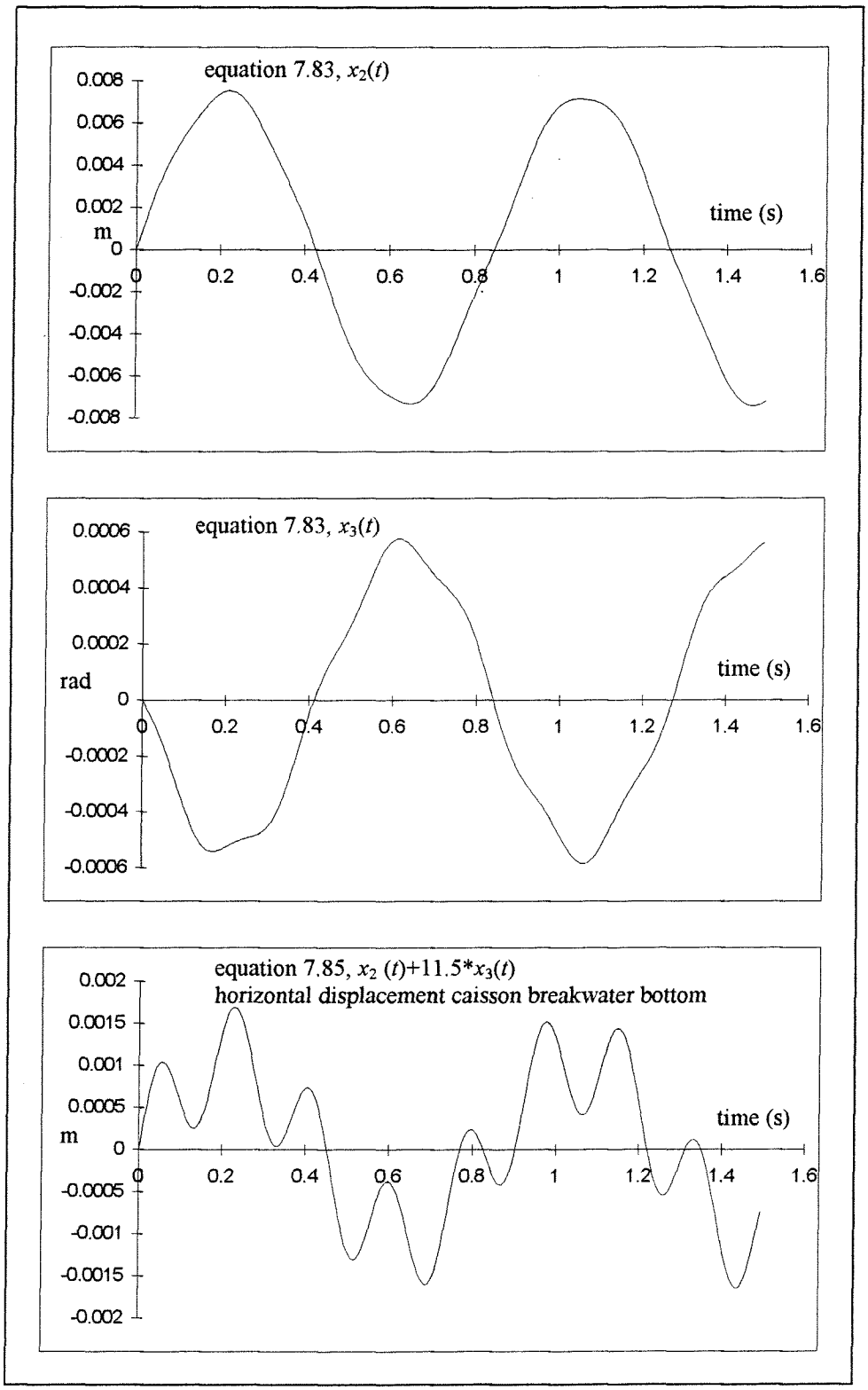

fig. 7.9 Results of the analytical calculation, see equation 7.83 and 7.85

In figure 7.10 the total displacement of the bottom of the caisson breakwater is sketched

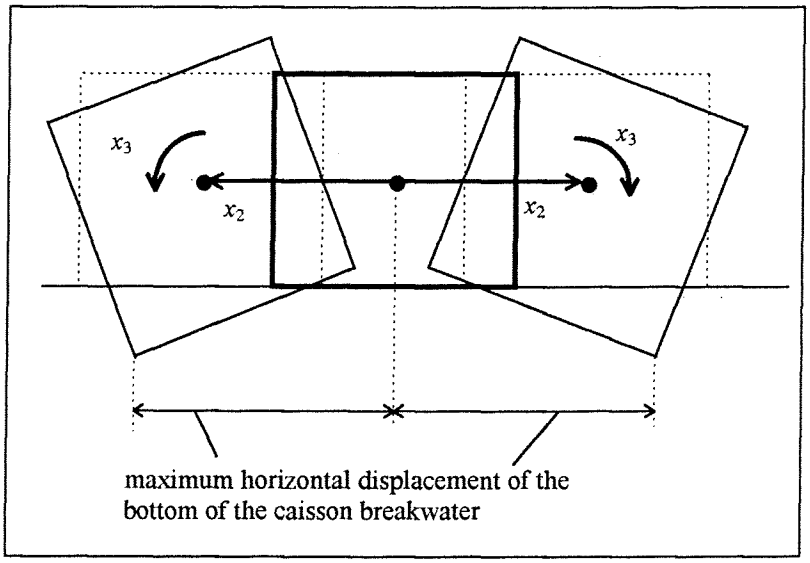

fig. 7.10 Total displacement bottom caisson

The maximum horizontal displacement of the bottom of the vertical breakwater is 1.0575+0.64525 = 1.70275 mm. The maximum horizontal force in the foundation is:

$$F_{foundation} = 1.70275*10^{-3}*k_2 = 1.70275*10^{-3}*1.5*10^{10} = 25.54*10^{6}\ \text{N} \qquad (7.86)$$

Only $\frac{25.54*10^{6}}{30*13422000} = 6.34\%$ of the wave impact force is "felt" in the foundation.

The maximum rotation of the vertical breakwater is $5.4739*10^{-4} + 3.7375*10^{-5} = 5.84765*10^{-4}$ rad.
The maximum moment in the foundation is:

$$M_{foundation} = 5.84765*10^{-4}*k_3 = 1.033*10^{-3}*5.0*10^{11} = 292.38*10^{6}\ \text{Nm} \qquad (7.87)$$

Only $\frac{292.38*10^{6}}{30*15*13422000} = 4.84\ \%$ of the moment caused by the wave impact force is "felt" in the foundation.

The force and moment in the foundation of the breakwater are reduced due to the dynamical behaviour of the caisson breakwater (inertia).

7.6.1 Stability against sliding

The caisson breakwater will not slide if the maximum horizontal foundation force of $25.54*10^6$ N (equation 7.86) is smaller than the friction force between the caisson breakwater and its foundation (see figure 7.11). This horizontal friction force (F_f) is related to the normal force of the vertical breakwater by the Coulomb friction coefficient (μ). The normal force F_n is the difference between the weight (W) of the caisson and the buoyancy (F_b) and the uplift force (F_u) under the caisson due to wave action.

$$F_n = W - F_b - F_u \tag{7.88}$$

$$F_f = \mu * F_n \tag{7.89}$$

It is assumed that F_u is caused by a column of water of 3.5 m equally distributed under the bottom of the caisson breakwater. This value is chosen for this vertical breakwater according to the Goda formula (see chapter 6). The Goda formula assumes a triangular uplift pressure [GODA (1992)]. The uplift pressure is zero at the side of the vertical breakwater which is not exposed to wave loads and approximately equal to a column of water of 7 m at the sea-side of the vertical breakwater. So, the average uplift pressure according to the Goda formula is equal to a column of water of 3.5 m. The weight is calculated for an unfavourable situation, only m_{cai} (equation 7.11) is taken into account.

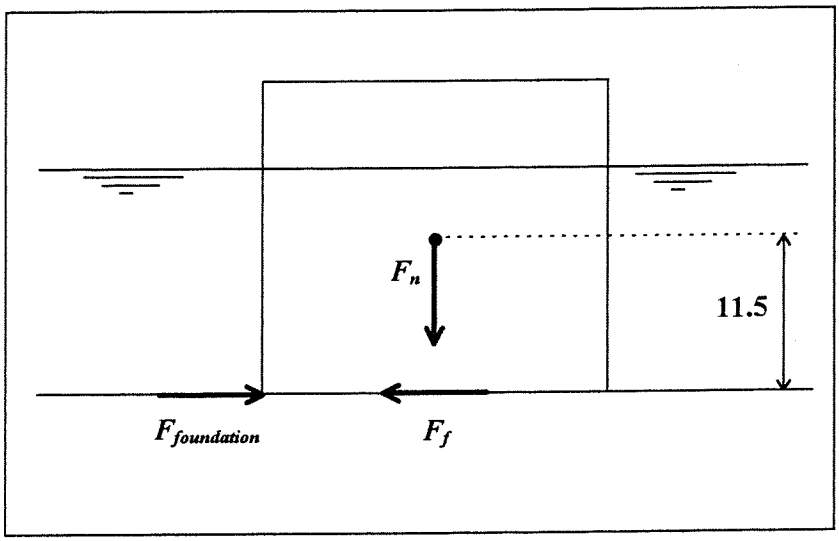

fig. 7.11 Forces on the vertical breakwater

Thus, F_n will be:

$$F_n = 26910.0 * 10^3 * 9.81 - 15 * 20 * 30 * 1025 * 9.81 - 3.5 * 20 * 30 * 1025 * 9.81$$
$$F_n = 152.4 * 10^6 \text{ N}$$

With $\mu = 0.5$ follows ($\mu = 0.5$ is a rather safe assumption, this Coulomb friction coefficient is usually taken as 0.6 in Japan [GODA (1992)]):

$$F_f = 0.5 * 152.4 * 10^6 = 76.20 * 10^6 \text{ N}$$

The caisson breakwater is safe against sliding because $F_f > F_{foundation}$ ($76.20*10^6 > 25.54*10^6$).

7.6.2 Stability against overturning

As explained in the EUROCODE, the stability against overturning is ensured by restricting the eccentricity to:

$$e < 0.3*B_c \quad = 0.3*20 = 6 \text{ m} \tag{7.90}$$

$$e = \frac{M_{foundation}}{F_n} = \frac{292.38 * 10^6}{152.4 * 10^6} = 1.92 \text{ m} \tag{7.91}$$

The condition which is described in equation 7.90 is fulfilled, it can be concluded that the breakwater is stable against overturning.

7.6.3 Collapse of the foundation

The foundation of the vertical breakwater will not collapse (or yield) if the pressure in the foundation does not become smaller than -700 kN/m^2 (the derivation of this value will be given in the next chapter, tension is positive and pressure is negative). The pressure in the foundation cannot exceed the value of 0 N/m^2 because the foundation soil cannot withstand tension; this condition is in fact fulfilled if the condition described in equation 7.90 is fulfilled. Thus, the following criterion must be fulfilled:

$$0 \geq \sigma_{foundation} \geq -700 \text{ kN/m}^2 \tag{7.92}$$

in which:

$$\sigma_{foundation} = -\frac{F_n}{B_c * L_c} \pm \frac{M_{foundation}}{\frac{1}{6} * L_c * B_c^2} \tag{7.93}$$

$$\sigma_{foundation} = -\frac{152.4 * 10^6}{20 * 30} \pm \frac{292.38 * 10^6}{\frac{1}{6} * 30 * 20^2} = -254.0 \pm 146.2 \text{ kN/m}^2$$

thus,

$\sigma_{foundation,\ max}$ = -107.8 kN/m^2

$\sigma_{foundation,\ min}$ = -400.2 kN/m^2

The criterion which is described in equation 7.92 is fulfilled, so the foundation of this vertical breakwater which is exposed to the (enormous) wave impact which is described in figure 7.8 does not collapse.

Conclusion:
Although the caisson breakwater is exposed to an enormous wave impact (12 ms, 13422 kN/m and a triangular load history), it will neither slide nor overturn. The wave impact force is only felt for approximately 6.34% in the foundation of the breakwater and the moment caused by the wave impact force for approximately 4.84%. From this case - with a conservative assumption like a wave impact which acts over the total length of the vertical breakwater - it can be concluded that enormous wave impacts with very high forces and very short durations are not important for the stability of vertical breakwaters within the framework of the given analysis.

7.7 Comments

The model as described in the previous sections has its limitations and its shortcomings but it gives a good first approximation of how a caisson breakwater reacts on an enormous wave impact of the transition type - a very high force and very short duration. The results found in this chapter show good agreement with the literature [MARINSKI et al. (1992)], [OUMERACI et al. (1992)].

The most important shortcomings and assumptions of the model which is described in this chapter are:

- The duration of the horizontal impact force (t_d) and the rise time (t_r) were partially neglected when the wave impact was schematised by a pulse force. In chapter 2 and chapter 3 was stated that these are very important. When a computer model of the caisson breakwater is made, the development in time of a wave impact force can easily be taken into account. It will then also be possible to see how the breakwater will react on a force history as is described in chapter 2, a double peaked force with low frequency force oscillations which are in the range of the eigenfrequencies of a vertical (caisson) breakwater. This type of wave impact can be far more dangerous than wave impacts with a very high peak force and a very short duration, relative to the eigenperiods of the caisson breakwater (see chapter 10).
- The structure is assumed to be rigid, this seems to be a reasonable assumption. For the derivation of the TILLY computer model the vertical breakwater will be assumed to be rigid as well, the structure cannot distort.
- It is assumed that there is no interlocking between the different individual caissons, this seems a reasonable assumption as well.
- The wave impact acts on the total length of the structure, this is a very conservative assumption.
- Only a rough estimation of the pressure distribution under the caisson breakwater has been made, the effect of a wave impact on the pressure distribution under the caisson breakwater has not been taken into account very accurately.
- No cyclic loads are taken into account (a few wave impacts after each other).
- Long time (dynamical) effects of the foundation soil are not taken into account.
- Liquefaction of the foundation of the vertical breakwater, which may probably be an important failure mode, has not been taken into account and this will not be done in the remainder of this study.
- The foundation was assumed to react elastic. This is a good assumption when the displacements of the vertical breakwater are small. Elasto-plastic springs should be applied if the displacements of the bottom of the breakwater are large, because the maximum bearing capacity of the foundation may be exceeded or sliding of the vertical breakwater may occur. In the computer model the foundation can be schematised by elasto-plastic springs.
- Damping is neglected.

In the next chapter the derivation of a more sophisticated model will be described. Most of the points which are mentioned above can then be taken into account (different load histories, elasto-plastic springs and damping). The results of this more sophisticated model will be calculated by the use of TILLY, which is a computer programme. These calculations and results of these calculations will be treated in the next chapters.

8 Derivation of a mass-spring-dashpot TILLY model of the vertical breakwater

8.1 Introduction

In this chapter the derivation of a mass-spring-dashpot model will be described. This mass-spring-dashpot model represents a vertical breakwater. In this case the mass-spring-dashpot model represents the vertical breakwater which has already been described in chapter 7. The model can be used to calculate the dynamical behaviour of the vertical breakwater which is exposed to wave impacts. Unlike the previous chapter, the springs in this model are not linear-elastic anymore. The behaviour of the foundation will be described more accurately by the use of elasto-plastic springs, in which the plastic part of the springs represent the yielding of the foundation soil ("collapse" of the foundation soil).

Calculations of the dynamical behaviour of the vertical breakwater exposed to wave impacts, by the use of this mass-spring-dashpot model with elasto-plastic springs, will be carried out by the use of TILLY 3.3, which is a computer programme. The possibilities of this computer programme are reflected by using the name of the programme itself:

T Transient and static loading
I Incremental loading, initial stresses and strains
L Linear and non linear behaviour
L Lumped masses, springs and dashpots
Y Young and aging material

In section 8.2 a mass-spring TILLY model will be derived. This model differs in some ways from the analytical model of chapter 7 (see figure 7.3). This is done because of the fact that the new model makes it easier to implement elasto-plastic springs. The results of the calculations of this TILLY model will be compared to the results of the analytical model of chapter 7 to show the validity of the TILLY model. In section 8.3 the derivation of the characteristics of the elasto-plastic springs which represent the foundation of the vertical breakwater (sub-section 8.3.1) and the magnitude of the damping of the vertical breakwater (sub-section 8.3.2), which is represented by dashpots, will be discussed. The elasto-plastic springs and the dashpots will be implemented in a mass-spring-dashpot TILLY model which can describe the dynamical behaviour of the vertical breakwater very accurately. This will be carried out in section 8.4. In section 8.4 also the results of two wave impact loading cases on the vertical breakwater which are calculated by the use of this TILLY model will be presented.

The TILLY model which is derived in this chapter is a very usefull one. It describes the behaviour of the foundation of the vertical breakwater accurately and does also take the damping of the system into account. The output (the result of the calculations) of the TILLY model gives a reliable estimation of the dynamical behaviour of the vertical breakwater in real nature, until the moment that the soil in the foundation yields (see also the remark at the end of section 8.4). In this chapter the calculations are carried out for one geometry of a breakwater. All calculations will be carried out for the same vertical breakwater as has been described in chapter 7 before: the length is $L_c = 30$, the height is $H_c = 23$ m and the width is $B_c = 20$ m. The effect of the variation of different parameters of the mass-spring-dashpot model will be presented in chapter 9. The importance of the different parameters of the mass-spring-dashpot model can be indicated by means of the calculation of the effect of the variation of the different parameters.

In the TILLY model the geometry of the vertical breakwater- and the characteristics of the foundation of the vertical breakwater - can be changed easily, so in fact this model can be used for any type of vertical breakwater. The loading on the breakwater can also be changed very easily (see also chapter 10). Thus, not only the dynamical behaviour of a vertical breakwater which is exposed to wave impacts can be calculated, but also the dynamical behaviour of a vertical breakwater which is exposed to any kind of load. So the TILLY model of a vertical breakwater can - with some slight changes - easily be adapted to any kind of vertical breakwater which can be exposed to any kind of (dynamical) load. In this way it can support the analysis of the dynamical behaviour of any kind of vertical breakwater.

8.2 Derivation of a mass-spring TILLY model

In the previous chapter the derivation of an analytical model of a vertical breakwater has been discussed. This mass-spring model consisted of three linear-elastic springs with an infinite strength: a horizontal, a vertical and a rotational spring. The TILLY model which will be derived in this section differs from the model of the previous chapter, instead of a horizontal, a vertical and a rotational spring, the TILLY model consists of six linear-elastic springs: five vertical springs and one horizontal spring (see figure 8.1)

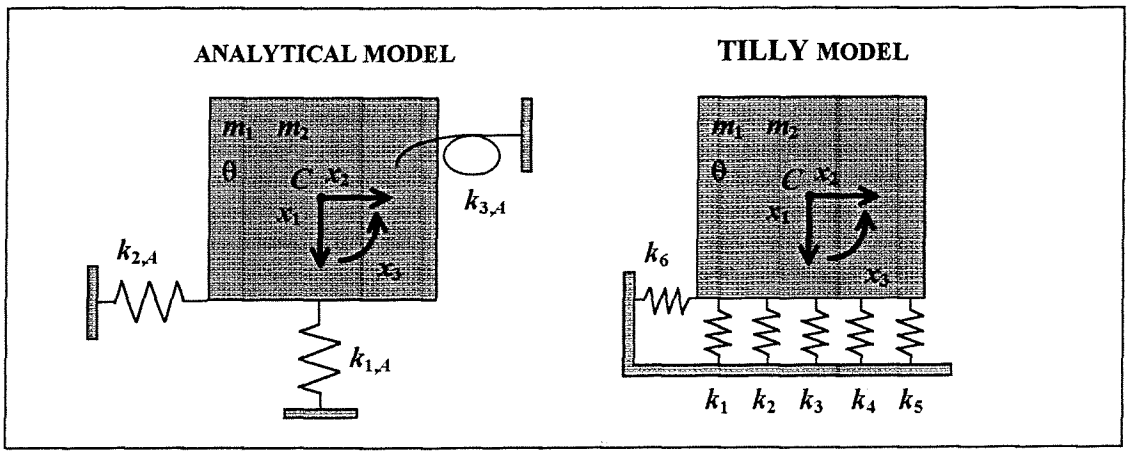

fig. 8.1 Comparison of the analytical model with the TILLY model

As can be seen in figure 8.1 the rotational spring in the analytical model has been replaced by the springs 1, 2, 4 and 5 in the TILLY model. Springs 1, 2, 4 and 5 represent not only the vertical stiffness of the foundation of the vertical breakwater but they can also represent the rotational stiffness of the foundation of the breakwater ($k_{3,A}$ in the analytical model) because of the fact that they are placed excentric relative to the centre of gravity (C) of the breakwater (spring k_3 in the TILLY model does not contribute to the rotational stiffness, but only to the vertical stiffness of the foundation see table 8.1).

The change in the TILLY model compared to the analytical model has been made because of the fact that in section 8.3 the linear-elastic springs will be changed into elasto-plastic springs. It is difficult to determine a rotational elasto-plastic spring. In the TILLY model the rotational spring is absent and only the elasto-plastic behaviour of the horizontal and the five vertical springs has to be determined, which is relatively easy. The determination of the elasto-plastic behaviour of the springs which represent the characteristics of the foundation will be carried out in sub-section 8.3.1. In this section, the springs will still be considered as linear-elastic.

The stiffnesses of the springs have to be determined in such a way that the results of the analytical and the TILLY calculations are the same. The magnitude of the different parameters of the analytical model is (see also figure 7.1 and section 7.3):

m_1	=	$29269.9*10^3$ kg			
m_2	=	$38956.2*10^3$ kg			
θ	=	$3.016*10^9$ kgm^2			
B_c	=	20 m	b	=	10.0 m
H_c	=	23 m	h	=	11.5 m
L_c	=	30 m	l	=	15.0 m
k_1	=	$1.5*10^{10}$ N/m			
k_2	=	$1.5*10^{10}$ N/m			
k_3	=	$5.0*10^{11}$ Nm/rad			

The horizontal stiffness in the analytical model and in the TILLY model are the same:

$$k_6 = k_{2,A} = 1.5*10^{10}\ \text{N/m} \tag{8.1}$$

The vertical stiffness of spring 1 ($k_{1,A}$) in the analytical model has to be the same as the total vertical stiffness of the five vertical springs in TILLY model. So:

$$k_1\ ,\ k_2\ ,\ k_3\ ,\ k_4\ ,\ k_5 = \frac{k_{1,A}}{5} = \frac{1.5*10^{10}}{5} = 3.0*10^9\ \text{N/m}. \tag{8.2}$$

The stiffnesses of the five vertical springs are known. Now the eccentricities (a and $2*a$) of the springs 1, 2, 4 and 5 have to be determined (see figure 8.2). These eccentricities determine in their way the rotational stiffness of the foundation of the vertical breakwater. The moment in the foundation of the vertical breakwater which is described by the analytical model is

$$x_3*k_{3,A} = 1*\ 5.0*10^{11} = 5.0*10^{11}\ \text{Nm} \tag{8.3}$$

if the vertical breakwater is given a unit rotation of 1 rad. The moment in the foundation of the TILLY model must be $5.0*10^{11}$ Nm as well, when x_3 (the rotational degree of freedom) in the TILLY model is also chosen as 1 rad. In that case the five vertical springs of the TILLY model exactly represent the rotational spring of the analytical model.

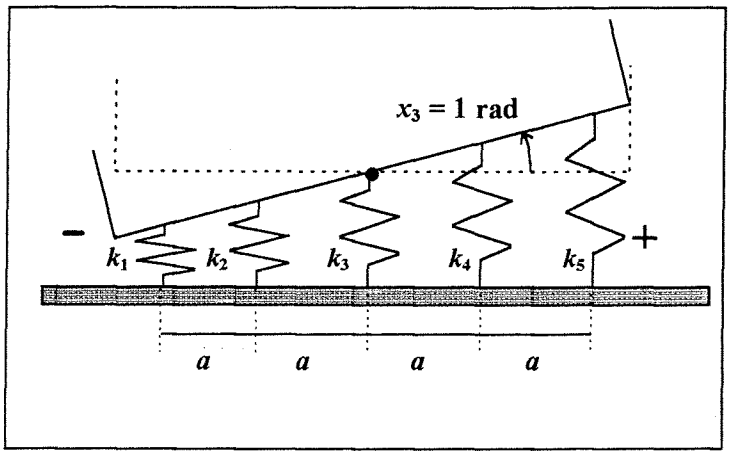

fig. 8.2 Eccentricity of the vertical springs

The total moment in the foundation of the breakwater in the TILLY model is $10*a^2*k$ (in this case k_1 , k_2 , k_3 , k_4 and k_5 are called k for reasons of simplicity) if the vertical breakwater is given a unit rotation of = 1 rad (see table 8.1). The total moment of $10*a^2*k$ must be equal to $5.0*10^{11}$ Nm.

spring	extension	force (x_3=1 rad)	lever arm	moment
1	$-2*a*x_3$	$-2*a*k$	$-2*a$	$4*a^2*k$
2	$-a*x_3$	$-a*k$	$-a$	a^2*k
3	0	0	0	0
4	$a*x_3$	$a*k$	a	a^2*k
5	$2*a*x_3$	$2*a*k$	$2*a$	$4*a^2*k$
			TOTAL	$10*a^2*k$

table 8.1 Moment in the foundation

So a is:

$$a = \sqrt{\frac{k_{3,A} * 1}{10 * k * 1}} = \sqrt{\frac{5.0 * 10^{11}}{10 * 3.0 * 10^9}} = 4.0825 \text{ m} \qquad (8.4)$$

The TILLY model can now be developed because all the input parameters of the model are known: the masses and the mass moment of inertia of the vertical breakwater, the stiffnesses of the springs and the eccentricities of the springs. All these parameters describe the vertical breakwater. This vertical breakwater can be exposed to different kinds of loads. These loads are an input for the model as well.

The validity of the TILLY model has to be checked. The analytical model of chapter 7 can serve as the check for the TILLY model, just as was mentioned in chapter 7 when the analytical model was derived. The vertical breakwater which is described by the TILLY model will be exposed to the same wave impact as has been described in chapter 7 before: a wave impact of the transition type with a triangular load history, with a peak force of 13422 kN/m and a duration of 12 ms (see figure 7.8). The load will act on the breakwater at Still Water Level (SWL) over a total length of 30 m, so 3.5 m eccentric relative to the centre of gravity of the vertical breakwater. (The centre of gravity of the vertical breakwater is 11.5 above the seabed, the water depth is 15 m, so when the wave impact acts on the vertical front wall of the breakwater at SWL, it acts 3.5 m eccentric relative to the centre of gravity of the vertical breakwater. If the results of the analytical and the TILLY model are the same, then the TILLY model has been derived correctly.

The output of the TILLY model will be determined for two cases. In the first case the homogeneous solution of the breakwater is determined, just as this has been carried out before in chapter 7 (section 7.5) where the wave impact of the transition type was schematised by a pulse load; so no external load on the vertical breakwater and only initial values which have been described in equations 7.65 an 7.66 before:

$$\underline{x}(0^+) = \begin{bmatrix} x_2(t) \\ x_3(t) \end{bmatrix} = \begin{bmatrix} 0 \\ 0 \end{bmatrix} \tag{7.65}$$

$$\underline{\dot{x}}(0^+) = \begin{bmatrix} \dot{x}_2(t) \\ \dot{x}_3(t) \end{bmatrix} = \begin{bmatrix} 0.0620173 \\ -0.0028036 \end{bmatrix} \tag{7.66}$$

The listing of the TILLY programme in which this model is described can be found in enclosure 8.1 at the end of this report.

In the other case the initial velocities and the initial displacements are zero. The input of the TILLY model is an external load (the triangular load with a peak force of 13422 kN/m and a total duration of 12 ms which acts over a total length of 30 m) which is described in the TILLY model as follows (see also figure 7.8):

$$\begin{array}{llll} t_i = 0.000 & \text{s} & F = 0 & \text{kN} \\ t_i = 0.006 & \text{s} & F = 402660 & \text{kN} \\ t_i = 0.012 & \text{s} & F = 0 & \text{kN} \end{array} \tag{8.5}$$

The listing of the TILLY programme in which this model is described can be found in enclosure 8.2.

The results of the calculations of the two TILLY models (described in enclosure 8.1 and enclosure 8.2) and the analytical model are summarised in figure 8.3. In figure 8.3 the horizontal displacement of the caisson breakwater bottom is sketched for the three cases which have been calculated for the same wave impact load situation.

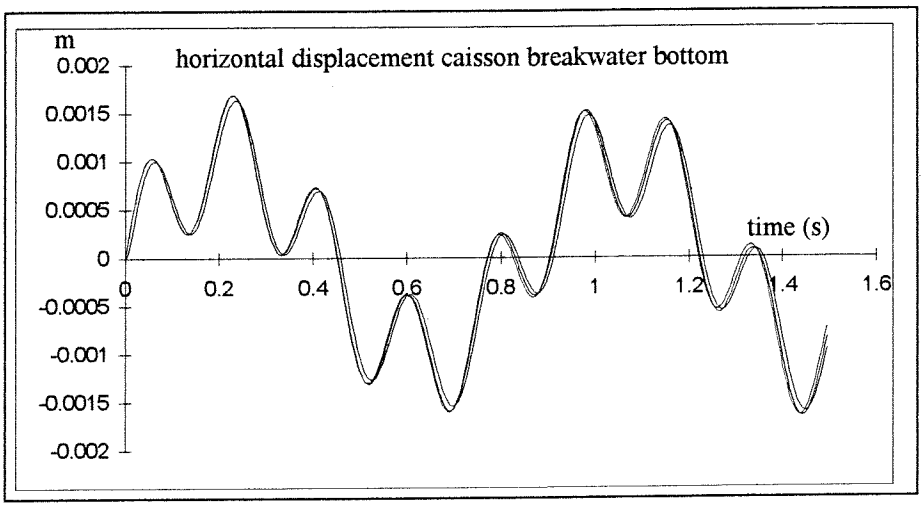

fig. 8.3 Comparison of the output of the analytical model and the two TILLY computations

The results show good agreement: there is hardly any difference between the output of the different models (the two TILLY models and the analytical model). So the following conclusions can be drawn:

Conclusions:
The TILLY model and the analytical model show good agreement. Henceforth, the calculations of the dynamical behaviour of a vertical breakwater exposed to a wave impact can be done by the use of the TILLY model which has been derived in this section. (This TILLY model will be improved in the next sections.)

In chapter 7, the wave impact of the transition type has been schematised by a pulse load, figure 8.3 shows that this was permitted.

In the next section the TILLY model will be extended, a more sophisticated model will be derived. Damping and elasto-plastic springs will be introduced.

8.3 Derivation of a TILLY model with elasto-plastic springs and damping

8.3.1 Elasto-plastic springs

So far, the springs which represent the foundation of the vertical breakwater have been considered as linear-elastic. The linear-elastic springs have got an infinite strength, there is not a certain displacement at which the springs (which represent the foundation) yield ("collapse"). In nature this is not true. If the forces in the foundation exceed a certain value, the foundation will react plastic instead of elastic, if this value is not exceeded the foundation will react elastic. When the foundation of the vertical breakwater becomes plastic, the foundation yields and permanent displacements in the foundation will occur. This combined elastic and plastic behaviour of the foundation can be schematised by elasto-plastic springs . In figure 8.4 an elasto-plastic spring is shown which can be used to schematise the real behaviour of the foundation soil.

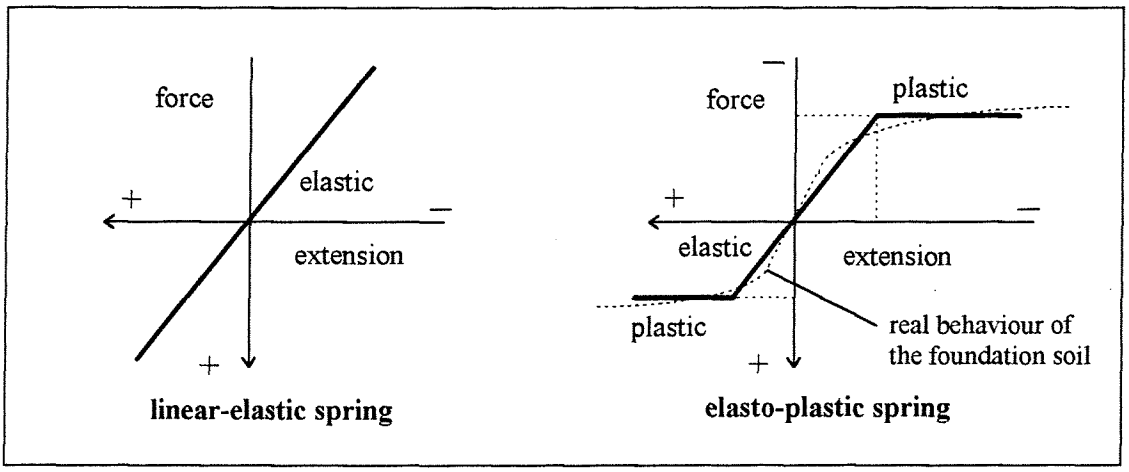

fig. 8.4 Linear-elastic spring and elasto-plastic spring

A negative extension of the spring can be seen as pressure in the spring and a positive extension of the spring can be seen as tension in the spring (see figure 8.4). Thus, a negative pressure in the soil is caused by a negative extension of the springs and a positive pressure in the soil is caused by a positive extension of the springs (tension).

The determination of the elasto-plastic behaviour of the foundation will be treated separately for the horizontal spring and the vertical springs because a different way of calculating is used for these two different types of springs.

Determination of the vertical elasto-plastic springs (spring 1, 2, 3, 4 and 5)

For the determination of the elasto-plastic behaviour of the foundation in the vertical direction, the theory of Brinch Hansen is used [VERRUIJT (1993)]. By the use of this theory, the maximum bearing pressure of a strip foundation can be determined. A strip foundation shows good agreement with the foundation of a vertical breakwater (see figure 8.5).

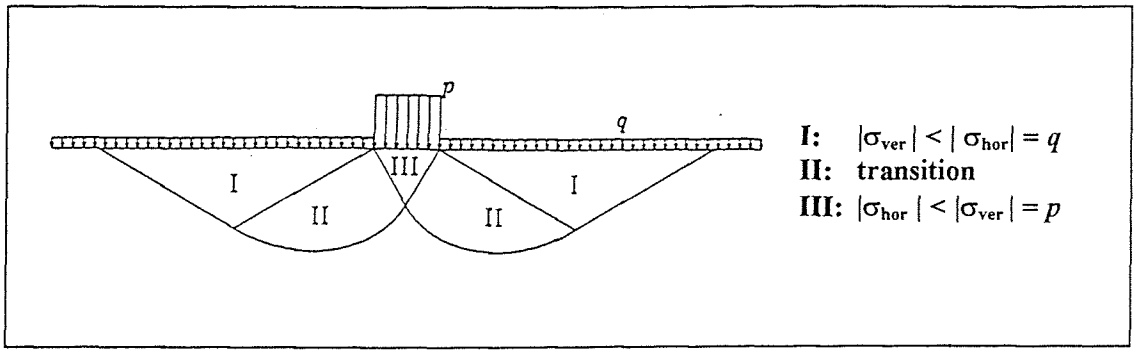

fig. 8.5 Definition sketch for the determination of the bearing pressure of a strip foundation [VERRUIJT (1993)]

The theory of Brinch Hansen has been the subject of a lot of discussions. Although the theoretical basis of the Brinch Hansen formula is weak at some points (the theoretical basis of some factors and constants), it can give a good approximation of the bearing pressure of the foundation. The theory has been derived for dry conditions.

Brinch Hansen used the theory of Prandtl and defined the bearing pressure of the strip foundation (p) (see also figure 8.5):

$$p = i_c s_c c N_c + i_q s_q q N_q + i_\gamma s_\gamma \tfrac{1}{2} \gamma_s B_{eff} N_\gamma \qquad (8.6)$$

in which:

p	=	maximum bearing pressure in the foundation	
i_c, i_q, i_γ	=	reduction factors related to direction of the load on the foundation	
s_c, s_q, s_γ	=	reduction factors related to the shape of the foundation (different from a strip)	
c	=	cohesion	
q	=	pressure next to the foundation	
γ_s	=	weight of the soil (kN/m^3). For soil under water: $\gamma_s = \gamma_{saturated} - \gamma_w$	
B_{eff}	=	$B_c - 2*e$ = effective width of the foundation	(8.7)
e	=	$\frac{M_{foundation}}{F_n}$ = eccentricity (see figure 8.6)	(8.8)
N_q	=	$\frac{1+\sin(\varphi)}{1-\sin(\varphi)} e^{[\pi * \tan(\varphi)]}$ = dimensionless constant	(8.9)
N_c	=	$(N_q-1)\cot(\varphi)$ = dimensionless constant	(8.10)
N_γ	=	$2(N_q-1)\tan(\varphi)$ = dimensionless constant	(8.11)
φ	=	angle of internal friction of the soil	

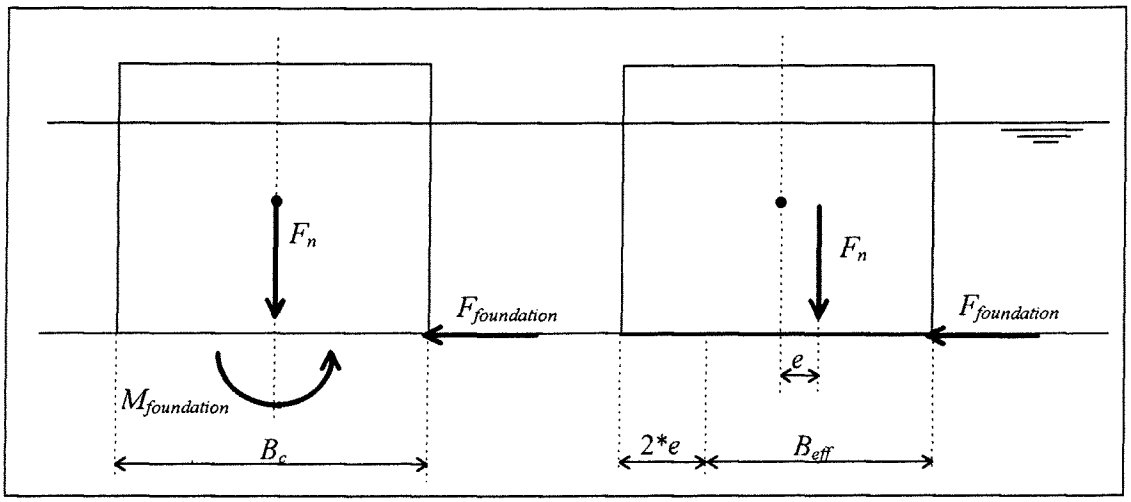

fig. 8.6 Definition sketch for the determination of B_{eff}

The maximum bearing pressure of the foundation must be reduced when besides a vertical load (F_n) a horizontal load ($F_{foundation}$) also acts on the foundation (see figure 8.7)

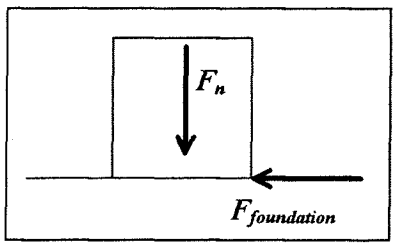

fig. 8.7 Horizontal and vertical load

If the breakwater does not slide ($F_{foundation} < \mu * F_n$, see chapter 7) the reduction factors i_c, i_q and i_γ are:

$$i_c = 1 - \frac{\frac{F_{foundation}}{B_{eff}}}{c + \frac{F_n}{B_{eff}} \tan(\varphi)} \qquad (8.12)$$

$$i_q = i_c^2 \qquad (8.13)$$

$$i_\gamma = i_c^3 \qquad (8.14)$$

The Brinch Hansen formula was derived for a strip foundation with an infinite length. A vertical breakwater consists of different individual caissons with a finite length. The following reduction factors (s_c, s_q and s_γ) must be applied if the foundation is rectangular instead of an infinite long strip.

$$s_c = 1 + 0.2 * \frac{B_{eff}}{L_c} \qquad (8.15)$$

$$s_q = 1 + \frac{B_{eff}}{L_c} \sin(\varphi) \qquad (8.16)$$

$$s_\gamma = 1 - 0.3 * \frac{B_{eff}}{L_c} \qquad (8.17)$$

For the determination of the parameters which are used in the Brinch Hansen formula, the same vertical breakwater is used as was described in chapter 7 and in section 8.2. The input parameters which are necessary for the calculation of the maximum bearing pressure of the foundation by means of the Brinch Hansen formula are as follows:

- The length of one section (one caisson) of the vertical breakwater is chosen as L_c = 30 m. This length is used for the determination of the reduction factors s_c, s_q and s_γ. The width of the caisson is B_c = 20 m.
- The foundation of the vertical breakwater is sand: mass density ρ_s = 2000 kg/m^3, γ_s = 10 kN/m^3, the cohesion c = 0 N/m^2 and the angle of internal friction is chosen as φ = 33°. The angle of internal friction of sand is somewhere in the range of 30-35°, so here a mean value of 33° is chosen.
- $F_n = 152.4*10^6$ N
  In chapter 7 was found that 6.34% of the wave impact force was felt in the foundation and 4.84% of the moment caused by the wave impact. These values are rather low due to the fact that the wave impact with a peak force of 13422 kN/m only has a small duration (12 ms). So, this wave impact only represents a small amount of momentum. For wave impacts with a longer duration - and a larger amount of momentum - it is expected that a greater part of the wave impact force and wave impact momentum is felt in the foundation. Here it is assumed that 7% (>2*3.33%) of the maximum wave impact force of 30*($15*\rho_w*g*H_b^2$) is felt in the foundation by means of a force and a moment (H_b = 10 m)

$$F_{foundation} = 0.07*30*(15*1025*9.81*10^2) = 31.67*10^6 \text{ N}$$
$$M_{foundation} = 15*31.67*10^6 = 475.1*10^6 \text{ Nm}$$
$$e = \frac{M_{foundation}}{F_n} \quad \frac{475.1*10^6}{152.4*10^6} = 3.11$$
$$B_{eff} = B_c\text{-}2*e = 20\text{-}2*3.11 = 13.78 \text{ m}$$

- q = 0 N/m^2.

The maximum bearing pressure in the vertical direction of the foundation can now be determined:

i_c	=	0.680	i_q	=	0.462	i_γ	=	0.314
s_c	=	1.092	s_q	=	1.250	s_γ	=	0.862
N_c	=	38.638	N_q	=	26.092	N_γ	=	32.590

$$p = i_c s_c c N_c + i_q s_q q N_q + i_\gamma s_\gamma \tfrac{1}{2} \gamma_s B_{eff} N_\gamma$$
$$= 0.680*1.092*0*38.638+0.462*1.250*0*26.092+0.314*0.862*0.5*10*13.78*32.590$$
$$= 608 \text{ kN/m}^2$$

This value is a good approximation for the maximum bearing pressure of the foundation of a vertical breakwater. One should bear in mind that the influence of the angle of internal friction on the results obtained is enormous. For example if φ = 35° is chosen, the maximum bearing pressure will be 1022.0 kN/m^3. In literature a value of 700 kN/m^2 is recommended as a maximum for the bearing pressure of deep water vertical breakwater (see formula 7.92). According to the Japanese standards the maximum value of the bearing pressure (at the toe of the caisson) was previously taken as 400 - 500 kN/m^2. The limit has been increased to 600 kN/m^2 or more, especially for deep-water breakwaters [PIANC (1996)]

Nota bene:

For the determination of the elasto-plastic behaviour of the foundation in the vertical direction, the theory of Brinch Hansen has been used. This theory has been derived for a **static** loading case. The calculations which are carried out in this study are for a **dynamical** loading case. The foundation of the vertical breakwater will react different on dynamical loads than on static loads. According to Verruijt [VERRUIJT (1996)] the theory of Brinch Hansen can be used under dynamical loading situations if the following condition is fulfilled:

$$\omega < \omega_0 \tag{8.18}$$

in which:

ω = the radian frequency of the oscillation(s) of the structure

$$\omega_0 = \frac{2 * c_s}{R} \tag{8.19}$$

$$c_s = \sqrt{\frac{E_s}{\rho_s}} = \text{wave velocity in the foundation soil} \tag{8.20}$$

in which:

E_s = elasticity modulus of the soil, approximated by $188*10^6$ N/m^2 (this estimation is a rather high value, but in chapter 7 has been stated that the vertical breakwater is founded on stiff soil, the derivation of this value can be found in sub-section 7.3.2).

R = radius of the loaded area, approximation: $R = \sqrt{\frac{B_c * L_c}{\pi}}$ (8.21)

$$c_s = \sqrt{\frac{188 * 10^6}{2000}} 307 \text{ m/s} \qquad R = \sqrt{\frac{30 * 20}{\pi}} = 13.8 \text{ m}, \text{ so:}$$

$$\omega_0 = \frac{2 * 307}{13.8} = 44.5 \text{ rad/s}$$

The eigenfrequencies of the vertical breakwater which have been found in chapter 7 are all smaller than 44.5 rad/s (ω_1 = 22.638 rad/s, ω_2 = 7.440 rad/s and ω_3 =33.959 rad/s), this means that the condition of equation 8.18 is fulfilled. So it is allowed to use the Brinch Hansen theory for the determination of the maximum bearing pressure of the foundation.

According to Verruijt [VERRUIJT (1996)] the geo-dynamical mass can be neglected when the condition of equation 8.18 is fulfilled because there will be no inertia of the foundation soil. But because of the fact that the magnitude of the geo-dynamic mass has been derived independent of the frequency of the oscillations of the structure - which is common within the framework of the MAST-project - it will still be taken into account, just as it has been done before in chapter 7.

The elasto-plastic springs can now be determined. The maximum bearing pressure of the foundation soil is 608 kN/m^2. The soil cannot withstand pressures greater than 0 kN/m^2 and smaller than - 608 kN/m^2. The springs which represent the foundation of the breakwater have got an initial negative extension due to the static load of the vertical breakwater. This negative extension is:

$$\Delta\ell = -\frac{F_n}{5*k} = -\frac{152.4*10^6}{5*3.0*10^9} = -10.16 \text{ mm} \qquad (8.22)$$

A negative extension causes a negative pressure in the soil and thus a negative force in the springs which represent the foundation of 30480 kN (= F_n /5 = 152.4*10^6/5).

The initial negative extension of the springs must be taken into account when the dynamical behaviour of the vertical breakwater is determined. The springs which represent the soil can be lengthened until the force in the springs is 0 kN, the initial force in the springs is -30480 kN.

The maximum and minimum forces in the springs can be determined if the area of the soil which is represented by each of the springs is known. The springs are determined for the total length of the structure (L_c = 30 m). Every spring represents a part of the width of the caisson. Spring 2, 3 and 4 represent 4.0825 m and spring 1 and 5 together represent the rest of the width of the caisson which is [20-(3*4.0825)]/2=3.8763 m (see figure 8.2). So:

- spring 2, 3 and 4 represent an area of: 4.0825*30 = 122.475 m^2
- spring 1 and 5 represent an area of: 3.8763*30 = 116.289 m^2

and:

- the minimum force in spring 2, 3 and 4 is: 122.475*-608 = -74464.8 kN
- the minimum force in spring 1 and 5 is: 116.289*-608 = -70703.7 kN
- The maximum force in all springs is: 0 kN

and:

- The stiffness of spring 1, 2, 3, 4 and 5 is 3.0*10^9 N/m.

The characteristics of spring 1, 2, 3, 4 and 5 are sketched in figure 8.8.

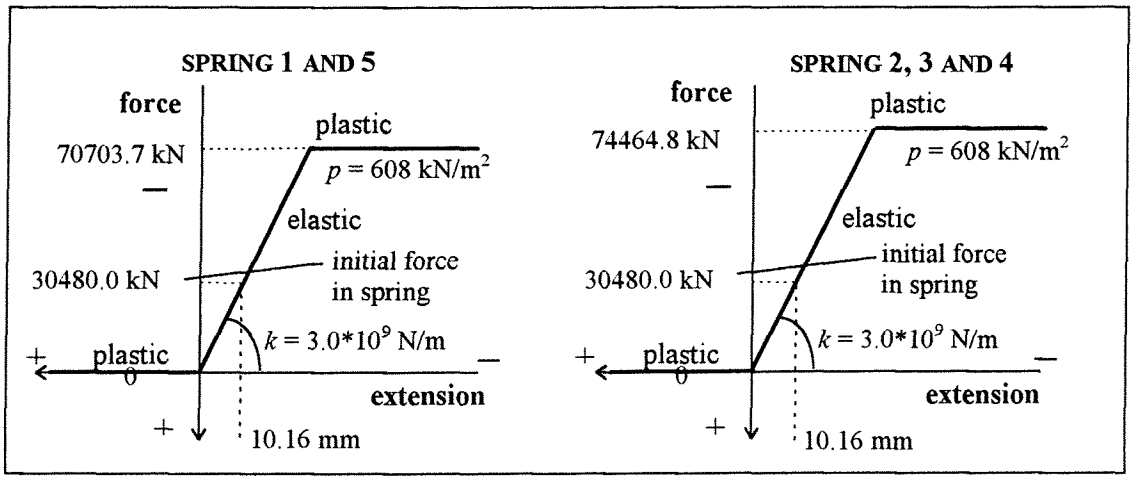

fig. 8.8 Spring characteristics of spring 1 and 5 and spring 2, 3 and 4

Check: 2*70703.7+3*74464.8 = 20*30*608 → OK!

Determination of the horizontal elasto-plastic spring (spring 6)

The elasto-plastic behaviour of the horizontal spring (spring 6) can be determined using the sliding criterion which has previously been described in chapter 7, sub-section 7.6.1 The maximum force in spring 6 is chosen equal to:

$$F_{spring\ 6,\ max} = \mu * F_n \tag{8.23}$$

The minimum force in spring 6 is equal to:

$$F_{spring\ 6,\ min} = -\mu * F_n \tag{8.24}$$

In equations 8.17 and 8.18 the Coulomb friction coefficient (μ) is used which is defined as:

$$\mu = \tan(\varphi) \tag{8.25}$$

The magnitude of the Coulomb friction coefficient can be determined as $\mu = \tan(33) = 0.65$. This value is higher than 0.50, the value which has been used in section 7.6.1, but lower than 0.6 the value which is usually used in Japan [GODA (1993)], [TAKAHASHI (1996)]. Delft Hydraulics [DELFT HYDRAULICS (1982)] has found values which are in the range of 0.60-0.70. The value of the friction coefficient μ has been investigated in models and in full scale studies. For a plane concrete slab resting on quarried rubble stones Takayama (1992) found, as an average, a static friction coefficient of $\mu = 0.636$ and a coefficient of variation of 0.15. Here, μ will be chosen as 0.60.

So, the maximum and minimum force in spring 6 are, with $F_n = 152.4*10^6$ N and $\mu = 0.60$:

- the maximum force in spring 6 is $0.60*152.4*10^6 = 91440.0$ kN
- the minimum force in spring 6 is $-0.60*152.4*10^6 = -91440.0$ kN.

The characteristics of spring 6 are sketched in figure 8.9.

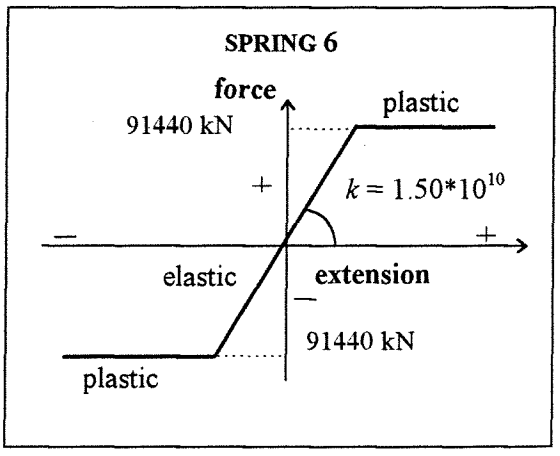

fig. 8.9 Spring characteristics of spring 6

8.3.2 Damping

Damping has been neglected in the TILLY model so far (as well as in the analytical model). This means that if energy is added to the system (in this case the vertical breakwater), this energy will not be dissipated. In other words, if the system is oscillating due to the addition of energy it will not stop oscillating (until an intervention). In nature energy will be dissipated. So in order to make a good model of the vertical breakwater, damping has also to be added. This can be done by means of dashpots (dampers).

In this section only the derivation of the mass-spring-dashpot *TILLY* model will be given. In the following intermezzo short attention is being paid to the *analytical* formula of a mass-spring-dashpot model which belongs to the model which is also sketched in this intermezzo. This model is almost the same model as the model which has been used in chapter 7 (only the dashpots with the friction coefficients are added).

Intermezzo

ANALYTICAL MODEL

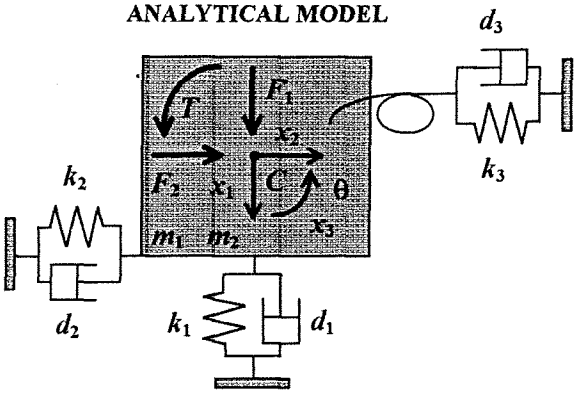

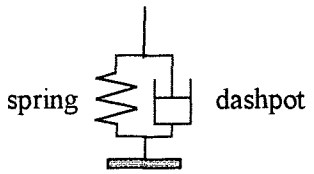

k = stiffness
d = friction coefficient

EQUATION WHICH DESCRIBES THE DYNAMICAL BEHAVIOUR OF THE MODEL

$$\begin{bmatrix} m_1 & 0 & 0 \\ 0 & m_2 & 0 \\ 0 & 0 & \theta \end{bmatrix} \begin{bmatrix} \ddot{x}_1 \\ \ddot{x}_2 \\ \ddot{x}_3 \end{bmatrix} + \begin{bmatrix} d_1 & 0 & 0 \\ 0 & d_2 & hd_2 \\ 0 & hd_2 & h^2 d_2 + d_3 \end{bmatrix} \begin{bmatrix} \dot{x}_1 \\ \dot{x}_2 \\ \dot{x}_3 \end{bmatrix} + \begin{bmatrix} k_1 & 0 & 0 \\ 0 & k_2 & hk_2 \\ 0 & hk_2 & h^2 k_2 + k_3 \end{bmatrix} \begin{bmatrix} x_1 \\ x_2 \\ x_3 \end{bmatrix} = \begin{bmatrix} F_1 \\ F_2 \\ T \end{bmatrix}$$

Energy dissipation can take place in the structure itself, in the foundation of the structure and by exciting water movements (e.g. waves) when the structure is moving:

- It is assumed that energy is not significantly dissipated in the caisson breakwater itself, which is assumed to be rigid (no internal distortion).

- Dissipation of energy by exciting water movements is negligible if [DELFT HYDRAULICS (1995)] the condition which is described in equation 8.26 is fulfilled:

$$\frac{\omega^2 L}{g} > 10 \qquad (8.26)$$

in which:

L = characteristic size of the structure
ω = radian frequency of the oscillation of the breakwater

The condition of equation 8.26 is usually fulfilled for caisson breakwaters which are exposed to waves and wave impacts.

The validity of the condition which is described in equation 8.26 can be shown by the following analysis. The maximum wave length of waves is the deep water wave length L_0:

$$L_0 = \frac{g * T^2}{2 * \pi} \tag{8.27}$$

It is assumed that the waves in the water around the vertical breakwater which are excited by the oscillating vertical breakwater itself have got the same periode as the period of the horizontal oscillation of the vertical breakwater. This period is $T_2 = 0.845$ s (equation 7.44), so L_0 becomes:

$$L_0 = \frac{9.81 * 0.845^2}{2 * \pi} = 1.11 \text{ m}$$

The condition for deep-water calculations is:

$$\frac{2 * \pi * d}{L} >> 1 \tag{8.28}$$

which is fulfilled in this situation:

$$\frac{2 * \pi * 15}{1.11} >> 1$$

if is assumed that $L \approx L_0$ (which is a conservative assumption)

The influence of the wave period is often described as a wave length and related to the wave height, resulting in a wave steepness. The wave steepness, s, can be defined by using the deep water wave length:

$$s = \frac{2 * \pi * H}{g * T^2} = \frac{H}{L_0} \tag{8.29}$$

According to Miche (1944) [BATTJES (1993)] the wave steepness is limited for deep water waves. The maximum height of (regular) deep water waves, H_{max} , is given by the following equation:

$$H_{max} \approx 0.14 * L_0 \qquad (s_{max} \approx 0.14) \tag{8.30}$$

So, in this case the maximum wave height which is possible for waves which are excited by the oscillating vertical breakwater is 0.14*1.11 = 0.15 m.

The influence of the waves which are excited by the oscillating vertical breakwater on the dynamical behaviour of the vertical breakwater itself is negligible (compared to the size and mass of the structure and compared to the hydraulic loads on the structure). Only very minor waves with a maximum wave height of 0.15 m and a maximum wave length of 1.11 m are generated by the oscillating structure. These waves are, for example, very small compared to the waves which can cause wave impacts on the vertical front wall of the structure, they can be as high as 10 m. So just as has been stated before by the condition which has been described in equation 8.26, no significant damping is expected due to the excitement of water movements due to the oscillating breakwater. So damping due to excitation of waves can be neglected.

- Damping in the foundation is the only significant damping. Damping will take place in horizontal and in vertical direction.

Damping in the TILLY model will be represented by five dashpots in the vertical direction with friction coefficients (d_1, d_2, d_3, d_4 and d_5) and one dashpot in the horizontal direction with a friction coefficient (d_6) (see figure 8.10)

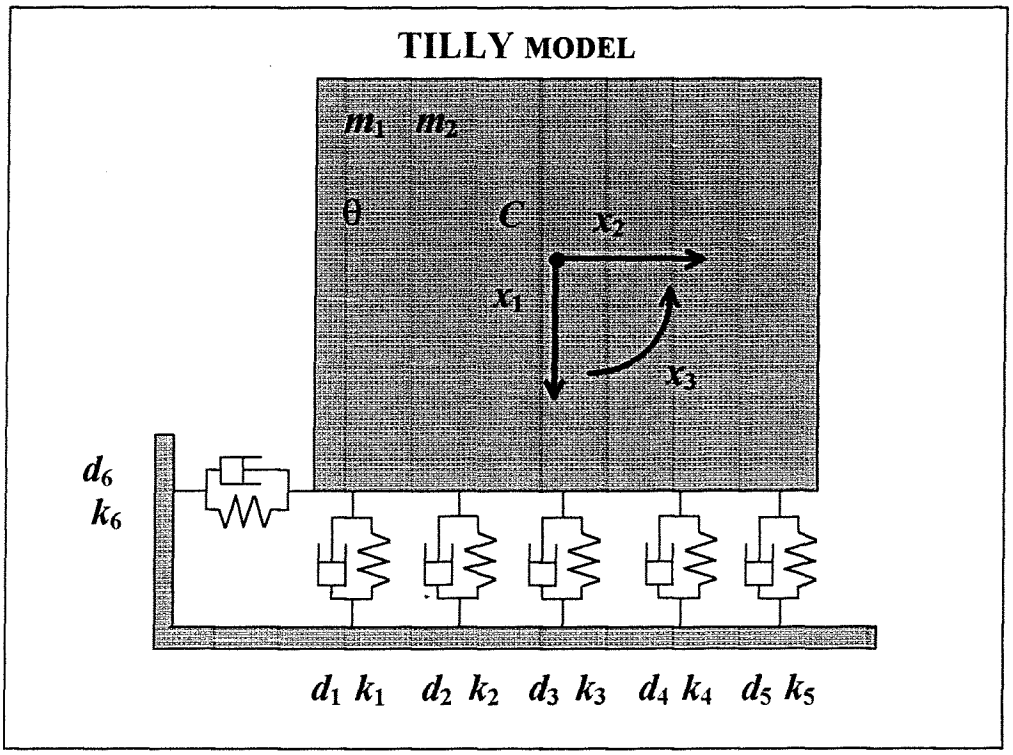

fig. 8.10 Mass-spring-dashpot model of the vertical breakwater

The vertical damping (represented by dashpots with friction coefficients d_1 to d_5) and the horizontal damping (represented by a dashpot with a friction coefficients d_6) will be chosen the same. The friction coefficients which represent the damping in the foundation of the vertical breakwater can be estimated using the following formula for the total magnitude of the damping in the vertical and the horizontal direction:

$$d_{hor,ver} = B_c * L_c * \sqrt{\rho_s * E_s} \tag{8.31}$$

$$d_{hor,ver} = 30 * 20 * \sqrt{2000 * 188 * 10^6} = 367.9 * 10^6 \text{ Ns/m}$$

So, the following friction coefficients for the different dashpots of the model can be derived:

$$d_1, d_2, d_3, d_4, d_5 = {}^1/_5 * 367.9 * 10^6 = 73.58 * 10^6 \text{ Ns/m} \tag{8.32}$$

$$d_6 = 367.9 * 10^6 \text{ Ns/m} \tag{8.33}$$

The horizontal dashpot and the five vertical dashpots are placed parallel relative to the springs (see figure 8.10). This means that the five vertical dashpots have got the same eccentricity relative the centreline of the bottom slab of the vertical breakwater as the five vertical springs, a = 4.0825 m (see equation 8.4).

Nota bene:

Within the MAST-project damping is often calculated using the formulae which are given by Richart et al. [RICHART et al. (1970)]. Richart et al. gives different friction coefficients for horizontal, vertical and rotational oscillations. The formula used for the determination of the damping in the foundation soil used in the analysis which is presented in this report gives, together with the chosen position of the dashpots (see figure 8.10 and 8.11), comparable results.

In the previous sub-section the elasto-plastic springs have been determined, in this sub-section the magnitude of the friction coefficients which represent the damping in each of the six dashpots has been calculated. In the next section the different aspects of the TILLY model will be summarised and some calculations will be done.

8.4 Implementation and summary

In this section a summary of the mass-(elasto-plastic)spring-dashpot TILLY model is given in figure 8.11. The programme listing of this TILLY model (exposed to the transition type wave impact) can be found in enclosure 8.3.

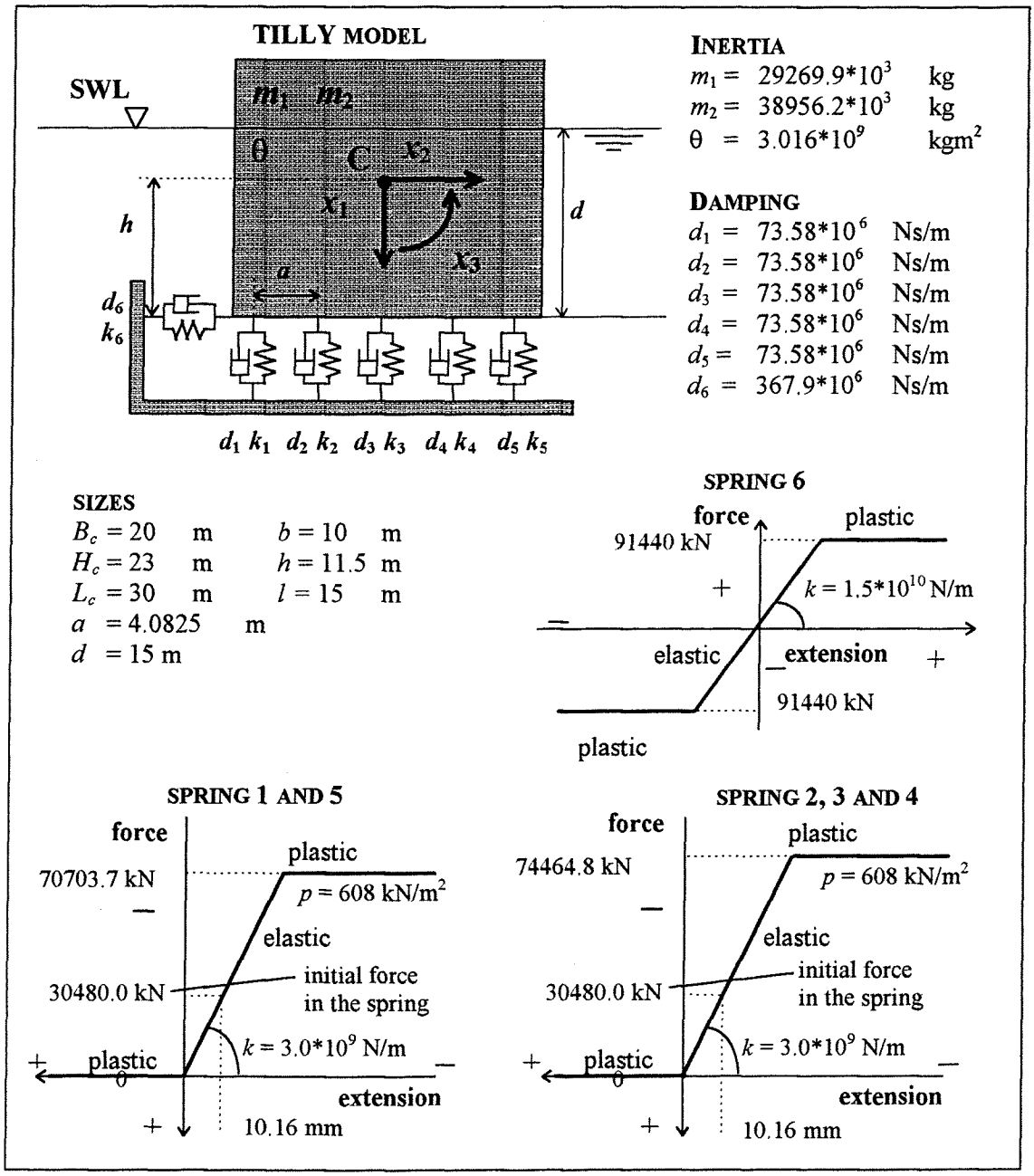

fig. 8.11 Summary of the mass-spring-dashpot TILLY model, elasto-plastic springs and damping

First example loading case

The vertical breakwater which is described in the TILLY model (see figure 8.11 and enclosure 8.3) will be exposed to the same wave impact as has been described before in chapter 7: a wave impact of the transition type with a triangular load history, with a peak force of 13422 kN/m and a duration of 12 ms which acts over a total length of 30 m (see figure 7.8). The load will act on the vertical front wall of the breakwater at Still Water Level (SWL), so 3.5 m excentric relative to the centre of gravity of the vertical breakwater. The result of this TILLY calculation - in this case the horizontal displacement of the bottom of the vertical breakwater - is shown in figure 8.12 together with the analytical solution which has been derived in chapter 7 before.

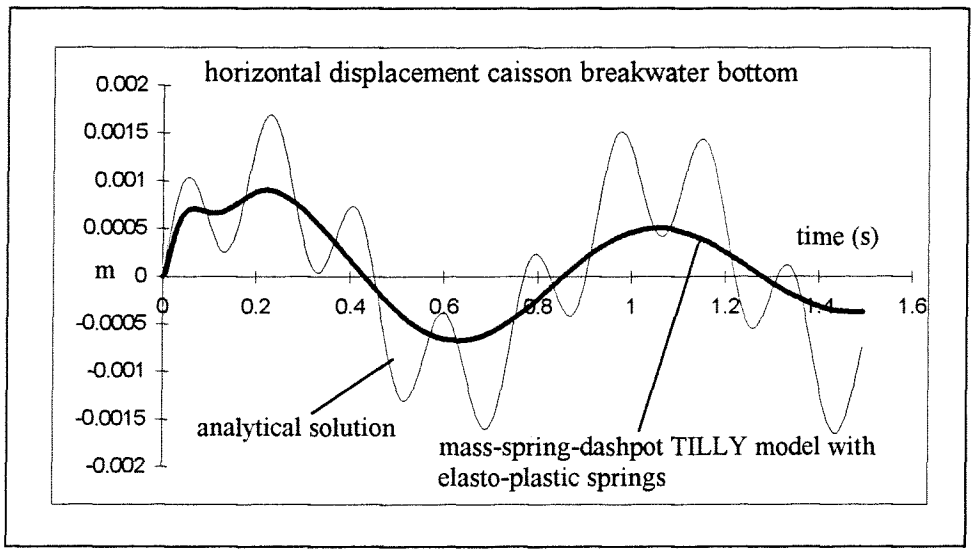

fig. 8.12 Comparison horizontal displacement analytical solution and mass-spring-dashpot TILLY model

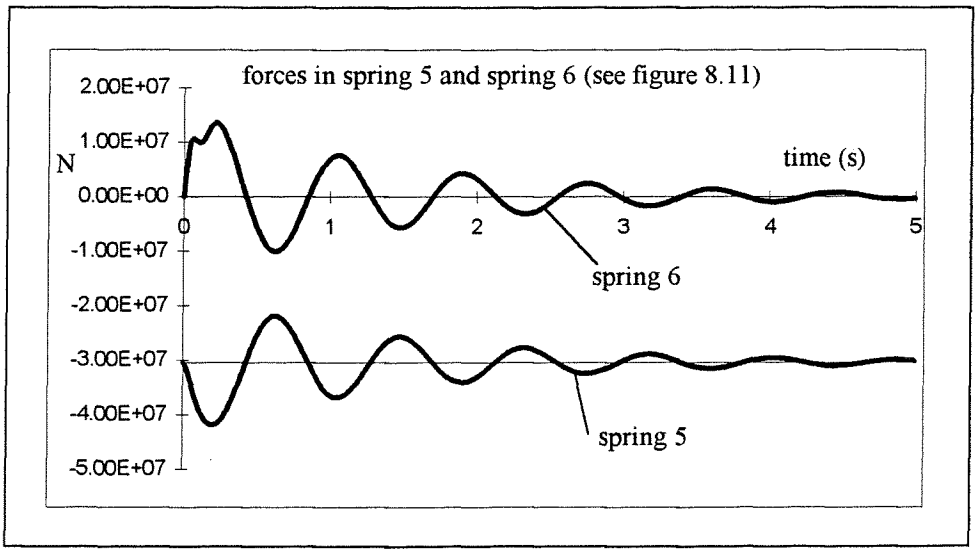

fig. 8.13 Forces in spring 5 and spring 6 calculated by using the TILLY model

In section 7.6 the most important failure modes of a vertical breakwater have been mentioned, these are: sliding, overturning and collapse (yielding) of the foundation. As can be seen in figure 8.12, the vertical breakwater does not slide. There are no residual displacements. In figure 8.13 can be seen that the foundation of the vertical breakwater does not collapse if the vertical breakwater is exposed to the wave impact with a peak force of 13422 kN/m and a duration of 12 ms (see figure 7.8. The springs do not become plastic.

The forces in spring 5, the most eccentric vertical spring and the forces in spring 6, the horizontal spring, do not exceed the value at which the springs become plastic. For spring 5 this value has a magnitude of -70703.7 kN and for spring 6 it is ±91440 kN. This means that both the vertical and the horizontal springs remain elastic and that there is no permanent - horizontal and vertical - displacement.

The fact that the breakwater does not overturn has already been proven in sub-section 7.6.2.

Second example loading case

The results of the last loading case on the vertical breakwater of this chapter can be found in figure 8.14 and in figure 8.15. In this example the vertical breakwater will be exposed to a load which causes foundation failure of the breakwater. The breakwater will be exposed to a maximum wave impact force of $15*\rho_w*g*H_b^2$ (15082.875 kN/m) which will act over the total length (30 m) of the vertical breakwater, the total force is $30*15*\rho_w*g*H_b^2$ = 452486.25 kN. The height of the wave is chosen as H_b = 10 m. The total duration of the wave impact is chosen as 0.25 s (250 ms) and the wave impact has a triangular load history. This duration of 250 ms is almost 20 times as large as the duration of the previous example which was 12 ms. It is assumed that the wave impact force acts on the vertical front wall of the vertical breakwater at Still Water Level (SWL), so 3.5 m excentric relative to the centre of gravity of the vertical breakwater. The listing of the TILLY programme in which this problem is described can be found in enclosure 8.4.

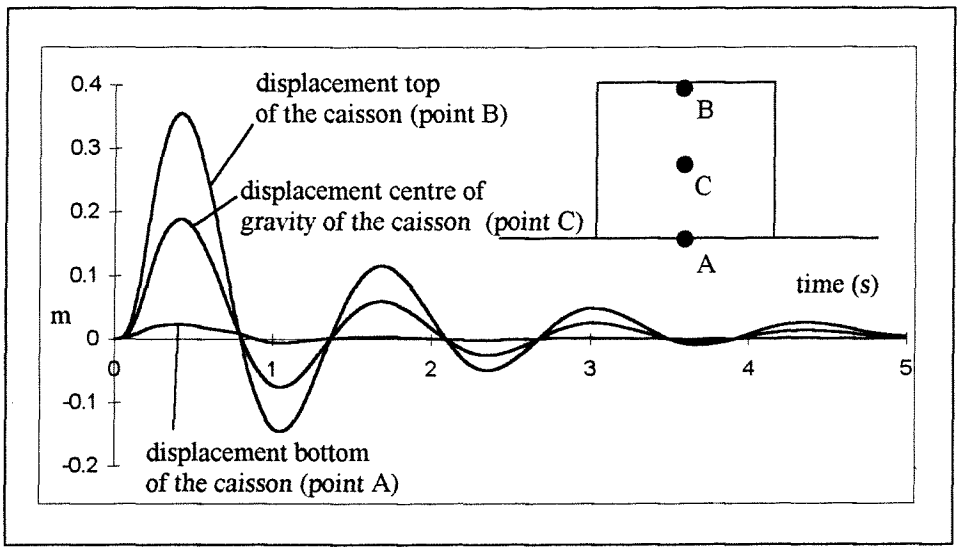

fig. 8.14 Horizontal displacement of different points on the caisson breakwater

As it can be seen in figure 8.14, there is no significant horizontal displacement of the bottom of the vertical breakwater, while figure 8.15 shows that the horizontal spring becomes plastic, the maximum force in spring 6 (91440 kN) is reached within the first second. The fact that there is almost no horizontal displacement of the bottom of the vertical breakwater is due to the fact that a wave impact not only causes a horizontal force but also a moment on the vertical breakwater. Because of this moment the vertical breakwater is forced to rotate. This rotation works against the horizontal translation of the bottom of the vertical breakwater. The net effect is almost no horizontal displacement of the bottom of the vertical breakwater. This effect which is described here is sketched in figure 7.10 and see also figure 8.17.

A better way to look at the horizontal displacement of the vertical breakwater is to look at the horizontal displacement of the centre of gravity, because the rotation of the vertical breakwater does not work against the horizontal translation of the vertical breakwater at that point. It can be seen that there is a significant displacement of the centre of gravity of the structure.

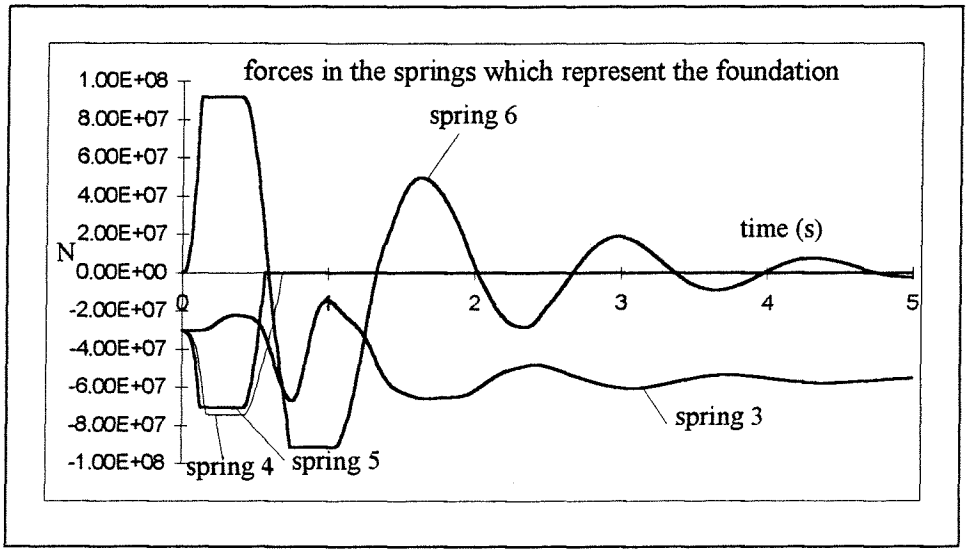

fig. 8.15 Forces in the springs which represent the foundation

In figure 8.15 it can be seen that spring 5 and spring 4 do not bear a load anymore after the first second. The consequence is that the vertical stiffness of the foundation, represented by five vertical springs decreases: some of the springs do not bear a load anymore. The effect of this is that the period of oscillation of the vertical breakwater will increase according to equation 8.34 which describes the period of oscillation of a single degree of freedom mass-spring model:

$$T = 2\pi\sqrt{\frac{m}{k}} \tag{8.34}$$

If k decreases than T increases. This is effect is clearly to be seen if the periods of the horizontal oscillation of the vertical breakwater sketched in figure 8.14 and figure 8.12 are compared.

The reason for this is that the foundation of the vertical breakwater has yielded ("collapsed"). The foundation is permanently displaced at the place of spring 4 and spring 5, as is sketched in figure 8.16. Spring 4 and 5 can only bear a load when the breakwater is loaded again and displaced that much that the bottom of the vertical breakwater has a renewed contact with the foundation soil. In figure 8.15 it can also be seen that spring 3 has to bear more load. This means that the vertical breakwater is permanently displaced downwards. Besides this downward displacement it is also rotated as can be seen in figure 8.14 and figure 8.17.

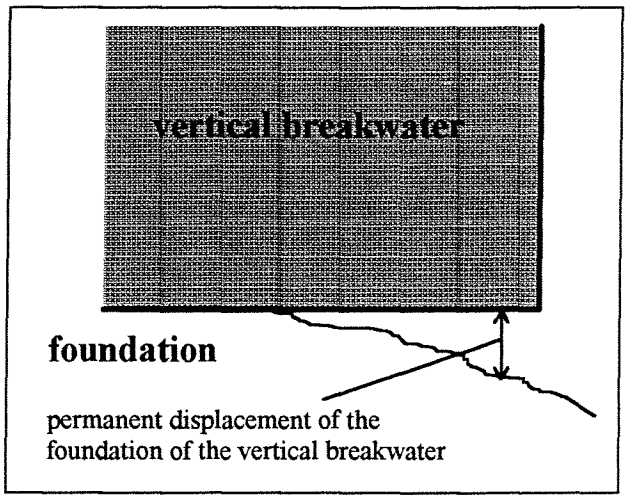

fig. 8.16 Permanent displacement foundation

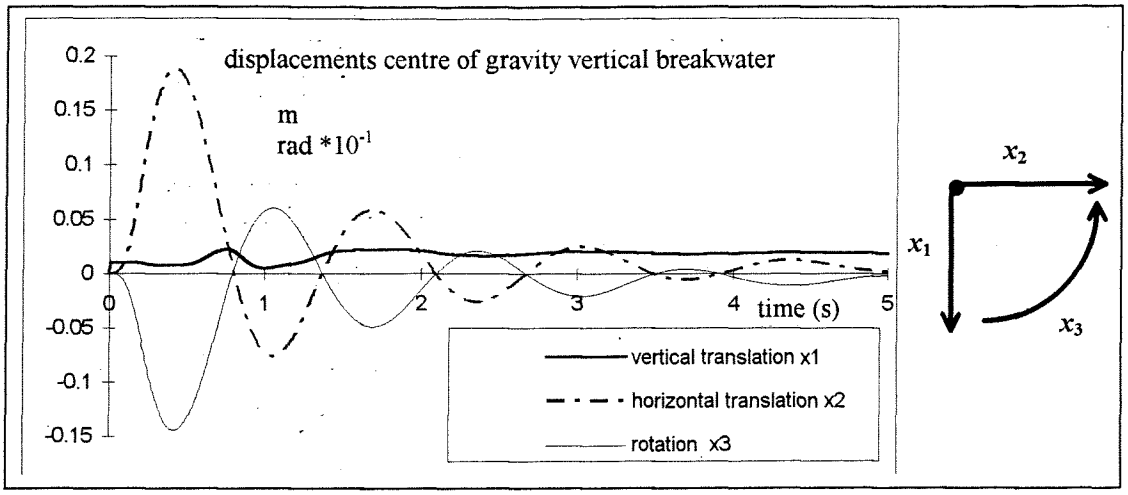

fig. 8.17 Horizontal and vertical translations and rotation of the centre of gravity of the vertical breakwater

The conclusions which have been drawn for this loading case before (described in enclosure 8.4) can be confirmed. According to figure 8.17 there are residual displacements of the centre of gravity of the vertical breakwater. If the wave impact acts on the left vertical front wall of the vertical breakwater there is a horizontal displacement to the right (positive in the direction of x_2) a positive downward displacement (positive in the direction x_1) and a rotation to the right (negative in the direction of x_3) as can be seen in figure 8.17.

Nota bene:

One should bear in mind that the model which is presented in this chapter can give a reliable estimation whether sliding of the vertical breakwater or failure - collapse or yielding - of the foundation of the vertical breakwater will occur. The precise sliding distance of the vertical breakwater and/or permanent displacement in the foundation of the vertical breakwater are very difficult to model. What precisely happens at the contact surface of the bottom slab of the vertical breakwater and the foundation soil during sliding of the breakwater or yielding of the foundation soil of the vertical breakwater is not very well known.

9 Analysis of the structure and foundation parameters of the vertical breakwater

9.1 Introduction

In the previous section the mass-(elasto-plastic)spring-dashpot TILLY model has been derived. In this chapter the effect of the variation of different parameters of that model on its dynamical behaviour will be described.

There are two basic sources of uncertainty when calculations of the dynamical behaviour of a vertical breakwater are being carried out. The first source of uncertainty is the wave impact load on the vertical breakwater. Which characteristics of wave impacts loads are important and which are not. The effect of the type of wave impact loading on the dynamical behaviour of the vertical breakwater and its stability will be treated in chapter 10. The second source is structural model itself, with is most relevant dynamical parameters (mass, stiffness and damping). The effect of the variation of the different parameters of the mass-(elasto-plastic)spring-dashpot model will be described in this chapter

The effect of changing the stiffness of the foundation soil of the vertical breakwater will be treated in section 9.2. The influence of the strength of the foundation soil of the vertical breakwater will be treated in section 9.3. In section 9.4 the effect of the variation of the last parameter concerning the foundation, the damping of the foundation, will be described. The effect of the variation of the masses and the mass moment of inertia of the vertical breakwater on its stability will be treated in section 9.5 by means of a variation of the total lay out of the vertical breakwater.

It is interesting to study the variation of the foundation parameters because of the fact that the foundation aspects are relatively more important with caisson breakwaters than with rubble mound breakwaters. The bearing capacity of the subsoil is often decisive for the dimensions of the caisson where the subsoil consists of clay and loose or even medium dense sand. [MAST II MSC (1995)].

The results of the variation of the parameters of the mass-(elasto-plastic)spring-dashpot model will be checked by comparing these results to the analytical solution of a mass-spring-dashpot model - with only one degree of freedom - which is exposed to a pulse load. A pulse load can, according to chapter 7 and 8, be used to schematise a wave impact. In that way the validity of the mass-(elasto-plastic)spring-dashpot TILLY model which has been derived in the previous chapter can be checked. The analytical solution of a mass-spring-dashpot model - with one degree of freedom - exposed to a pulse load which can schematise a wave impact is shown in figure 9.1.

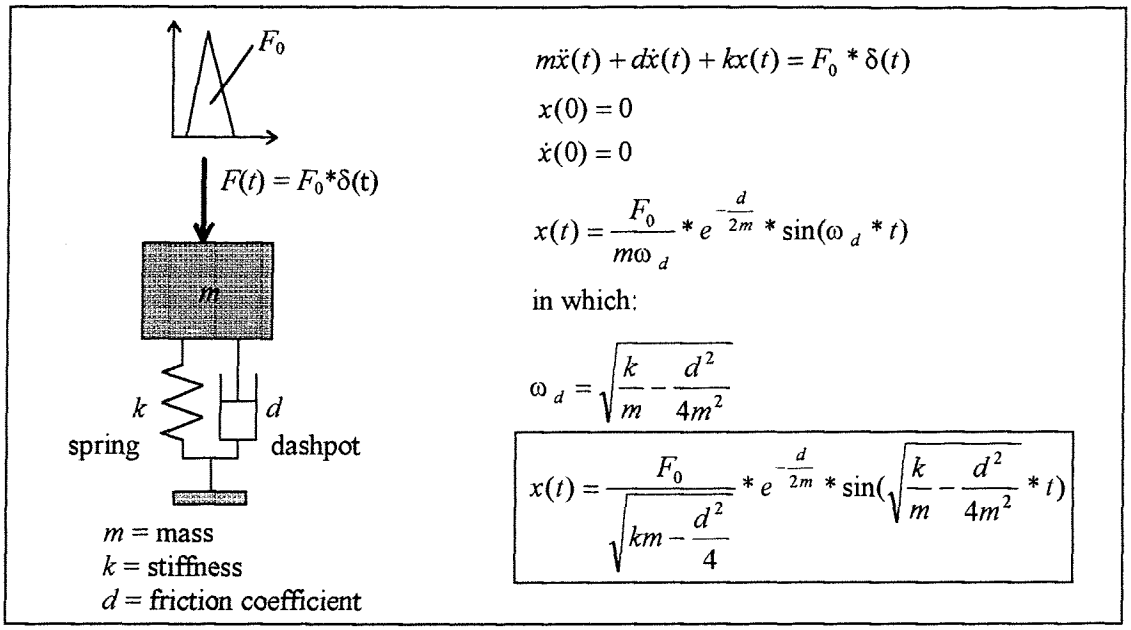

fig. 9.1 Analytical solution of a mass-spring-dashpot model with one degree of freedom exposed to a pulse load

The breakwater lay-out which is used for the analysis of the foundation parameters which is presented in section 9.2 to 9.4 is the same as the one which has been described in chapter 7 and chapter 8 before, see figure 9.2 and 8.11. In these sections will be referred to figure 9.2 repeatedly.

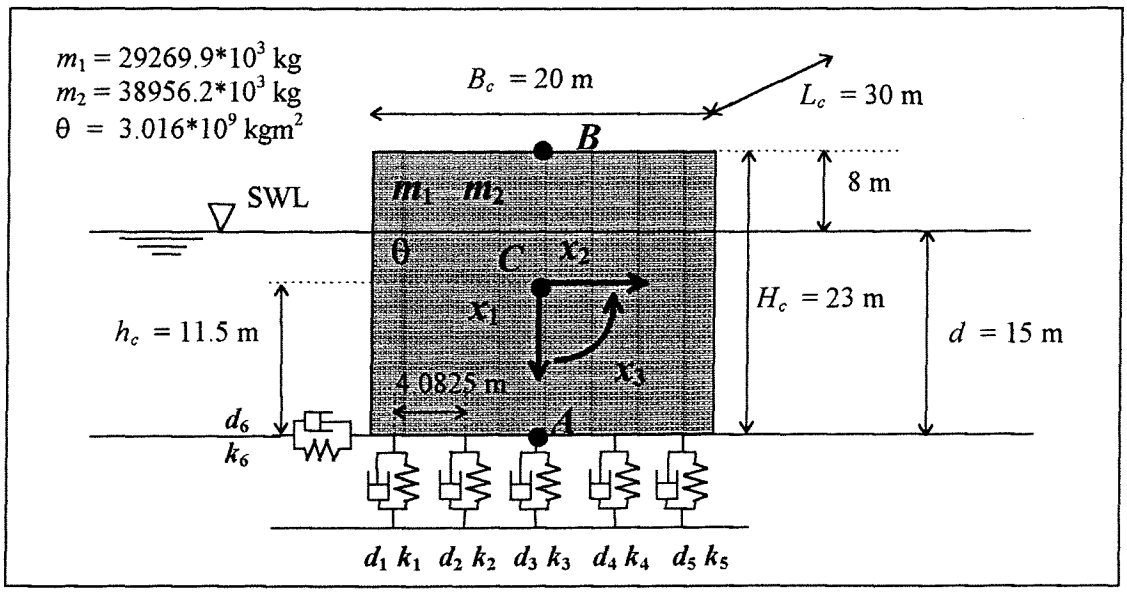

fig. 9.2 Configuration used for the benefit of the analysis in section 9.2, 9.3 and 9.4

The only load on the vertical breakwater which is of relevance for the analysis of the dynamical behaviour of the vertical breakwater, in this chapter as well as in chapter 10, is a horizontal wave impact load. All other loads on the vertical breakwater (the quasi-static wave forces, the buoyancy and the uplift force) are assumed to be constant. They will not influence the dynamical behaviour of the vertical breakwater which is exposed to a wave impact load. The only force of relevance (the wave impact force) is shown in figure 9.3 together with the constant forces (and the weight) which are represented by a dotted arrow. According to Oumeraci et al. [OUMERACI et al. (1994)] neglecting of the quasi-static forces in the calculation of the dynamical behaviour of the vertical breakwater is valid if one is only interested in the maximum response of the vertical breakwater. For reasons of simplicity it is assumed that the uplift force is constant and according to the prediction of the design formulae of Goda which have been treated before in chapter 6. The magnitude of this force has been given in chapter 7 before and has been calculated by assuming an equally distributed uplift pressure with a magnitude of approximately 35 kN/m^2.

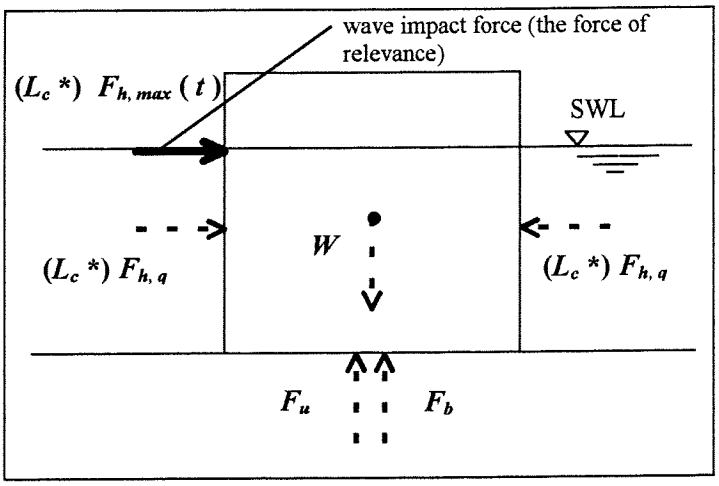

fig. 9.3 Forces on the vertical breakwater

The only failure mechanisms which can - and will - be investigated by the use of the dynamical TILLY model in this chapter and in chapter 10 are sliding of the vertical breakwater over its foundation and failure (collapse or yielding) of the foundation soil. However, this is very usefull because these failure mechanisms are very important ones. Other failure mechanisms which have been presented in chapter 1 are neglected (e.g. slip of the foundation or liquefaction of the foundation soil due to building up of groundwater pressure).

In chapter 8 it has been stated that the Brinch Hansen theory can be used for an estimation of the strength of the foundation soil depending on the frequency of oscillation of the structure. Changing the parameters of the mass-(elasto-plastic)spring-dashpot TILLY model will among other things change the frequency of oscillation of the vertical breakwater. But for reasons of simplicity it will be assumed that the Brinch Hansen theory will be applicable constantly.

Nota bene:

It must be stated that the conclusions which will be drawn in this chapter and in the next chapter are only (directly) valid for the model as it is presented here in this report, within the framework of this study. However, some conclusions are generally applicable

9.2 Variation of the stiffness of the foundation

The influence of the magnitude of the stiffness of the foundation on the dynamical behaviour of the vertical breakwater which is described in figure 9.2 will be investigated in this section. The strength of the foundation soil, the damping in the foundation soil and the masses and mass moment of inertia will not be varied. Thus, the maximum bearing pressure of the foundation soil is 608 kN/m^2 and the damping coefficients d_1 to d_5 are 73.58*10^6 Ns/m and d_6 is 367.9*10^6 Ns/m as has been derived in chapter 8 (see figure 8.11).

Nota bene:

It seems reasonable that a stiff foundation soil will be stronger as well (and the other way around). A stiffer soil may also lead to more damping because of the fact that the elasticity modulus of the foundation soil changes. However, these effects will be neglected in this study, but it is very interesting to do research on this topic: the relation between the strength, stiffness and maximum bearing pressure of the foundation.

All results in this chapter will be derived for the breakwater described in figure 9.2 and which is exposed to a wave impact force with a triangular load history. The quasi-static part is neglected again just as it has been done before in the previous chapters. This wave impact is sketched in figure 9.4 and will not lead to foundation failure or sliding for the mass-(elasto-plastic)spring-dashpot TILLY model which has been described before in chapter 8, figure 8.11 (k_1 to k_5 are 3.0*10^9 N/m and k_6 = 1.5*10^{10} N/m, in the remainder of this section called: "the reference case" or case 1). The wave impact is supposed to act at Still Water Level (SWL).

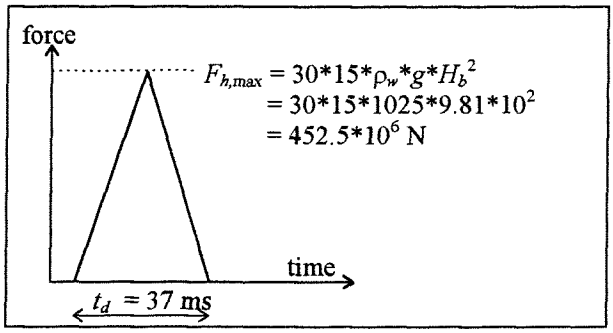

fig. 9.4 Wave impact force on the vertical breakwater

The influence of the stiffness of the springs on the dynamical behaviour will now be investigated for two cases and compared to the reference case (see figure 8.11):

- case 1: the reference case (see figure 8.11):
  k_1, k_2, k_3, k_4 and k_5 : $3.0*10^9$ N/m
  k_6 : $1.5*10^{10}$ N/m

- case 2: the stiffness of the foundation will be halved:
  k_1, k_2, k_3, k_4 and k_5 : $1.5*10^9$ N/m
  k_6 : $0.75*10^{10}$ N/m

- case 3: the stiffness of the foundation will be doubled:
  k_1, k_2, k_3, k_4 and k_5 : $6.0*10^9$ N/m
  k_6 : $3.0*10^{10}$ N/m

The horizontal displacement of the bottom of the vertical breakwater (A, see figure 9.2) for each of the cases is sketched in figure 9.5. The horizontal displacement of the centre of gravity (C, see figure 9.2) of each of the cases is sketched in figure 9.6 and the horizontal displacement of the top of the vertical breakwater (B, see figure 9.2) of each of the cases is sketched in figure 9.7. The forces in spring 1, spring 5 and spring 6 are sketched in figure 9.8 for case1, in figure 9.9 for case 2 and in figure 9.10 for case 3. Spring 1 and spring 5 are the two most eccentric vertical springs and spring 6 is the horizontal spring (see figure 9.2).

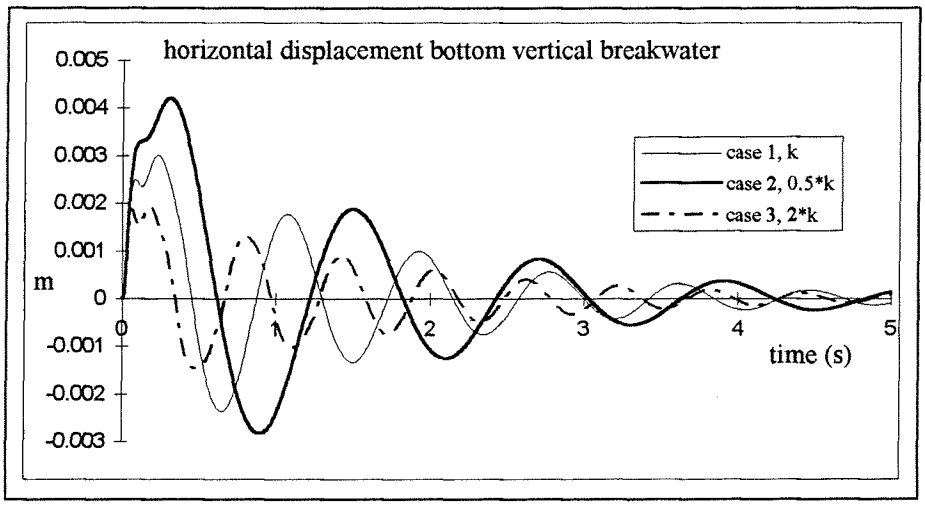

fig. 9.5 Horizontal displacement of the bottom vertical breakwater (A) for three cases

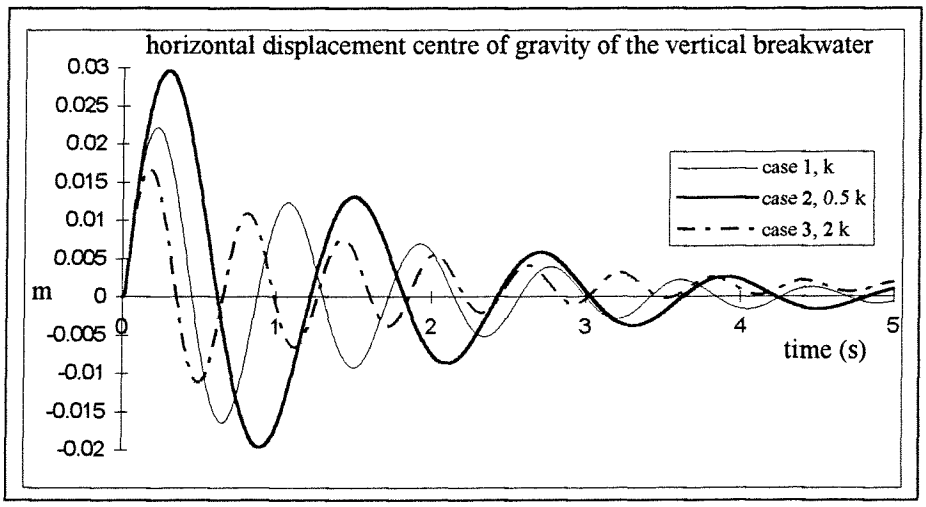

fig. 9.6 Horizontal displacement of the centre of gravity (C) of the vertical breakwater for three cases

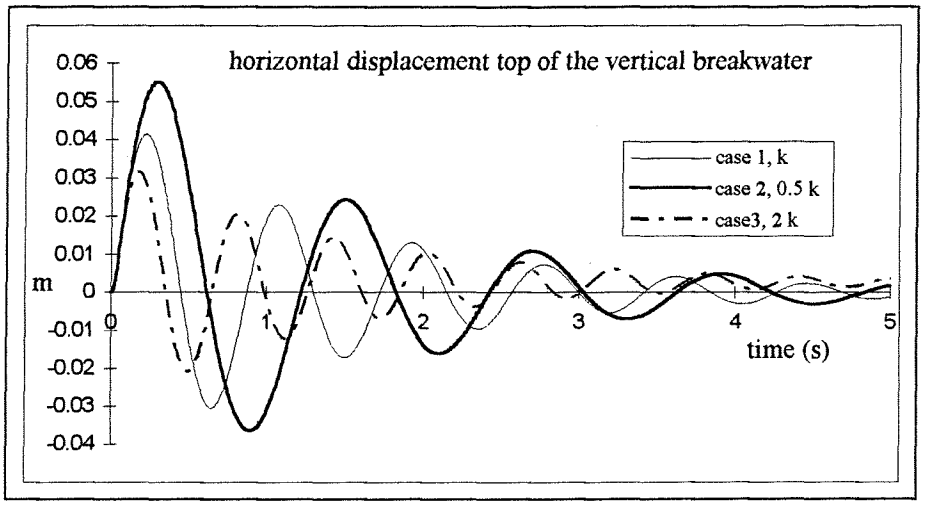

fig. 9.7 Horizontal displacement of the top (B) of the vertical breakwater for three cases

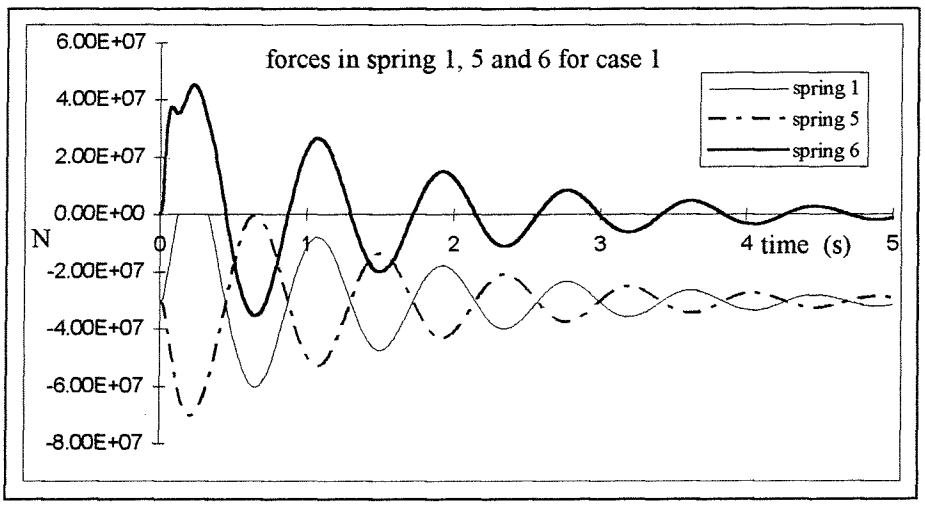

fig. 9.8 Forces in spring 1, 5 and 6 for case 1

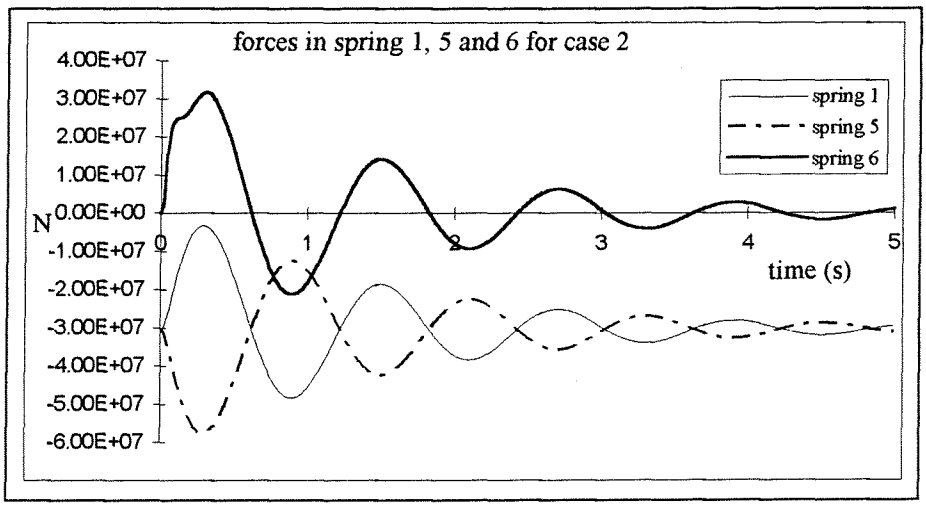

fig. 9.9 Forces in spring 1, 5 and 6 for case 2

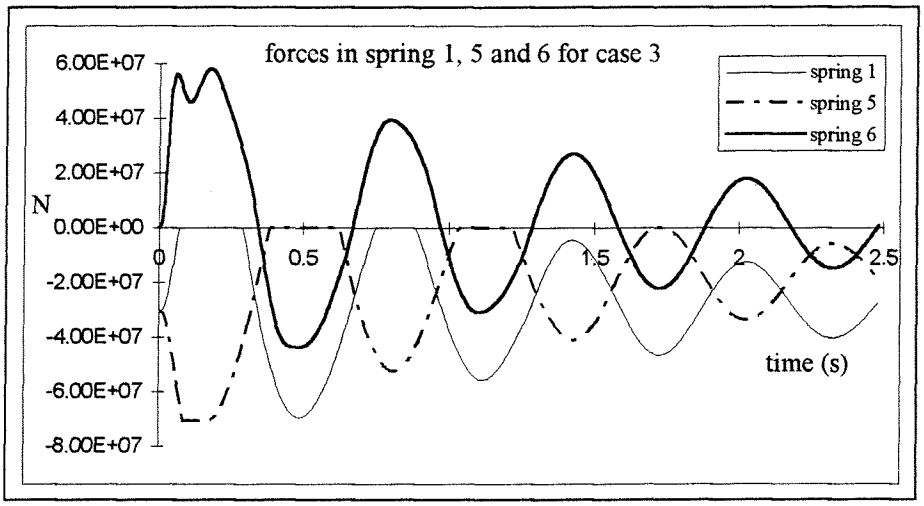

fig. 9.10 Forces in spring 1, 5 and 6 for case 3

Some effects of the change of the stiffness of the foundation will be discussed now. The results of this change of the stiffness of the foundation are presented in figure 9.5 to 9.10. The influence of the stiffness on the period of the horizontal oscillation of different points on the vertical breakwater, the behaviour of the springs which represent the stiffness of the foundation as well as the magnitude of the horizontal displacements of different points (point *A*, *B* and *C*) on the vertical breakwater will be discussed.

Period of horizontal oscillation for case 1, case 2 and case 3

It can be seen from figure 9.5 to 9.7 that the period of the horizontal oscillation of the vertical breakwater changes when the stiffness of the foundation changes while the masses, mass moment of inertia and the damping of the foundation remain constant. The periods of the horizontal oscillations of the different cases are:

- case 1 (reference case): $T = 0.85$ s
- case 2 (halved stiffness): $T = 1.23$ s
- case 3 (doubled stiffness): $T = 0.60$ s

The period of the horizontal oscillation of the vertical breakwater increases if the stiffness of the foundation decreases and the other way around. This is in accordance with the formulae presented in figure 9.1 where ω_d is the radian frequency of the damped eigenoscillation. If the stiffness, k, decreases then ω_d decreases and T increases because $T = 2\pi/\omega_d$.

Behaviour of the springs for case 1, case 2 and case 3

The behaviour of the springs which represent the stiffness of the foundation of the vertical breakwater is shown in figure 9.8 to 9.10. In figure 9.8 the forces in spring 1, spring 5 (the two most eccentric vertical springs, see figure 9.3) and spring 6 (the horizontal spring, see figure 9.2) of case 1, the reference case, are shown. Just as it has been stated before in the introduction, the force which is sketched in figure 9.4 will not lead to foundation failure for the reference case. This is true according to figure 9.8: it can be seen that spring 1 and 5 do not have to bear forces which become less than - 70703.7 kN.

Note that the force spring 1 becomes 0 kN and thus spring 1 will react "plastic" for a short moment (see figure 8.11). However, this will not considered to be foundation failure because the soil is not permanently deformed. When the minimum vertical force in the foundation is reached (-70703.7 kN) the soil is really deformed. It can be seen from figure 9.8 that the forces in the springs return to their initial value which is 0 kN for spring 6 and -30480.0 kN for spring 1 and 5. This confirms the statement that a force of 0 kN in a spring does not mean foundation failure. The fact that the force in spring 1 becomes 0 kN means in fact that the vertical breakwater is not safe against overturning (see equation 7.90). However, this failure mechanism is neglected in the remainder of this study because in can be seen form figure 9.8 that the fact that the force becomes 0 kN in spring 1 has no influence on the characteristics of that spring and the other springs because there is no permanent vertical residual displacement.

From figure 9.9 it can be seen that if the stiffness of the foundation is reduced, the forces in the springs are reduced as well. The minimum force in spring 5 of case 1 (the reference case) is approximately -70000.0 kN while the minimum force in spring 5 of case 2 (the case where the magnitude of the stiffness is halved). is approximately -58000 kN. It is obvious to see from figure 9.9 that none of the springs become plastic.

The opposite is the case for case 3 as can be seen in figure 9.10 (note that - relative to figure 9.8 and 9.9 - the scale of the time axis has been changed). The stiffness of the foundation of case 3 is doubled compared to the reference case. Now the foundation yields, the minimum force of -70703.7 kN is reached. This will lead to permanent displacements (vertical, horizontal and rotational) of the vertical breakwater. The permanent horizontal displacement of the vertical breakwater for case 3 can clearly be seen in figure 9.6 to 9.8, although it is a very small horizontal displacement. Note that because of the fact that spring 5 becomes plastic, the other springs have to bear more load. This will cause a downward displacement and a permanent rotation of the vertical breakwater as well.

The phenomenon that the springs which represent a stiff foundation of a vertical breakwater become plastic while the springs of a foundation with a smaller stiffness are still elastic - when the breakwater is exposed to the same wave impact load - can be explained (see figure 9.11). For this explanation *positive* forces and *positive* extensions are used in contrast to the situation of case 3 where the foundation yields for at the maximum *negative* force at a *negative* extension.

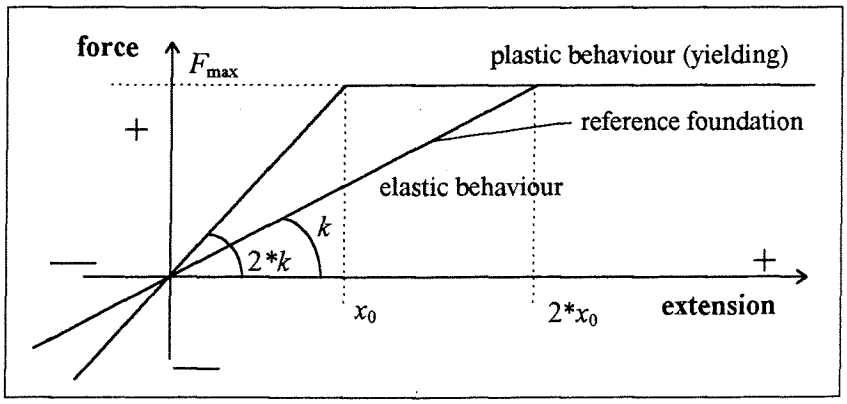

fig. 9.11 Characteristic of an elasto-plastic spring

From figure 9.11 it can be seen that for a reference foundation, with a stiffness k, the maximum extension - before yielding of the foundation soil - is equal to $2*x_0$. The maximum extension before yielding of the foundation soil for a foundation which is twice as stiff as the reference foundation ($2*k$) is x_0. Thus, the foundation of a soil which is twice as stiff as a reference foundation yields at an extension which is twice as twice small as the extension at which the reference foundation would yield.

But, according to the formulae presented in figure 9.1, the displacement of a vertical breakwater which is placed on a stiff foundation also becomes smaller because of the fact that the stiffness is larger. However, this displacement is only reduced by a factor which is proportional to the square root of the stiffness of the foundation, according to equation 9.1. Equation 9.1 denotes the amplitude of the movement of a mass-spring-dashpot model with one degree of freedom which is exposed to a wave impact load represented by F_0.

$$\frac{F_o}{\sqrt{km - \frac{d^2}{4}}} \tag{9.1}$$

Conclusion:
Wave impact loads are the most dangerous for the foundation (and the stability) of a vertical breakwater if the foundation is rather stiff. A stiff foundation of a vertical breakwater is more likely to yield than a foundation of a vertical breakwater with a smaller stiffness, if it is exposed to the same wave impact load (F_0 is equal for both situations) and the other parameters of the model are maintained constant (e.g. the strength of the foundation soil). Even if the reduction of the maximum displacement - because of the fact that magnitude of the stiffness of the foundation is larger - of a vertical breakwater placed on a stiff foundation is taken into account. Thus, it is favourable to have a foundation with a small stiffness, e.g. clay. The disadvantage of such a foundation soil is that it is less strong than a foundation with a large stiffness e.g. sand or gravel and that the vertical breakwater may not be stable against quasi-static wave loading because of the fact that the eigenperiod of oscillation of the vertical breakwater increases if the stiffness decreases.

This phenomenon can also be explained by calculating the maximum load ($F_{0,\,max}$) which is necessary to let the foundation of a vertical breakwater, which is exposed to wave impacts, yield. The maximum load which is necessary to led a foundation with a stiffness k yield is proportional to (see figure 9.11):

$$F_{0,\,max,\,stiffness\ k} \propto 2 * \sqrt{k} * x_0 \tag{9.2}$$

while for a foundation of a vertical breakwater with a stiffness $2*k$ a load with a magnitude proportional to

$$F_{0,\,max,\,stiffness\ 2*k} \propto \sqrt{2*k} * x_0 = \sqrt{2} * \sqrt{k} * x_0 \tag{9.3}$$

is necessary to let the foundation yield. Thus, the load which is needed to let a foundation yield with a stiffness k is larger than the load which is needed to let a foundation yield with a stiffness $2*k$. This fact confirms previous conclusion.

If spring 5 which only represents a part of the foundation of the vertical breakwater becomes plastic, the foundation yields. It is interesting to see from figure 9.10 that the force in spring 5 does not return to its initial value of 30480.0 kN anymore after it has become plastic (after the foundation soil has yielded, compare this case to the cases presented in figure 9.8 and 9.9 where this phenomenon does not occur). This is because of the fact that the negative extension in spring 5 is less in the final situation than in the initial situation because of the fact that due to the yielding of the foundation the soil is - so to say - "pushed away". This phenomenon is sketched in figure 8.16 for an extreme situation where the soil is totally pushed away.

The following could be found in the literature regarding the stiffness of the foundation soil of vertical breakwaters: "Stiff soil often yields the highest sensitivity to wave impacts, because the natural period becomes closer to the impact duration. On the other hand stiff soil is usually much stronger then elastic soil" (see section 9.3) [MAST II MSC (1995)].

Horizontal displacement for case 1, case 2 and case 3

It can be seen from figure 9.5 to 9.7 that the maximum horizontal displacement increases if the stiffness of the foundation decreases. The maximum horizontal displacement of the bottom of the vertical breakwater for the different cases is (see figure 9.5):

- case 1 (reference case): $x_{max} = 3.0$ mm
- case 2 (halved stiffness): $x_{max} = 4.2$ mm
- case 3 (doubled stiffness): $x_{max} = 1.9$ mm

It can be seen in figure 9.6 and 9.7 that the maximum horizontal displacement of the centre of gravity and of the top of the vertical breakwater are approximately a factor 10 in magnitude larger than the maximum horizontal displacement of the bottom of the vertical breakwater. This is caused by the rotation of the vertical breakwater, which reduces the horizontal displacement of the bottom, but enlarges the horizontal displacement of the top of the vertical breakwater.

Not that because of the fact that spring 5 in case 3 has become plastic permanent displacements of the vertical breakwater will occur (horizontal, vertical as well as rotational displacements). as well as the magnitude of the horizontal displacements of different points (point A, B and C) on the vertical breakwater will be discussed.

The fact that a stiffer foundation leads to a smaller horizontal displacement in accordance with the formulae presented in figure 9.1. The horizontal displacement of the vertical breakwater is proportional to:

$$\frac{F_o}{\sqrt{km - \frac{d^2}{4}}} \tag{9.1}$$

So, if the stiffness of the foundation k increases the horizontal displacement decreases.

The last case which will be examined in this section is case 4. In case 4 the horizontal stiffness is halved in relation to the reference case. In literature it is often suggested that the horizontal stiffness may be (much) smaller than the vertical stiffness. The effect of the change in the horizontal stiffness for the mass-(elasto-plastic)spring-dashpot TILLY model of the vertical breakwater as it is presented in this study will be reflected by means of a comparison between the reference case and case 4. The load on the vertical breakwater is sketched in figure 9.4.

- case 1: the reference case (see figure 8.11):
  k_1, k_2 k_3 k_4 and k_5 : $3.0*10^9$ N/m
  k_6 : $1.5*10^{10}$ N/m
- case 4: the horizontal stiffness is halved:
  k_1, k_2 k_3 k_4 and k_5 : $3.0*10^9$ N/m
  k_6 : $0.75*10^{10}$ N/m

The horizontal displacement of the bottom (A), the centre of gravity (C) and the top (B) of the vertical breakwater is shown in figure 9.12, 9.13 and 9.14 respectively. The forces in spring 1, spring 5 and spring 6 for case 4 are presented in figure 9.15.

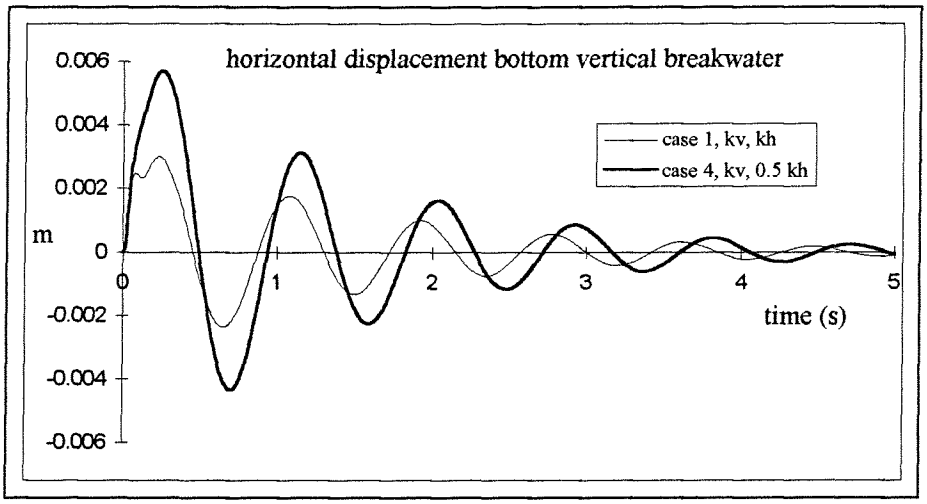

fig. 9.12 Horizontal displacement of the bottom of the vertical breakwater (A)

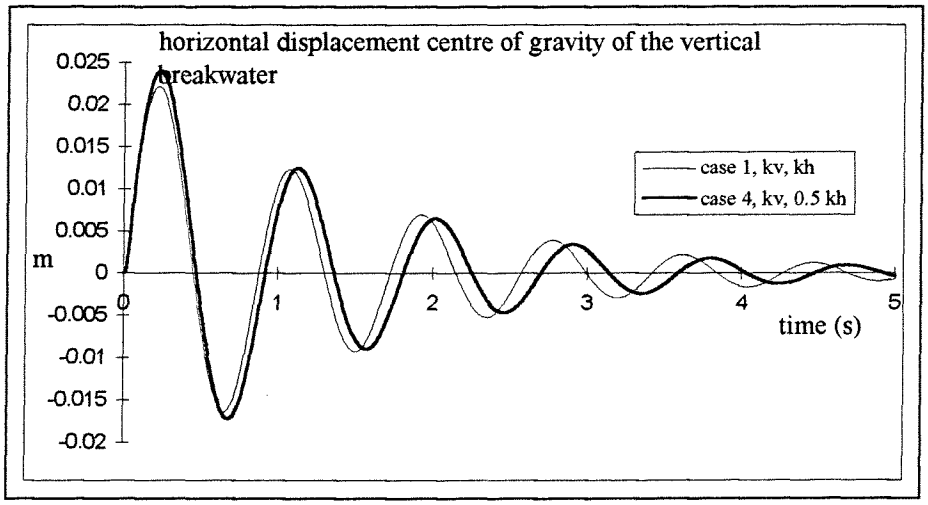

fig. 9.13 Horizontal displacement of the centre of gravity (C) of the vertical breakwater

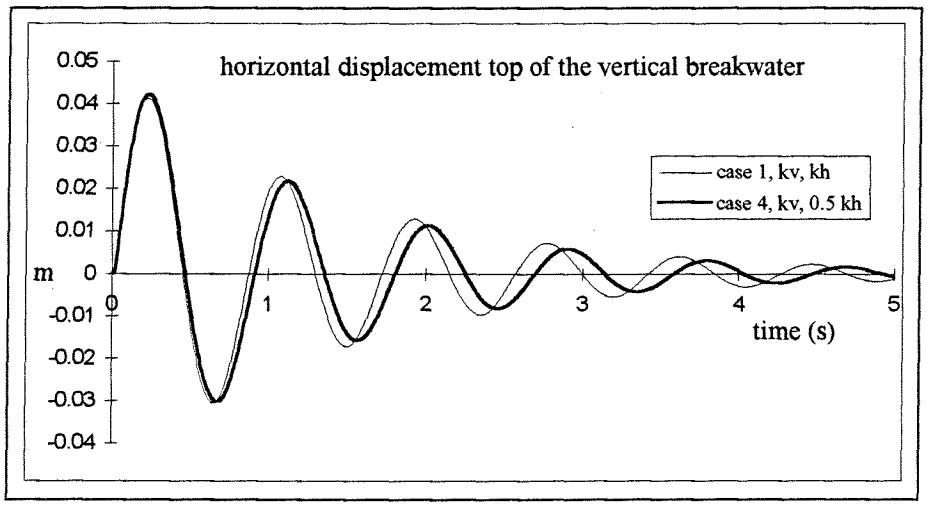

fig. 9.14 Horizontal displacement of the top (*B*) of the vertical breakwater

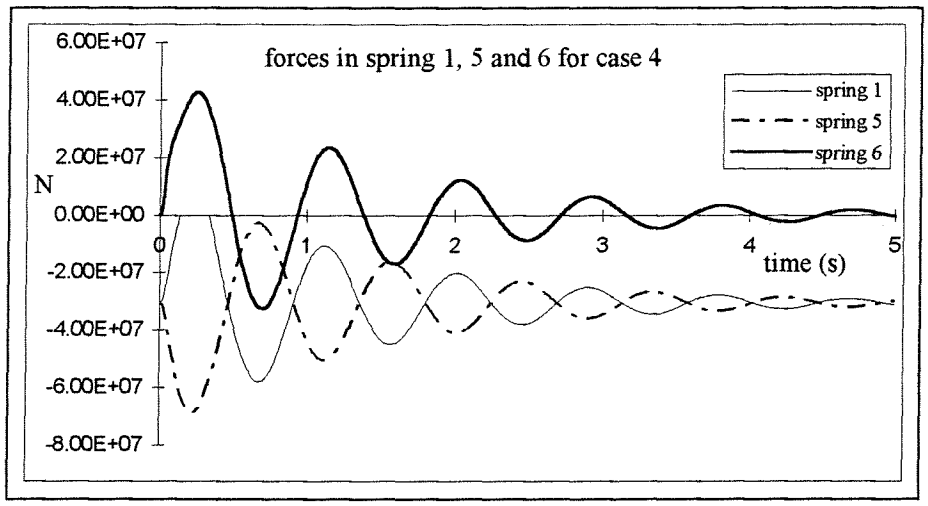

fig. 9.15 Forces in spring 1, 5 and 6 for case 4

From figure 9.12 to 9.13 it can be seen that the influence of the horizontal stiffness on the horizontal displacement of the vertical breakwater is relatively large for the horizontal displacement of the bottom of the vertical breakwater but negligible for the horizontal displacement of the centre of gravity and the top of the vertical breakwater.

As is to be expected the period of the horizontal oscillation increases if the stiffness of the horizontal spring decreases.

Horizontal springs with a small stiffness can withstand lager forces before they become plastic compared to horizontal springs with a large stiffness as has been shown in this section before. So case 4 makes the vertical breakwater safer against sliding compared to the reference case because the horizontal stiffness is smaller and therefore a larger load is necessary to provoke breakwater sliding.

Nota bene:

It must be stated that in this section - and in the remainder of this chapter - only a few relevant parameter studies are being carried out. Of course, it is possible to vary all individual springs, dampers etc. individually but that is beyond the scope of this study.

9.3 Variation of the strength of the foundation

Previous deterministic and probabilistic studies of the effect of quasi-static wave loads on vertical breakwaters have shown that failure of the foundation (yielding of the foundation soil) is the most important an most probable failure mechanism for vertical breakwaters with a conventional rectangular shape [HAILE (1996)]. Sliding of vertical breakwaters is only dominant in the case of vertical breakwaters with a large ratio of width / height. In figure 9.10 it can be seen that - within the framework of that given analysis - this conclusion can be confirmed for wave impacts as well. Reference is being made to chapter 10 where this conclusion will be treated more extensively.

However, this conclusion can change if other parameters of the model are changed (see section 9.5) or for instance if the strength of the foundation soil is varied. If the strength of the soil of the foundation is very high or, the other way around, if the Coulomb friction coefficient is smaller in magnitude than expected, sliding of the caisson may be more probable than failure (collapse or yielding) of the foundation.

In this study the strength of the foundation has been determined using the theory of Brinch Hansen. The calculated strength is dependent on the angle of internal friction of the foundation soil. One of the governing factors in the determination of the strength of the foundation soil is the dimensionless factor N_γ which changes dramatically with the angle of internal friction of the foundation soil. A large angle of internal friction means a large strength of the foundation soil. In sub-section 8.3.1 it was found that the strength of the chosen foundation soil in this study with an angle of internal friction of 33° is 608 kN/m^2, while for an angle of internal friction of 35° the strength of the soil can be as high as 1022 kN/m^2.

Just as has been said in the previous section, there will be a relation between the strength of the foundation soil and the stiffness.

Recapitulating: it is to be expected that there is a large influence of the strength of the foundation soil and the magnitude of the Coulomb friction coefficient on the conclusions which can be drawn. In the remainder of this study, the following values will still be used:

- maximum bearing pressure of the foundation soil: 608 kN/m^2
- magnitude of the Coulomb friction coefficient (μ): 0.6

Within the framework of MAST the following could be found; "A low value of the friction angle between caisson bottom and the gravel or rubble or bedding layer or mound, may bring about the risk of sliding of the caisson over this layer. A reliable prediction of this angle may be essential. The quantification is not yet clear. The favourable effect of a rough caisson bottom or ribs cannot yet be quantified" [MAST II MSC (1995)].

9.4 Variation of the damping of the foundation

In this section the magnitude of the damping of the foundation of the vertical breakwater will be varied. It has been shown that the damping values obtained from experimental results exhibit a considerable scatter [OUMERACI et al. (1992a)]. In order to assess the effect of this scatter on the results of the computations of the dynamical behaviour of the vertical breakwater, three different cases have been investigated:

- case 1: the reference case (see figure 8.11):
  d_1, d_2, d_3, d_4 and d_5 : $73.58*10^6$ Ns/m
  d_6 : $367.9*10^6$ Ns/m

- case 5: the damping of the foundation will be halved:
  d_1, d_2, d_3, d_4 and d_5 : $36.79*10^6$ Ns/m
  d_6 : $183.95*10^6$ Ns/m

- case 6: the damping of the foundation will be doubled:
  d_1, d_2, d_3, d_4 and d_5 : $147.16*10^6$ Ns/m
  d_6 : $735.80*10^6$ Ns/m

The breakwater will be exposed to the wave impact load which has been sketched in figure 9.4.

The stiffnesses of the springs and the strength of the foundation will not be varied and these values are according to the values reflected in figure 8.11. Thus, the maximum bearing pressure of the foundation soil is 608 kN/m^2 and the stiffnesses of the springs k_1 to k_5 is $3.0*10^9$ N/m and the stiffness of spring k_6 is $1.5*10^{10}$ N/m as has been derived in chapter 8 (see figure 8.11).

The influence of the magnitude of the friction coefficients on the horizontal displacement of the vertical breakwater is shown for the bottom of the vertical breakwater (point A, see figure 9.2) in figure 9.16, for the centre of gravity (C) in figure 9.17 and for the top (B) of the caisson in figure 9.18. In each figure, case 5 and case 6 are compared to the reference case, case 1

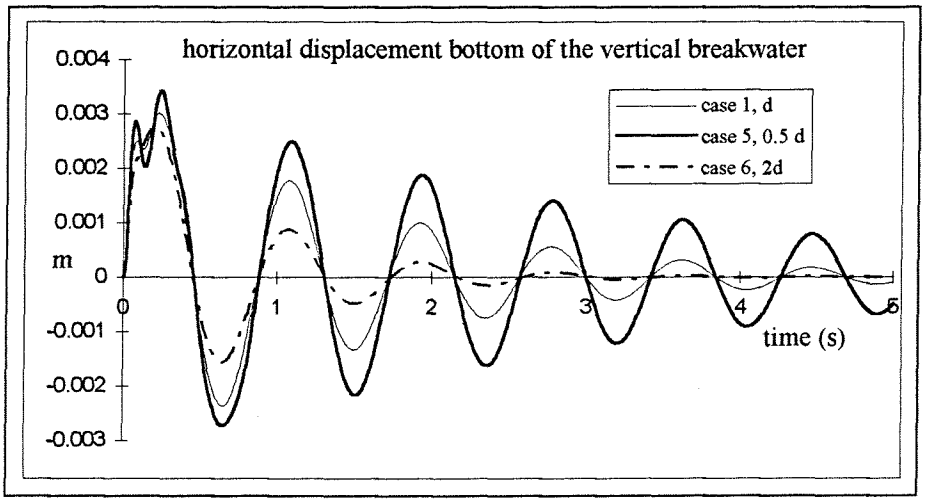

fig. 9.16 Horizontal displacement of the bottom of the vertical breakwater (A)

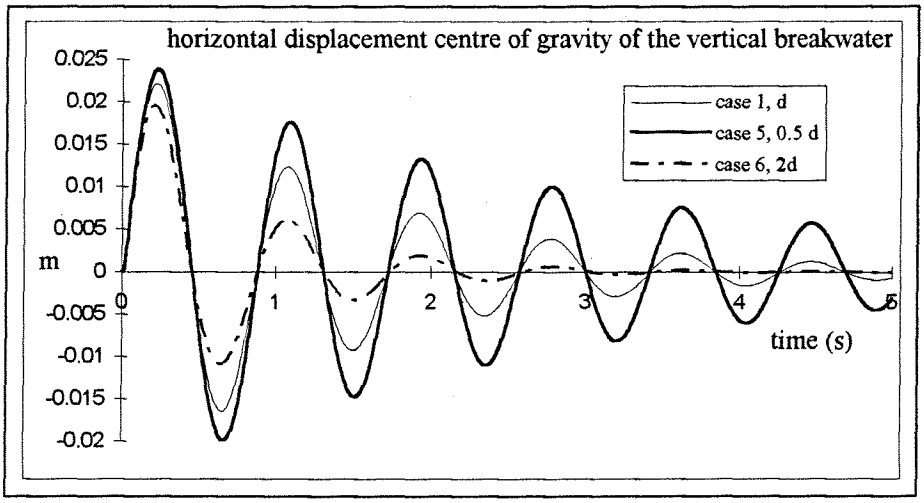

fig. 9.17 Horizontal displacement centre of gravity (C) of the vertical breakwater

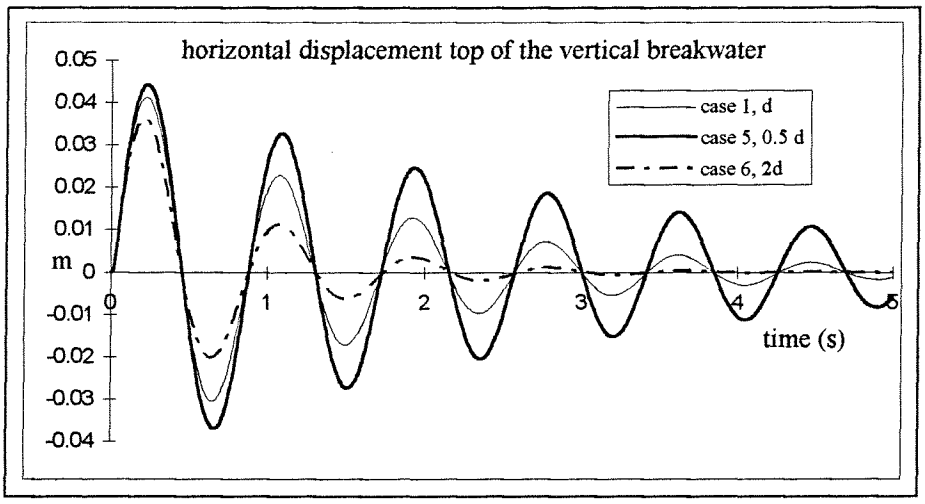

fig. 9.18 Horizontal displacement top (B) of the vertical breakwater

The results of the computations are shown in figure 9.16 to 9.18. The conclusion found by Oumeraci et al. [OUMERACI et al. (1994)]: "As is to be expected, the period of the oscillations and the maximum amplitude of the response of the first cycle are almost not affected by the variation of the damping terms d" is confirmed by the computations carried out in this section.

As can be seen from fig 9.16 to 9.18 large variations of the damping of the foundation of the vertical breakwater have much less influence on the maximum horizontal displacement of the vertical breakwater than large variations of the stiffness of the foundation. The maximum displacements do not differ that much from case to case as could be found in figure 9.5 to 9.7 for the variation of the stiffness of the foundation from case to case, see table 9.1.

	maximum horizontal displacement bottom of the vertical breakwater for variation of the stiffness (see figure 9.5)		**maximum horizontal displacement bottom of the vertical breakwater for variation of the damping (see figure 9.16)**
case 1: reference case *k*	3.0 mm	**case 1: reference case *d***	3.0 mm
case 2: 0.5*k	4.2 mm	**case 2: 0.5*d**	3.4 mm
case 3: 2*k	1.9 mm	**case 3: 2*d**	2.7 mm
ratio: case 2 / case 3	2.21	**ratio: case 5 / case 6**	1.26

table 9.1 Comparison maximum horizontal displacements for variation of the stiffness and damping

On the other hand, the damping strongly affects the magnitude of the amplitude of the oscillations after the first cycle. This is according to the formulae presented in figure 9.1. See equation 9.4 which represents the amplitude of a mass-spring-dashpot model with one degree of freedom which is exposed to a wave impact:

$$\frac{F_0}{\sqrt{km - \frac{d^2}{4}}} * e^{-\frac{d}{2m}} \tag{9.4}$$

If the magnitude of the friction coefficients increases (the damping d increases) than the amplitude of the (horizontal) movement of the breakwater decreases: the two factors of which equation 9.4 consists do both decrease.

Because of the fact that the damping has only got a minor influence on the maximum displacement of the bottom of the vertical breakwater, the effect of the variation of the damping will not be investigated as intensively as the effect variation of the stiffness of the foundation has been done.

Note that the springs do not become plastic in the reference case. The displacements of the vertical breakwater - horizontal, as shown in figure 9.16 to 9.18 but also vertical - for case 5 are somewhat larger than for the reference case. This means that spring 5 of case 5 will become plastic for a short moment. But as can be seen in figure 9.16 to 9.18 this does not cause any significant residual horizontal displacement of the vertical breakwater.

9.5 Variation of the masses and mass moment of inertia of the vertical breakwater

The effect of the variation of the mass and mass moment of inertia of the vertical breakwater will be studied by means of a variation of the total lay-out of the vertical breakwater as can be seen in figure 9.19. Note that this is the only section of the report in which the lay out of the (chosen) vertical breakwater will be changed. All other calculations in the report will be done for the lay out of the reference case, case 1, described among other things in figure 8.11 and 9.19.

The reference case is case 1 and the breakwater with the different geometry is case 7. The breakwater of case 7 is considered to be a vertical composite breakwater: a vertical wall breakwater (a caisson) placed on a rubble mound. The ratio height / width is chosen the same for both cases. So the width of the caisson of case 7 is: (16/23)*20 $\approx$ 14 m.

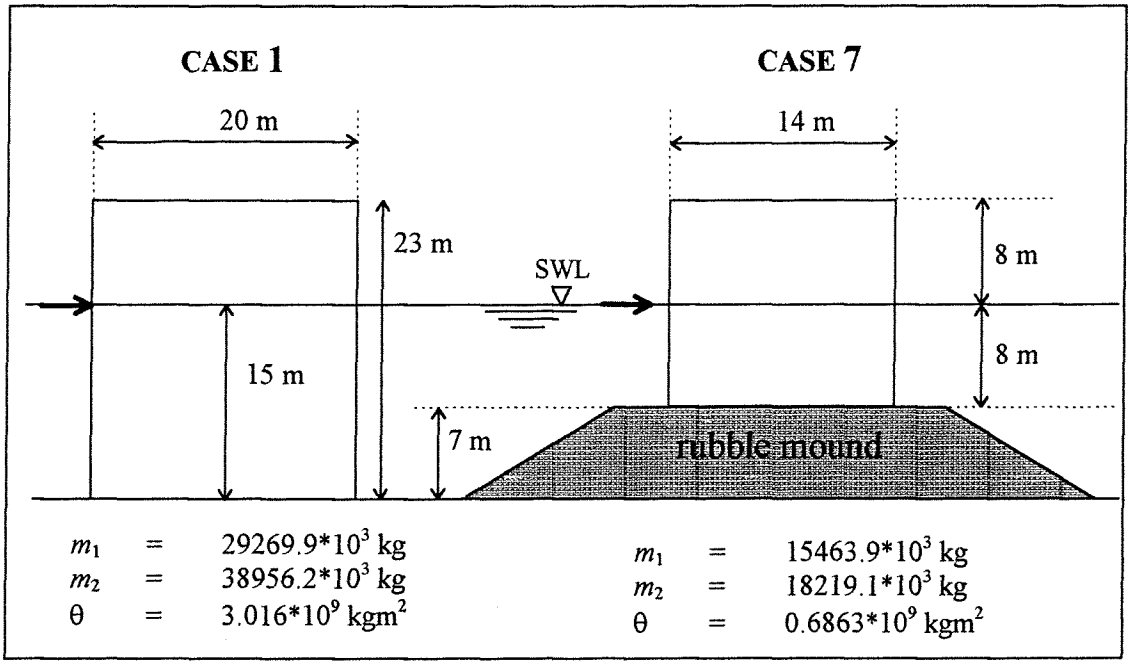

fig. 9.19 Lay-out vertical breakwater case 1 and case 7

The masses and mass moment of inertia of the vertical breakwater of case 1 are according to the values which are presented in figure 8.11 or 9.2. The masses and mass moment of inertia of case 7 have to be determined now:

m_{cai} = 30*14*16*1950 = 13104.0*10^{3}kg (see equation 7.11)
$m_{hyd,\ hor}$ = 30*1.4*1025*8^2 = 2755.2*10^3 kg (see equation 7.13)
$m_{hyd,\ ver}$ = 0 kg (see equation 7.14)
$m_{geo,\ hor}$ = 2359.9*10^3 kg (see equation 7.15)
$m_{geo,\ ver}$ = 2359.9*10^3 kg (see equation 7.15)

m_1 = 13104*10^3 + 2359.9*10^3 = 15463.9*10^3 kg (see equation 7.16)
m_2 = 13104*10^3 + 2755.2*10^3 + 2359.9*10^3 = 18219.1*10^3 kg (see equation 7.17)
θ = $^1/_{12}$ *18219.1*10^3*(14^2+16^2) = 0.6863*10^9 kg (see equation 7.20)

The stiffness and the damping of the foundation soil are the same for each case and according to figure 8.11. In fact the stiffnesses of the springs and the magnitude of the damping is dependent on the surface of the bottom slab of each individual caisson as has been derived in chapter 7. But for reasons of comparison it is assumed that the stiffness and the damping of the foundation soil are maintained constant for both cases in order to assess the effect of the variation of the masses and mass moment of inertia of a vertical breakwater more clearly.

The strength of the horizontal springs is assumed to be the same for both cases as well. According to the theory of Brinch Hansen, which has been used before to calculate the strength of the foundation soil, the strength of the foundation soil of case 7 can be different from the reference case because the strength of the foundation soil is dependent on the surface of the bottom slab of the vertical breakwater. However this effect is neglected here. Because of the fact that the weight of the vertical breakwater of case 7 is much smaller than the weight of the vertical breakwater of case 1, a smaller force is needed to provoke breakwater sliding. If the same uplift pressure is assumed for both cases ($\approx$35 kN/m^2) than the normal force on the foundation for case 7 is equal to (see equation 7.88)

$$F_n = 13104.0*10^3*9.81-8*14*30*1025*9.81-3.5*14*30*1025*9.81 = 79.98*10^6 \text{ N}$$

If the Coulomb friction coefficient is $\mu = 0.6$ than the maximum and minimum force in spring 6 are:

$$F_{spring\ 6,\ max,\ min} = 0.6 * 79.98*10^6 = \pm 47.99*10^6 \text{ N}$$

A berm with a large width will significantly change the height of the breaking waves against the vertical wall. The rubble mound of case 7 is considered to be narrow. It is assumed that it does not change the breaking conditions of waves on the vertical front wall of the breakwater compared to case 1. So it is assumed that the same wave impact load acts on the two breakwaters sketched in figure 9.19. This wave impact load is sketched in figure 9.20 and is the same wave impact as the one which has been shown before in figure 9.4.

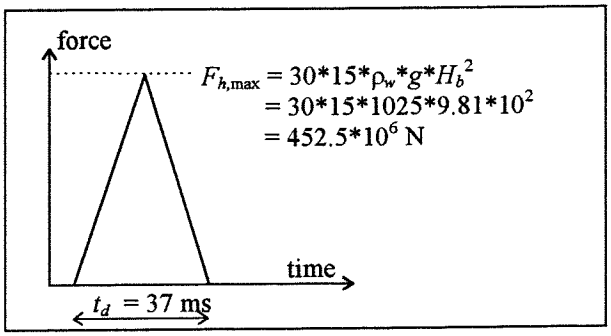

fig. 9.20 Wave impact force on the vertical breakwater

The wave impact, described in figure 9.20 is assumed to act on Still Water Level (SWL) The wave impact acts different on the two breakwaters relative to their centre of gravity because of the fact that the lay-out of the two breakwaters is different. The wave impact acts 3.5 m eccentric relative to the centre of gravity for case 1 and 0 m eccentric relative to the centre of gravity for case 7 because the centre of gravity is exactly placed at Still Water Level for case 7. It is assumed that the mass of the vertical breakwater is equally distributed over its height, length and width just as it has been said before in chapter 7.

Now all input parameters are known for case 7. In figure 9.21 the displacements of the centre of gravity of the vertical breakwater of case 7 are shown. Some results of the calculations of case 1 can be found in figure 9.5 to 9.8.

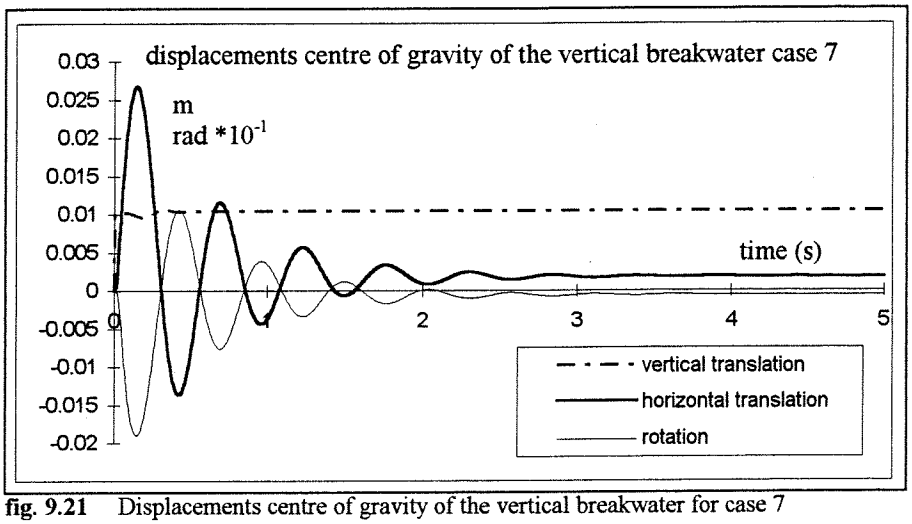

fig. 9.21 Displacements centre of gravity of the vertical breakwater for case 7

As it can be seen in figure 9.21 the vertical breakwater slides. There is a residual horizontal displacement of several mm. The breakwater slides to the right if the wave impact acts on the left vertical front wall of the breakwater (see figure 9.19). From this it can be concluded that it is unfavourable for the stability of a vertical breakwater to have a small mass. The displacements of a vertical breakwater will be larger for a "light" caisson than for a "heavy" caisson with a rectangular cross-section which are both exposed to the same wave impact. This conclusion can be confirmed by the formulae given in figure 9.1. The maximum displacement of a vertical breakwater exposed to a wave impact is proportional to:

$$\frac{F_o}{\sqrt{km - \frac{d^2}{4}}} \tag{9.1}$$

If the mass m increases, than the maximum displacement of the vertical breakwater decreases if all other parameters remain constant. This can also be found in figure 9.6 and figure 9.21. The maximum horizontal displacement of the centre of gravity for case 1, the "heavy" caisson, is 22 mm, while the maximum horizontal displacement of the centre of gravity of case 7, the "light" caisson is 27 mm. It can be concluded that the heavier the caisson, the safer the caisson is against sliding, so it is favourable for the stability of a vertical breakwater to have a large mass.

This conclusion is only valid if the breakwater of case 1 and case 7 are exposed to the same wave impact load. Thus, it is unwise to design a breakwater with a high rubble mound with a small width and a small caisson - with a relatively small mass - placed on it because this breakwater will be exposed to the same wave impact load as a large vertical breakwater of the caisson type which is placed on a small berm. If a rubble mound with a large width is made than probably waves with a smaller height will break against the vertical front wall because of the fact that the water depth is significantly reduced in front of the vertical breakwater and waves might have been broken before they reach the vertical front wall of the breakwater. It is part of an economical analysis to choose the best design alternative (a large rubble mound can be expensive!).

A large mass of the vertical breakwater is favourable for its stability. However, a vertical breakwater with a larger mass will cause higher initial pressures in the foundation soil if the dimensions of a vertical breakwater are fixed. This is unfavourable. Thus, a larger mass of a vertical breakwater should be combined with larger dimensions: a larger width B_c for example. Note that a larger width will also cause an increase in the stiffness of the foundation according to the formulae presented in chapter 7, if an individual caisson has got a fixed length L_c.

In figure 9.6 and 9.21 it can also be seen that if the mass of the vertical breakwater decreases, the period of the oscillation decreases as well. This is in accordance with the formulae presented in figure 9.1 where ω_d is the radian frequency of the damped eigenoscillation. If the mass, m, decreases then ω_d increases and T decreases because $T = 2\pi/\omega_d$. In figure 9.22 the forces in the springs are shown for case 7.

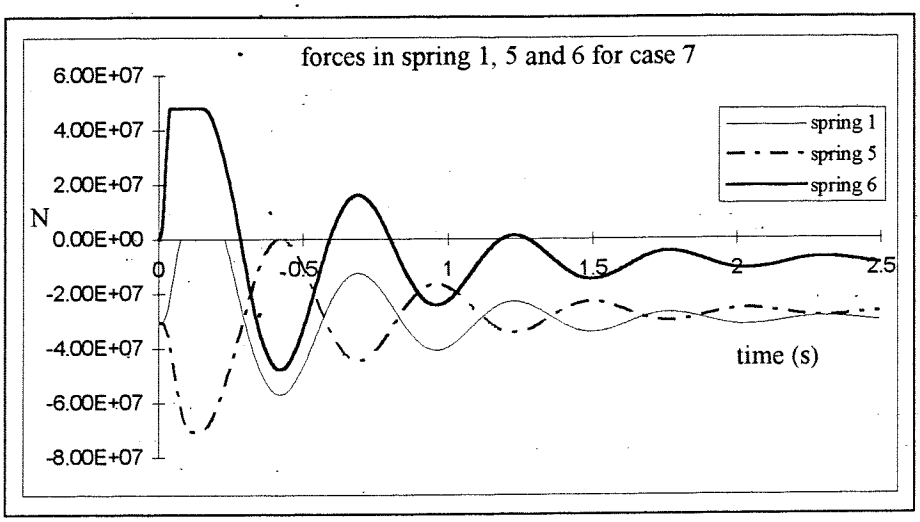

fig. 9.22 Forces in spring 1, 5 and 6 for case 7

It can be seen from figure 9.22 that in this case sliding is detrimental for the stability of the vertical breakwater. Firstly the horizontal spring becomes plastic while secondly vertical spring 5 becomes plastic, in other words: the breakwater slides before the foundation yields. This confirms what has been said before in section 9.3: changing the parameters of mass-(elasto-plastic)spring-dashpot model might as well change the conclusion which vertical breakwater failure mechanism is the most probable one. In figure 9.10 could be found that for that case yielding of the foundation was the most detrimental failure mechanism. In chapter 10 it this conclusion will be found as well for the vertical breakwater described in figure 8.11 (case 1).

The following could be found in the literature about the influence of the magnitude of the added mass, the geo-dynamic and the hydro-dynamic mass: "Depending on the motions of the structure and the nature of the foundation soil, the geo-dynamic mass and the hydro-dynamic mass may reach values of more than 5% and 50% of the mass of the oscillating structure, respectively. Not properly accounting for these added masses will introduce some mistakes in the period as well as in the amplitude of the oscillations. In this respect it has already been pointed out by Oumeraci et al. [OUMERACI et al. (1992a)] that neglecting the geo-dynamic mass and the hydro-dynamic mass would result in a decrease up to 10% and 25% of the natural period of oscillation respectively" [OUMERACI et al. (1994)].

Nota bene:

In this chapter different parameters of the mass-(elasto-plastic)spring-dashpot model have been varied. In order to assess the effect of the variation of each parameter all other parameters have been maintained constant. In this way it has been possible to properly indicate the influence of the different parameters on the stability and the dynamical behaviour of a vertical breakwater exposed to wave impacts. However, it is assumed that the initial values of the different parameters of the mass-(elasto-plastic)spring-dashpot TILLY model belonging to case 1 and described in figure 8.11 are the correct values. All calculations in the next chapter will be carried out for this model. Different conclusions which have been presented in this chapter, concerning the parameter variation of the mass-(elasto-plastic)spring-dashpot model of a vertical breakwater, are summarised in chapter 11 as well.

C

Analysis of different types of wave impact loads on a vertical breakwater and conclusions

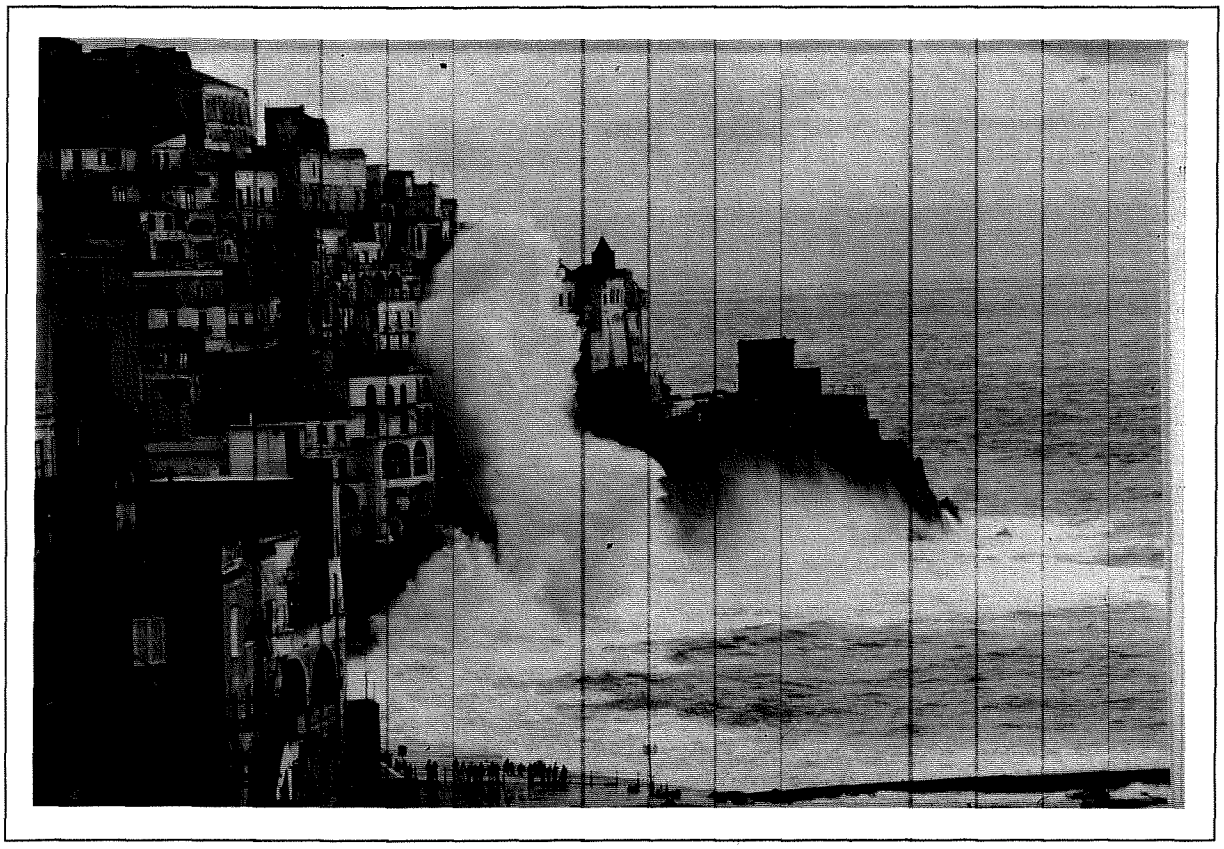

Naples (Italy), 11th of January 1987, H = 7 m

10 Analysis of different types of wave impact loads on a vertical breakwater

10.1 Introduction

The TILLY model which has been derived in chapter 8 can be used to analyse the effect of the variation of the magnitude of different parameters which are related to the dynamical behaviour of a vertical breakwater which is exposed to wave impacts. In the previous chapter the effect of the variation of the parameters related to the mass-(elasto-plastic)spring-dahpot TILLY model itself has been investigated. In this chapter the characteristics of a wave impact load on a vertical breakwater will be varied in order to determine the effect of wave impacts. Which wave impacts are important and which are not for the stability of the investigated vertical breakwater? In this chapter it is tried to find an answer to this question.

All calculations of the effects of different types of wave impacts on a vertical breakwater will be carried out for the vertical breakwater of which the mass-(elasto-plastic)spring-dashpot model has been derived in chapter 8. A summary of this dynamical model of the vertical breakwater can be found in figure 8.11 on page 8-18 but is reflected here as well in figure 10.1.

The effect of the variation of the magnitude of the different parameters of the model - which has been described in the previous chapter - has to be kept in mind when the effect of different types of wave impacts on the stability of the vertical breakwater is examined. The magnitude of the different parameters of the model of the vertical breakwater is chosen fixed in this chapter, see figure 10.1. All conclusions which will be drawn in this chapter are directly valid for the chosen model. However, it must be stated that some conclusions are generally applicable. The chosen magnitude of the parameters seem to represent a very reasonable estimation of the real values in nature. However, conclusion might dramatically change if the governing parameters of the model are changed (e.g. the masses and mass moment of inertia or the stiffness of the foundation).

The following will be treated in this chapter:

- In section 10.2 the effect of a variation of the position of the point where the resultant of the wave impact pressures acts on the vertical front wall of the breakwater.
- An analysis of the formula of Schmidt et al. [SCHMIDT et al. (1992)] in section 10.3. This formula can among other thing be found in section 4.3 equation 4.21. It will be shown that the duration of a wave impact is very important. Failure of the breakwater (foundation failure) can occur if the duration of a single peak wave impact (a wave impact of the transition type, see chapter 2) is in the range of the eigenperiods of the vertical breakwater.
- In section 10.4 an analysis of the formulae of which the derivation has been presented in chapter 4 can be found. In that chapter horizontal wave impact force prediction formulae have been derived using a consideration of momentum of a breaking wave.
- A comparison between the effect of a single peaked wave impact force (due to a wave impact with almost no trapped air) and a double peaked wave impact force (due to a wave impact with a large trapped air pocket) will be given in section 10.5.
- In section 10.6 the effect of wave impacts with low frequency force oscillations will be described. These low frequency force oscillations originate from pulsating air pockets of a well developed plunging breaker on a vertical wall which encloses a large air pocket.

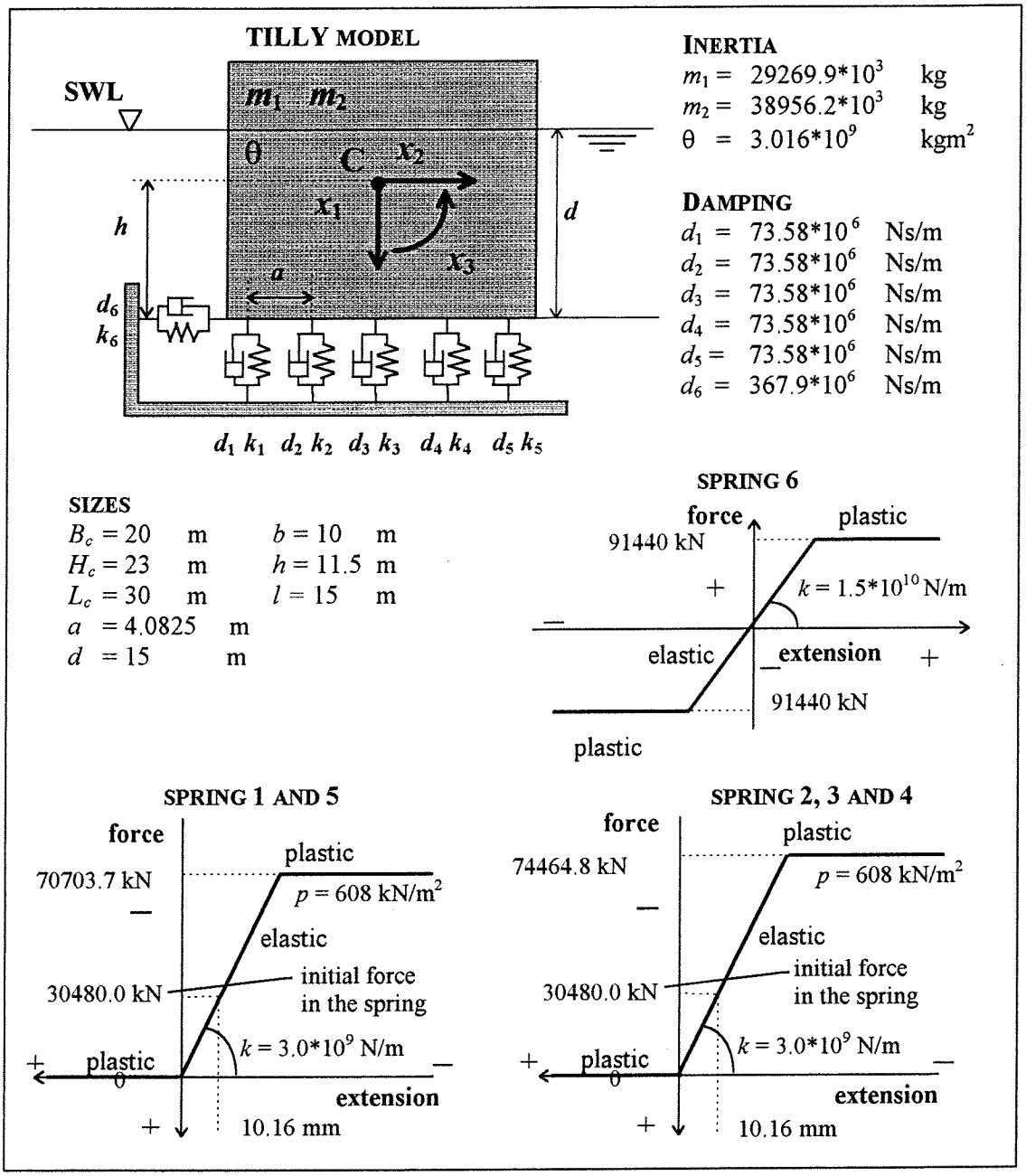

fig. 10.1 Summary of the mass-(elasto-plastic)spring-dashpot TILLY model

As has been stated before in chapter 9 on page 9 - 3, the only load on the vertical breakwater which is assumed to be of relevance for the benefit of the analysis of the dynamical behaviour of the vertical breakwater which is exposed to different kinds of wave impact loads in this chapter, is the horizontal wave impact load (see for example figure 9.3). All other loads on the vertical breakwater are assumed to be constant. They will not influence the dynamical behaviour of a vertical breakwater which is exposed to a wave impact load. More can be found on page 9 - 3, where a more extensive explanation of this assumption has been given.

For the benefit of the calculations in this chapter an estimation of the height of the breaking waves on the vertical breakwater has to be made. The height of the breaking waves on the vertical breakwater sketched in figure 10.1 can be calculated using the formula presented in equation 4.12 [OUMERACI et al. (1994a)].

$$H_b = L_b * \left[0.1025 + 0.0217 * \left(\frac{1 - K_r}{1 + K_r} \right) \right] * \tanh\left(\frac{2 * \pi * d_b}{L_b} \right) \qquad (4.12)$$

It is assumed that the peak period of the breaking waves is equal to T_p = 12 s and the reflection coefficient K_r is equal to 0, which means that the waves are not reflected at all (a conservative assumption according to equation 4.12). The breaking depth of the waves is d_b = 15 m. The height of the breaking waves can be calculated if the wave length of the breaking waves L_b is known. This wave length can be calculated using equation 10.1:

$$L_b = \frac{g T_p^{\,2}}{2\pi} \tanh\left(\frac{2\pi}{L_b} \right) \qquad (10.1)$$

It can be found that L_b = 134 m. Using equation 4.12 the height of the breaking waves can be calculated as: H_b = 10.09 m.

In all calculations which will be carried out in this chapter, the peak period of the waves is assumed to be T_p = 12 s and the height of the breaking waves is assumed to be H_b = 10 m.

Nota bene:

All calculations of which the results will be presented in this chapter in section 10.2 to 10.6 have been carried out assuming that the different wave impacts act over the total length of the vertical breakwater or a section of the vertical breakwater (e.g. a single caisson with a length of 30 m). This means that the waves which approach the vertical breakwater are assumed to be long crested while in nature this may often not be the case. It should be kept in mind that this is a very conservative assumption.

10.2 Effect of the position of the wave impact force

In this section the influence of the position of the wave impact force on the front wall of a vertical breakwater is investigated for wave impacts with high peak force and a short duration (wave impacts of the transition type). The model specifications of the investigated breakwater can be found in figure 10.1.

In the previous chapters the wave impact load (the total wave impact force, which is the resultant of the wave impact pressures on the front wall of the vertical breakwater) has been assumed to act on the vertical breakwater at Still Water Level (SWL). Thus, 15 m above the seabed (the water depth is 15 m). Takahashi [TAKAHASHI (1995)] concludes that the pressure intensity peaks at a waterdepth h_m. If the Irribarren number ξ>0.5 then impulsive pressures may occur (see chapter 2) and the ratio of the water depth at the structure d and h_m determines the type of wave impact load as follows:

$$\begin{aligned} 1.0 < \frac{d}{h_m} \le 1.2 &\quad \text{ventilated shock, Wagner type pressures} \\ \frac{d}{h_m} = 1.0 &\quad \text{vertical wave front, Transition type pressures} \\ 0.7 \le \frac{d}{h_m} < 1.0 &\quad \text{trapped air pocket, Bagnold type pressures} \end{aligned} \qquad (10.2)$$

As can be seen in the equations 10.2 the maximum wave impact pressure will act somewhere around SWL. This can also be seen in figure 4.4. The total wave impact force on the vertical breakwater and the position of this resultant of the wave impact pressures can be calculated if the distribution of the wave impact pressures on the front wall of the vertical breakwater is known. As can be seen in figure 4.4 this total wave impact force is located slightly below SWL.

Three different TILLY calculations have been carried out for three different positions of the resultant of the wave impact pressures on the model described in figure 10.2. All calculations have been carried out for a transition type wave impact which has been schematised by a triangular load. One for a total wave impact force (integrated pressures on the front wall of the vertical breakwater) which acts at SWL (case 1), one for a wave impact force which acts 2 m below water SWL (case 2) and one wave impact force which acts 2 m above SWL (case 3) (see figure 10.2). The magnitude of the wave impact of the transition type which has been investigated is also sketched in figure 10.2. A maximum wave impact force of $F_{h,max} = 15*\rho_w*g*H_b^2 = 15083$ kN/m with a duration of 15 ms is chosen which acts over the total length (30 m) of the structure; $t_r = 0.5*t_d$.

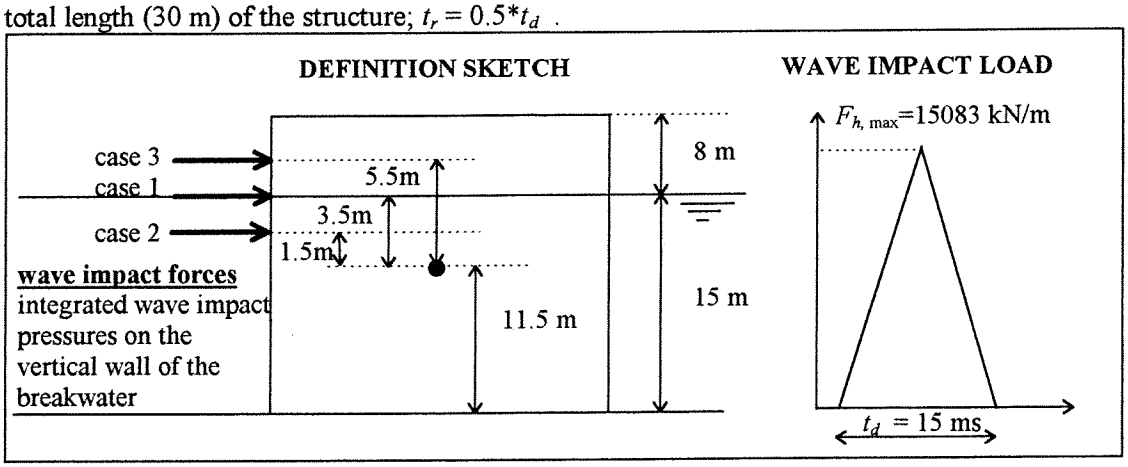

fig. 10.2 Position of different wave impact forces of the transition type and triangular load history

Results of the TILLY calculations can be found in figure 10.3, figure 10.4 and figure 10.5. In figure 10.3 the horizontal displacement of the bottom of the vertical breakwater is sketched for the three different cases. A description of the three different cases can be found in figure 10.2. In figure 10.4 the forces in the spring 6, the horizontal spring (see figure 10.1) are sketched for the three cases. The forces of spring 1 and spring 5, the two most eccentric vertical springs (see figure 10.1) are sketched in figure 10.5.

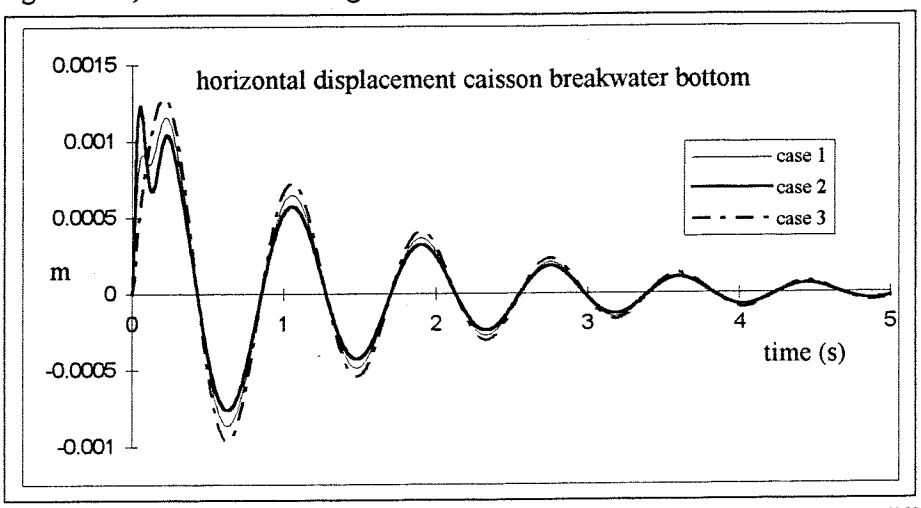

fig. 10.3 Horizontal displacement of the bottom of the vertical breakwater for the three different cases

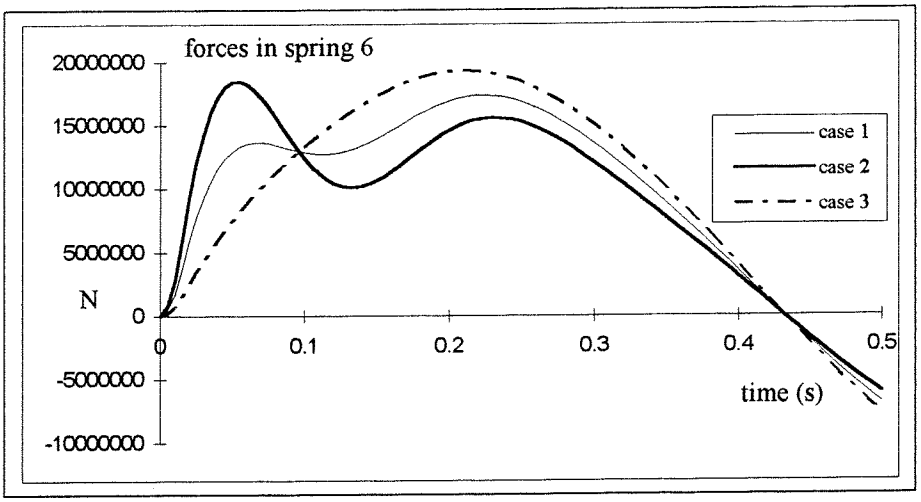

fig. 10.4 Forces in spring 6 (the horizontal spring) of the vertical breakwater for the three different cases

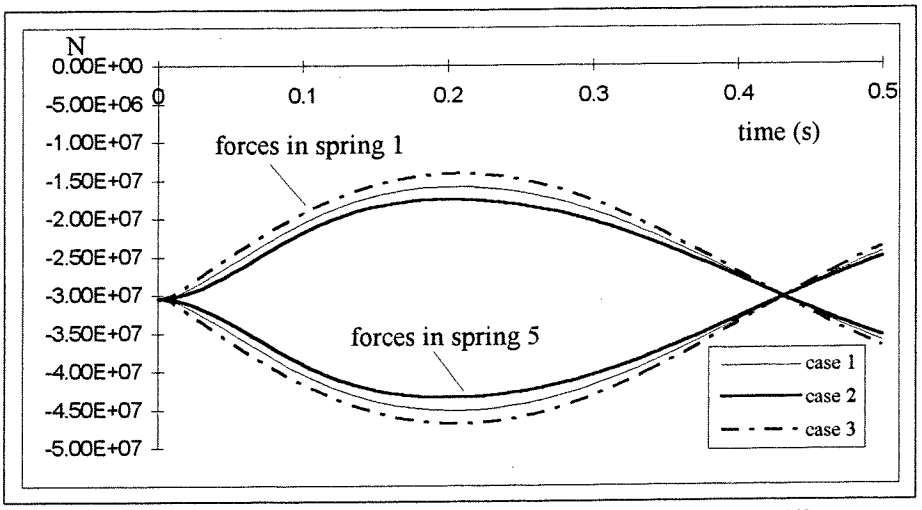

fig. 10.5 Forces in spring 1 and spring 5 of the vertical breakwater for three different cases

As it can be seen in figure 10.3 the maximum horizontal displacement of the bottom of the vertical breakwater does not differ very much for the different cases. The initial displacement is to the right because the wave impact acts on the left side of the vertical breakwater. It can be seen in figure 10.4 that spring 6 (the horizontal spring) does not become plastic under the different wave impact conditions. The same counts for spring 1 and spring 5 (the most eccentric vertical springs, see figure 10.1). The foundation of the breakwater does not fail (no yielding of the foundation soil) and the vertical breakwater does not slide. Another failure mode, besides sliding of the vertical breakwater and foundation failure, is overturning. The most dangerous condition for breakwater overturning is a wave impact force which acts very high; case 3 is determinative: the force acts 2 m above SWL. It can be seen in figure 10.5 that the forces in the vertical spring do not reach the value of 0 kN. This means that the condition described in equation 7.90 is fulfilled. The vertical breakwater is safe against overturning for all cases.

$$e < 0.3*B_c \quad = 0.3*20 = 6 \text{ m} \tag{7.90}$$

Overturning will not be considered as a failure mode anymore in this study because of the fact that the foundation soil does not yield when the force in the springs becomes 0 kN. The only failure mechanisms which will be taken into account are sliding and yielding of the foundation.

Thus, it can be concluded that the breakwater is save against sliding, overturning and breakwater failure for every case, case 1, case 2 and case 3.

The position of resultant of the enormous wave impact pressures to which the vertical breakwater (with a very common - rectangular - shape) has been exposed does not influence the displacement of the vertical breakwater very much. The vertical breakwater is safe against sliding, overturning and foundation failure for every investigated position of the resultant of the wave impact pressures on the vertical breakwater. The conclusion that the position of the wave impact force is not important is only valid if the foundation of the vertical breakwater does not fail, and that is true in this case.

In chapter 7 and 8 it has already been found that wave impacts with a very short duration but a very high peak force are not dangerous for the stability of the examined vertical breakwater. The results found in this section confirm this conclusion again. An addition to this conclusion can be given: it does not matter where the wave impact force of the transition type - very high peak force with a very short duration - acts on the vertical front wall of the breakwater. The maximum displacement does not change for the different positions if these positions are within a reasonable range of 2 m above and 2 m below Still Water Level.

Nota bene:

In this report the waterdepth is assumed to be constant: d is 15 m. In nature there will among other things be an influence of the vertical tide. This vertical tide causes different water depths in front of the vertical breakwater. This may have the following consequences:

- If the water depth at the vertical front wall of the breakwater changes, the height of the breaking waves against the vertical will also change.
- The position of the wave impact forces on the vertical front wall will change
- There will be different buoyancy forces for each water level

This all means that the stability of the vertical breakwater has to be examined for each water level which can occur at the site where the vertical breakwater is planned to be built.

In the remainder of this report, all calculations will be carried out for a waterdepth of $d = 15$ m.

10.3 Analysis of the formula of Schmidt et al.

In this section an analysis of the formula of Schmidt et al. [SCHMIDT et al. (1992)], see equation 4.21, will be treated. In the previous chapters, as well as in the previous section, the wave impact of the transition type has been described by a triangular shaped load history. A wave impact of the transition type is a wave impact on a vertical wall where only a small amount air is trapped (see chapter 2). As has been shown in chapter 2 before, a wave impact of the transition type should in fact be schematised by a "church-roof" load history: a large peak force with a very short duration, followed by the actual "roof" of the church: a quasi-static wave force with a much longer duration (see chapter 2 and figure 10.6).

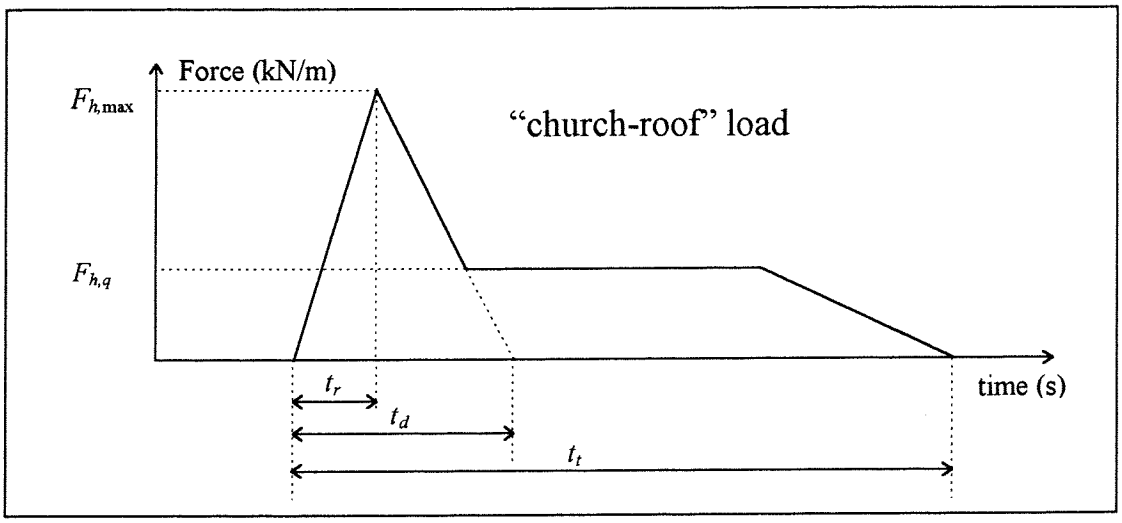

fig. 10.6 Church-roof load history

However, in the previous chapters the quasi-static wave force of the "church-roof" load has been neglected in the calculations. According to Oumeraci et al. [OUMERACI et al. (1994)] neglecting of the quasi-static force in the calculations is valid if one is only interested in the maximum response: "The procedure of substituting the actual impact loads by triangular loads may lead to useful results with respect to engineering application provided that:

- the rise time and the load duration of the triangular pulse are well selected, and
- the actual impact load does not exhibit oscillations after the peak value which may excite the structure at quasi-resonant conditions."

(the oscillations after the peak value of the wave impact force which may excite the structure at quasi-resonant conditions is treated in section 10.6)

In chapter 7 and chapter 8 the dynamical behaviour of a vertical breakwater due to a wave impact of the transition type with a very high peak force (13422 kN/m) and a very short duration (12 ms) has been investigated. The duration of the wave impact and the peak force have been determined using the formula of Schmidt et al. [SCHMIDT et al. (1992)] see equation 4.21. The main point of interest has been the maximum response of the structure. This maximum response has been used in the calculations of foundation failure and breakwater sliding of the vertical breakwater. Thus, according to Oumeraci et al [OUMERACI et al. (1994)] it has been valid to use only a triangular load history for this analysis of the dynamical behaviour of the vertical breakwater and its stability. In this section a same kind of analysis will be carried out so here the quasi-static wave impact force of the "church-roof" wave impact load will be neglected as well .

In the previous chapters the influence of a wave impact with a very high peak force of 13422 kN/m and a very short duration of 12 ms on the stability of the vertical breakwater - which among other things is described in figure 10.1 - has been treated. It has been extensively shown that such a kind of wave impact does not threaten the stability of the vertical breakwater. This was an important conclusion because a lot of measurements are carried out all over the world just to measure these very high peaks forces with very short durations, while these forces seem to be not important for the stability of the vertical breakwater as can be shown by a dynamical stability analysis.

Other wave impacts of the transition type can be more dangerous than the one with the shortest duration and the highest peak, as will be shown further on in this section. A wave impact of the transition type described by the formula of Schmidt et al. [SCHMIDT et al. (1992)], with a duration which is in the range of the eigenperiods of the vertical breakwater, is the most dangerous wave impact for the stability (stability against sliding and foundation failure) of the vertical breakwater.

For the benefit of the analysis presented in this chapter the quasi-static part of the wave impact force will be neglected. Within the framework of the given analysis this is permitted according to Oumeraci et al. [OUMERACI et al. (1994)]. Thus, the transition type wave impact - a single peak wave impact - will be schematised by a triangular force history as is shown in figure 10.7.

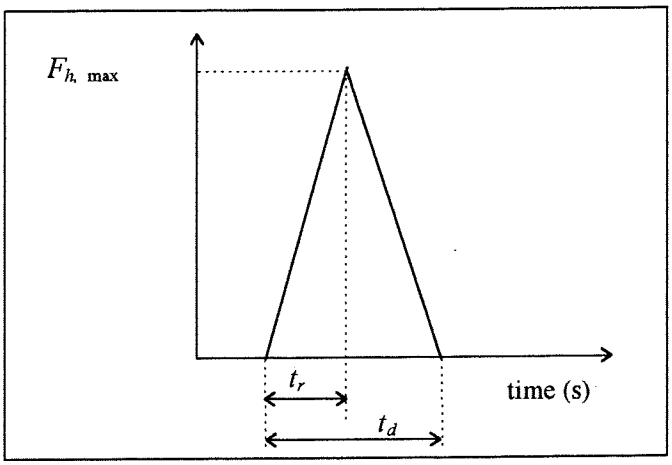

fig. 10.7 Triangular force history

In this section it is assumed that the rise time (t_r) of the wave impact force is the half of the total duration (t_d) of the wave impact with a triangular load history. This seems a reasonable assumption according to what Schmidt et al. [SCHMIDT et al. (1992)] found in their large scale hydraulic model tests, see equation 4.23:

$$0.3 \leq \frac{t_r}{t_d} < 0.65 \tag{4.23}$$

The duration of a transition type wave impact and the maximum horizontal force of a wave impact on a vertical breakwater are related. In chapter 4, equation 4.21 has been treated which describes this relationship between the maximum horizontal wave impact force and the duration of the wave impact [SCHMIDT et al. (1992)]:

$$\frac{F_{h,\max}}{\rho_w g H_b^2} = 1.24\left(\frac{t_d}{T_P}\right)^{-0.344} \tag{4.21}$$

in which:

H_b	=	breaker height at the front wall of the vertical breakwater
T_p	=	peak period of the waves
ρ_w	=	mass density of sea water (1025 kg/m^3)
t_d	=	total peak duration
$F_{h,\max}$	=	maximum horizontal wave impact force on a vertical breakwater per linear meter

Calculations of the response of the vertical breakwater to different kinds of wave impacts of the transition type are carried out by the use of the TILLY model which is summarised in figure 10.1). The wave impact load of the transition type is supposed to act at Still Water Level (SWL). The response of the vertical breakwater has been calculated for five different cases. The input parameters of the formula of Schmidt et al. [SCHMIDT et al. (1992)] are: g = 9.81 m/s^2, H_b = 10 m, T_p = 12 s and ρ_w = 1025 kg/m^3.

The most relevant eigenperiod of the vertical breakwater for the stability analysis (sliding and foundation failure) using the horizontal wave impact force prediction formula of Schmidt et al. [SCHMIDT et al. (1992)] is the eigenperiod of the horizontal oscillation of the vertical breakwater: T_2 = 0.845 s. The magnitude of this eigenperiod has already been determined in chapter 7 (see equation 7.44). In figure 8.12 as well as in figure 8.13 it can be seen that the (horizontal) displacement and the forces (vertical as well as horizontal) in the springs of the vertical breakwater, which is described by the mass-(elasto-plastic)-spring TILLY model (figure 10.1), are determined by an oscillation with a period which is approximately equal to the eigenperiod of the horizontal oscillation of the vertical breakwater. This eigenperiod of 0.845 s is slightly influenced by the amount of damping according to the formulae presented in figure 9.1. It is to be expected that the eigenperiod of the horizontal oscillation is the most important eigenperiod of the vertical breakwater for the determination of the stability of the vertical breakwater using the horizontal wave impact force prediction formula of Schmidt et al. [SCHMIDT et al. (1992)].

In case 3 the duration of the wave impact force of the transition type is 0.5* T_2 = 0.4225 s, in case 4 the duration of the wave impact force of the transition type is T_2 = 0.845 s and finally in case 5 the duration of the wave impact force is 2*T_2 = 1.69 s. In table 10.1 the wave impact force per linear meter can be found for each investigated case. In table 10.1 the maximum momentum: $I_{\max}$ = 0.5*t_d *$F_{h,\max}$ (see figure 4. 14) for each case is given as well. Note that all calculations will be done for the total length of the vertical breakwater (L_c = 30 m) and that all wave impact loads in table 10.1 are smaller than 15*ρ_w*g*H_b^2 = 15083 kN/m.

	t_d [s]	t_d / T_p [-]	$F_{h,\max}$ [kN/m]	$I_{\max}$ [Ns/m]
case 1	0.012	0.001	13422	80532
case 2	0.12	0.01	6079	364725
case 3	0.4225	0.03521	3942	832847
case 4	0.845	0.07042	3106	1312324
case 5	1.69	0.1	2447	2067838

table 10.1 Different loading cases

In figure 10.8 the maximum impact force versus the maximum impact duration is shown for the tests which have been carried out by Schmidt et al [SCHMIDT et al. (1992)]. The different cases which are described in table 10.1 are shown in this figure as well.

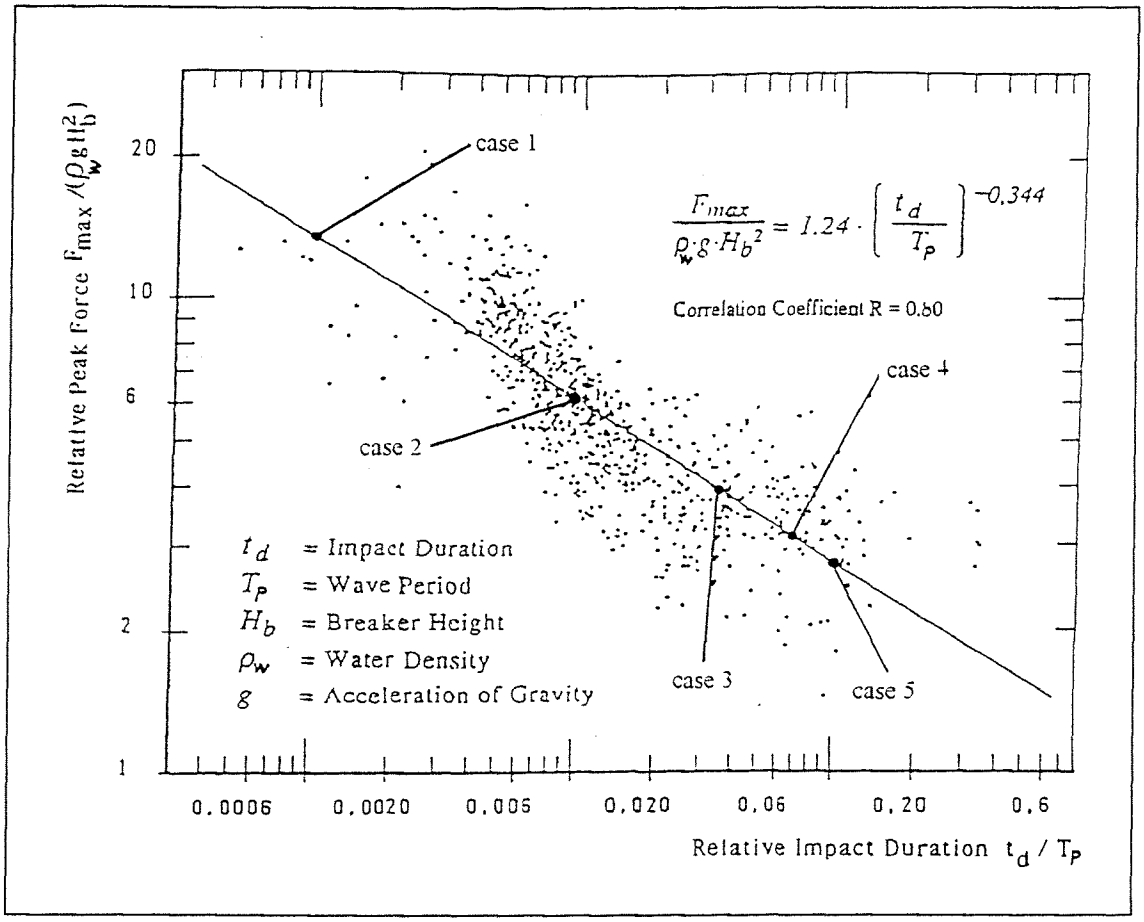

fig. 10.8 Maximum impact force versus impact duration [SCHMIDT et al. (1992)]

The horizontal displacement of the vertical breakwater bottom for the five different cases is shown in figure 10.9.

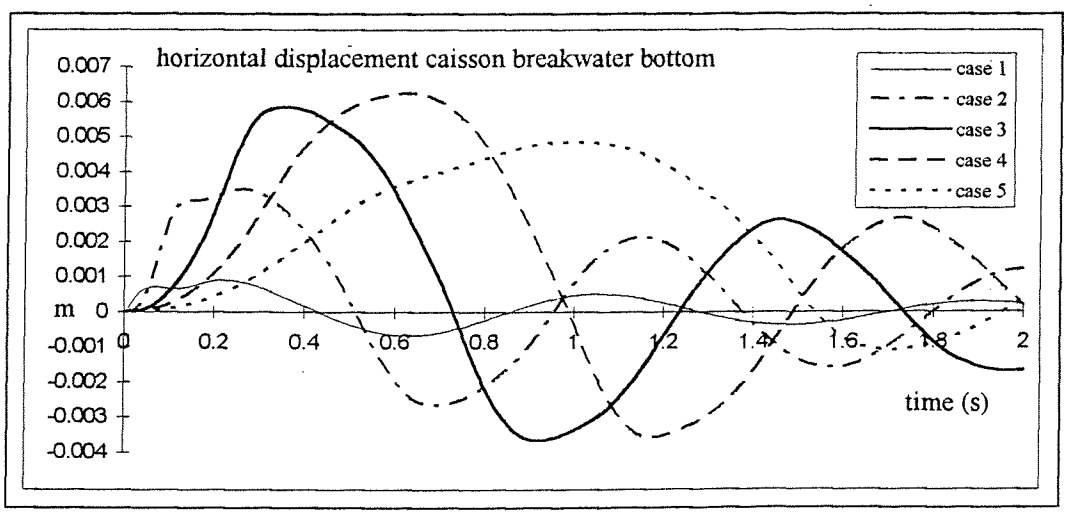

fig. 10.9 Horizontal displacement of the bottom of the vertical breakwater for five different cases

It can be seen in figure 10.9 that for this breakwater the most dangerous wave impact of the transition type which is described by the formula of Schmidt et al. [SCHMIDT et al. (1992)] is the wave impact with a duration of 0.845 s (case 4) and a magnitude of 3106 kN/m (assuming t_r=0.5*t_d for all loading cases). The wave impact of case 4 causes the largest horizontal displacements of the bottom of the vertical breakwater. The duration of this wave impact is equal to the most relevant eigenperiod of the vertical breakwater for the stability analysis: the eigenperiod of the horizontal oscillation of the vertical breakwater: T_2 = 0.845 s (see again figure 8.12 and figure 8.13).

The following can be concluded using the wave impact force prediction formula of Schmidt et al. [SCHMIDT et al. (1992)] and assuming that the rise time of a wave impact is the half of the total duration of a wave impact for all loading conditions. As long as the duration of the wave impact force is smaller than the eigenperiod of the horizontal oscillation of the vertical breakwater: the larger the amount of momentum of a wave impact (see table 10.1), the larger the maximum displacement of the breakwater (see figure 10.9). The maximum displacement of the vertical breakwater occurs for the wave impact load which has got the same total duration as the most relevant eigenperiod of the vertical breakwater for the stability analysis (the eigenperiod of the horizontal oscillation of the vertical breakwater). When the total duration of the wave impact force becomes longer, then the maximum displacement of the vertical breakwater decreases while the total amount of momentum of the wave impact still increases. This means that besides the total amount of momentum of a wave impact, the total duration relative to the eigenperiod of horizontal oscillation of the vertical breakwater is detrimental for the maximum displacement of a vertical breakwater according to the formula of Schmidt et al. [SCHMIDT et al. (1992)]

The forces in some springs which represent the foundation of the vertical breakwater are shown in figure 10.10 (for a definition of the different springs see figure 10.1).

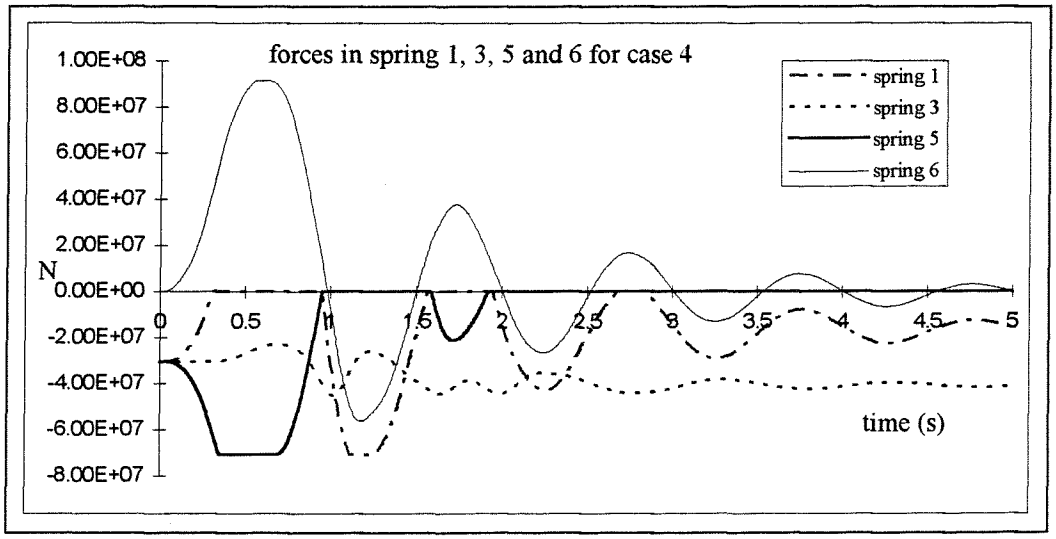

fig. 10.10 Forces in spring 1, 3, 5 and 6

It is obvious to see that the foundation of the vertical breakwater will fail for case 4. In figure 10.10 the forces in spring 1, spring 3, spring 5 and spring 6 are shown. As can be seen in figure 10.1 spring 1 and spring 5 are the two most eccentric vertical springs, spring 3 is the centre vertical spring and spring 6 is the horizontal spring. As has been stated before in this report foundation failure of vertical breakwaters is more likely to occur than sliding. This can be seen in figure 10.10 again. Spring 5 becomes plastic before spring 6 becomes plastic. Failure of the foundation seems to be the most important failure mechanism for vertical breakwaters. Not only for quasi-static loads, as has been shown in previous deterministic and probabilistic studies, but as well as for wave impact loads. Spring 6 reaches its maximum force of 91440 kN only for a very short while. So only little sliding of the vertical breakwater occurs.

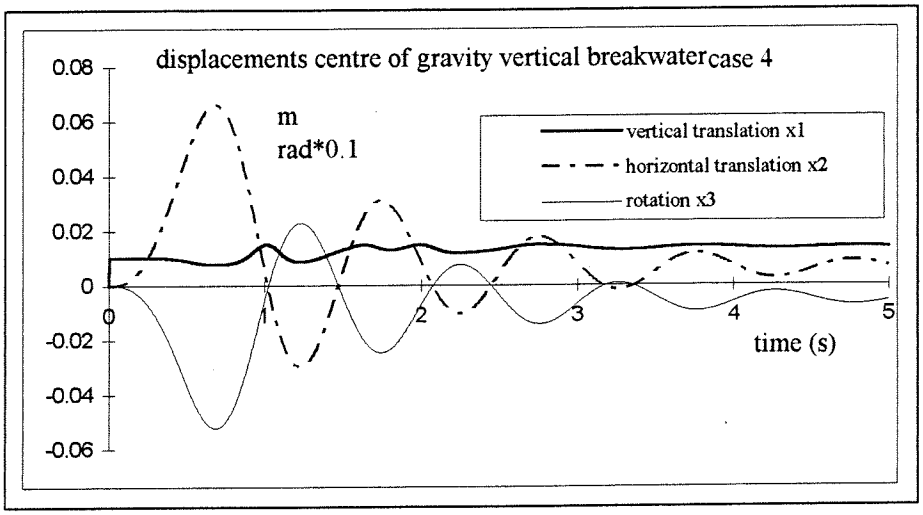

fig. 10.11 Displacements centre of gravity vertical breakwater

There may be almost no horizontal displacement of the bottom of the vertical breakwater but as can be seen in figure 10.11 where the displacements of the centre of gravity are shown for case 4 the breakwater is displaced downwards and there is a residual rotation to the right. Note that the consequence of this residual displacement is that the centre of gravity and the top of the vertical breakwater are permanently displaced to the right as can be seen in figure 10.12

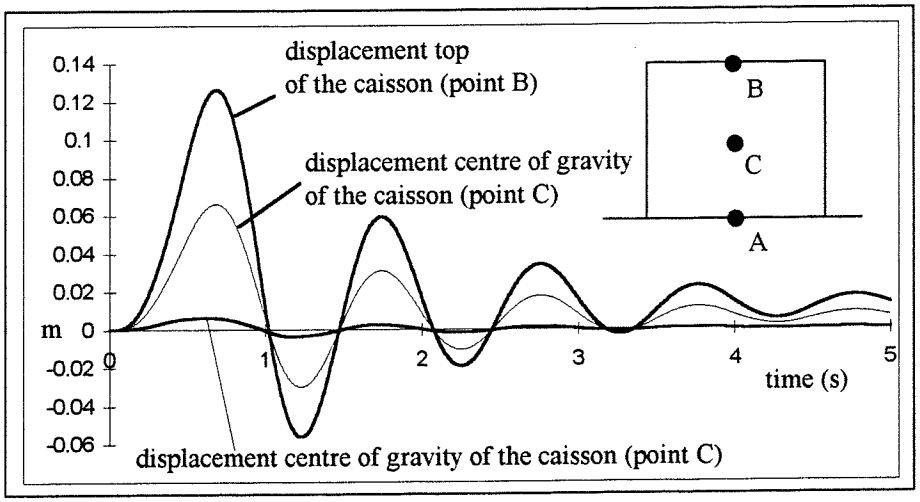

fig. 10.12 Horizontal displacement of different points on the vertical breakwater

Figure 10.12 is used for the benefit of the sketch of the residual displacement of the vertical breakwater after the wave impact of case 4. To show the effect of the wave impact on the vertical breakwater of case 4 the scale of figure 10.13 is distorted.

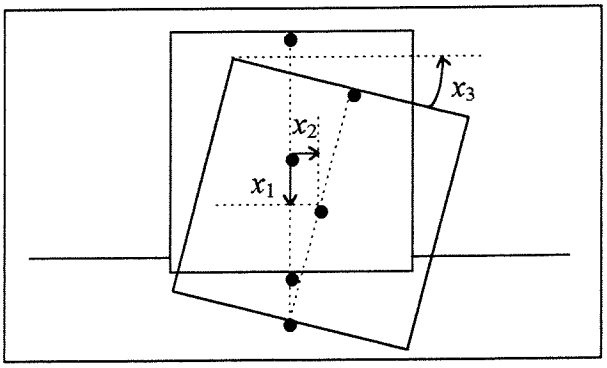

fig. 10.13 Residual displacement of the vertical breakwater (distorted scale)

In the next section it will be shown that the vertical breakwater which is described in figure 10.1 is safe against sliding and yielding of its foundation soil as long as the momentum of the wave impact to which the breakwater is exposed is less than I = 279000 Ns/m. If a triangular load history is assumed (see figure 10.7) then the maximum amount of momentum of a wave impact according to the formula of Schmidt et al. [SCHMIDT et al. (1992)] (equation 4.21) can be approximated by:

$$I_{max} = 0.5 * t_d * F_{h,max} = 0.5 * t_d * 1.24 * \rho_w * g * H_b^2 * \left(\frac{t_d}{T_p}\right)^{-0.344}$$

Now, the combination of a horizontal wave impact force and total duration of that wave impact force, according to the formula of Schmidt et al., can be determined which will not cause breakwater sliding or yielding of its foundation soil (T_p = 12 s, H_b = 10 m):

$F_{h,max}$ = 6996 kN/m $\qquad$ t_d = 0.080 s = 80 ms $\qquad$ I_{max} = 279000 Ns/m

If this result is compared with the dominant eigenperiod of the oscillation of the vertical breakwater (T_2 = 0.845 s) than it can be derived that, according to the formula of Schmidt et al. [SCHMIDT et al. (1992)], wave impacts with a total duration smaller than 9.5% of the most dominant eigenperiod of the investigated vertical breakwater (see figure 10.1) are not dangerous for its stability.

Conclusion of the analysis presented in this section:
Using the formula of Schmidt et al. [SCHMIDT et al. (1992)] the following conclusions can be drawn: one cannot say in general which kind of wave impact of the transition type (a wave impact with a small amount of trapped air) is the most dangerous one according to the formula of Schmidt et al [SCHMIDT et al. (1992)]. Calculations in this section show that the most dangerous wave impact has got a duration which is equal to the most dominant period of the eigenoscillation of the vertical breakwater. Thus, the most dangerous wave impact of the transition type can only be determined if the dynamical properties of the vertical breakwater are known. Every vertical breakwater has its own unique dynamical properties, and thus its "own" most dangerous wave impact of the transition type according to the formula of Schmidt et al. [SCHMIDT et al. (1992)]. In the design phase of a vertical breakwater a lot of attention should be paid to the occurrence of wave impacts and their relation to the dynamical properties of the vertical breakwater itself in order to design a safe and reliable vertical breakwater.

For prototype scale, wave impacts of the transition type with very high peak forces and very short durations were found not to be dangerous for the stability of the vertical breakwater. For the investigated vertical breakwater in this section this was the case for wave impacts with a total duration smaller than 9.5% of the most dominant eigenperiod of the vertical breakwater. Nevertheless, a lot of model tests are carried out all over the world to measure the very high peak forces and the very shorts durations even more accurately. These calculations seem not to be very relevant for the over-all dynamical stability analysis of a vertical breakwater.

The calculations in this section show again that failure of the foundation of the vertical breakwater (the maximum bearing capacity of the foundation soil is exceeded) is more likely to occur than sliding of the vertical breakwater.

The following could be found in literature: "Wave impacts with relatively long duration, although with a relatively low load maximum, are often most dangerous for the stability of caisson breakwaters, as the duration approaches the same order of magnitude as the natural oscillation period of the caisson with its foundation" [MAST II MSC (1995)]. This conclusion can be confirmed according to the analysis of the formula of Schmidt et al. [SCHMIDT et. al (1992)] in this section. The results found in this section are according to what Oumeraci et al. [OUMERACI et al.(1994)] found. When the wave impact of the transition type is schematised by a triangular load history and $t_r = 0.5t_d$ then the maximum response of the vertical breakwater may be expected for a wave impact with a total duration t_d which is equal to the most dominant eigenperiod of the vertical breakwater, in this case the eigenperiod of the horizontal oscillation of the vertical breakwater.

10.4 Analysis of the effect of maximum wave impact forces and momentum

In chapter 4 the derivation of different horizontal wave impact force prediction formulae has been treated using the consideration of momentum of a breaking wave on a plane vertical front wall of a breakwater. In chapter 4 the following figure has been presented for the determination of maximum wave impact forces related to the rise time of wave impacts (see figure 10.14).

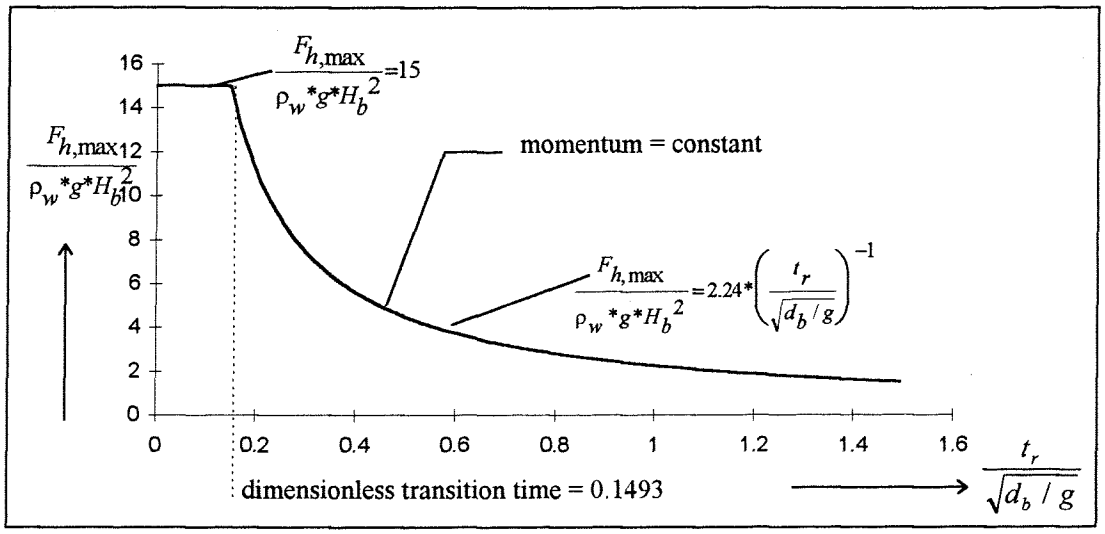

fig. 10.14 Prediction formula of wave impact forces with the maximum dimensionless wave impact force of 15

Maximum wave impact forces are not important for the stability of a vertical breakwater as long as the total duration of these wave impact forces is very short since the maximum wave impact force is limited. According to figure 10.14 the maximum dimensionless wave impact force is (equation 4.20):

$$\frac{F_{h,max}}{\rho_w * g * H_b^2} = 15 \qquad (4.20)$$

One of the governing factors for the stability of vertical breakwaters is the amount of momentum of the wave impacts to which the vertical breakwater is exposed as will be shown in this section and has been shown in the previous section before.

The maximum amount of momentum of wave impacts per linear meter, using the horizontal wave impact prediction formulae presented in figure 10.14, is presented in figure 10.15. The following input parameters have been used (for a detailed derivation of figure 10.15, see section 4.4):

- $g = 9.81$ m/s^2
- $H_b = 10$ m
- $d_b = 15$ m
- $\rho_w = 1025$ kg/m^3
- $t_r = 0.30 * t_d$ and $t_r = 0.65 * t_d$ according to the large scale hydraulic model tests of Schmidt et al. [SCHMIDT et al.(1992)], see equation 4.23:

$$0.3 \leq \frac{t_r}{t_d} < 0.65 \qquad (4.23)$$

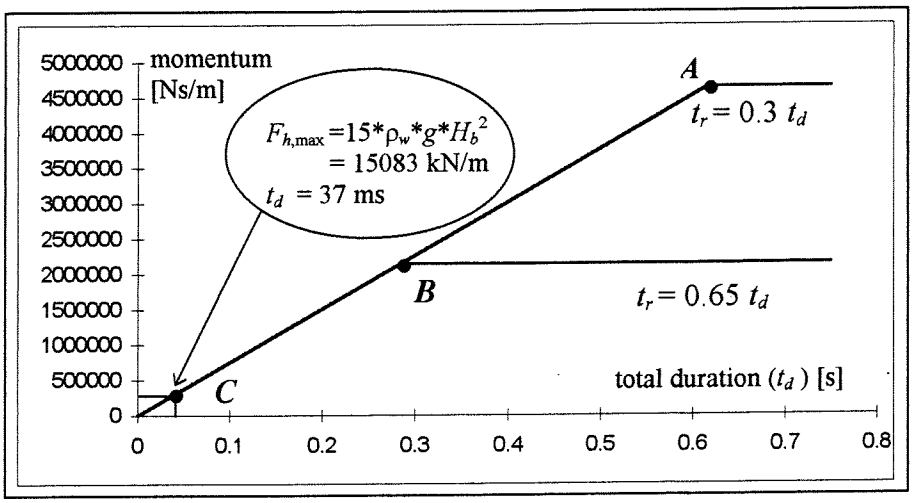

fig. 10.15 Maximum momentum for H_b = 10 m, d_b = 15 m and $t_r = 0.65*t_d$ and $t_r = 0.30*t_d$

The maximum amount of momentum of a wave impact which the vertical breakwater - described in figure 10.1 - can resist before the foundation of the vertical breakwater yields has been calculated by using the TILLY model described in figure 10.1. Yielding of the foundation soil was found to be the dominant failure mechanism of the vertical breakwater again. This maximum amount of momentum was found to be:

I = 279000 Ns/m

According to figure 10.15 this means a wave impact with a maximum force of $F_{h,max} = 15*\rho_w*g*H_b^2$ = 15083 kN/m and a total duration of 37 ms (point C). In this section a triangular wave impact force history is used again to schematise a wave impact force, according to figure 10.7. It can be seen in figure 10.15 that this amount of momentum is only very small compared to the maximum amount of momentum calculated by using the wave impact prediction formulae which are sketched in figure 10.14. It can be seen in figure 10.16 where the displacements of the centre of gravity of the vertical breakwater are shown and in figure 10.17 where the forces in spring 1, spring 5 and spring 6 are shown, that the combination of this wave impact force and this total duration will not lead to foundation failure, sliding and permanent displacements of the vertical breakwater. So it can be concluded that the vertical breakwater described in figure 10.1 is save against foundation failure and sliding for a wave impact with the maximum wave impact force of $F_{h,max} = 15*\rho_w*g*H_b^2$ and a total duration of 37 ms or smaller than 37 ms.

For the calculation, of which the results are presented in figure 10.16 and figure 10.17, it has been assumed that $t_r = 0.5*t_d$. Note that for this very short total duration (37 ms) the load duration t_d is predominant for the response of the vertical breakwater, the ratio t_r / t_d does not influence the maximum response of the vertical breakwater according to Oumeraci et al. [OUMERACI et al. (1994)] and Delft Hydraulics [DELFT HYDRAULICS (1994)]. In their studies it has been shown that for impulsive loads of short total duration ([t_d] / [the period of the most dominant eigenoscillation] < 0.25) the response seems to be almost independent of the load shape and is essentially determined by the area under the wave impact load curve (momentum): $0.5*t_d*F_{h,max}$ according to figure 10.7. The relation of t_r and / or t_d to the eigenperiod(s) of an investigated vertical breakwater is important.

It can be seen in figure 10.15 that the amount of momentum of two wave impacts with the same total duration (and which are in the constant branches of the graph) is larger for the wave impact with the shortest rise time. This wave impact will be the most dangerous for the stability (stability against sliding or foundation failure) of a vertical breakwater. This is logical because according to the horizontal wave impact force prediction formulae which have been derived in chapter 4, using the consideration of momentum of a breaking wave, the wave impact with the shortest rise time causes the largest wave impact force.

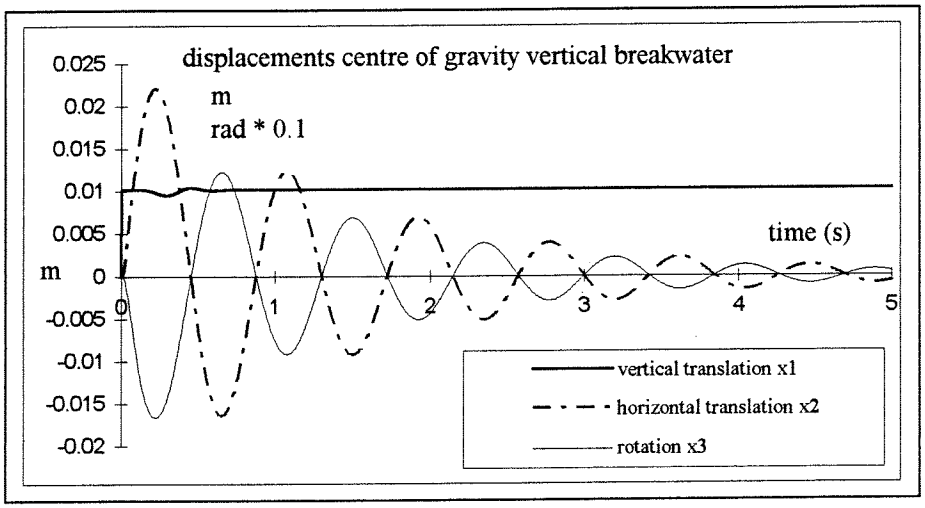

fig. 10.16 Displacements centre of gravity of the vertical breakwater loading case point *C* in figure 10.15

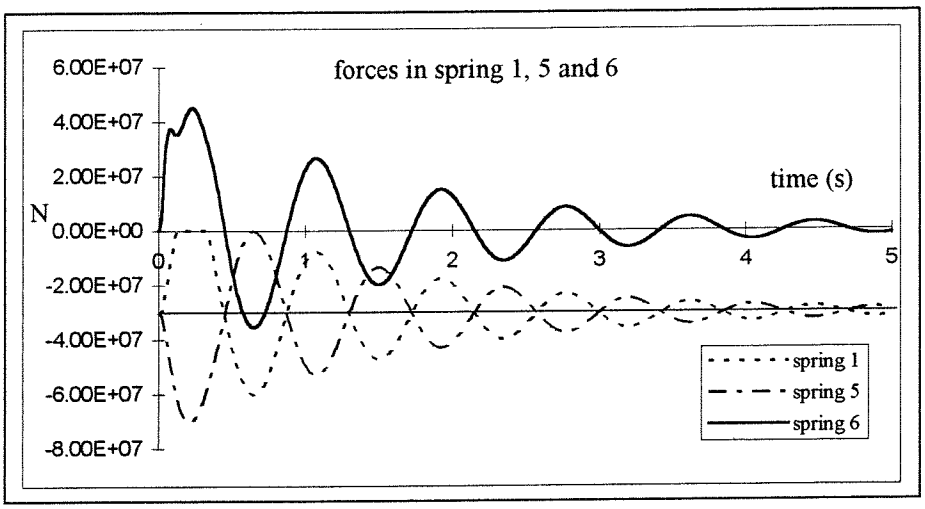

fig. 10.17 Forces in spring 1, 5 and 6 loading case point *C* figure 10.15

In chapter 4 it has been found that the maximum momentum of a wave impact can be calculated by using equation 4.42 which has been derived using the formula (equation 4.19) presented in figure 10.14:

$$\frac{F_{h,\max}}{\rho_w * g * H_b^{\,2}} = 2.24 * \left(\frac{t_r}{\sqrt{d_b / g}} \right)^{-1} \tag{4.19}$$

$$\text{If } t_r > \frac{2.24}{15} * \sqrt{\frac{d_b}{g}} \qquad I_{\max} = 0.5 * \rho_w * g * H_b^{\,2} * 2.24 * \sqrt{\frac{d_b}{g}} * \frac{t_d}{t_r} \tag{4.42}$$

It can be shown that the maximum response of a vertical breakwater which is exposed to wave impacts which represent the same maximum amount of momentum according to equation 4.42 - see the horizontal, constant, branches in figure 10.15 - is the largest for the wave impact with the shortest total duration (and the highest peak force). This is point *A* in figure 10.15, point *A* is the intersection of the horizontal and linear branch of the graph. This phenomenon can be seen in figure 10.18 where the horizontal displacement of the bottom of the vertical breakwater - described in figure 10.1 - is given for two loading cases of wave impacts which represent the same maximum amount of momentum, this maximum amount of momentum is equal for both loading cases.

The first loading case is the loading case indicated by point A in figure 10.15 and is a wave impact with a rise time equal to:

$$t_r = \frac{2.24}{15} * \sqrt{\frac{d_b}{g}} = 0.1493 * \sqrt{\frac{15}{9.81}} = 0.1847 \text{ s},$$

The maximum response of the vertical breakwater can be expected for the shortest rise times relative to the total duration: $t_r = 0.3*t_d$ (equation 4.23). According to figure 10.15 these wave impacts represent the largest amounts of momentum. So t_d can be calculated as:

$t_d = 0.1847/0.3 = 0.6155$ s

Using equation 4.19, the maximum force of a wave impact with a rise time of 0.1847 s is:

$F_{h,max} = 15*\rho_w*g*H_b^2 = 15083$ kN/m

$I = 0.5*0.6155*15083*10^3 = 4641953$ Ns/m (Check figure in 10.15 → OK!)

The other loading case is a wave impact with a total duration equal to the dominant eigenperiod of the vertical breakwater, according to section 10.3, this period is the eigenperiod of the horizontal oscillation of the vertical breakwater, which is $T_2 = 0.845$ s. So:

$t_d = 0.8450$ s
$t_r = 0.3*0.8450 = 0.2535$ s

Using equation 4.19, the maximum force of a wave impact with a rise time of 0.2535 s is:

$F_{h,max} = 10987$ kN/m
$I = 0.5*0.8450*10987*10^3 = 4641953$ Ns/m (Check in figure 10.15 → OK!)

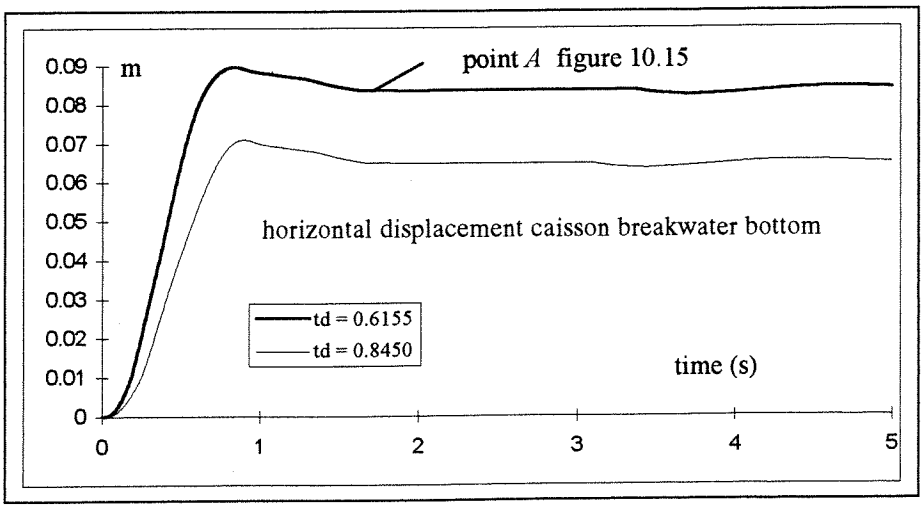

fig. 10.18 Horizontal displacement bottom of the vertical breakwater for maximum wave impact momentum

It can be seen that point A in figure 10.15 gives the largest response of the vertical breakwater: the maximum response is approximately 9 cm, see figure 10.18. Thus, the wave impact belonging to point A in figure 10.15 is more dangerous for the stability of the vertical breakwater than the wave impact with a total duration equal to the dominant eigenperiod of the oscillation of the vertical breakwater because it causes the largest response. In general it can be concluded that if a vertical breakwater is exposed to two different wave impacts, which both represent the same amount of momentum, the wave impact with the shortest total duration and rise time causes the largest response of the vertical breakwater. This is confirmed by the studies of Oumeraci et al. [OUMERACI et al (1994)] and Delft Hydraulics [DELFT HYDRAULICS (1994)]. Both wave impacts here represent the same amount of momentum. Thus, the maximum response for wave impacts with an equal amount of momentum can be expected for the point at the intersection of the linear and the constant branch in figure 10.15 (point A) if the horizontal wave impact force prediction formulae described in figure 10.14 are used for the benefit of the calculation of the maximum response of the vertical breakwater exposed to wave impacts. This is in contrast to what has been found in the previous section! There it has been found that the most dangerous wave impact for the vertical breakwater was a wave impact with a total duration equal to the most dominant eigenperiod of the oscillation of the vertical breakwater. So it needs once again to be stressed that the conclusion which has been drawn in the previous section, that the wave impact force with a duration equal to the most dominant eigenperiod of the vertical breakwater is the most dangerous wave impact force, is only valid when the formula of Schmidt et al. [SCHMIDT et al. (1992)] is applied in breakwater design and when it is assumed that $t_r = 0.5 * t_d$ for all loading cases.

The forces in the springs of the loading case belonging to point A in figure 10.15 ($(t_d = 0.6155$ s, $F_{h,max} = 15083$ kN/m) are shown in figure 10.19. Note that if the forces in the vertical springs are added, a value which is approximately equal to $F_n = 152.4 * 10^6$ N (see equation 7.88) can be found.

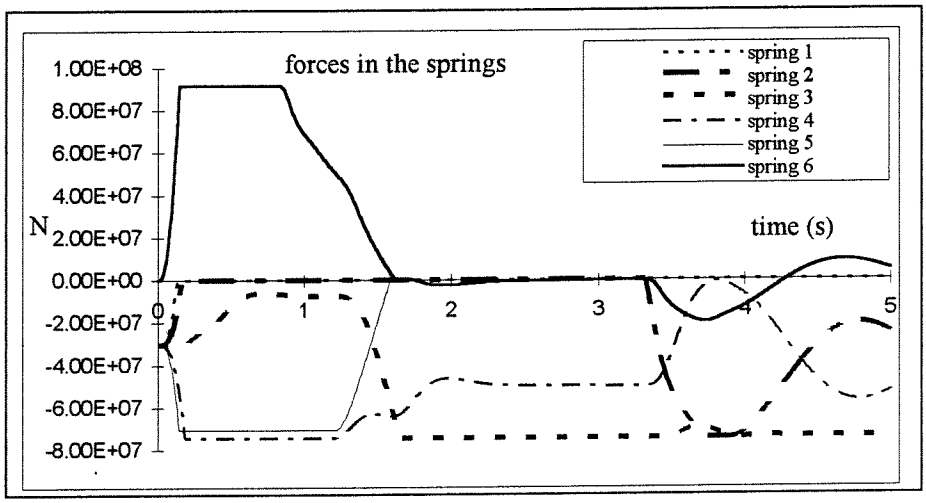

fig. 10.19 Forces in the springs for wave impact loading case point A in figure 10.15

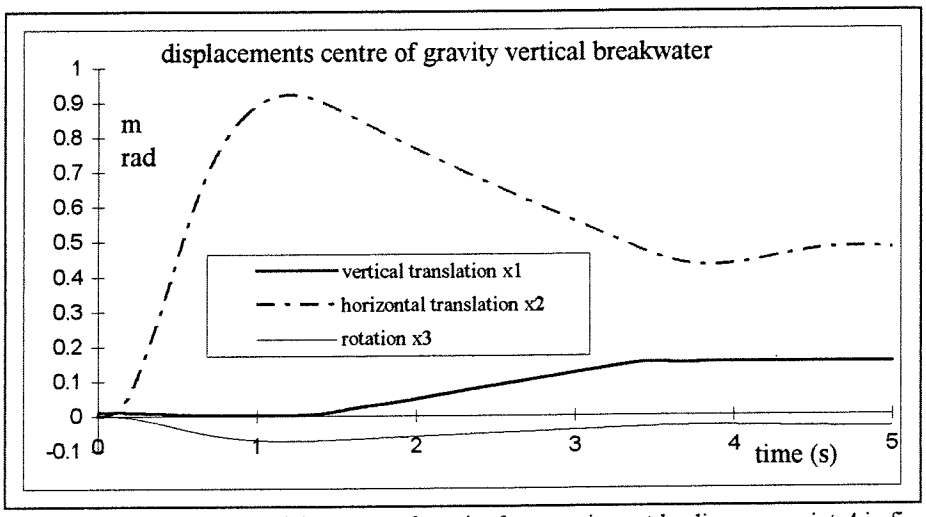

fig. 10.20 Displacements of the centre of gravity for wave impact loading case point *A* in figure 10.15

Figure 10.20 is used for the benefit of the sketch of the residual displacement of the vertical breakwater after the breakwater has been exposed to a wave impact with a duration and a force belonging to point *A* in figure 10.15. To show the effect of this wave impact (t_d = 0.6155 s, $F_{h,\max}$ = 15083 kN/m) on the vertical breakwater, the scale of figure 10.21 has been distorted.

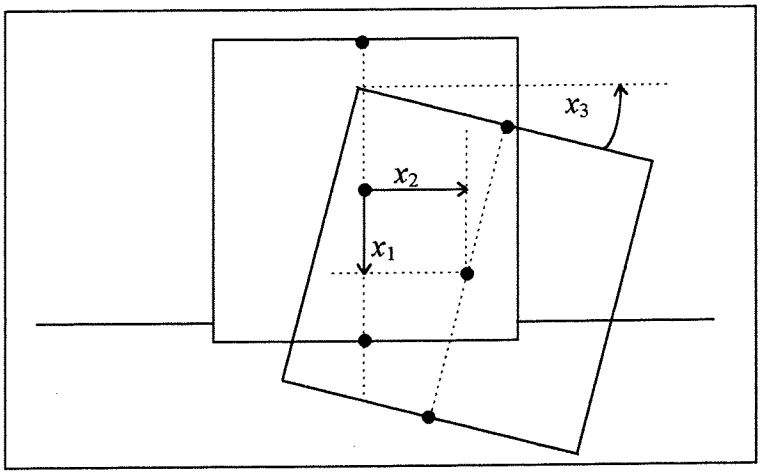

fig. 10.21 Residual displacement of the vertical breakwater (distorted scale)

The conclusion of this section can be written in terms of formulae. If the formula of Klammer et al. [KLAMMER et al. (1996)] (equation 4.16) is used, together with the maximum dimensionless wave impact force of 15 (see figure 10.14), for the benefit of the analysis of the dynamical behaviour of the vertical breakwater which is described in figure 10.1, then the maximum response of a vertical breakwater can be expected for the force $F_{h,\max}$ and the rise time t_r described in equation 10.3 and 10.4 (see among other things figure 10.14 and 10.15 e.g. point *A* or *B*):

$$t_r = \frac{2.24}{15} * \sqrt{\frac{d_b}{g}} \tag{10.3}$$

$$F_{h,\max} = 15 * \rho_w * g * H_b^2 \tag{10.4}$$

The formula derived by Klammer et al. [KLAMMER et al. (1996)] is given in equation 4.19:

$$\frac{F_{h,\max}}{\rho_w * g * H_b^2} = 2.24 * \left(\frac{t_r}{\sqrt{d_b / g}} \right)^{-1} \tag{4.19}$$

If $t_r > \frac{2.24}{15} * \sqrt{\frac{d_b}{g}}$ then the maximum momentum of a wave which causes a wave impact is given by equation 4.42 (derived using equation 4.19):

$$I_{max} = 0.5 * \rho_w * g * H_b^2 * 2.24 * \sqrt{\frac{d_b}{g}} * \frac{t_d}{t_r} \tag{4.42}$$

In chapter 4 a horizontal wave impact force prediction formula has been derived which takes the peak period T_p of the waves into account:

$$\frac{F_{h,max}}{\rho_w * g * H_b^2} = 0.38 * \left(\frac{t_d}{T_p}\right)^{-1} \tag{4.31}$$

If $t_d > \frac{0.38}{15} * T_p$ then the maximum momentum of a wave which causes a wave impact is given by equation 4.44 (derived using equation 4.31)

$$I_{max} = 0.5 * \rho_w * g * H_b^2 * 0.38 * T_p \tag{4.44}$$

The maximum wave height of a breaking wave with the maximum amount of momentum on the vertical front wall of the breakwater which will not cause breakwater sliding or foundation failure for the most dangerous combination of $F_{h,max}$ and t_d or t_r (see figure 10.15, e.g. point *A* or *B*) can be calculated knowing that the vertical breakwater which has been described in figure 10.1 is safe against foundation failure and sliding for a total amount of momentum of I=279000 Ns/m. This has been carried out for different ratios of t_r / t_d using equation 10.3 and 4.42, see table 10.2 as well as for equation 4.44 also given (T_p = 12 s). The maximum response of the vertical breakwater using equation 4.31 and 4.44 will occur for t_d = (0.38/15)*T_p according to the results presented in this section (according to equation 10.3).

		$H_{b,max}$
equation 4.19 / 4.42	$t_r = 0.3\ t_d$	2.45 m
	$t_r = 0.5\ t_d$	3.17 m
	$t_r = 0.65\ t_d$	3.61 m
equation 4.31 / 4.44		3.49 m

table 10.2 Maximum breaker height allowed

For the calculation of these maximum allowed breaker heights on the vertical breakwater, the effect of the shape of the wave impact load history (see figure 10.7) on the maximum response of the vertical breakwater has been neglected.

For wave impacts caused by breakers with these maximum wave heights the vertical breakwater sketched in figure 10.1 is safe against sliding and foundation failure for all possible total durations of wave impacts if equation 4.19, derived by Klammer et al. [KLAMMER et al. (1996)], or equation 4.31 is used for the design of the vertical breakwater together with the maximum dimensionless horizontal wave impact force of 15 (see among other things figure 10.14). It is to be seen in table 10.2 that these wave heights are only very small compared to the waterdepth d = 15 m. This again confirms the fact that the horizontal wave impact force prediction formula derived by Klammer et al. [KLAMMER et al. (1996)] and equation 4.31 are very conservative.

Using the conservative horizontal wave impact force prediction formula of Klammer et al. [KLAMMER et al. (1996)] together with the maximum dimensionless wave impact force of 15, higher breaking waves than presented in table 10.2 against the vertical front wall of the breakwater - which will not cause sliding or foundation failure - are for instance possible if the dynamical properties of the breakwater itself are changed.

In the previous chapter is has been stressed that increasing the mass of the vertical breakwater and decreasing the stiffness of the foundation are possible solutions for making a vertical breakwater more safe against wave impacts, because of the fact that the maximum response of the vertical breakwater will decrease. However, decreasing the stiffness of the foundation may result in a vertical breakwater which is less stable against quasi-static wave loads because of the fact that the eigenperiod of the oscillation of the vertical breakwater increases when the stiffness of the foundation decreases. The following other comments must be made as well: the initial pressure in the foundation soil of the vertical breakwater will increase if the mass of the vertical breakwater is enlarged without changing the dimensions of the vertical breakwater. This is unfavourable for the stability of the vertical breakwater against foundation soil failure. Increasing the stiffness of the foundation is unfavourable and decreasing the stiffness of the foundation is favourable for the stability of the vertical breakwater against sliding and foundation failure. However, a foundation soil with a low stiffness will probably have got a smaller strength compared to a stiff foundation soil. Changing the dynamical properties of the vertical breakwater can have contradictory effects, as can be seen. So one must be very careful when changing the properties of the vertical breakwater and its foundation.

The conclusions found in this section are somewhat different from the conclusions found in the previous section. In contrast to the previous section where a horizontal wave impact force prediction formula has been used which does not represent a constant amount of momentum (the formula of Schmidt et al. [SCHMIDT et al. (1992)], equation 4.21), the period of the wave impact load relative to the most dominant eigenperiod of the vertical breakwater (e.g. the period of horizontal oscillation as has been found in this study) was found to be not normative anymore if a formula is used which has been derived using the consideration of momentum of a breaking wave for calculating the response of a vertical breakwater. In this section it has been found that if a vertical breakwater is exposed to two different wave impacts which both represent the same amount of momentum, the wave impact with the shortest total duration and rise time causes the largest response of the vertical breakwater.

These two different conclusions - found in this section and in the previous section - do both indicate the fact that an extensive analysis of the wave impacts to be expected at the site were a vertical breakwater is planned to be build is necessary. For the design of a vertical breakwater it is essential to know which wave impacts are to be expected. The types of wave impacts and the dynamical properties of a planned vertical breakwater determine the effect of wave impacts on the (dynamical) behaviour of a vertical breakwater. A (very) large and stiff hydraulic scale model - which is preferable to overcome scaling problems - can be used to analyse the different wave impacts to be expected at the location where a vertical breakwater is planned to be built. It is very important to know which kinds of wave impacts are to be expected. Knowing these wave impacts: rise times, total durations and peak forces and the dynamical properties of a vertical breakwater which has been designed, the effect of different wave impacts can be indicated. This can be done by using the results of the calculations carried out by the use of a mass-(elasto-plastic)spring-dashpot model of a designed vertical breakwater exposed to wave impacts, as has been carried out in this study. The results of the analysis of the dynamical behaviour of the designed vertical breakwater can be used to adapt the actual vertical breakwater to the wave impacts which are to be expected. Another important thing is that a probabilistic approach for vertical breakwater design concerning wave impacts seems to be necessary as has been mentioned before in chapter 4. The chance of occurrence of a maximum wave impact load can be a governing factor in the design of vertical breakwaters.

The conclusion found in this section has been confirmed by Oumeraci et al. [OUMERACI et al. (1994)] and by [DELFT HYDRAULICS (1994)]. For different wave impacts with the same amount of momentum the wave impacts with the shortest rise times and total durations are the most dangerous ones.

10.5 Effect of a double peaked wave impact

In chapter 5 the effect of a trapped air pocket on the wave impact load on a vertical breakwater has been discussed. Two aspects of the trapped air pocket have been treated:

- the double-peaked force history and
- the low frequency force oscillations.

This results in two different kinds of wave impact loads, a double peaked wave impact force and a wave impact with a peak force followed by low frequency force oscillations.

The second peak of the double-peaked force history is in fact the first peak of the low frequency force oscillations. So one could say that it is wrong to consider the second peak and the low frequency force oscillations separately. This is not true. The first peak of the low frequency force oscillations is not likely to be damped very much while the other maximum forces after this peak - or the amplitude - of the low frequency force oscillations (thus, apart from the first one) are likely to be damped out very soon: the amplitude of these low frequency force oscillations diminishes very rapidly. Then, one can see two peaks and only very minor force oscillations in the load history (see figure 10.22). Only under special conditions the low frequency force oscillations can play an important role in stability of a vertical breakwater against foundation failure and sliding. The effect of the low frequency force oscillations on the dynamical behaviour of the vertical breakwater will be shown in the next section. In this section the effect of a double peaked force history on the vertical breakwater will be treated.

When an air pocket is trapped between the breaker and the caisson front, the impinging breaker tongue first strikes the wall and induces a first peak (F_1) in the impact force history. It is then followed by a second peak (F_2) resulting from the subsequent compression of the air pocket caused by the advancing breaker front. (see figure 10.22)

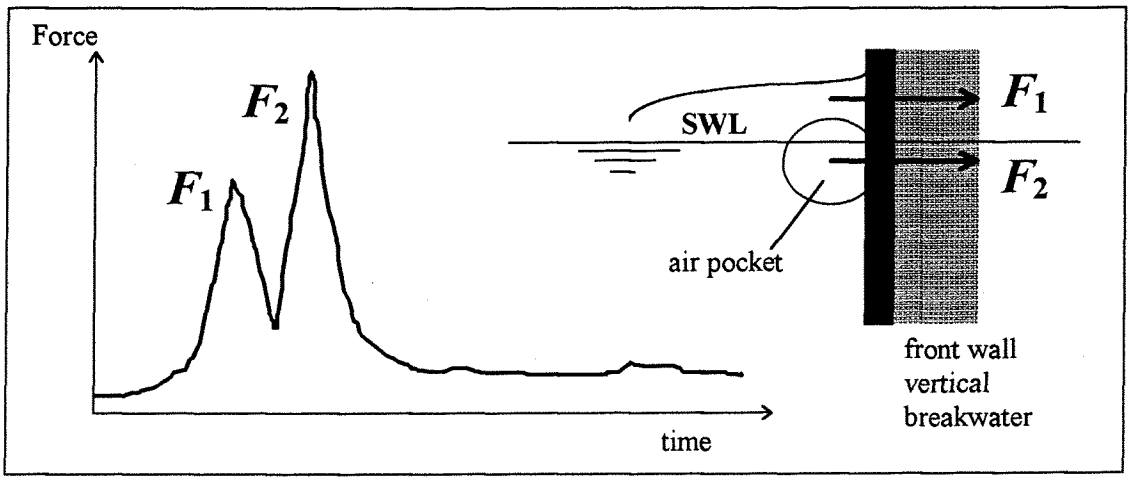

fig. 10.22 Force history of a double peaked wave impact force

If the second peak occurs within a time:

$$t < T/4 \quad \text{or} \quad {}^3/_4T < t < T \tag{10.5}$$

in which:

T = dominant period of the oscillation of the vertical breakwater

that means while the caisson is moving shoreward, it will have to overcome no or at least only a part of the structure's inertia. The cumulative response is expected to be higher than it would be if only a single impact occurred or if the second peak was applied at a time t with $T/4 < t < {}^3/_4T$.

Schmidt et al. [SCHMIDT et al. (1992)] have shown that in the case of a well developed plunging breaker with a large trapped air pocket - which is the case in this section - the spatial integration of the impact pressures generally leads, besides a double peaked wave impact load, to a total force with a duration which may be much larger than usually assumed. The duration of the total impact force may reach values in the range of 0.15 - 0.6 s in full scale situations. According to Walkden et al. [WALKDEN et al. (1995)] the reduction in the impact force and the associated increase in the impact duration are due to the combined influence of the increase in compressibility of the air/water mixture and the observed change in the wave profile at the impact. So if a large air pocket is trapped between the breaking wave and the vertical front wall of the breakwater not only a double peak force may be expected but also a longer duration of the wave impact.

A comparison has been made between a transition type wave impact which is a single peaked wave impact (case 1, see figure 10.23) and a double peaked wave impact due to a large trapped air pocket (case 2, see figure 10.23) by the use of the results of the computations of the mass-(elasto-plastic)spring-dashpot TILLY model described in figure 10.1. The vertical breakwater which has been described in figure 10.1 is exposed to these two different wave impact loads (see figure 10.23). The effect of the longer duration of the impact force in the case of a plunging breaker which encloses a large pocket of air between the breaker and the vertical front wall of the breakwater, which also causes the double peaked wave impact force, has also been taken into account. According to figure 4.4 on page 4 - 6 the horizontal wave impact force (the resultant of the wave impact pressures) in case of a well-developed plunging (which encloses a large air pocket between the breaker and the vertical front wall of the breakwater) acts below Still Water Level. In this case the wave impacts are assumed to act on the front wall of the vertical breakwater 2 m below SWL. The two load histories have been derived in such a way that a reliable comparison can be made between the results of the two different kinds of wave impacts on the TILLY model described in figure 10.1 and the results of the two different kinds of wave impact loads on the large scale hydraulic model tests which have been carried out by Oumeraci [OUMERACI (1991)].

The two different wave impacts are sketched in figure 10.23.

An estimate of the time between the first peak and the second peak can be made by using the propagation velocity of shallow water waves. The propagation velocity of waves in water with a depth of d = 15 m is and a wave height of H_b = 10 m is:

$$c = \sqrt{g(d + 0.5 * H_b)} = \sqrt{9.81 * (15 + 0.5 * 10)} = 14.01 \text{ m/s} \tag{10.6}$$

If the large trapped air pocket has a thickness of approximately D = 2.0 m, then the time between the first and the second peak Δt can be approximated by:

$$\Delta t = \frac{D}{c} = \frac{2.0}{14.01} = 0.143 \tag{10.7}$$

The period T of the dominant oscillation of the vertical breakwater is approximately 0.845 s. $T/4$ = 0.211 s, so the second peak can occur within the time(s) given by equation 10.5.

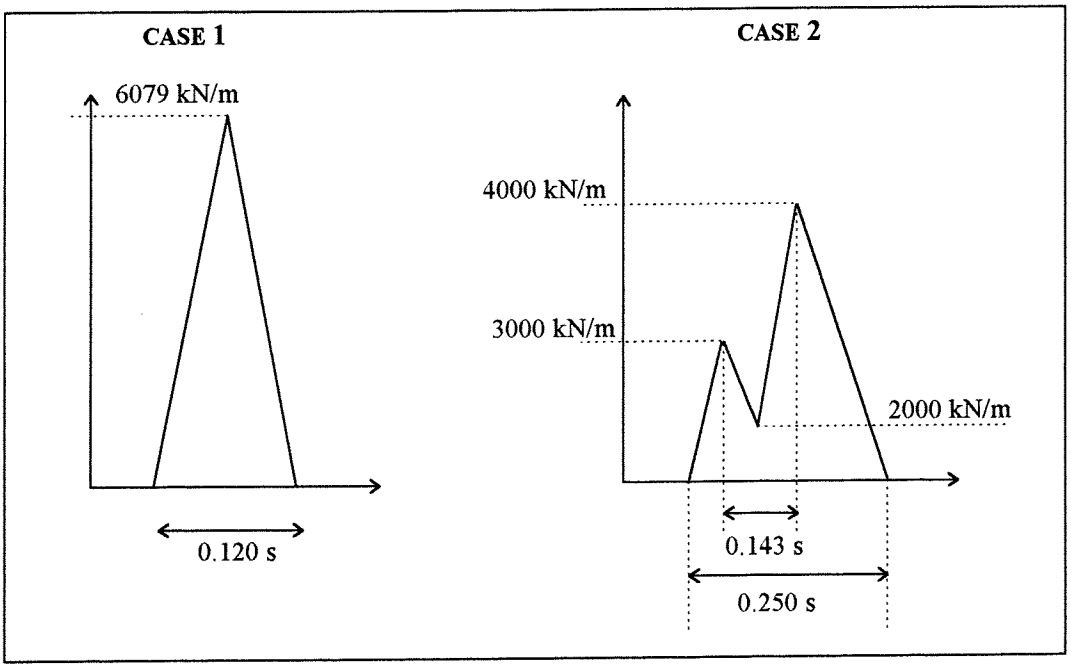

fig. 10.23 Force history of the two wave impact loading cases

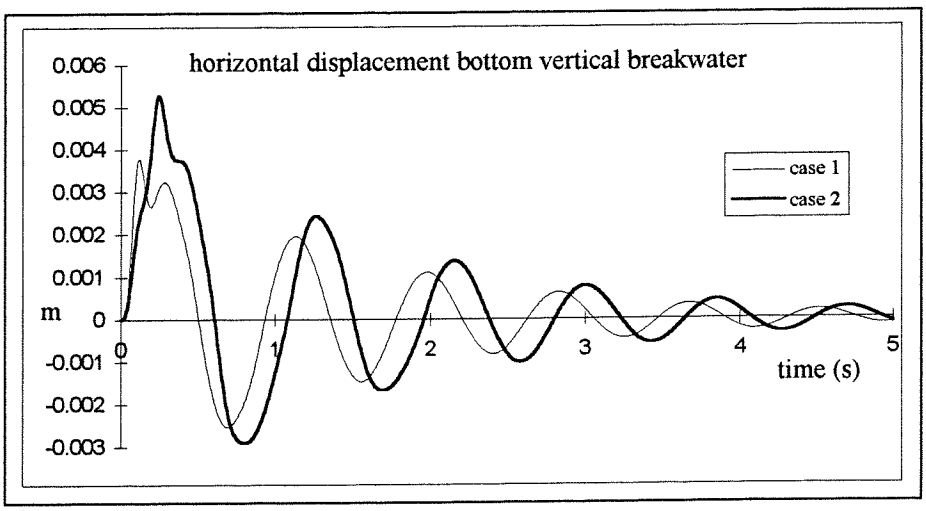

fig. 10.24 Horizontal displacement of the caisson breakwater bottom

It can be seen in figure 10.24 that a double peaked wave impact force causes a larger response of the vertical breakwater than a single peaked wave impact force. This confirms the theory which has been presented before: double peaked wave impacts can be more dangerous than single peaked wave impacts. The larger response of the double peaked wave impact is caused by:

- the fact that the second peak occurs while the caisson is moving shoreward (in the direction of the harbour), the second peak does have to overcome no or at least only a part of the structure's inertia and
- the fact that the double peaked wave impact force represents a slightly larger amount of momentum - in spite of the fact that the peak force is smaller - due to the fact that wave impacts which enclose a large air pockets have got longer total durations.

The results of the comparison of the two different wave impact types carried out by the use of the TILLY model described in figure 10.1 show good agreement with the results which have been found in large scale model tests (see figure 10.25) by Oumeraci [OUMERACI (1991)].

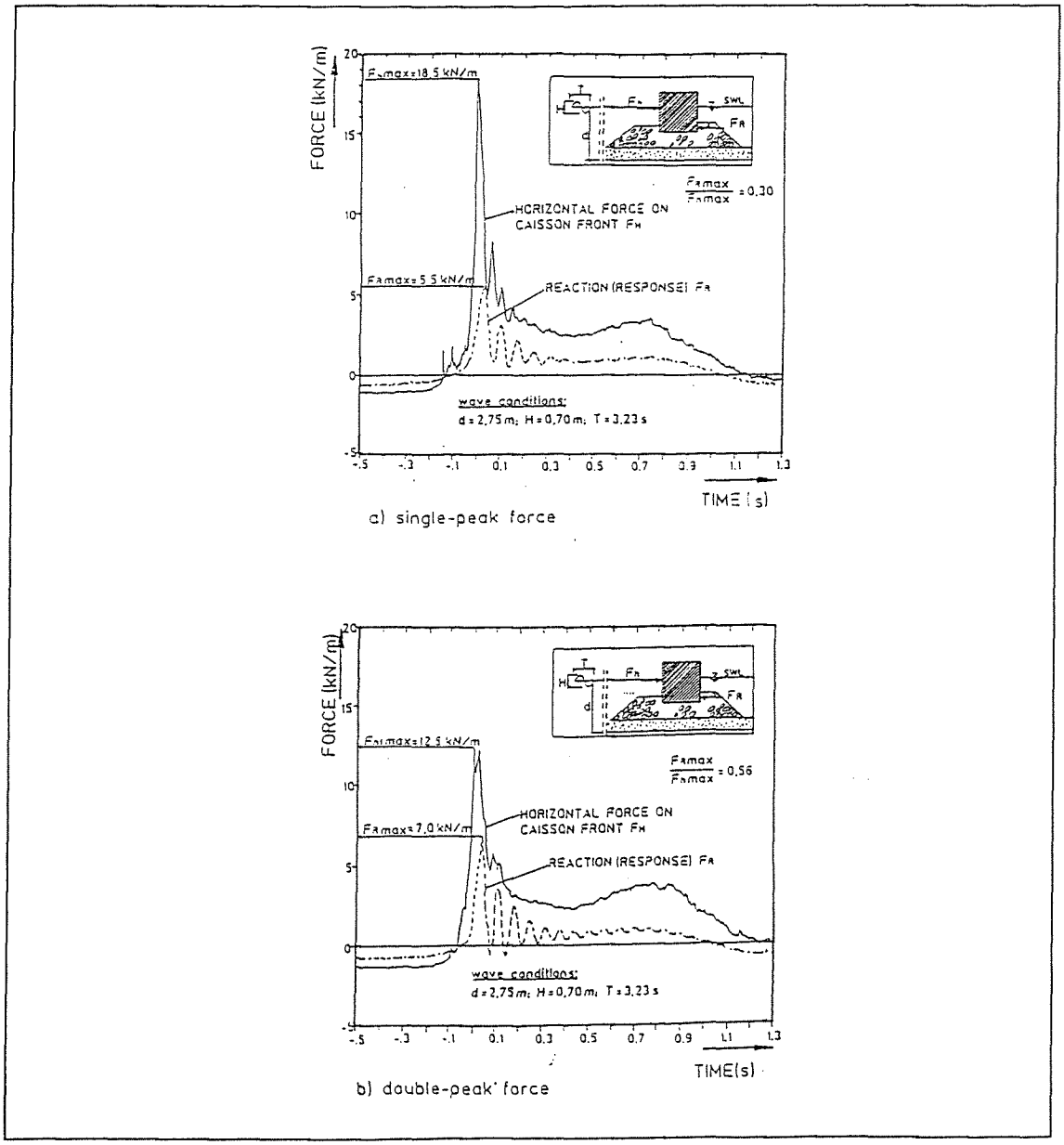

fig. 10.25 Influence of the shape of loading history on the structure response [OUMERACI (1991)]

10.6 Wave impact force with low frequency force oscillations

When a large amount of air is trapped between a well developed plunging breaker and the front wall of the vertical breakwater which is described in figure 10.1, low frequency force oscillations can occur due to the expanding and compressing of the large trapped air pocket.

The period of these force oscillations can be equal to one of the most dominant eigenperiods of the vertical breakwater as can be calculated with the equation which has been derived in chapter 5. The relationship between the period of pulsations T_{0w} (in seconds) and the incident wave height H (in cm) has been found to be:

$$T_{0w} = 0.75*10^{-3} * H \qquad (10.8)$$

The most dominant eigenperiod of the vertical breakwater which has been described by the use of the TILLY model is 0.845 s. So the wave height H needed is 11.27 m to cause low frequency force oscillations with a period of 0.845. This is more than the wave height which has been used in the calculations which have been carried out in the previous sections. But to demonstrate the effect of low frequency force oscillations due to large amounts of trapped air it is assumed that the period of the low frequency force oscillations of 0.845 s can occur near the vertical breakwater which has been described in figure 10.1.

According to Oumeraci et al. [OUMERACI et al. (1994)] the wave impact force loading history cannot be schematised anymore by a triangular load history as it has been done before in the previous sections if the maximum response of the vertical breakwater is of interest because of the fact that the actual wave impact load is now supposed to exhibit oscillations after the peak value which may excite the structure at quasi-resonance conditions.

A calculation has been made by the use of the TILLY model described in figure 10.1. The wave impact load with the low frequency force oscillations to which the vertical breakwater described in figure 10.1 will be exposed is described in figure 10.26. The wave impact has got a triangular load history with a peak force of 13422 kN/m and a duration of 12 ms (the first peak, this peak is schematised by a single peaked force for reasons of simplicity, while it could have been a double peaked force according to the previous section), followed by three periods of low frequency force oscillations (in total 3*0.845=2.535 s). The amplitude of these oscillation is approximated by 1678 kN/m (which is $^1/_8$ *13422 kN/m, approximately according to figure 5.15 on page 5 - 18), the minimum force of the low frequency force oscillations is 0 kN and the maximum force is 2*1678 = 3356 kN/m. Note that the scale of the sketch of the load history in figure 10.26 is distorted and that the sinusoidal low frequency oscillations are schematised by a saw-toothed force history.

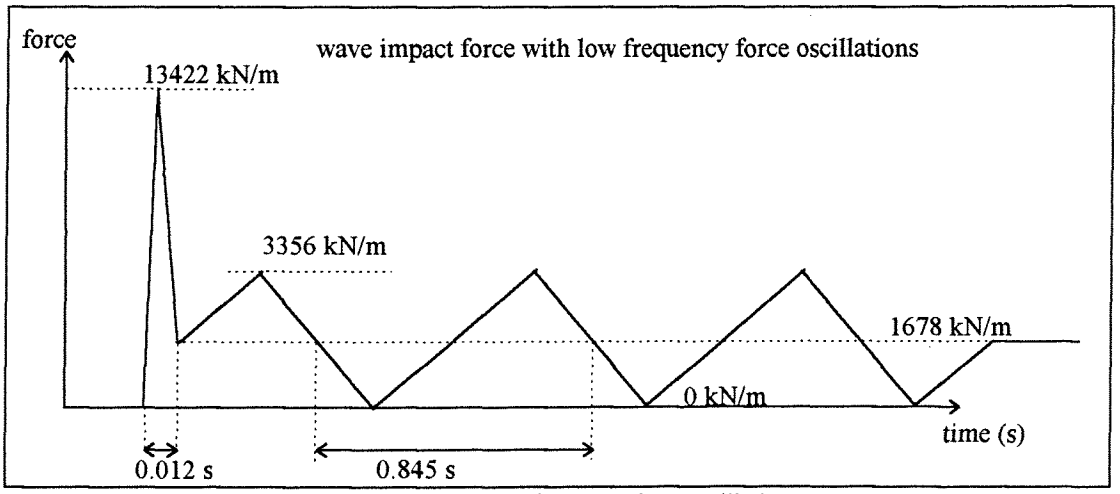

fig. 10.26 Wave impact force: a peak force with low frequency force oscillations

The wave impact with the low frequency force oscillations is assumed to act 2 m below Still Water Level just as it has been described in the previous section and can be seen in figure 4.4 on page 4 - 6. The results of this calculation of the load history described in figure 10.26 are plotted in figure 10.27. In figure 10.27 the response of a vertical breakwater exposed to only the first peak of the wave impact load history, so a wave impact with a triangular load history with a peak force of 13422 kN/m and a total duration of 12 ms is sketched as well for reasons of comparison.

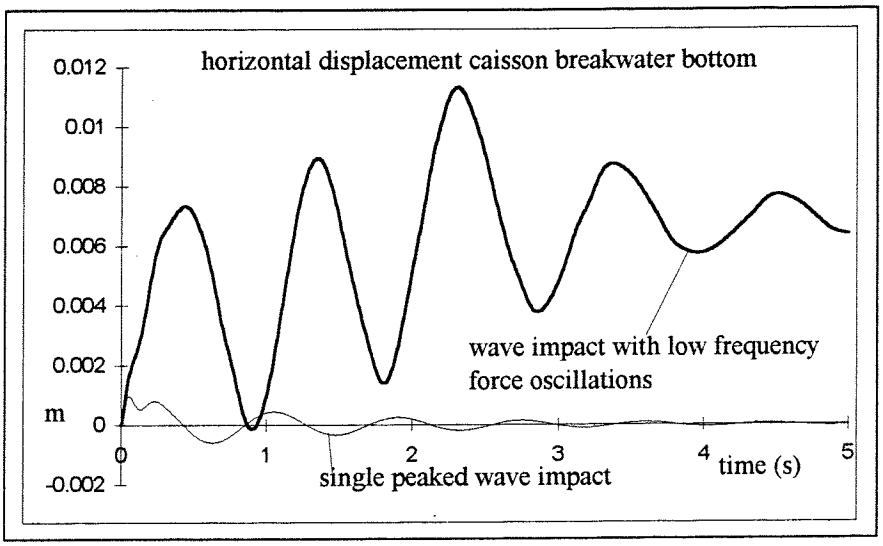

fig. 10.27 Horizontal displacement caisson breakwater bottom due to wave impact with low frequency force oscillations

As it can be seen in figure 10.27, the permanent displacement of the bottom of the vertical breakwater due to the wave impact described in figure 10.26, the wave impact peak force followed by low frequency force oscillations, is approximately 7.5 mm. The wave impact with only the single peaked force and the triangular load history does not cause permanent displacements. The maximum displacements do also differ a lot: the maximum displacement of the vertical breakwater which is exposed to the single peaked wave impact is approximately 1 mm, while the wave impact with the low frequency force oscillations causes a maximum displacement of approximately 11 mm. It can be concluded that the wave impacts with low frequency force oscillations after the first peak must be regarded as very dangerous. The occurrence of this kind of wave impacts should be prevented by changing the design of a planned vertical breakwater if this kind of wave impacts is likely to occur.

However, the wave impact load described in this section will very rarely occur.

Dr. Shigeo Takahashi told me:

"The low frequency force oscillations are not so important for practical design of vertical breakwaters, compared with the first and second peak of the force history of a wave impact caused by a plunging breaker because:

- the trapped air will leak out during compression and the oscillation will damp out (diminish soon)
- and this leakage will be encouraged due to short-crested waves and oblique waves, as well as wave overtopping. (Actually the low-frequency force oscillations can be large only in two dimensional experiments with a very high crown wall.)"

In my opinion this kind of wave impact load should not be neglected, especially not in the case where the sections of the vertical breakwater (the individual caissons) are not placed accurately relative to each other or due to other reasons (other kinds of loads on the vertical breakwater) shifted relative to each other (see figure 10.28).

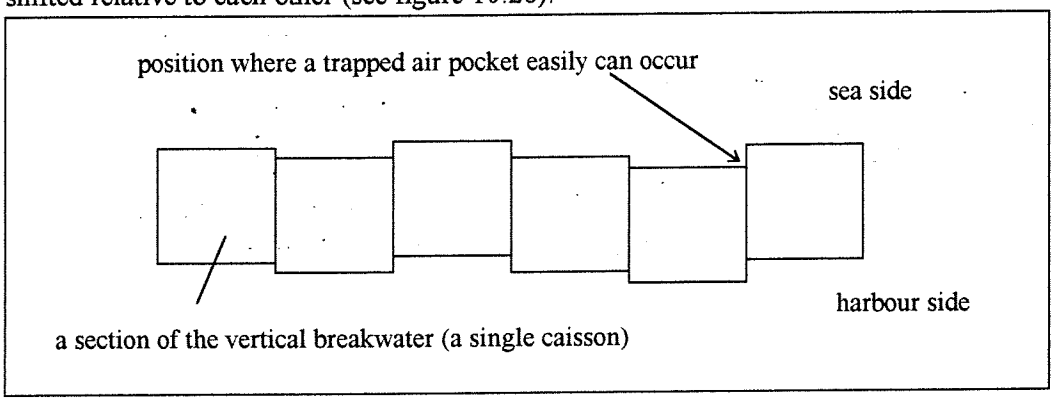

fig. 10.28 Caissons shifted relative to each other

It is very likely that a wave impact with low frequency force oscillations will occur at the spot indicated in figure 10.28, because a large trapped air pocket can be formed relatively easy and the air can not leak out because of the vertical concrete walls of the caissons at that spot. This will cause the breakwater to slide even more and a kind of domino effect may occur, which can end in displacements of several meters.

The same phenomenon can probably occur at the intersection of two vertical breakwater alignments, see figure 10.29.

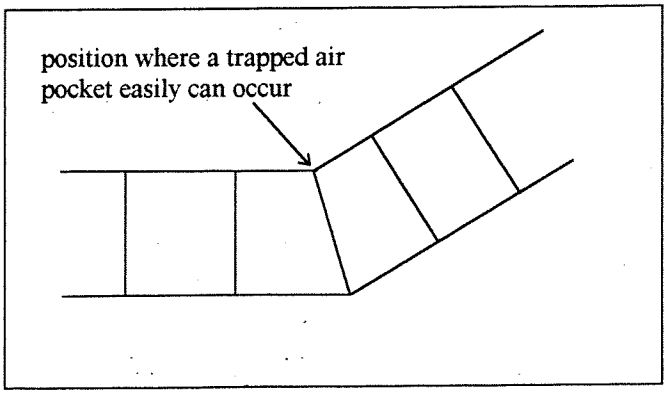

fig. 10.29 Intersection of two breakwater alignments

11 Conclusions and recommendations

11.1 Introduction

In this chapter, the final chapter, the conclusions and the most important results of this study on wave impacts on vertical breakwaters will be presented. Throughout the whole report conclusions and interim results have been presented by using the results of: an extensive study of literature, own findings and the calculations which have been carried out by means of a mass-(elasto-plastic)spring-dashpot computer model of a vertical breakwater which is exposed to wave impacts. This computer model of a vertical breakwater has been used to study the effect of the variation of the different dynamical properties of a vertical breakwater (e.g. masses, mass moment of inertia, stiffness and damping) and the effect of different types of wave impacts.

In this chapter a summary of the most important conclusions and results can be found in section 11.2. Some of these conclusions do end up in recommendations which should - in my opinion - be taken into account when vertical breakwaters are designed. These recommendations will be formulated in section 11.3. Despite the research which has been carried out within the framework of this graduation project a lot of gaps remain open. Therefore, some recommendations for future research will also be given, these can be found in section 11.3 as well.

11.2 Conclusions and results

This study, which has been carried out within the framework of a graduation project at the faculty of Civil Engineering of the Delft University of Technology, has put forward the following conclusions:

- The shape of the breaking waves considerably influences the resulting impact force histories. There is not one type of wave impact. Three types of wave impacts on breakwaters with a plane vertical front wall can be distinguished:
  1. Wave impacts of the *Wagner* type: caused by upward deflected breakers, no air is trapped between the breaker and the plane vertical front wall of a breakwater.
  2. Wave impacts of the *transition* type: caused by breaking waves of the plunging type with an almost vertical front at the instant of the impact: a small amount of air is trapped between the breaking wave and the plane vertical front wall of a breakwater. This type of wave impact causes a very high (single peaked) force with a small total duration. This type of wave impacts gives the highest total horizontal peak force on vertical breakwaters.
  3. Wave impacts of the *Bagnold* type: caused by well-developed plunging breakers, a large amount of air is trapped between the breaking wave and the plane vertical front wall of a breakwater. This type of wave impact causes a (double peaked) force which can be followed by low frequency force oscillations caused by the cyclic compression and expansion of the large amount of trapped air under highly transient pressure fields. The period of these low frequency force oscillations is related to the amount of trapped air: the period increases if the amount of trapped air increases. The second peak of the double peaked wave impact force, which is in fact the first peak of the low frequency force oscillations is more likely to occur in nature than the low frequency force oscillations, which will probably diminish soon in most cases due to the leaking out of air.
- The upper limit of wave impact pressures can be found by using the shock wave model.

- The derivation of different horizontal wave impact force prediction formulae has been treated using the consideration of momentum of a wave which breaks onto a plane vertical front wall of a vertical breakwater. These formulae (see equation 4.19 and equation 4.31) do all give conservative results. Horizontal wave impact forces will most likely always be smaller in magnitude.

- The larger the amount of trapped air between a breaking wave and the plane vertical front wall of a breakwater, the longer the rise time of a wave impact and the smaller the peak force of this wave impact

- If a horizontal wave impact force prediction formulae is used which has been derived by using the consideration of momentum of a wave which breaks onto a plane vertical front wall of a vertical breakwater and if a triangular wave impact load history is assumed, then the largest amount of momentum of two wave impacts with the same total duration can be expected for the wave impact with the shortest rise time because this wave impact gives the highest impact force and will thus represent the largest amount of momentum since the total duration is equal. The latter wave impact will be the most dangerous of the two for the stability of a vertical breakwater. The amount of momentum is one of the governing properties of a wave impact load concerning the stability of a vertical breakwater. Another important characteristic of a wave impact is the relation of t_r and / or t_d to the eigenperiod(s) of a vertical breakwater.

- Goda [GODA (1994)] suggests that there is a maximum force of wave impacts which is $F_{h,\max} = 15 * \rho_w * g * H_b^2$. Numerous measurements of small scale and large scale hydraulic models have been investigated. The conclusion of Goda can be confirmed. Although a very few impacts were found which gave a slightly larger force.

- It is well accepted that wave impact forces in small scale hydraulic model tests will be greater in magnitude, but shorter in duration than their equivalents at full-scale in invariably aerated sea water. Compression of trapped air by breaking waves and subsequent oscillations of air bubbles give model scales which deviate from Froude's scale law. Impact loads converted by Froude scaling will over-estimate full-scale loads and will therefore give an upper limit to the impact force to be expected. By means of the results of hydraulic scale model tests it has been shown that lower impact forces can be expected from sea water wave impacts than from similar fresh water wave impacts.

- It has been shown that the low frequency force oscillation after a (double peaked) wave impact force which is caused by wave impacts with a large trapped air pocket (Bagnold type wave impacts) is a phenomenon purely caused by a breaking wave itself. The period of these low frequency force oscillations is proportional to the wave height. The period of the low frequency force oscillations must be transferred form a hydraulic scale model to full-scale situations by multiplying the hydraulic scale model value by a length scale instead of the square root of a length scale (the latter is according to the Froude scaling law).

- A mass-(elasto-plastic)spring-dashpot computer model of a vertical breakwater has been derived which can be used to describe the dynamical behaviour of a vertical breakwater which is exposed to wave impacts. A description of this model can be found in chapter 8 in figure 8.11. The main sources of uncertainty of the calculations which have been carried out by the use of the model of the vertical breakwater which has been derived in this study are:
  1. The dynamical properties of the vertical breakwater and its foundation:
     - the masses and mass moment of inertia of the vertical breakwater
     - the stiffness of the foundation soil
     - the strength of the foundation soil and the magnitude of the Coulomb friction coefficient
     - the damping of the foundation soil
  2. The type of wave impact load and its most relevant characteristics

- The influence of the magnitude of the different parameters of the model of the vertical breakwater (which is described in chapter 8 in figure 8.11) on its dynamical behaviour and stability has been studied by subsequently varying one of the parameters while remaining all other parameters constant, including the wave impact load to which the breakwater is exposed. This parameter study of the mass-(elasto-plastic)spring-dashpot computer model has proved that especially the masses and mass moment of inertia and the stiffness of the foundation are detrimental for the maximum response and the stability of the investigated vertical breakwater:
  1. The effect of increasing the stiffness of the foundation is that the maximum response of the vertical breakwater decreases. However, if the strength of the soil is not changed increasing of the stiffness of the foundation will enlarge the danger of foundation failure (i.e. exceeding the maximum bearing capacity of the foundation soil of the vertical breakwater). It can be concluded that a stiff foundation soil is unfavourable for the stability of caisson breakwaters, it yields the highest sensitivity to wave impacts.
  2. Changing the strength of foundation or the Coulomb friction coefficient may change the fact which of the investigated failure mechanisms of the vertical breakwater (sliding or foundation failure) is the most probable failure mechanism.
  3. The maximum response of the vertical breakwater which is exposed to wave impacts is almost not affected by the variation of the damping of the foundation.
  4. A large mass of a vertical breakwater is favourable for its stability. The larger the mass the smaller the (maximum) response of the breakwater. In this respect is must be stated that it is very unwise to design a vertical composite breakwater with a high rubble mound with a small width and only a small upright section placed on it. If this vertical breakwater is exposed to the same wave impacts as a basic vertical breakwater placed on a thin rubble mound foundation (and with a large mass) it has got a higher probability of failure. If the upright section of a vertical (composite) breakwater is placed on a high rubble mound, this rubble mound must have a large width to ensure the fact that the breaking wave conditions onto the vertical wall of the breakwater change relative to the design without a high rubble mound (smaller breaking waves onto the vertical front wall of the upright section).

- The formula of Schmidt et al. [SCHMIDT et al. (1992)] (see equation 4.21) is the most widely used horizontal wave impact force prediction formula within the MAST project. This formula can be used to describe wave impacts of the transition type. For the benefit of the analysis of this formula which has been presented in this study it has been assumed that the rise time of the wave impact is the half of the total duration of the wave impact for all loading conditions. For the vertical breakwater which has been investigated in this study (see chapter 8 in figure 8.11) the eigenperiod of the horizontal oscillation is the most dominant period of oscillation. Using the formula of Schmidt et al. [SCHMIDT et al. (1992)] wave impacts with a duration equal to this dominant period of oscillation of the investigated vertical breakwater will yield the largest response, although the maximum wave impact force belonging to this duration (according to the formula of Schmidt et al. [SCHMIDT et al. (1992)]) is small compared to wave impacts with an extremely short duration of say milliseconds. According to the formula of Schmidt et al. [SCHMIDT et al. (1992)] one cannot say which wave impact is the most dangerous one for the stability (stability against sliding and foundation failure i.e. exceeding the bearing capacity of the foundation soil) of a vertical breakwater. The most dangerous wave impact can only be determined if the dynamical properties of the vertical breakwater which is exposed to wave impacts are known.

- For prototype scale, wave impacts of the transition type with very high peak forces and very short total durations were found not to be dangerous for the stability of the vertical breakwater which has been investigated in this study (see chapter 8 in figure 8.11). For the investigated vertical breakwater this was the case for wave impacts with a total duration smaller than 9.5% of the most dominant period of oscillation of the vertical breakwater (using the formula of Schmidt et al. [SCHMIDT et al. (1992)] with T_p = 12 s and H_b = 10 m). It has been shown that for the investigated vertical breakwater a wave impact of 12 ms with a triangular load history (it is assumed that the rise time is the half of the total duration of the wave impact) and a peak force of 13422 kN/m is only felt for approximately 4.5 - 6.5% in the foundation soil of the vertical breakwater. Nevertheless, a lot of hydraulic scale model tests are being carried out all over the world just to measure the very high peak forces with the very shorts durations even more accurately. These measurements seem not to be very relevant for the over-all dynamical stability analysis of a vertical breakwater.

- For the maximum dimensionless wave impact force of 15, the investigated vertical breakwater (see chapter 8 in figure 8.11) is safe against sliding and foundation failure (i.e. exceedance of the bearing capacity of the foundation soil) for a wave impact with a total duration smaller than 37 ms, assuming H_b = 10 m.

- Of two wave impacts which both represent the same amount of momentum, the wave impact with the shortest rise time and / or total duration has been found to cause the largest response of the vertical breakwater even if the wave impact with the longest duration has got a total duration equal to the most dominant period of oscillation of the vertical breakwater (this is the eigenperiod of horizontal oscillation in the case of the investigated vertical breakwater in this study, see chapter 8 in figure 8.11).

- Two phenomena of the Bagnold type wave impact have been studied for the vertical breakwater which can be found in chapter 8 in figure 8.11:
  1. *Double peaked wave impacts* can be dangerous when second peak occurs within such an interval that the structure is moving in the same direction as the direction of the wave impact (i.e. while the vertical breakwater is moving shoreward). The cumulative maximum response is higher than if only a single impact occurred or if the second peak would occur while the vertical breakwater is moving in the direction of the open sea.
  2. If the period of the low *frequency force oscillations* (due to a large air pocket which is trapped between a breaking wave of the Bagnold type and the plane vertical front wall of the breakwater) is in the range of the most dominant eigenperiod of the vertical breakwater resonance or near resonance phenomena occur. The consequence is that large permanent displacements of the vertical breakwater are possible if it is exposed to such a wave impact. However, this wave impact loading type will rarely occur on a long plane vertical front wall of a vertical breakwater and it seems to be a loading case which can typically be found in two dimensional hydraulic scale model tests. However, large trapped air pockets which cause low frequency force oscillations can occur at the intersection of two breakwater alignments or when different individual caissons of a vertical breakwater are shifted relative to each other.

- Two failure mechanisms of the investigated vertical breakwater have been treated extensively: sliding and foundation failure. If foundation and structure parameters are chosen in accordance with full-scale situations (see chapter 8 in figure 8.11) then foundation failure i.e. exceeding of the maximum bearing pressure of the foundation soil (approximately 600 kN/m^2) is more probable than sliding of the vertical breakwater over its rubble mound foundation (if a Coulomb friction coefficient of 0.6 is used) under wave impact loading conditions.

- Changing the dynamical properties of a vertical breakwater may be a solution to make a vertical breakwater more stable against sliding or foundation failure. Increasing the mass of a vertical breakwater and decreasing the stiffness of the foundation are the most effective solutions to make a vertical breakwater more safe against wave impacts, because the maximum response of the vertical breakwater will decrease. However, changing the dynamical properties of a vertical breakwater can have contradictory effects. So if one wants to design a safe vertical breakwater one must be very careful when changing the magnitude of the parameters which represent the vertical breakwater and its foundation. For instance:
  1. Decreasing the stiffness of the foundation, which is favourable for the stability of a vertical breakwater against wave impacts, may result in a vertical breakwater which is less stable against quasi-static loads because of the fact that the eigenperiods of the vertical breakwater increase when the stiffness of the foundation decreases.
  2 However, a foundation soil with a low stiffness will probably have a smaller strength compared to a stiff foundation soil.
  3. The initial pressure in the foundation soil of the vertical breakwater will increase if the mass of the vertical breakwater is increased without changing the dimensions of the vertical breakwater. This is unfavourable for the stability of the vertical breakwater against foundation soil failure.
  4. However, according to the Mohr-Coulomb model, the strength of the foundation soil will increase if the magnitude of the load on the foundation soil is increased.

Returning to the question which has been presented in chapter 1 on page 1 - 3 and page 1 - 5 (*"Are wave impacts important for the stability of vertical breakwaters?"*) the following answers can be given:

- **Wave impacts with a very short total duration relative to the eigenperiod(s) of a vertical breakwater are not important for the stability of a vertical breakwater (stability against sliding and exceeding of the maximum bearing pressure of the foundation soil) because the total amount of momentum of the breaking wave is to small. For the investigated vertical breakwater (see chapter 8 in figure 8.11) the following results have been found in this study:**
  1. **Using the formula of Schmidt et al. [SCHMIDT et al. (1992)] with T_p = 12 s and H_b = 10 m, wave impacts with a total duration t_d smaller than 80 ms are not dangerous for the stability of the vertical breakwater (80 ms is 9.5% of the eigenperiod of horizontal oscillation (T = 0.85 s) of the vertical breakwater).**
  2. **Using the maximum horizontal wave impact force ($F_{h,max}$ =15*ρ_w*g*H_b^2 N/m) with H_b = 10 m, wave impacts with a total duration t_d smaller than 37 ms are not dangerous for the stability of the vertical breakwater (37 ms is 4.4% of the eigenperiod of horizontal oscillation (T = 0.85 s) of the vertical breakwater).**

- **However, a lot of research all over the world is carried out just to measure these wave impacts with very short total durations. These measurements do not seem to be very relevant for the over-all dynamical stability analysis of a vertical breakwater. In my opinion these measurements seem to be unwise and a waste of money.**

- **The stability of a vertical breakwater against wave impacts does entirely depend on the type of wave impact load (rise time, total duration, magnitude of the peak force, amount of trapped air) and the dynamical properties of a vertical breakwater and its foundation soil (masses, mass moment of inertia, stiffness and damping). The maximum peak force of a wave impact does not necessarily induce the maximum dynamical response. Wave impacts with relatively low peak forces (relative to $F_{h,max}$ =15*ρ_w*g*H_b^2 N/m) and long total durations (relative to the eigenperiod(s) of a vertical breakwater), double peaked wave impact forces and wave impacts with low frequency force oscillations have proved to be more dangerous for the stability of a vertical breakwater. The amount of momentum is one of the governing properties of a wave impact load concerning the response and stability of a vertical breakwater. The suggestion commonly found in the literature that impacts are totally not significant and should not be used for the design of vertical breakwaters could not be confirmed.**

11.3 Recommendations

Recommendations which can be used for the design of vertical breakwaters:

- In the design phase of a vertical breakwater a lot of attention should be paid to the occurrence of wave impacts and their relation to the dynamical properties of the vertical breakwater and its foundation in order to design a safe and reliable vertical breakwater. The types of wave impacts which are to be expected and the dynamical properties of the planned vertical breakwater determine the effect of wave impacts on the (dynamical) behaviour of the vertical breakwater. Knowing these wave impacts: rise times, total durations and peak forces and the dynamical properties of a vertical breakwater which has been designed, the effect of different wave impacts can be indicated. A dynamic analysis of the behaviour of a vertical breakwater by means of a mass-(elasto-plastic)-spring-dashpot model should in my opinion become a necessary part of the design process for caisson breakwaters which are exposed to breaking wave loads. The results of the analysis of the dynamical behaviour of the designed vertical breakwater can be used to adapt the actual vertical breakwater to the wave impacts which are to be expected. Uncertainties concerning the type of the wave impact loads on, and the dynamical properties of a vertical breakwater which is the subject of a design study can be reduced by performing large-scale hydraulic model test and / or full-scale measurements (site investigations).

- Wave impact forces are very complicated functions of the wave conditions and the geometry of the structure. Different types of wave impacts can be distinguished. Each type of wave impact has got different effects on the dynamical behaviour and stability of breakwaters with plane vertical front walls (i.e. the type of vertical breakwater which has been used in this study). So, it is very import to investigate which kinds of wave impacts are to be expected at a site where a vertical breakwater is planned to be built. It is therefore recommended to perform hydraulic scale model tests, at least for the final design of important (expensive) vertical breakwaters. These hydraulic scale model tests should be performed in a large and stiff hydraulic scale model in order to partly overcome scaling problems. In these hydraulic scale model tests a lot of attention should be paid to the wave impacts with relatively long durations and low peak forces. Because of the fact that, for instance, wave impacts with a total duration which is in the range of the dominant eigenperiod of oscillation of a vertical breakwater have proved to be very dangerous for its stability. To do research on the subject of the duration of wave impacts seems to be very interesting and necessary. The wave impacts with high peak forces but very short durations (relative to the dominant eigenperiod of oscillation of the vertical breakwater) were found no to be dangerous for the stability of a vertical breakwater. However a lot of attention is being paid to the latter in hydraulic scale model test. This seems to be wasted time. It seems to be not necessary to do research on the subject of wave impacts with durations shorter than say 10% of the most dominant eigenperiod of the vertical breakwater

- Uncertainties concerning the dynamical properties of the vertical breakwater and its foundation itself can be reduced by site investigations. The results of these site investigations can be used to make a reliable estimation of the stiffness and damping of the foundation. An important parameter which has to be investigated thoroughly is the Coulomb friction coefficient. For example: a low friction coefficient will make sliding the most probable failure mechanism instead of failure of the foundation (i.e. exceeding of the bearing capacity of the foundation soil) which has found to be the most probable failure mechanism of a vertical breakwater in this study.

- If the analysis by the use of a mass-(elasto-plastic)spring-dashpot model will indicate that wave impacts will be threatening the stability of a breakwater with a plane vertical front wall, then the dynamical properties of the structure and foundation can be adapted to a situation in which wave impacts will not be threatening its stability. However, this adaptation (replacing for instance the stiffness of the foundation or the mass of the vertical breakwater by changing the existing foundation soil by another type of foundation soil) is possible within certain bounds as has been indicated in this report. Other possibilities to make a vertical breakwater safe against wave impacts may then become interesting such as: armour blocks (natural and / or artificial) in front of the vertical wall of a caisson breakwater, a sloping top of the caisson, a perforated front wall. These construction alternatives are usually more expensive than a caisson with a rectangular shaped cross-section. An economical analysis will have to indicate which alternative may be the most promising one.

- If the upright section of a vertical (composite) breakwater is placed on a high rubble mound, this rubble mound must have a large width to ensure the fact that the breaking wave conditions onto the vertical wall of the breakwater change relative to the design without a high rubble mound (smaller breaking waves onto the vertical front wall of the upright section)

- Spots where large trapped air pockets are to be expected have been indicated in chapter 10 (see figure10.28 and figure 10.29) and have to be prevented because of the fact that at these spots Bagnold type wave impacts can easily occur. Bagnold type wave impacts have proved to be very dangerous for the stability of vertical breakwaters.

Some recommendations for future research:

<u>The most important recommendations for future research are in my opinion:</u>

- In this study uplift forces were assumed to be constant in time for different wave loading conditions. It has been stressed that this is a usefull approximation for the relatively simple analysis which has been carried out in this study. However, in reality uplift forces are not constant in time and they vary for different wave (impact) loading conditions. Uplift forces should not be neglected in the final design phase of a vertical breakwater, they should be taken into account in a dynamical stability analysis of a vertical breakwater. Full-scale measurements of uplift forces under breaking wave conditions seems the only way to overcome the large scaling problems concerning uplift forces in hydraulic scale model tests. Factors of influence of uplift forces are the permeability and the geometry of the rubble mound.

- It is interesting to do more research on the subject of the occurrence of wave impact loads. As could be seen in figure 4.10 there is still not a very reliable statistical distribution of wave impact forces. The return period of the most dangerous wave impact forces (a combination of a peak force and a total duration or rise time) may be an important parameter in a probabilistic design approach of vertical breakwaters.

- There is still a lot of work to do on the subject of scaling of wave impact loads, for instance the effect of the salinity of the water on the magnitude, the rise time and the total duration of wave impact forces and the effect of the stiffness of the scale models which are used.

- Wave impacts with long total durations (relative to the eigenperiod(s) of a vertical breakwater) but relatively low peak forces (relative to $F_{h,max}=15*\rho_w*g*H_b^2$) have proved to be very dangerous for the stability of vertical breakwaters. Especially wave impacts with total durations which may lie in the range of the most dominant eigenperiod of the oscillation of a vertical breakwater. It is detrimental to do a lot of research (large hydraulic scale model tests) on the subject of wave impacts with relatively long durations. It seems to be wasted time to do more research on the subject of wave impacts with durations shorter than say 10% of the most dominant eigenperiod of the vertical breakwater which has to be investigated.

Other recommendations for future research are:

- In this study it has been assumed that the wave impacts act over the total length of the vertical breakwater, the waves which cause the wave impacts were assumed to be long-crested. This is a conservative assumption. Attention should be paid the effect of short-crested waves. Reviewing short-crested waves may lead to a load reduction on the vertical breakwater.

- It is interesting to study the effect of water level differences between the sea-side and the harbour-side of a vertical breakwater. In relation to this it is the influence of the horizontal tide on the stability of a vertical breakwater is a very interesting point of research. The tide may influence the buoyant forces as well as the conditions of the breaking waves onto the plane vertical front wall of the breakwater.

- It is interesting to investigate the interface of the concrete bottom slab of a vertical breakwater and its (rubble mound) foundation. Interesting questions to solve are which processes do take place when a vertical breakwater slides or when the maximum bearing capacity of the foundation soil is exceeded.

- Liquefaction of the foundation soil due to the storage of pore pressures or residual pore pressures may be an important failure mechanism of vertical breakwaters. Research on this subject is difficult but may be important.

- The effect of cyclic wave impact loading on the vertical breakwater has not been investigated. Cyclic wave impact loading may for instance lead to a different behaviour of the foundation soil and may lead to totally different conclusions concerning the stability of a vertical breakwater

- It is interesting to find a reliable relationship between the stiffness of the foundation soil and the maximum bearing capacity of the foundation soil which has in this study been derived using the theory of Brinch Hansen.

- Research on alternative foundations of vertical breakwaters, for instance foundation on piles, seems to be interesting in relation to the stability of vertical breakwaters.

- The vertical breakwater has been assumed to be rigid. The effect of the rigidity of the concrete caisson on its dynamical behaviour under wave impact conditions is an interesting point to investigate.

- It may be possible to extend the mass-(elasto-plastic)spring-dashpot TILLY model which has been derived in this study to include more failure mechanisms. So far only sliding of the vertical breakwater over its rubble mound foundation and exceedance of the bearing capacity of the foundation soil have been taken into account. Seaward tilting of the vertical breakwater has been neglected but can be examined by the use of the TILLY model as well. Only a different loading situation has to be implemented in the programme listing.

- Local failure can lead to overall failure of a vertical breakwater. Rupture of the concrete front wall of a vertical breakwater of the caisson type may have the consequence that the fill will flow out of the cells of the caisson. The consequence is that the weight of the caisson decreases and that overall failure such as sliding of the caisson may occur. Thus, it is evident that local failure modes must be investigated as well.

- A vertical breakwater consists of individual caissons. In stability calculations it is assumed that these individual caissons are not connected: the individual caissons cannot transfer forces to each other. It is to be expected that when individual caissons are connected that the total stability of the connected caissons will increase. It is interesting to study the reliability of this idea.

- The reliability of the extension of the Goda formula by Takahashi, concerning wave impacts, must be investigated. A comparison between the results of this quasi-static approach of wave impacts and the dynamical approach of wave impacts as it has been presented in this study is an interesting subject.

References

ALLSOP, N.W.H., VICINANZA, D. and MCKENNA, J.E. (1996) *"Wave forces on vertical and composite breakwaters"* Report SR 443. Hydraulics Research, Wallingford, United Kingdom

BAGNOLD, R.A. (1939) *"Interim report on wave pressure research"*. Journal of the Institution of Civil Engineers Vol. 12 pp. 202-226. Institution of Civil Engineers, Londen, United Kingdom

BATTJES, J.A. (1990) *"Vloeistofmechanica"* lecture notes B70 (in Dutch). Delft University of Technology, Delft, the Netherlands

BATTJES, J.A. (1993) *"Korte golven"* lecture notes B76 (in Dutch). Delft University of Technology, Delft, the Netherlands

BURCHARTH, H.F., J. DALSGAARD SØRENSEN and CHRISTIANI, E. (1994) *"On the Evaluation of Failure Probability of Monolithic Vertical Wall Breakwaters"*. Proceedings second workshop MCS-project, Milan, Italy

CERC (1984) *"Shore protection manual"* fourth edition. U.S. Government Printing Office, Washington, D.C. 20402, United States of America

COOKER M.J. and PEREGRINE D.H. (1990) *"Computations of violent motion due to waves breaking against a wall"*. A.S.C.E., Proceedings of the 22nd International Conference on Coastal Engineering, pp. 164-176, Delft 1990. Delft, the Netherlands

CUR/RIJKSWATERSTAAT (1995) *"Manual on the use of rock in hydraulic engineering"* CUR/Rijkswaterstaat publication 169. Centre for civil engineering research and codes, Gouda, the Netherlands

DELFT HYDRAULICS (1979) *"Golfklappen: een literatuuroverzicht en schaaleffecten in modelonderzoek"* stormvloedkering Oosterschelde, verslag studie M 1335 deel III (in Dutch). Delft Hydraulics, Delft, the Netherlands

DELFT HYDRAULICS (1982) *"Civitavecchia Harbour, Italy; Three-dimensional tests on the stability of the breakwater"* report on model investigations, M1869 Volume I. Delft Hydraulics, Delft, The Netherlands

DELFT HYDRAULICS (1993) *"Wave impacts on a circular and square caisson"*. Prepared for MAST II, Monolithic (Vertical) Coastal Structures Commission of the European Communities. Delft Hydraulics, Delft, The Netherlands

DELFT HYDRAULICS (1994) *"Dynamisch gedrag van waterbouwkundige constructies bij stroming en golfklappen; deel B: Constructies in golven"* concept, 21 september 1994 (in Dutch). Delft Hydraulics, Delft, the Netherlands

DELFT HYDRAULICS (1995) *"Dynamisch gedrag van waterbouwkundige constructies bij stroming en golfklappen; deel C: Methoden van rekenen en experimenteel onderzoek"* concept, 27 februari 1995 (in Dutch). Delft Hydraulics, Delft, the Netherlands

DIETERMAN, H.A., SPIJKERS, J., KLAVER E. and VROUWENVELDER A. (1993) *"Dynamica van constructies"* deel 2, lecture notes B9 (in Dutch). Delft University of Technology, Delft, the Netherlands

DIETERMAN, H.A. (1994) *"Algemene Mechanica II"* deel II inleiding Dynamica van Constructies, lecture notes B8 (in Dutch). Delft University of Technology, Delft, the Netherlands

FÜHRBÖTER (1969) *"Laboratory investigation of impact forces"* preprints, symposium on research on wave action. Delft, the Netherlands

GODA, Y. (1985) *"Random seas and design of maritime structures"*. University of Tokyo press, Tokyo, Japan

GODA, Y. (1992) *"The design of upright breakwaters"*. Design and reliability of coastal structures, proceedings of the short course on design and reliability of coastal structures. Venice, Italy

GODA, Y. (1994) *"Dynamic response of upright breakwaters to impulsive breaking wave forces"*. Coastal Engineering 22 (1994) pp. 135-158. Elsevier Science B.V., Amsterdam, the Netherlands

GROOT, M.B. DE (1996) *"Desired wave force information for foundation design"* (prepared for task 1 group of MAST III/PROVERBS) June 1996. Delft Geotechnics, Delft, the Netherlands

HAILE, A. (1996) *"Probabilistisch Ontwerpen van Verticale Golfbrekers"* (in Dutch). MSc thesis, Delft University of Technology, Delft, The Netherlands

HATTORI, M., ARAMI, A and YUI, T (1994) *"Wave impact pressure on vertical walls under breaking waves of various types"*. Coastal Engineering 22 (1994) pp. 79-114. Elsevier Science B.V., Amsterdam, the Netherlands

KINSMAN, B., (1965) *"Wind waves, their generation and propagation on the ocean surface"*. Prentice Hall, Incorporated, Englewood Cliffs, New Jersey, United States of America

KLAMMER, P. KORTENHAUS, A. and OUMERACI, H. (1996) *"Wave impact loading of vertical face structures for dynamic stability analysis - prediciton formulae -"* Leichtweiß-Institut, TU Braunschweig, Braunschweig, Germany

KOLKMAN, P.A. (1992) *"Maximale golfdrukken volgens stromingsdrukmodel, schokgolfmodel en waterpistonmodel"* Notitie SL1 in Notities van P.A. Kolkman in de periode 1969-1990 (in Dutch). Delft Hydraulics, Delft, the Netherlands

KORTENHAUS, A., OUMERACI, H., KOHLHASE, S. and KLAMMER, P. (1994) *"Wave Induced Uplift Loading of Caisson Breakwaters"*. A.S.C.E., Proceedings of the 24th International Conference on Coastal Engineering (I.C.C.E.), pp. 1298-1311, Kobe 1994. Kobe, Japan

KORTENHAUS, A., C. MILLER and OUMERACI, H., (1996) *"Design of vertical walls against storm surge"*. Leichtweiß-Institut, TU Braunschweig, Braunschweig, Germany

LAMB, H. (1932) *"Hydrodynamics"* sixth edition. pp. 31-61. Cambridge University Press, Londen, United Kingdom

LAMBERTI, A. and MARTINELLI, L. (1996) *"Verification by prototype measurements, preliminary phase"*. University of Bologna, Bologna, Italy

LUNDGREN, H. (1969) *"Wave shock forces: an analysis of deformation and forces in the wave and in the foundation"* Proceedings of the Symposium on Research on Wave Action, Vol. 2, paper 4. Delft Hydraulics, Delft, the Netherlands

MASSIE, W.W., AGEMA, J.F., BIJKER, E.W., LOO, L.E. VAN and PAAPE, A. (1986) *"Coastal Engineering, volume III Breakwater design"* lecture notes F5. Delft University of Technology, Delft, the Netherlands

MAST II MSC (1995) *"Monolithical Vertical Structures"* Annex I General Document Foundation Design of Caisson Breakwaters.

MITSUYASU, H. (1962) *"Experimental study on wave force against a wall"*. Coastal Engineering in Japan, Vol. 5, pp. 23-47, 1962. Tokyo, Japan

MARINSKI, J.G. and OUMERACI, H. (1992) *"Dynamic Response of Vertical Structures to Breaking Wave Forces - Riview of the CIS Design Experience"*. A.S.C.E., Proceedings of the 23rd International Conference on Coastal Engineering, pp. 1357-1370, Venice 1992. Venice, Italy

MURAKI, Y. (1966) *"Field investigations on the oscillations of breakwaters caused by wave action"*. Coastal Engineering in Japan, Vol. 9, 1966. Tokyo, Japan

OUMERACI, H. (1991) *"Dynamic loading and response of caisson breakwater - results of large-scale model tests"*. Franzius-Institut, University of Hannover, Hannover, Germany

OUMERACI, H. (1994) *"Review and analysis of vertical breakwater failures - lessons learned"*. Coastal Engineering 22 (1994) pp. 3-29. Elsevier Science B.V., Amsterdam, the Netherlands

OUMERACI, H (1994a) *"Multi-disciplinary research experience in Europe on vertical breakwaters"*. Proceedings of the international workshop on Wave Barriers in Deep Waters, January 10-14, 1994, pp. 267-278. Port and Harbour Research Institute, Ministry of Transport, Nagase, Yokosuka, Japan

OUMERACI, H. and PARTENSCKY, H.W. (1991) *"Breaking Wave Impact Loading of Vertical Structures - Effect of Entrapped Air on Structure Response"* . Paper 8 in the proceedings of the first workshop on project 2 : Wave impact loading of vertical structures, MAST G6-S

OUMERACI, H., PARTENSCKY, H.W. and TAUTENHAIN, E. (1992) *"Breaking wave loads on vertical gravity structures"*. Proceedings of the 2nd International Conference of Offshore and Polar Engineering, ISOPE'92, Volume 3, pp. 532-539. San Francisco, United States of America

OUMERACI, H., PARTENSCKY, H.W. KOHLHASE, S. and KLAMMER, P. (1992a) *"Impact loading and dynamic response of caisson breakwaters - Results of large-scale model tests"*. A.S.C.E., Proceedings of the 23rd International Conference on Coastal Engineering, pp. 1475-1488, Venice 1992. Venice, Italy

OUMERACI, H. and KORTENHAUS, A. (1994) *"Analysis of the dynamic response of caisson breakwaters"*. Coastal Engineering 22 (1994) pp. 159-183. Elsevier Science B.V., Amsterdam, the Netherlands

OUMERACI, H., KLAMMER, P. and KORTENHAUS, A. (1994a) *"Impact Loading and Dynamic Response of Vertical Breakwaters - Review of Experimental Results - "*. Proceedings of the international workshop on Wave Barriers in Deep Waters, January 10-14, 1994, pp. 374-359. Port and Harbour Research Institute, Ministry of Transport, Nagase, Yokosuka, Japan

OUMERACI, H., BRUCE, T., KLAMMER, P. and EASSON, W.J. (1995) *"PIV-Measurement of Breaking Wave Kinematics and Impact Loading of Caisson Breakwaters"*. Proceedings of the International Conference on Coastal and Port Engineering in Developing Countries pp. 2394-2410. Rio de Janeiro, Brazil

PEDERSEN, J. (1994) *"Dynamic Response of Rubble Mound Breakwater Crown Walls"*. Proceedings of the Second Project Workshop, April 14-15 1994, Milan, Italy

PEREGRINE D.H. (1994) *"Pressure on breakwaters: a forward look"*. Proceedings of the international workshop on Wave Barriers in Deep Waters, January 10-14, 1994, pp. 553-571. Port and Harbour Research Institute, Ministry of Transport, Nagase, Yokosuka, Japan

PEREGRINE, D.H. and THAIS, L. (1995) *"The effect of entrained air in violent water wave impacts"*. Final Proceedings, MAST II, MCS-project: Monolithic (Vertical) Coastal Structures

PIANC (1996) *"Identification and evaluation of design tools"* draft February 1996. PIANC PTCII, report of Working Group 28, Brussels, Belgium

RAMKEMA, C (1978) *"A model law for wave impacts on coastal structures"* Delft Hydraulics publication no. 207. Delft Hydraulics, Delft, the Netherlands

RICHART, F.E., HALL, J.R. and WOODS, R.D. (1970) *"Vibrations of soils and foundations"*. Prentice-Hall Inc., Englewood Cliffs, New Jersey, United Sates of America

ROUVILLE, M.A., BESSON, P. and PETRY, P. (1938) *"État actuel des Études internationales sur les efforts dus aux lames"*. Annales des Ponts et Chaussées vol. 108 (II), pp. 5 -113. Paris, France

SCHIERECK, G.J. (1995) *"Introduction to bed, bank and shore protection"* lecture notes F4. Delft University of Technology, Delft, the Netherlands

SCHMIDT, R., OUMERACI, H. and PARTENSCKY, H.W. (1992) *"Impact loads induced by plunging breakers on vertical structures"*. A.S.C.E., Proceedings of the 23rd International Conference on Coastal Engineering, pp. 1545-1558, Venice 1992. Venice, Italy

SPIJKERS, J., DIETERMAN, H.A., KLAVER E. and VROUWENVELDER A. (1993) *"Dynamica van constructies"* deel 1, lecture notes B9 (in Dutch). Delft University of Technology, Delft, the Netherlands

TAKAHASHI, S. (1995) *"Design of breakwaters"*. Port and Harbour Research Institute, Ministry of Transport, Nagase, Yokosuka, Japan

TAKAHASHI, S., TANIMOTO, K. and SUZUMARA, S. (1983) *"Generation mechanism of impulsive pressure by breaking wave on a vertical wall"*. Vol. 22, No. 4, pp 3-31. Port and Harbour Research Institute, Ministry of Transport, Nagase, Yokosuka, Japan

TAKAHASHI, S., TANIMOTO, K. and SHIMOSAKO, K. (1993) *"Experimental study of impulsive pressures on composite breakwaters - fundamental feature of impulsive pressure and the impulsive pressure coefficient"*. Vol. 31, No. 5 (March 1993). Port and Harbour Research Institute, Ministry of Transport, Nagase, Yokosuka, Japan

TAKAHASHI, S., TANIMOTO, K. and SHIMOSAKO, K. (1994) *"Dynamic Response and Sliding of Breakwater Caissons against Impulsive Breaking Wave Forces"* Proceedings of the international workshop on Wave Barriers in Deep Waters, January 10-14, 1994, pp. 362-399. Port and Harbour Research Institute, Ministry of Transport, Nagase, Yokosuka, Japan

TOPLISS, M.E., COOKER, M.J. and PEREGRINE, D.H. (1992) *"Pressure oscillations during wave impact on vertical walls"*. A.S.C.E., Proceedings of the 23rd International Conference on Coastal Engineering, pp. 1639-1650, Venice 1992. Venice, Italy

VERRUIJT, A (1993) *"Grondmechanica"* (in Dutch). Delftse Uitgevers Maatschappij, Delft, The Netherlands

VERRUIJT, A. (1996) *"Soil Dynamics"*. lecture notes B28. Delft University of Technology, Delft, the Netherlands

WALKDEN, M.J.A., HEWSON, P.J. BULLOCK, G.N. and GRAHAM, D.I. (1995) *"The influence of artificially entrained air upon wave impact pressures at model scale in fresh water"*. Final Proceedings, MAST II, MCS-project: Monolithic (Vertical) Coastal Structures

WALKDEN, M.J.A.and HEWSON, P.J. (1995a) *"Comparison of model scale waves (University of Plymouth) with large scale model tests (GWK, Franzius Institute Hannover)"*. Final Proceedings, MAST II, MCS-project: Monolithic (Vertical) Coastal Structures

Enclosures

On the next pages different enclosures are to be found.

Enclosure 8.1: Listing TILLY program

```
$ Graduation project "Wave Impacts on Vertical Breakwaters"
$ Project: model vertical breakwater
$       six springs, all of them linear-elastic
$       no damping
$       inital velocities caused by a wave impact load of the transition type
$ H.A.Th. Vink, 22 April 1997

INERTIA
1 29269.9e3
2 38956.2e3
3 3.016e9

KINEMATICS
1 ndof=3 1 -1 2 0   3  -8.1649658
2 ndof=3 1 -1 2 0   3  -4.0824829
3 ndof=3 1 -1 2 0   3  0
4 ndof=3 1 -1 2 0   3  4.0824829
5 ndof=3 1 -1 2 0   3  8.1649658
6 ndof=3 1  0 2 1   3  11.5

ELEMENTS
1  spring1 kine 1
2  spring2 kine 2
3  spring3 kine 3
4  spring4 kine 4
5  spring5 kine 5
6  spring6 kine 6

SPRING
1 3.0e9
2 3.0e9
3 3.0e9
4 3.0e9
5 3.0e9
6 15.0e9

INITIAL VELOCITIES
2  0.0620173
3 -0.0028036

EXECUTIVE COMMANDS
DYNAMIC DIRECT INTEGRATION NSTEP=1000 LSTEP=0.005 &
LINEAR GAMMA2=-1 &
PSC=1 POU=10 PGR=1

PLOT FILE
STEP
TIME
DISPLACEMENTS 1 2 3
E 1 2 3 4 5 6
S 1 2 3 4 5 6
```

Enclosure 8.2: Listing TILLY program

```
$ Graduation project "Wave Impacts on Vertical Breakwaters"
$ Project: model vertical breakwater
$       six springs, all of them linear-elastic
$       no damping
$       load: wave impact of the transition type
$ H.A.Th. Vink, 22 April 1997

INERTIA
1 29269.9e3
2 38956.2e3
3 3.016e9

KINEMATICS
1 ndof=3 1 -1 2 0   3  -8.1649658
2 ndof=3 1 -1 2 0   3  -4.0824829
3 ndof=3 1 -1 2 0   3   0
4 ndof=3 1 -1 2 0   3   4.0824829
5 ndof=3 1 -1 2 0   3   8.1649658
6 ndof=3 1  0 2 1   3  11.5

ELEMENTS
1  spring1 kine 1
2  spring2 kine 2
3  spring3 kine 3
4  spring4 kine 4
5  spring5 kine 5
6  spring6 kine 6

SPRING
1 3.0e9
2 3.0e9
3 3.0e9
4 3.0e9
5 3.0e9
6 15.0e9

LOADING
ti=0.000        2 0             3 0
ti=0.006        2 4.0266e8      3 -1.40931e9
ti=0.012        2 0             3 0

EXECUTIVE COMMANDS
DYNAMIC DIRECT INTEGRATION NSTEP=1000 LSTEP=0.005 &
LINEAR GAMMA2=-1 &
PSC=1 POU=10 PGR=1

PLOT FILE
STEP
TIME
DISPLACEMENTS 1 2 3
E 1 2 3 4 5 6
S 1 2 3 4 5 6
```

Enclosure 8.3: Listing TILLY program

```
$ Graduation project "Wave Impacts on Vertical Breakwaters"
$ Project: model vertical breakwater
$       six springs, all of them elasto-plastic
$       damping
$       load: wave impact of transition type
$ H.A.Th. Vink, 25 April 1997

INERTIA
1 29269.9e3
2 38956.2e3
3 3.016e9

KINEMATICS
1 ndof=3 1 -1 2 0   3  -8.1649658
2 ndof=3 1 -1 2 0   3  -4.0824829
3 ndof=3 1 -1 2 0   3  0
4 ndof=3 1 -1 2 0   3  4.0824829
5 ndof=3 1 -1 2 0   3  8.1649658
6 ndof=3 1  0 2 1   3  11.5

ELEMENTS
1  hygade1 kine 1
2  hygade2 kine 2
3  hygade3 kine 3
4  hygade4 kine 4
5  hygade5 kine 5
6  sprelpla6 kine 6
11 fric1 kine 1
12 fric2 kine 2
13 fric3 kine 3
14 fric4 kine 4
15 fric5 kine 5
16 fric6 kine 6

HYGADE
1 3e9 -70.7037e6 0 degr a=0 c=1 init 0 1e8
2 3e9 -74.4648e6 0 degr a=0 c=1 init 0 1e8
3 3e9 -74.4648e6 0 degr a=0 c=1 init 0 1e8
4 3e9 -74.4648e6 0 degr a=0 c=1 init 0 1e8
5 3e9 -70.7037e6 0 degr a=0 c=1 init 0 1e8

SPRELPLA
6 1.5e10 plastic -91.440e6 91.440e6

FRICTION
1 viscous 73.58e6
2 viscous 73.58e6
3 viscous 73.58e6
4 viscous 73.58e6
5 viscous 73.58e6
6 viscous 367.9e6

LOADING
ti=0.000  1 152.4e6   2 0              3 0
ti=0.006              2 402.66e6       3 -1409.31e6
ti=0.012              2 0              3 0

INITIAL DISPLACEMENTS
1 0.01016

EXECUTIVE COMMANDS
DYNAMIC DIRECT INTEGRATION NSTEP=1000 LSTEP=0.005 &
LINEAR GAMMA2=-1 &
PSC=1 POU=10 PGR=1

PLOT FILE
STEP
TIME
DISPLACEMENTS 1 2 3
E 1 2 3 4 5 6
S 1 2 3 4 5 6
```

Enclosure 8.4: Listing TILLY program

```
$ Graduation project "Wave Impacts on Vertical Breakwaters"
$ Project: model vertical breakwater
$       six springs, all of them elasto-plastic
$       damping
$       load: maximum wave impact load with triangular load history
$ H.A.Th. Vink, 25 April 1997

INERTIA
1 29269.9e3
2 38956.2e3
3 3.016e9

KINEMATICS
1 ndof=3 1 -1 2 0   3  -8.1649658
2 ndof=3 1 -1 2 0   3  -4.0824829
3 ndof=3 1 -1 2 0   3  0
4 ndof=3 1 -1 2 0   3  4.0824829
5 ndof=3 1 -1 2 0   3  8.1649658
6 ndof=3 1  0 2 1   3  11.5

ELEMENTS
1  hygade1 kine 1
2  hygade2 kine 2
3  hygade3 kine 3
4  hygade4 kine 4
5  hygade5 kine 5
6  sprelpla6 kine 6
11 fric1 kine 1
12 fric2 kine 2
13 fric3 kine 3
14 fric4 kine 4
15 fric5 kine 5
16 fric6 kine 6

HYGADE
1 3e9 -70.7037e6 0 degr a=0 c=1 init 0 1e8
2 3e9 -74.4648e6 0 degr a=0 c=1 init 0 1e8
3 3e9 -74.4648e6 0 degr a=0 c=1 init 0 1e8
4 3e9 -74.4648e6 0 degr a=0 c=1 init 0 1e8
5 3e9 -70.7037e6 0 degr a=0 c=1 init 0 1e8

SPRELPLA
6 1.5e10 plastic -91.440e6 91.440e6

FRICTION
1 viscous 73.58e6
2 viscous 73.58e6
3 viscous 73.58e6
4 viscous 73.58e6
5 viscous 73.58e6
6 viscous 367.9e6

LOADING
ti=0.000  1 152.4e6   2 0                  3 0
ti=0.125              2 452.48625e6        3 -1583.7019e6
ti=0.250              2 0                  3 0

INITIAL DISPLACEMENTS
1 0.01016

EXECUTIVE COMMANDS
DYNAMIC DIRECT INTEGRATION NSTEP=1000 LSTEP=0.005 &
LINEAR GAMMA2=-1 &
PSC=1 POU=10 PGR=1

PLOT FILE
STEP
TIME
DISPLACEMENTS 1 2 3
E 1 2 3 4 5 6
S 1 2 3 4 5 6
```

Canarias 7
CANARIAS A DIARIO

MIERCOLES,
19 de febrero de 1997
Año XVI / Número 5.208
Precio: 125 ptas.

FERNANDO OJEDA

El Dique Reina Sofía se convierte en laboratorio europeo

La ampliación del Dique Reina Sofía del Puerto de La Luz y Las Palmas se ha convertido en un inmejorable laboratorio para expertos europeos, que analizan estos días en la capital grancanaria las características de una obra revolucionaria que cuenta además con la singularidad de aportar datos fiables sobre el impacto del mar en la estructura de hormigón. Expertos de ocho países visitaron ayer el Dique Reina Sofía, considerado «un hito» en su categoría. La imagen recoge un momento de la visita de los ingenieros a la obra portuaria.